

# Investigation of intraoperative accelerometer data recording for safer and improved target selection for deep brain stimulation

**Inaugural dissertation**

to

be awarded the degree of Dr. sc. med.  
presented at  
the Faculty of Medicine  
of the University of Basel

by

Ashesh Shah  
Vadodara, India

Basel, 2018

Original document stored on the publication server of the University of  
Basel [edoc.unibas.ch](http://edoc.unibas.ch)



Approved by the Faculty of Medicine  
On application of

Prof. Dr. Simone Hemm-Ode  
*Primary Advisor*

Prof. Dr. med. Raphael Guzman  
*Secondary Advisor*

Prof. Dr. Erik Schkommodau  
*Further Advisor*

Dr. Ethan Taub  
*Further Advisor*

Prof. Dr. med. Lars Timmermann  
*External Expert*

Basel, .....

.....

Prof. Dr. Primo L. Schär  
*Dean, Faculty of Medicine*



This thesis is dedicated to my son Vihaan



# Summary

**Background:** Deep Brain Stimulation (DBS) is a well established surgical treatment for Parkinson's Disease (PD) and Essential Tremor (ET). Electrical leads are surgically implanted in the deeply seated structures in the brain and chronically stimulated. The location of the lead with respect to the anatomy is very important for optimal treatment. Therefore, clinicians carefully plan the surgery, record electrophysiological signals from the region of interest and perform stimulation tests to identify the best location to permanently place the leads. Nevertheless, there are certain aspects of the surgery that can still be improved. Firstly, therapeutic effects of stimulation are estimated by visually evaluating changes in tremor or passively moving patient's limb to evaluate changes in rigidity. These methods are subjective and depend heavily on the experience of the evaluator. Secondly, a significant amount of patient data is collected before and during the surgery like various CT and MR images, surgical planning information, electrophysiological recordings and results of stimulation tests. These are not fully utilized at the time of choosing the position for lead placement as they are either not available or acquired on separate systems or in the form of paper notes only. Thirdly, studies have shown that the current target structures to implant the leads (Subthalamic Nucleus (STN) for PD and Ventral Intermediate Nucleus (VIM) for ET) may not be the only ones responsible for the therapeutic effects. The objective of this doctoral work is to develop new methods that help clinicians subdue the above limitations which could in the long term improve the DBS therapy.

**Method:** After a thorough review of the existing literature, specifically customized solutions were designed for the shortcomings described above. A new method to quantitatively evaluate tremor during DBS surgery using acceleration sensor was developed. The method was then adapted to measure acceleration of passive movements and to evaluate changes in rigidity through it. Data from 30 DBS surgeries was collected by applying these methods in two clinical studies: one in Centre Hospitalier Universitaire (CHU), Clermont-Ferrand and another multi-center study in Universitätsklinik Basel and Inselspital Bern in Switzerland. To study the role of different anatomical structures in the therapeutic and adverse effects of stimulation, the data collected during the study was analysed

using two methods. The first classical approach was to classify the data based on the anatomical structure in which the stimulating contact of the electrode was located. The second advanced approach was to use patient-specific Finite Element Method (FEM) simulations of the Electric Field (EF) to estimate the spatial distribution of stimulation in the structures surrounding the electrode. Such simulations of the adverse effect inducing stimulation current amplitudes are used to visualize the boundaries of safe stimulation and identify structures that could be responsible for these effects. In addition, the patient-specific simulations are also used to develop a new method called "Improvement Maps" to generate 2D and 3D visualization of intra operative stimulation test results with the patient images and surgical planning. This visualization summarized the stimulation test results by dividing the explored area into multiple regions based on the improvement in symptoms as measured by the accelerometric methods.

**Results:** The accelerometric method successfully measured changes in tremor and rigidity. Standard deviation, signal energy and spectral amplitude of dominant frequency correlated with changes in the symptoms. Symptom suppressing stimulation current amplitudes identified through quantitative methods were lower than those identified through the subjective methods. Comparison of anatomical targets using the accelerometric data showed that to suppress rigidity in PD patients, stimulation current needed was marginally higher for Fields of Forel (FF) and Zona Incerta (ZI) compared to STN. On the other hand, the adverse effect occurrence rate was significantly lower in ZI and FF, indicating them to be better targets compared to STN. Similarly, for ET patients, other thalamic nuclei like the Intermediolateral (InL) and Ventro-Oral (VO) as well as the Pre-Lemniscal Radiations (PLR) are as efficient in suppressing tremor as the VIM but have lower occurrence of adverse effects. Volumetric analysis of spatial distribution of stimulation agreed with these results suggesting that the structures other than the VIM could also play a role in therapeutic effects of stimulation. The visualization of the adverse effect simulations clearly show the structures which could be responsible for such effects e.g. stimulation in the internal capsula induced pyramidal effects. These findings concur with the published literature. With regard to the improvement maps, the clinicians found them intuitive and easy to use to identify the optimal position for lead placement. If the maps were available during the surgery, the clinicians' choice of lead placement would have been different.

**Conclusion:** This doctoral work has shown that modern techniques like quantitative symptom evaluation and electric field simulations can suppress the existing drawbacks of the DBS surgery. Furthermore, these methods along with 3D visualization of data can simplify tasks for clinicians of optimizing lead placement. Better placement of the DBS lead can potentially reduce adverse effects and increase battery life of implanted pulse generator, resulting in better therapy for patients.

# Acknowledgements

This doctoral work would not have been possible without the efforts and encouragement of various people.

First and foremost, I would like to thank **Prof. Dr. Simone Hemm-Ode** for letting me pursue this work under her supervision. I am extremely grateful for her relentless support, especially during testing times. I am indebted to her for generously taking the time for discussions and sharing her knowledge.

I am also very thankful to **Prof. Dr. Erik Schkommodau** for giving me the opportunity to work in his Institute for Medical and Analytical Technologies (IMA) at the Fachhochschule Nordwestschweiz (FHNW). I appreciate his trust in me and granting full freedom to pursue the tasks for this work. His technical queries and insights have on various occasions challenged me to find better solutions to my hurdles and resulted in many fold improvements in my work.

I have immense gratitude for **Prof. Dr. med. Raphael Guzman** and **Dr. Ethan Taub** for graciously taking time to supervise my work, despite their busy schedules as neurosurgeons at the **Universitätsspital Basel**. Their crucial inputs from the medial point of view have significantly increased my understanding and vastly improved the practical aspects of this doctoral work. I am also grateful to Dr. Taub for kindly allowing me to participate in and record data during his surgeries.

It would not have been possible to collect sufficient data for this doctoral work without the efforts of **Prof. Dr. Jean-Jacques Lemaire** and **Dr. Jérôme Coste** at the **CHU, Clermont-Ferrand**. Prof. Lemaire benevolently shared his neuro-anatomical knowledge and surgical planning data with me to use during this work. Dr. Coste helped me in every surgery to set up the data recording apparatus and also translated all necessary information from French to English. He has patiently answered many of my trivial and non-trivial questions in person as well as through emails. I am extremely grateful to both of them for all of the above and more and for making me feel comfortable at CHU, Clermont-Ferrand.

I also want to thank **Prof. Dr. med. Claudio Pollo** and **PD. Dr. med. Michael Schüpbach** at the Inselspital Bern for helping me collect data for this work.

Prof. Pollo shared his in-depth knowledge of the DBS surgical procedure and the surgical planning data for my analysis. Dr. Schüpbach gave important inputs from a neurologist's point of view which helped me tune my methods for better clinical use. He graciously provided his patient evaluation notes taken during the surgery to compare them with results from accelerometer data analysis.

The improvement maps technique would not have been possible without the fruitful collaboration with the Institutionen för medicinsk teknik (IMT) headed by **Prof. Dr. Karin Wårdell** at the Linköping University (LiU). They kindly shared their knowledge about electric field simulations and adapted it for the needs of the project. **Daniela Pison** in IMA and **Fabiola Alonso** in IMT worked extensively on patient-specific electric field simulations for intraoperative stimulation tests. The resultant data formed the basis for the improvement maps. I am extremely grateful to all of them for openly discussing their methods, their challenges and their solutions which helped me to improve the improvement maps.

Apart from Prof. Hemm-Ode and Prof. Schkommodau, I have also received advice and encouragement from **Prof. David Hradetzky** and **Prof. Markus Degen**. Many colleagues have help me keep a sane and calm mind while trying to solve typographical errors in my scripts. Various discussion with Daniela Pison in the lab and outside have helped me get through difficult times. **Dorian Vogel**, who is now pursuing his PhD in the same field, has help me by reviewing this document and has provided valuable inputs on various occasions. He along with **Denise, Quentin, Florian, Daniel, John, Yves, Chris, Gregor and Pascal** have entertained me every day through the gaming breaks after lunch. I am thankful to all of them for the wonderful time I have had.

I would not have been able to finish this doctoral work without the persistent support of my family. My parents, **Atul** and **Parul** have helped me in various ways, especially by visiting me here in Switzerland in times of need. Having my brother **Ankit** and his wife **Ankini** nearby in Germany has helped me many times to blow off some steam by visiting them, even on short notice. Most of all, I am thankful to my wife **Nikita** for having the courage and patience to travel this road with me, for providing continuous motivation, for standing beside me on various challenging and crucial occasions, and I am also thankful to my son **Vihaan** who is an eternal source of happiness for me.

# Contents

<b>Summary</b>	<b>i</b>
<b>Acknowledgements</b>	<b>iii</b>
<b>Contents</b>	<b>v</b>
<b>Abbreviations</b>	<b>viii</b>
<b>List of Figures</b>	<b>xi</b>
<b>List of Tables</b>	<b>xiv</b>
<b>1 Introduction</b>	<b>1</b>
1.1 Motivation . . . . .	2
1.2 Aims . . . . .	3
1.3 Outline . . . . .	4
<b>2 Background</b>	<b>5</b>
2.1 Basal ganglia and motor circuit . . . . .	5
2.1.1 Motor Cortex . . . . .	5
2.1.2 Cerebellum and Inferior Olivary Nucleus . . . . .	6
2.1.3 Thalamus . . . . .	6
2.1.4 Basal Ganglia . . . . .	7
2.2 Parkinson's Disease (PD) . . . . .	9
2.2.1 PD Rating Scales . . . . .	12
2.2.2 Pathology . . . . .	16
2.2.3 Treatments . . . . .	18
2.3 Essential Tremor (ET) . . . . .	19
2.3.1 ET Rating Scales . . . . .	21
2.3.2 Pathology . . . . .	23
2.3.3 Treatments . . . . .	24
2.4 Deep Brain Stimulation (DBS) . . . . .	24
2.4.1 Surgical Procedure . . . . .	27
2.4.2 Risks and Complications . . . . .	33

2.4.3	Mechanism of Action . . . . .	35
2.5	Symptom Evaluation During DBS Surgery . . . . .	37
2.5.1	Quantitative tremor evaluation . . . . .	39
2.5.2	Quantitative rigidity evaluation . . . . .	42
2.6	Anatomical Targets for DBS Lead Implantation . . . . .	43
2.6.1	Identifying structures . . . . .	43
2.6.2	STN implantation . . . . .	44
2.6.3	VIM implantation . . . . .	45
2.7	Data Management and Visualization for DBS Lead Placement . . . . .	45
<b>3</b>	<b>Clinical Data Acquisition</b>	<b>49</b>
3.1	Accelerometer Data Recording Setup . . . . .	49
3.1.1	Technical Requirements . . . . .	49
3.1.2	Clinical Requirements . . . . .	50
3.1.3	Hardware . . . . .	52
3.1.4	Software . . . . .	52
3.1.5	Synchronization . . . . .	53
3.1.6	Laboratory tests . . . . .	53
3.2	Clinical Studies . . . . .	55
3.2.1	Study 1: Clermont-Ferrand . . . . .	55
3.2.2	Study 2: Basel and Bern . . . . .	56
3.2.3	Data Recording Protocol . . . . .	58
<b>4</b>	<b>Quantitative Tremor Evaluation during DBS Surgery</b>	<b>59</b>
4.1	Paper 1: Case Study for Quantitative Tremor Evaluation . . . . .	60
4.2	Paper 2: Clinical Study for Quantitative Tremor Evaluation . . . . .	65
<b>5</b>	<b>Assistive Rigidity Evaluation during DBS Surgery</b>	<b>80</b>
5.1	Paper 3: Clinical Study for Assistive Rigidity Evaluation . . . . .	81
<b>6</b>	<b>Quantitative Target Selection</b>	<b>96</b>
6.1	Paper 4: Anatomical analysis of stimulating contact position . . . . .	99
<b>7</b>	<b>Spatial Effects of Stimulation</b>	<b>105</b>
7.1	Paper 5: Anatomical analysis of spatial effect of stimulation . . . . .	107
<b>8</b>	<b>Data Visualization during DBS Surgery</b>	<b>122</b>
8.1	Paper 6: Visual analysis of adverse effects . . . . .	125
8.2	Paper 7: Visual tool for Lead placement . . . . .	130
<b>9</b>	<b>Synthesis, Discussion and Perspective</b>	<b>161</b>
9.1	Summary of Key Findings . . . . .	161
9.2	General Discussion . . . . .	162
9.2.1	Symptom Evaluation during DBS Surgery . . . . .	162
9.2.2	Anatomical Targets for DBS Lead Implantation . . . . .	163

<i>CONTENTS</i>	vii
9.2.3 Data Visualization for DBS Lead Placement . . . . .	164
9.2.4 Mechanisms of Action of DBS . . . . .	167
9.3 Perspective . . . . .	167
<b>10 Conclusion</b>	<b>169</b>
<b>References</b>	<b>170</b>

# Abbreviations

**BG** Basal Ganglia

**cGMP** Cyclic guanosine monophosphate

**CHU** Centre Hospitalier Universitaire

**CT** Computed Tomography

**DBS** Deep Brain Stimulation

**DRTT** Dentato-Rubro Thalamic Tract

**EF** Electric Field

**EMG** Electromyography

**ET** Essential Tremor

**FEM** Finite Element Method

**FF** Fields of Forel

**FHNW** Fachhochschule Nordwestschweiz

**fMRI** Functional Magnetic Resonance Imaging

**GPe** Globus Pallidus externus

**GPI** Globus Pallidus internus

**GPS** Global Positioning System

**IC** Internal Capsule

**IMA** Institute for Medical and Analytical Technologies

**IMT** Institutionen för medicinsk teknik

**InL** Intermediolateral

**IPG** Implanted Pulse Generator

**LFP** Local Field Potential

**LiU** Linköping University

**MDS** Movement Disorder Society

**MEMS** Micro Electro Mechanical Systems

**MER** Micro-Electrode Recording

**MR** Magnetic Resonance

**MRI** Magnetic Resonance Imaging

**PD** Parkinson's Disease

**PET** Positron Emission Tomography

**PLR** Pre-Lemniscal Radiations

**PMC** Primary Motor Cortex

**PPN** Pedunculo-pontine Nucleus

**preMC** Premotor Cortex

**PSA** Posterior Sub-thalamic Area

**SMA** Supplementary Motor Area

**SNc** Substantia Nigra pars compacta

**SNr** Substantia Nigra pars reticulata

**SPECT** Single-photon emission computed tomography

**STN** Subthalamic Nucleus

**TETRAS** Tremor Research Group Essential Tremor Rating Assessment Scale

**UPDRS** Unified Parkinson's Disease Rating Scale

**VIM** Ventral Intermediate Nucleus

**VO** Ventro-Oral

**VTA** Volume of Tissue Activated

**WAIR** White Matter Attenuated Inversion Recovery

**WHIGET** Washington Heights-Inwood Genetic Study of Essential Tremor

**ZI** Zona Incerta

# List of Figures

2.1	Human Motor Cortex and Cerebellum . . . . .	6
2.2	Thalamus . . . . .	7
2.3	Human motor circuit connections . . . . .	8
2.4	Basal Ganglia . . . . .	8
2.5	Basal Ganglia Circuits . . . . .	9
2.6	Parkinson's patient sketch . . . . .	10
2.7	UPDRS Tremor Evaluation Question . . . . .	14
2.8	UPDRS Rigidity Evaluation Question . . . . .	15
2.9	Braak Staging in PD . . . . .	16
2.10	Classical Model of PD Pathophysiology . . . . .	18
2.11	Fahn-Tolosa-Marin Tremor Rating Scale . . . . .	22
2.12	DBS components . . . . .	25
2.13	Commercial DBS Leads . . . . .	26
2.14	Surgical planning software . . . . .	27
2.15	Commercial stereotactic frame . . . . .	28
2.16	Electrode insertion during surgery . . . . .	29
2.17	Example of MER and LFP data . . . . .	30
2.18	Summary of steps for DBS surgery . . . . .	31
2.19	Note-taking during stimulation tests . . . . .	32
2.20	Neuron structure . . . . .	36
2.21	Rigidity evaluation . . . . .	38
2.22	Tremor recorded through EMG and accelerometer . . . . .	40
2.23	Inertial Sensors . . . . .	41
2.24	Mechanical setup to evaluate rigidity . . . . .	43
2.25	Structures around the STN . . . . .	44
2.26	Thalamic nuclei around VIM . . . . .	45
2.27	Paper notes during stimulation tests . . . . .	47
3.1	Accelerometer use for rigidity evaluation . . . . .	51
3.2	Sensor used in this study . . . . .	52
3.3	Data Recording Software . . . . .	54
4.1	Acceleration sensor for tremor evaluation . . . . .	61

4.2	Raw and filtered tremor acceleration . . . . .	62
4.3	Comparison of tremor suppressing parameters 1 . . . . .	63
4.4	Comparison of tremor suppressing parameters 2 . . . . .	63
4.5	Comparison of tremor suppressing parameters 3 . . . . .	63
4.6	Data recording setup for tremor evaluation . . . . .	69
4.7	Raw acceleration data and outcome measures . . . . .	71
4.8	Comparison of quantitative and visual tremor evaluation . . . . .	74
4.9	Comparison of tremor suppressing amplitudes . . . . .	75
5.1	Data recording setup for rigidity evaluation . . . . .	85
5.2	Rigidity acceleration data and outcome measures . . . . .	86
5.3	Sensor on patient vs evaluator . . . . .	87
5.4	Interrater variations for rigidity evaluation . . . . .	88
5.5	Comparison of rigidity suppressing parameters . . . . .	89
5.6	Comparison of STN, ZI and FF as target structures . . . . .	90
5.7	Outcome measures sensor on patient vs evaluator . . . . .	94
5.8	Intra-rater variations in outcome measures . . . . .	95
6.1	Labelling of anatomical structures . . . . .	97
6.2	Comparison of tremor suppressing parameters . . . . .	102
6.3	Comparison of thalamic nuclei as target structures . . . . .	103
7.1	MR image and corresponding brain model . . . . .	106
7.2	Surgical workflow and data acquisition . . . . .	110
7.3	VIM and neighbouring structures . . . . .	111
7.4	Brain map generation workflow . . . . .	112
7.5	Exploration electrode and its FEM model . . . . .	113
7.6	Example of volumetric calculations . . . . .	114
7.7	Example of simulated electric field isosurface . . . . .	115
7.8	Classical comparison of thalamic nuclei for therapeutic effect . . . . .	116
7.9	Volumetric comparison of thalamic nuclei for therapeutic effect . . . . .	117
8.1	3D view of thalamic nuclei . . . . .	126
8.2	Orthogonal sections through adverse effect simulations . . . . .	129
8.3	Diagrammatic representation of EF simulations . . . . .	139
8.4	Improvement map creation workflow . . . . .	140
8.5	Sagittal view of EF simulations and respective improvement map for patient data . . . . .	141
8.6	Diagrammatic representation of maximum improvement map . . . . .	141
8.7	Improvement map for patient 5 right hemisphere . . . . .	143
8.8	Improvement map for patient 1 right hemisphere . . . . .	153
8.9	Improvement map for patient 2 left hemisphere . . . . .	154
8.10	Improvement map for patient 2 right hemisphere . . . . .	155
8.11	Improvement map for patient 3 left hemisphere . . . . .	156
8.12	Improvement map for Patient 3 right hemisphere . . . . .	157

8.13 Improvement map for Patient 4 left hemisphere . . . . .	158
8.14 Improvement map for Patient 4 right hemisphere . . . . .	159
8.15 Improvement map for Patient 5 left hemisphere . . . . .	160

# List of Tables

3.1	Patients recruited in Study 1 . . . . .	57
3.2	Patients recruited in Study 2 . . . . .	58
4.1	DBS surgical procedure differences . . . . .	68
4.2	List of patients for tremor evaluation . . . . .	70
4.3	Categorization of tremor improvement . . . . .	73
5.1	List of patients for rigidity evaluation . . . . .	85
5.2	Applied statistical tests and results . . . . .	86
5.3	Lead placement position based on accelerometer data . . . . .	90
6.1	Anatomical categorization of results . . . . .	103
7.1	List of simulations per patient . . . . .	114
8.1	Patient data used for adverse effect maps creation . . . . .	127
8.2	Adverse effect areas for different patients . . . . .	128
8.3	Patients used for improvement map creation . . . . .	138
8.4	Lead placement positions based on Improvement maps . . . . .	144
8.5	Summary of nine improvement maps . . . . .	145

# Chapter 1

## Introduction

Essential Tremor (ET) and Parkinson's Disease (PD) are two of the most common progressive neurodegenerative *movement disorders*. For decades, researchers have studied the abnormalities in the human motor circuits of patients suffering from these diseases to pin-point the cause. Through these efforts, some pathological findings have been associated with the diseases e.g. dopamine depletion in Substantia Nigra pars compacta (SNc) is associated with PD. However, the precise aetiology of these diseases remains elusive. This may be one of the reasons that a *cure* for either of the diseases *does not exist*. Current treatments are only symptomatic, i.e. they are designed to suppress the progressively worsening symptoms. The first approach to treat the symptoms is to use pharmaceutical drugs which supplement the loss of necessary compounds in the brain like dopamine. As the disease progresses, the dosage of the drug is increased but only till the therapeutic effects outweigh the adverse effects. If the increased dosage causes severe adverse effects, a surgical treatment called *Deep Brain Stimulation (DBS)* is considered to decrease the drug dosage without worsening the symptoms.

In DBS, electrical leads are implanted in specific regions of the brain and stimulated continuously using a pulse generator implanted in the thoracic or pelvic cavity. Over the years, certain brain structures have been established as ideal targets for different diseases e.g. Subthalamic Nucleus (STN) for PD. For a successful outcome of DBS therapy, the *implant location of the lead* plays a very crucial role. Before the surgery, the clinicians use commercial planning software in combination with Computed Tomography (CT) and/or Magnetic Resonance (MR) images of the patients' brain to identify the target structure and the best path to reach it. During the surgery, electrophysiological activity is recorded using Micro-Electrode Recording (MER) to verify the planned path and validate the target structure through its typical signal pattern. In addition, to ensure that the lead is implanted in the optimal location, intraoperative stimulation

tests are performed at planned locations along the path to check for therapeutic and adverse effects. The lead is implanted at a location where therapeutic effects are observed at low stimulation current amplitudes and where adverse effects are not observed or only when stimulating at very high currents.

## 1.1 Motivation

In the past three decades since DBS has been used as a treatment for movement disorders, more than 150000 patients have been treated. For a majority of these patients, the motor symptoms have been significantly suppressed. But reports of inadequate therapeutic effects have also been published, some of which have been attributed to *suboptimal placement of the DBS lead*. Despite the abundant tools and techniques available to optimize lead placement, from an engineering perspective, there are some areas which can be improved.

One area that needs further engineering research is the *symptom evaluation technique* used during surgery to estimate the therapeutic effects of stimulation. For patients with ET and tremor-dominant PD, the therapeutic effects are evaluated by visually observing the changes in tremor. For rigidity-dominant PD patients, changes in rigidity are measured by passive movements of patient's limb (mostly upper) about a joint. In most centres, changes in the symptoms are evaluated in a relative manner, i.e. by comparing the symptom severity during stimulation to a baseline severity noted before stimulation starts. Such relative changes can be rated in two ways: i) by direct rating i.e. a score is given from 0 to 4 where 0 indicates no change and 4 indicates symptom alleviation or ii) using parts of a clinical scale like the Unified Parkinson's Disease Rating Scale (UPDRS) for severity evaluation for baseline and during stimulation. In its current form, the evaluation of therapeutic effects for stimulation is very subjective i.e. the rating during the surgery depends heavily on the experience of the evaluator.

Another aspect of DBS surgery that can be improved concerns the *management of data* obtained during surgery. The results of stimulation tests i.e. stimulation parameters resulting in therapeutic and adverse effects are noted using pen and paper. On completion of the stimulation tests, to optimally place the leads, the surgical team discusses the results using these notes and "mentally" visualizes the information with respect to the patient's anatomy. If the software used for planning the surgery is available for intraoperative use, which is not a typical case, the clinicians have to manually enter the intraoperative data to visualize it. Nevertheless, the software packages currently available are not capable of visualizing all the information obtained during the stimulation tests.

The success of DBS as a therapy for PD and ET has prompted clinicians to apply it to other neurological diseases. However, one hurdle that they have yet to overcome is to completely understand the functioning of DBS. Despite the

application of DBS to so many patients, the *mechanisms* by which it reduces the patient's symptoms are still not fully known. Since its first use, the scientific community has proposed various hypothesis based on different research techniques, but none of these can explain all the effects of DBS on their own. It is known that stimulation in the brain causes changes in the electrical activity of the neurons surrounding the lead, but how these changes affect the functioning of the brain is only partially understood. Some studies have been performed where DBS has been applied to other neurological diseases, and while its application to some e.g. Dystonia has been very successful, application to other diseases like Alzheimer's has produced mixed results. Information regarding the mechanisms of action of DBS will not only speed-up its application as a therapy to other neurological diseases, but also result in an optimization of the commercial DBS devices as well.

## 1.2 Aims

In the last three decades, since the first DBS surgery, significant technical advancements have been made in the field of medicine. Clinical engineers and researchers working in the field of DBS have observed that DBS has not kept up with these developments as the fundamental procedure remains the same. This doctoral work attempts to resolve some practical drawbacks by introducing modern techniques to the surgical procedure of DBS lead implantation and to use the data collected to answer theoretical questions pertaining to DBS therapy in general. This thesis aims to:

**Improve intraoperative symptom evaluation** Current methods to evaluate tremor and rigidity during the surgery are adapted from the routine clinical methods which were not designed for intraoperative use. The first goal of this thesis is to develop a method using an acceleration sensor to quantitatively evaluate the changes in tremor and rigidity during intraoperative stimulation tests to overcome the limits of the current methods.

**Improve target selection** The current target structures for DBS lead implantation have been adapted from lesioning surgeries, and researchers are in search of more efficient and alternative targets. Another goal of this thesis is to compare the efficiency of different anatomical structures stimulated during the surgery using the results of the quantitative symptom evaluation data.

**Improve lead placement** The final implant position for the DBS lead is chosen based on the results of intraoperative stimulation tests that are noted using pen and paper. These results are mentally visualized by the individual member of the surgical team and discussed to make the choice. This thesis aims to assist the surgical team in the decision making process by visualizing the results of the intraoperative stimulation tests on the

patient's images and other relevant data.

**Further the understanding of mechanisms of action of DBS** The mechanisms by which DBS alleviates patient's symptoms are not fully known. Various hypotheses have been proposed, but none of them are able to explain all the effects of DBS. All the data collected during this thesis will also be analysed with the aim to obtain more information about the effect caused by stimulation of different anatomical structures.

### 1.3 Outline

The contents of the thesis are divided into *9 chapters* which also include the published peer-reviewed articles. The current chapter provides a basic introduction to this thesis. **Chapter 2** contains necessary background information about the anatomy and physiology of the human motor circuit, PD, ET and DBS. This section also provides details about the different shortcomings of DBS that this doctoral work attempts to overcome. **Chapter 3** contains details about the equipment used to record tremor and rigidity movement data and the clinical studies conducted to collect data from DBS surgeries. **Chapter 4** describes the method developed for quantitative tremor evaluation during DBS and the results obtained by applying it in 15 surgeries. This is followed by the description of method to evaluate rigidity during surgery using an acceleration sensor and its application for 9 patients in **Chapter 5**.

**Chapter 6** introduces the "classical" approach to compare the therapeutic effect of stimulation in different anatomical structures, i.e. based on the position of the stimulating contact with respect to these structures. The application of this method to 5 ET patients and the results are also described in this chapter. **Chapter 7** describes the limitations of using the classical approach and introduces a method to overcome them by estimating the spatial effects stimulation using patient-specific simulations. This is followed by the details of the application of this method to the same Electric Field (EF) patients and the consequent results.

**Chapter 8** describes the various data that is collected for one DBS surgery and introduces a new data visualization method called improvement maps developed to improve lead placement. The details of the method and its application to 5 patients are also included in the chapter. **Chapter 9** summarizes the main results of this doctoral work with respect to the aims set forth in the section above. This is followed by further discussion of the results in the context of current DBS practice as well as the main advantages and the limitations of each of the methods. It also contains details about the immediate follow-up tasks as well as the long term projections of this doctoral work. **Chapter 10** concludes this thesis.

## Chapter 2

# Background

### 2.1 Basal ganglia and motor circuit

Human motor control is regulated through various structures in the brain including parts of the cortex, thalamus, basal ganglia and the cerebellum.

#### 2.1.1 Motor Cortex

There are three areas in the frontal lobe of the cortex which are associated with motor function (**Figure 2.1**). The Primary Motor Cortex (PMC) is in the dorsal region of the frontal lobe, just anterior to the central sulcus. Its histological composition is similar to other parts of cortex apart from the distinctively giant pyramidal neurons called Betz cells.<sup>27</sup> It has well defined somatotopy i.e. point-for-point correspondence of specific area of the structure to an area of the body. The Premotor Cortex (preMC) and the Supplementary Motor Area (SMA) are located anteriorly to the PMC but are structurally different as the Betz cells are less common and smaller. Their somatotopical organization is not as well defined as that of the PMC. These three areas directly innervate the synapse in the brain stem for control of the head and face movements and in the spinal cord for the rest of the body. They are also connected to other cortical areas, basal ganglia nuclei, thalamus, red nucleus and cerebellum.

The different areas of the motor cortex are responsible for different aspects of motor physiology. Signals of the PMC encode movement related information like the force, speed, direction and extent. The preMC is associated with preparation of a movement based on the sensory and behavioural information. The SMA is associated with relating a movement to spatial dimensions acquired from sensory organs, bilateral and mental exercise of movements. All the three areas in conjunction with other sensory parts of the brain plan and execute movements of the human body.

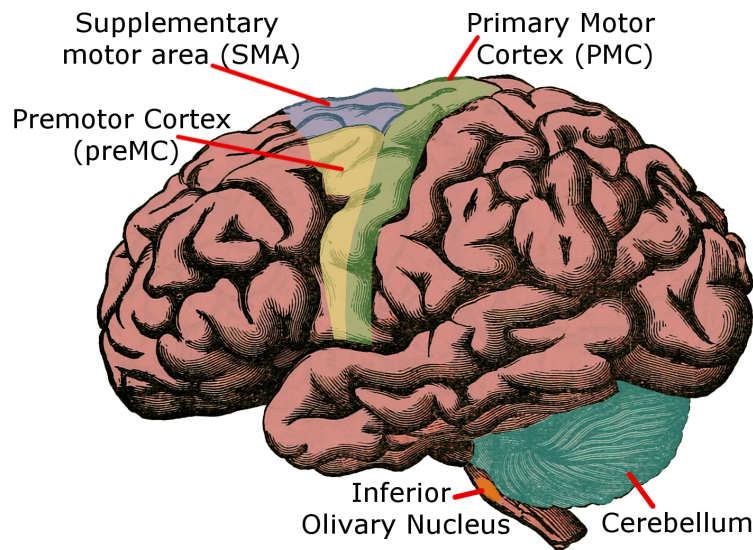


**Figure 2.1:** Approximate locations of the different areas of the motor cortex and the cerebellum in humans.

### 2.1.2 Cerebellum and Inferior Olivary Nucleus

The cerebellum (**Figure 2.1**) is a part of the metencephalon located below the cerebral hemispheres behind the fourth ventricle, pons and medulla. It is mostly built up of neurons and contains 3.6 times the number of neurons in the neocortex.<sup>145</sup> It receives inputs from motor and sensory part of the brain as well as the spinal cord through the inferior olivary nucleus. As a part of the motor circuit, it helps in coordination and timing of the movements but does not initiate any movements by itself.<sup>110</sup> Apart from its clearly established role in motor function, the cerebellum has also been associated with cognitive functions like attention and language.<sup>287</sup>

The inferior olivary nucleus is located in the medulla oblongata in the brain-stem, anterior to the cerebellum (**Figure 2.1**). Distinct fibers from the inferior olivary nucleus called "climbing fibers" form a major input to the neurons of the cerebellum. One neuron is innervated with only one climbing fiber, but it makes contact on multiple sites by wrapping around the dendrite.<sup>225</sup> The inferior olivary nucleus is believed to act as a filter in providing sensory information to the cerebellum.<sup>69</sup> It has also been shown to play a role in learning and coordinating movements along with the cerebellum.<sup>313</sup>

### 2.1.3 Thalamus

The thalamus is located at the center of a brain hemisphere in the forebrain and is the largest part of the diencephalon. It is made up of a group of gray

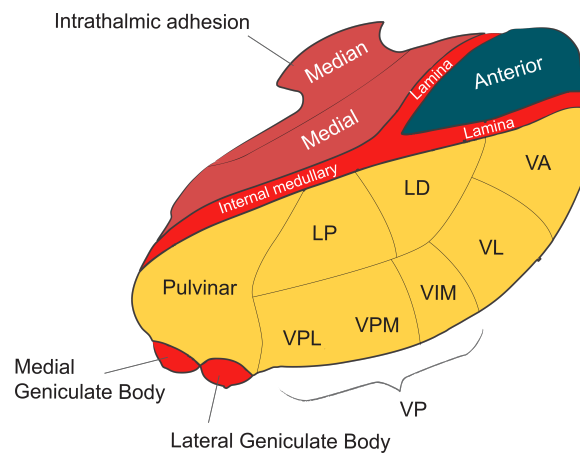


**Figure 2.2:** The thalamus and its nuclei represented in three regions: anterior, medial and lateral (yellow). LP: Lateral posterior nucleus; LD: Lateral dorsal nucleus; VA: Ventral anterior nucleus; VL: Ventral lateral nucleus; VP: Ventral posterior nucleus VIM:Ventral intermediate nucleus; VPM: Ventral posteromedial nucleus; VPL: Ventral posterolateral nucleus. Modified from Wikimedia (Madhero88 <https://commons.wikimedia.org/wiki/File:Thalamus.png>, "Thalamus", VI renamed to VIM, without legend) under the CC BY-SA 3.0 license (<https://creativecommons.org/licenses/by-sa/3.0/legalcode>)

matter nuclei which can be separated using a longitudinal thin sheet of white matter called internal medullary lamina (**Figure 2.2**). The thalamus has connections to most of the cerebral cortex, some basal ganglia nuclei, cerebellum, spinal cord and various other nuclei in the brain.<sup>108</sup> Most of the connections are bidirectional while some are unidirectional. Physiologically, the thalamus is believed to act as a relay station responsible for transferring information from other parts of the brain to the cortex.<sup>149</sup> The ventral lateral (VL) thalamic nucleus receives input signals from the basal ganglia and cerebellum and has bidirectional connections to all the three motor areas of the cortex. The ventral anterior (VA) thalamic nuclei also receives input signals from the basal ganglia and has bidirectional communication with the preMC. Through these connections (**Figure 2.3**), the thalamus provides feedback for motor control and may also be involved in planning and initiating movements.<sup>34</sup>

#### 2.1.4 Basal Ganglia

The substantia nigra (pars compacta: SNc and pars reticulata: SNr), along with the striatum (caudate nucleus, putamen, nucleus accumbens), the STN, the globus pallidus (internal: GPi and external: GPe) and the ventral pallidum, collectively form the Basal Ganglia (BG) (**Figure 2.4**). The BG were traditionally thought to be involved only in the motor functions of the brain, but recent research has shown that they are involved in various functions like attention,

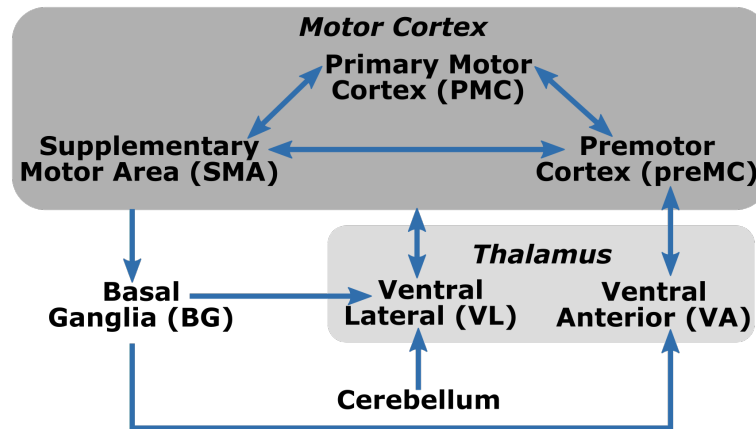


**Figure 2.3:** A diagrammatic representation of the connections between the different structures involved in the motor function. Arrow heads indicate signal direction.

learning, habit formation, etc.<sup>148,314,315,374</sup> Along with the thalamus and the cortex, the BG form 3 segregated circuits for motor, associative and limbic functions.<sup>4,249</sup> Striatum and STN are the input nuclei of BG while GPi and SNr are the output nuclei projecting into the thalamus.

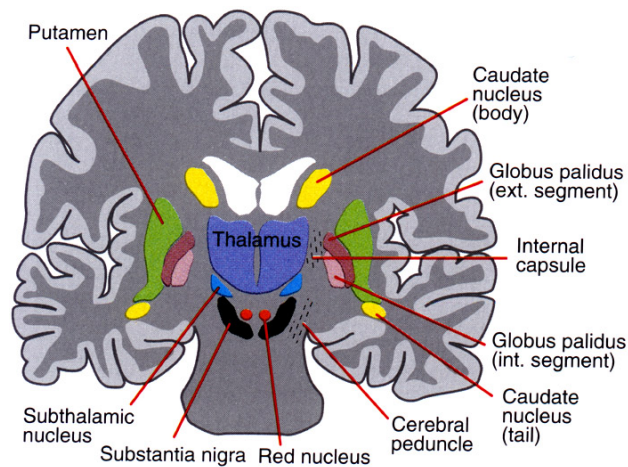


**Figure 2.4:** Anatomical location of the basal ganglia nuclei along with other deep brain structures. Reproduced from Leisman et al.<sup>185</sup> under the CC BY 3.0 license (<https://creativecommons.org/licenses/by/3.0/>).

There are two pathways in BG between the input and the output nuclei<sup>62</sup> (**Figure 2.5a**):

- i) the *direct pathway* in which the striatal neurons project directly into the GPi and

- ii) the *indirect pathway* where striatal signal passes through GPe and STN to reach GPi and SNr.

The direct and indirect pathways have opposing effects on movements (via the thalamus). The stimulation of direct pathway reduces inhibitory output of the GPi to the thalamus and facilitates movement. The indirect pathway, on the other hand, increases GPi/SNr activity inhibiting the thalamocortical system and reducing movement. Neurons of both the pathways have dopamine receptors, but of different kinds. The receptors on the direct pathway are of D1 type which facilitate the activation of the pathway in presence of dopamine and the receptors on the indirect pathway are of D2 type which inhibit the activation of the pathway in presence of dopamine<sup>109</sup> (**Figure 2.5b**). In addition to these two pathways within the BG, the direct input from cortex to the STN forms the hyperdirect pathway<sup>245</sup> (**Figure 2.5a**). While its existence has been acknowledged for some time, its anatomical organization and functional role in BG physiology including motor control is not completely known.<sup>224</sup>

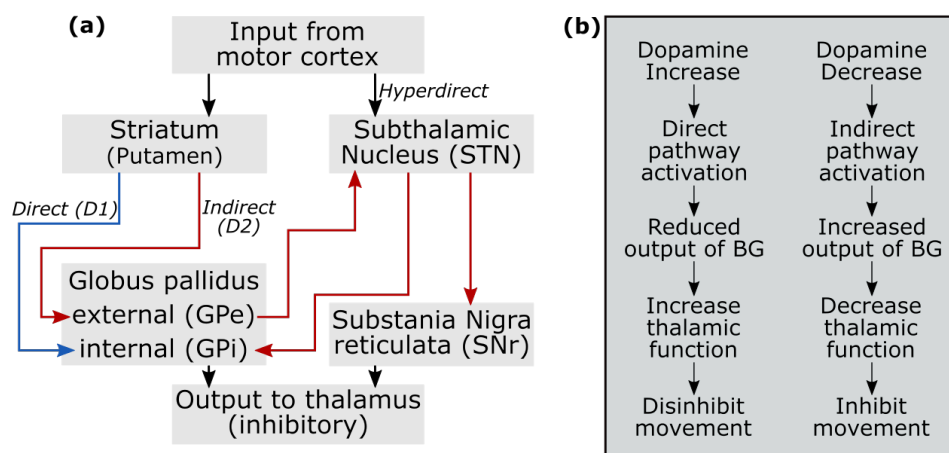


**Figure 2.5:** (a) The three pathways playing a role in motor function: direct (blue), indirect (red) and hyperdirect. (b) The influence of dopamine on the motor function through the thalamus.

## 2.2 Parkinson's Disease (PD)

Parkinson's Disease (PD) is one of the *most common neurodegenerative movement disorders*.<sup>276</sup> Some well-known people like Michael J. Fox and Davis Phinney who have been diagnosed with PD have used their image to create significant public awareness and support for research in PD through their foundations. Description of PD like symptoms can be found in various texts since biblical times. In 1817, James Parkinson published his essay titled "An essay on the Shaking Palsy" where he describes 6 patients having PD symptoms (**Figure**



**Figure 2.6:** The early sketch of a Parkinson's patient by Sir William Richard Gowers. Public domain image reproduced from Wikimedia Commons<sup>369</sup>

**2.6)** and how their disease progressed with age.<sup>265</sup> The French Neurologist Jean-Martin Charcot, known as the father of modern neurology, was the first to term the disease as "la maladie de Parkinson" (Parkinson's disease) because he noted that tremor is not always present in human PD.<sup>293</sup> A significant contribution that he made towards PD was distinguishing between rigidity, weakness and bradykinesia.<sup>184</sup>

Based on literature published in *PD epidemiology*, there are approximately 7 million people in the world suffering from PD.<sup>16</sup> The prevalence (proportion of a population at any given time) for PD is about 0.3% across ages, increases to 1% for people over 60 and to 4% for population over 80.<sup>348</sup> The median age of onset of the disease is 60 years and the mean duration of the disease (from diagnosis to death) is 15 years.<sup>182</sup> About 5-10% of PD cases are classified as young onset PD where the age of diagnosis is between 20 to 50 years.<sup>304</sup> Studies show men have higher chances of PD and at slightly younger (average) age compared to women.<sup>182</sup> The number of PD patients in Switzerland is estimated to be about 18,000.<sup>217</sup> Additionally, studies estimate that the incidence (number of new cases per year) of PD is between 8 and 18 per 100,000 person-years.<sup>348</sup> Economic burden of PD varies from country to country e.g. \$23 billion in USA in 2010<sup>332</sup> and about £449 million in UK in 2006,<sup>97</sup> but researchers agree that the cost of PD increases significantly as the disease progresses,<sup>175</sup> mostly because of increasing cost of institutional care.<sup>295</sup> With increasing quality of life and life expectancy, the PD related costs are expected to increase in the future.

In most PD patients, there is no external identifiable cause of the disease and such PD is termed as *primary or idiopathic*. Research has identified several risk factors like pesticides, dairy products, alcohol etc. and some protective factors like tobacco, caffeine, exercise etc. associated with PD. Ascherio et al.<sup>9</sup> describes the various risk and protective factors of PD and studies their effect on the epidemiology of PD. A small percentage of PD cases have been associated to genetic factors and are classified as *familial or hereditary PD*. In recent years, researchers have identified several genes whose mutations have been associated to PD which has led them to believe that all forms of PD are caused by a variable combination of environmental and genetic factors.<sup>327</sup> Of the different genes associated with PD, mutations in alpha-synuclein ( $\alpha$ -Syn, SCNA<sup>274</sup>) and leucine-rich repeat kinase 2 (LRRK2<sup>381</sup>) cause autosomal-dominant form of PD while mutations in PRKN (parkin, PARK2), PINK1 (PARK6), and DJ-1 (PARK7), cause autosomal-recessive forms of PD.<sup>190</sup>

PD is diagnosed based on the symptoms observed in the patients.<sup>340</sup> The *diagnostic criteria* for PD have been changed over the years based on various research studies. At present, the UK brain bank criteria<sup>156</sup> are the most commonly used. The Movement disorder's society has revised these criteria once in 2003<sup>115</sup> and very recently in 2016.<sup>113</sup> Based on the latest revision, the diagnosis of PD is still centered on the motor symptoms viz. bradykinesia (slowness of movement) and akinesia/hypokinesia (decreased movement amplitude), rigidity and rest tremor.<sup>277</sup> Elaborate details about tremor and rigidity are provided below due to their relevance to this doctoral work. In addition, certain "absolute exclusion" criteria are also defined like medical history of diseases known to cause PD secondarily (Alzheimer's disease). Studies show that accuracy of diagnosis (confirmation only through autopsy) is 75-90% depending on the duration of the disease and experience of the clinician.<sup>254</sup> PD patients also exhibit other motor symptoms like gait and postural instability and speech disturbances. In addition, various non-motor symptoms like sleep disturbances,<sup>229</sup> autonomic and sensory dysfunction<sup>165</sup> are also observed, some of which may be present before the diagnosis of the disease.<sup>310</sup>

### **Tremor**

Tremor is defined as the rhythmic oscillation of a body part.<sup>202</sup> Tremor is observed in 80%<sup>340</sup> of the PD patients. The following characteristics of PD tremor help clinicians to distinguish it from other types of tremor:<sup>5</sup>

- Tremor onset is unilateral, but with disease progression can become bilateral.
- Most patients present with upper limb tremor.
- PD patients have rest tremor which is attenuated by voluntary movement.

- It is often called pill-rolling because the thumb and the index finger tend to get into contact and perform circular movement.<sup>159</sup>
- Tremor has a tendency to increase with cognitive tasks or walking.
- The amplitude of tremor is moderate at onset and tends to increase with time.
- The age of onset for PD tremor is mostly after 60.
- Frequency of tremor is between 3-4 Hz which is lower compared to other types.
- Idiopathic PD patients tend to be more tremulous than other parkinsonian conditions.

### **Rigidity**

Rigidity is defined as resistance to passive movement caused by an involuntary increase in muscle tone and can affect all muscle groups.<sup>355</sup> PD patients describe rigidity as muscle stiffness or sometimes pain. The severity of rigidity is evaluated passively by repeated flexion and extension of the respective muscle about the corresponding joint. Based on the resistance observed by the clinicians, rigidity is described as either "lead-pipe" (smooth; constant resistance) or "cog-wheel" (jerky; potentially because of tremor).<sup>355</sup> Rigidity of a limb increases when patients are asked to perform movements on the contralateral limb (Froment's maneuver<sup>100</sup>). To distinguish between the two types, they are termed as "rest rigidity" and "activated rigidity."<sup>365</sup>

### **2.2.1 PD Rating Scales**

The symptoms of PD worsen with the progression as it is a neurodegenerative disease. To study the progression of the disease in general and in each patient individually, clinical scales that assign numbers to the severity of the symptoms are necessary. Currently, there are two rating scales that are widely used in clinical practice: i) Unified Parkinson's Disease Rating Scale (UPDRS)<sup>89</sup> and ii) Hoehn and Yahr Stage Scale.<sup>152</sup>

#### **Unified Parkinson's Disease Rating Scale (UPDRS)**

The UPDRS is the most widely used clinical rating scale for PD and is the international gold standard.<sup>162</sup> It was proposed in 1995 as a collaborative effort to provide an efficient and comprehensive scale to evaluate PD and related disorders.<sup>89</sup> The scale consists of 4 parts:<sup>115</sup>

**Part I Mentation, Behaviour and Mood** has 4 items to evaluate the mental dysfunction and mood of the patient.

**Part II Activities of Daily Living** has 13 items related to the disability that patients face in daily tasks due to the motor symptoms

**Part III Motor** has 14 items to evaluate the severity of the motor symptoms. Some items are divided further to evaluate the severity of each limb (**Figure 2.7 and 2.8**).

**Part IV Complications** is to be used to assess any motor or non-motor complications that arise due to medication.

Each item of the scale is rated between 0 (normal) and 4 (severe). Some items in the scale are rated by interviewing the patient while others are rated by examining the symptoms. The ratings of each part are summed to estimate the severity and to evaluate the progression of the disease with time (longitudinal evaluation). The average time taken by clinicians to administer the full UPDRS test is between 10 and 20 minutes.<sup>223</sup> The wide usage of UPDRS can be attributed to the availability of a *teaching tape*.<sup>116</sup> This tape provides examples of rating the motor symptoms of PD patients by a panel of 3 movement disorder specialists having extensive experience of using the scale. It also includes some UPDRS motor examinations that trainees can self-administer and compare the results with that of the panel.

UPDRS has also been extensively tested from a clinimetric point of view due to its wide usage. It is the most used scale in various clinical research studies and is relied upon by the US and European<sup>87</sup> regulatory agencies. Various studies have found that the UPDRS as a whole has good intra-rater (reproducibility of the same evaluators rating on different occasions/test-retest) and inter-rater (reproducibility of ratings by multiple evaluators of the same patient) reliability. However, Post et al<sup>275</sup> showed that the ratings *depend* heavily on the *experience of the evaluator*. Other studies have shown that some items of the motor part including speech, facial expression, posture, body bradykinesia, action tremor and rigidity have comparatively lower inter-rater reliability.<sup>223,278,289</sup> Other shortcomings of UPDRS include redundancy of items in Part II and Part III,<sup>223</sup> inconsistencies in item allocation<sup>115</sup> and cultural bias in Part II.<sup>113</sup>

The Movement Disorder Society (MDS) sponsored a think-tank to evaluate the limitations of UPDRS and propose the necessary steps to overcome them.<sup>117</sup> This revised version of the UPDRS known as *MDS-UPDRS* was proposed in 2008. It retains the number of parts and the 5-point rating system of the original UPDRS but the titles, items and their number for each parts have been altered. Part I has 13 items related to the non-motor experiences of daily living, Part II has 13 items related to the motor experiences of daily living, Part III has 18 items, some with sub-items, related to motor symptoms evaluation and Part IV has 6 items to describe complications arising due to medication. The time taken to administer the test is about 30 minutes. Compared to UPDRS, the MDS-UPDRS emphasized the non-motor components of PD, increased emphasis on

<b>Tremor At Rest</b>	<b>Severity</b>				
<b>Body Part</b>	0	1	2	3	4
Face	<input type="radio"/>				
Right Upper Extremity	<input type="radio"/>				
Left Upper Extremity	<input type="radio"/>				
Right Lower Extremity	<input type="radio"/>				
Left Lower Extremity	<input type="radio"/>				
Guidelines: 0 = Absent. 1 = Slight and infrequently present 2 = Mild in amplitude and persistent. Or moderate in amplitude, but only intermittently present. 3 = Moderate in amplitude and present most of the time. 4 = Marked in amplitude and present most of the time.					
<b>Action or Postural Tremor of hands</b>	<b>Severity</b>				
<b>Body Part</b>	0	1	2	3	4
Right Upper Extremity	<input type="radio"/>				
Left Upper Extremity	<input type="radio"/>				
Guidelines: 0 = Absent. 1 = Slight, present with action. 2 = Moderate in amplitude with action. 3 = Moderate in amplitude with posture holding as well as action. 4 = Marked, interferes with feeding.					

**Figure 2.7:** The figure shows the questions in UPDRS related to evaluation of tremor.

Rigidity	Severity				
Body Part	0	1	2	3	4
Neck	○	○	○	○	○
Right Upper Extremity	○	○	○	○	○
Left Upper Extremity	○	○	○	○	○
Right Lower Extremity	○	○	○	○	○
Left Lower Extremity	○	○	○	○	○
Guidelines: Judged on passive movement of major joints with patient relaxed in sitting position. Cogwheeling to be ignored. 0 = Absent. 1 = Slight or detectable only when activated by mirror or other movements. 2 = Mild to moderate. 3 = Marked, but full range of motion easily achieved. 4 = Severe, range of motion achieved with difficulty.					

**Figure 2.8:** The figure shows the questions in UPDRS related to evaluation of rigidity.

mild impairments and disabilities, increased cultural sensitivity,<sup>113</sup> improved the wordings of the different items, and resolved other ambiguities. The MDS also provides a teaching-tape which can be used to train clinicians in rating PD patients using the scale to increase reliability.

### Hoehn and Yahr Stage Scale

The Hoehn and Yahr Stage scale for PD was proposed in 1967 by Melvin Yahr and Margaret Hoehn.<sup>152</sup> It combines functional deficits (disability) and objective signs (impairment) in a descriptive form to estimate PD severity. It was originally designed as a five point scale (0-5), to which 0.5 increments were added in 1990 for some clinical trials.<sup>161</sup> The scale describes *PD symptoms in five stages* i.e. from unilateral (Stage 1) to bilateral (Stage 2), followed by presence of postural instability (Stage 3), loss of independence (Stage 4) and being wheelchair- or bed-bound (Stage 5). This scale was used to report the longitudinal effects of drugs on PD patients in various clinical studies between 1967 and 1998. In 2004, MDS also set up a task force to evaluate the Hoehn and Yahr scale.<sup>114</sup> They reported that the simplicity of the scale allows it to be used even by non-clinical people. However, they also point to the issues of the scale like neglect of upper limb disability, lack of assessment of some motor and non-motor impairments (tremor, depression), absence of teaching tape, etc.

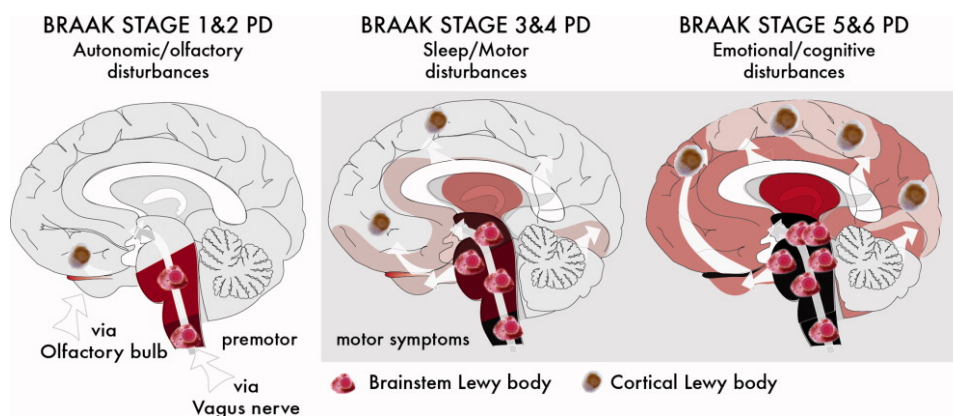


**Figure 2.9:** The Braak stages in different areas of the brain. Reproduced with permission from Halliday et al.<sup>130</sup>

## 2.2.2 Pathology

Besides being classified as a movement disorder, PD is also a neurodegenerative disease because of pathology. The symptoms of the patient worsen with increasing duration of the disease due to progressive and selective death of neurons in different parts of the brain. A pathological indication of PD is the presence of Lewy bodies (insoluble proteinaceous structures) in the neurons that survived until post-mortem.<sup>254</sup> Brack et al.<sup>35</sup> studied 168 brains obtained at autopsy (41 with clinical PD diagnosis, 69 without PD diagnosis and 58 age-matched controls) and proposed that the neuronal damage follows a specific sequence (Brack Staging, **Figure 2.9**) starting from motor nuclei in brain stem and the anterior olfactory nucleus (Stages 1 and 2) moving upwards to substantia nigra (Stage 3), mesocortex (Stage 4), neocortex (Stage 5) and terminating in premotor areas (Stage 6). However, the deposition of Lewy bodies does not correlate with neuronal cell loss and in turn with the progressing clinical severity of PD.<sup>163</sup> Traditionally, it was believed that the accumulation of Lewy bodies results in neuronal death, but, further research has led to a growing consensus that mechanisms taking place inside as well as originating from outside the neuron result in their death.<sup>151</sup> Researchers have proposed other hypotheses like mitochondrial dysfunction,<sup>309</sup> neuroinflammation,<sup>279</sup> etc. for the neuronal cell death in PD, but a complete explanation is yet to be established. Further discussion about the histo-pathology of PD will deviate from the topic of this thesis as its relevance is limited. On the other hand, a detailed introduction to the pathophysiology of PD is necessary for discussing the mechanisms of action of DBS.

### Pathophysiology

Neuronal degeneration in different areas of the brain causes different symptoms of PD. Studies have shown that

- i) degeneration of dopaminergic neurons in the pars compacta of substantia nigra results in the cardinal symptoms (bradykinesia/akinesia, rigidity and tremor) of PD<sup>142,293</sup>
- ii) degeneration of cholinergic neurons in nucleus basalis is associated to cognitive dysfunction and hallucinations<sup>19</sup>
- iii) gait disturbances may be a result of damage in pedunculopontine nucleus (PPN).<sup>258</sup>

Pathophysiology resulting due to the death of non-dopaminergic neurons is not well-understood due to lack of an animal model while the effects of dopaminergic degeneration can be modeled in animals using toxins like 1-methyl-4-phenyl-1, 2, 3,6-tetrahydropyridine (MPTP<sup>180</sup>), or 6-hydroxydopamine (6-OHDA<sup>350</sup>). Therefore, studies of pathophysiology of PD have vastly concentrated on the effects caused by degeneration of dopaminergic neurons.

Over the years, various models have been suggested for the pathophysiology of PD. The earliest model<sup>3,161</sup> (also referred to as *classical* or *rate model*) suggests that the depletion of dopamine in the brain has a two-fold effect on BG: reduced activation of the direct pathway resulting in lower movement initiation and disinhibition of the indirect pathway resulting in higher opposition to movement (**Figure 2.10**). Proof of this model can be obtained from animal and patient studies of effects of STN or GPi inactivation.<sup>6,15,18,24,129,178,358</sup> Despite the appeal of this model due to its simplicity, it only serves as a starting point because it provides no explanation for some motor and non-motor symptoms.

Electrophysiological studies have revealed *abnormalities in the firing activity of neurons* in PD patients and animals. The most notable pattern is the increase of burst discharges in extrastriatal BG<sup>25,36,368</sup> and thalamus.<sup>126,236,268</sup> Another observed pattern is abnormal oscillations in alpha and beta frequency ranges in the GPe, GPi and STN.<sup>107,192,293</sup> Graybiel<sup>120</sup> suggests that in a normal functioning BG, the subcircuits do not have any correlation in their firing patterns and activities. Hammond<sup>134</sup> revealed that, due to depletion of dopamine, cross connections are developed in the subcircuits of BG causing unwanted synchronization in their firing activity. Other researchers have used Positron Emission Tomography (PET) and Functional Magnetic Resonance Imaging (fMRI) to show that parts of BG that are normally used in only one subcircuit are also active during activities of other subcircuits in PD patients.<sup>172,215</sup>

Abnormal synchronization and oscillations are not just limited to BG in PD patients. Such patterns are also found in recordings of the cortex and the tha-

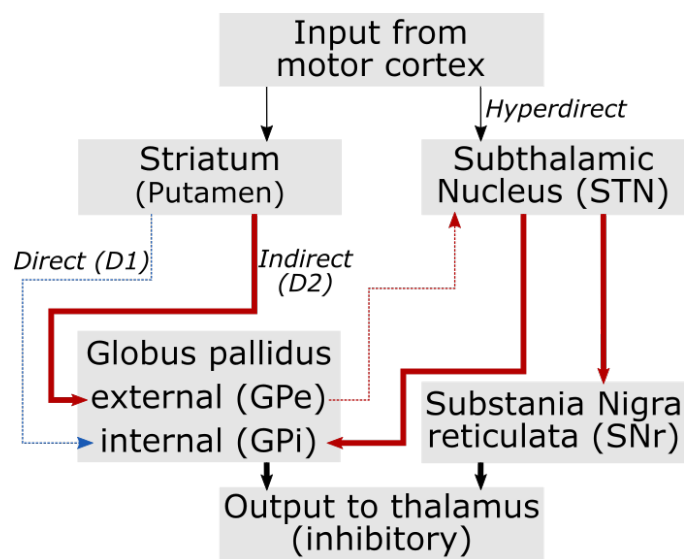


**Figure 2.10:** The influence of loss of dopamine in the basal ganglia on the circuits with respect to motor function. Activation of the direct pathway is reduced (indicated by dashed line) while that of the indirect pathway is increased (indicated by thick solid line). For comparison with normal circuit functions check Figure 2.5.

lamus.<sup>38, 39, 118, 325, 361</sup> Helmich<sup>142</sup> proposed a "dimmer-switch model" saying that tremor in PD is a resultant of combined actions from the BG and the cerebello-thalamo-cortical circuit. In addition, researchers have also shown that lesions in the Pedunculopontine Nucleus (PPN) in the brainstem of monkeys produce akinesia<sup>173, 246</sup> suggesting its involvement in PD. Studies of blood flow and metabolism in the motor cortex report differences in PD patients compared to healthy subjects during movements: increased activity in the PMC has been repeatedly shown<sup>138, 299, 377</sup> whereas reports of activity in the preMC<sup>138, 299</sup> and SMA<sup>272, 377</sup> show different results. Studies have also shown impaired motor learning ability in PD patients<sup>78, 98</sup> which agrees with the understanding that dopamine in motor cortex facilitates motor learning skills. Others have shown that the well-defined somatotopy of the motor cortex is blurred in PD<sup>96</sup> and restored through treatment<sup>37, 354</sup> indicating it to be essential for alleviating PD symptoms. Nevertheless, it is still unclear if abnormal cortical activities are due to dopamine depletion in the BG only or also because of dopamine depletion in the cortex itself.<sup>193</sup> Further research is necessary to completely understand changes in the brain of PD patients to develop a comprehensive model of pathophysiology of PD.

### 2.2.3 Treatments

A cure for PD does not exist and so current treatments of PD aim to maintain independence of patients as long as possible by treating the motor and

non-motor symptoms (symptomatic treatments). Treatments have to be individualized for each patient based on the symptoms and their severity, patient's response to medication and other conditions. The dopamine depletion cannot be treated directly with dopamine based drugs because it cannot cross the blood brain barrier. However, its precursor, levodopa (L-Dopa) can. Since Cotzias<sup>55, 88</sup> showed levodopa's capability to treat PD, it has been the most effective oral treatment. To prevent peripheral breakdown of levodopa, it is administered with dopadecarboxylase inhibitors (carbidopa or benserazide), allowing upto 4 fold reduction in levodopa dosage for the same effect. In addition, patients are also given catechol-O-methyltransferase (COMT) inhibitors to completely suppress the peripheral breakdown of levodopa. For patients with tremor dominant Parkinson's disease, if the levodopa treatment does not suppress tremor, anticholinergic drugs are used in addition.

High doses of levodopa are known to induce dyskinesias. With the worsening of symptoms, the therapeutic benefit of higher doses of levodopa are surpassed by the adverse effects. PD patients may be treated with dopamine agonists or other drugs in the early stages of the disease to delay the use of levodopa and in-turn levodopa induced dyskinesias. For patients with advanced PD, complimentary treatments are used to reduce the levodopa dosage while still retaining similar therapeutic effect. Continuous subcutaneous apomorphine infusion is one such therapy where apomorphine is delivered via a pump through a catheter with a subcutaneous needle in the abdominal wall or thigh. Symptoms that respond to levodopa improve allowing for a typical reduction in levodopa dosage of 50%. Another option is to administer levodopa in gel form (duodopa) by a tube placed in the jejunum allowing similar reductions in oral levodopa.

Before levodopa was introduced, surgical ablation of parts of thalamus (thalamotomy) or sub-thalamic nucleus (subthalamotomy) or the pallidum (pallidotomy) were used to treat PD patients. Thalamotomy was the most preferred due to lower adverse effects compared to others. These procedures have been largely replaced by their electrical stimulation through a neurostimulator via surgically implanted electrodes collectively known as DBS (Section 2.4). Bilateral stimulation of the subthalamic nucleus is currently the most used treatment for advanced PD patients. Apart from reducing levodopa-responsive symptoms, it also reduces tremor. Lower number of adverse effects, adaptability to worsening disease and reversibility compared to thalamotomy makes it a very compelling choice for treating advanced PD patients.

## 2.3 Essential Tremor (ET)

Essential tremor (ET) is one of the most common neurological diseases and the most common form of pathological tremor.<sup>200</sup> An Italian professor of medicine, Pietro Buresi, was the first to use the term "essential tremor" in 1847 to

describe a 18 year old man with severe, isolated action tremor.<sup>44,205</sup> The traditional image of ET as a benign, monosymptomatic (action tremor) condition has changed significantly since then.<sup>82</sup> It is now considered to be a progressive neurological disease with action tremor as a primary symptom and other motor and non-motor symptoms often disabling for the patients.<sup>203</sup> The expression of the disease varies significantly among patients in terms of evolution and severity of the symptoms. In addition, postmortem studies have shown different structural changes in the brains of ET patients raising concerns that ET could be a family of diseases.<sup>23,199</sup>

Epidemiological studies of ET report significant variations in data because of variations in the definition of ET among other things. Prevalence of the disease across all ages has been reported at 1% which rises to 4-5% for patients above 40<sup>73</sup> and between 6-9% for population above 60.<sup>73,200</sup> Studies concur that the prevalence rises rapidly with age.<sup>73,200</sup> In population based studies the age of onset was found to be 60 years,<sup>206</sup> while that in studies based on tertiary referrals was found to peak at 20 years and 60 years.<sup>206</sup> The onset of clinical symptoms of ET in childhood have been frequently reported with studies estimating between 5 and 15% of ET cases occurring during childhood.<sup>206,288</sup> ET occurrence does not vary with gender, but ethnic variations have been reported.<sup>204,212</sup>

Research has shown that ET patients have first and second-degree relatives suffering from the disease, indicating that ET has genetic causes and autosomal-dominant inheritance pattern. Studies have linked ET and regions on chromosomes 2p,<sup>147</sup> 3q<sup>127</sup> and 6p,<sup>322</sup> but have not been successfully replicated.<sup>8,65,174,216</sup> ET genes are yet to be identified, but polymorphisms in certain genes like LINGO1,<sup>52,64,334,356</sup> dopamine receptor D3,<sup>64</sup> etc. have been linked to ET. On the other hand, in ET twin studies, concordance in monozygotic twins was found to be about 60%,<sup>197,345</sup> suggesting role of environmental causes in ET. Familial aggregation studies have reported that more than 50% of ET patients do not have affected first or second-degree relatives.<sup>71,209,303</sup> Several studies have identified  $\beta$ -carboline alkaloids (e.g. harmine) and lead as environmental factors in ET.<sup>72,198</sup> Ongoing research in the field of etiology of ET will provide more details in the future.

The diagnosis of ET is made by history and physical examination.<sup>210</sup> Three diagnostic clinical criteria have been proposed that are similar and focus mainly on the severity and characteristics of the kinetic tremor.<sup>67,81,211</sup> ET is one of the most commonly misdiagnosed neurological disease with 30-50% of ET patients having other diseases.<sup>157,311,312</sup> Family history of ET and tremor response to alcohol are supportive features for diagnosis of ET. It is important to distinguish ET from other tremor disorders like PD, enhanced physiological tremor, dystonic tremor, etc. by careful physical examination.<sup>210</sup> Caffeine, cigarettes and some medications can alter other tremor conditions to resemble ET which necessitates through investigation of patient's history. Certain laboratory evaluations like

thyroid function tests to eliminate signs of hyperthyroidism, serum ceruloplasmin level for Wilson's disease etc. are useful to ensure correct diagnosis of ET.<sup>210</sup>

**Action tremor** of the hands is the hallmark of ET. It has the following characteristics:

- It is symmetric or only mildly asymmetric.
- It is kinetic (occurs during guided voluntary movements) or postural (during a position against gravity).
- The frequency of tremor is between 4 and 12 Hz and is inversely related to age.
- It is most common in the arms, but head tremor is also observed in patients (higher tendency in women).
- Amplitude of kinetic tremor increases with age and patient with longer duration of disease may also present rest tremor.
- Tremor causes flexion extension of the wrists, and/or abduction movement of the fingers.

Recent studies have observed other motor symptoms like postural instability and ataxic gait in ET patients<sup>93,336</sup> Minor abnormalities in the eye movements have also been described.<sup>141</sup> Some non-motor symptoms have also been identified. Social phobia,<sup>329</sup> depressive symptoms,<sup>183</sup> anxiety,<sup>49</sup> etc. were noted in few studies. It is not uncommon that ET patients later develop PD,<sup>201</sup> and recent studies have shown increased risk of Alzheimer's type dementia.<sup>158</sup>

### 2.3.1 ET Rating Scales

Clinicians use different rating scales to evaluate patients and estimate the severity of the disease. In clinical literature, the *Fahn-Tolosa-Marin*<sup>90</sup> scale is the most widely used (**Figure 2.11**). The scale was designed to rate tremor due to any disease. It has 10 items to rate tremor in different body parts (part A), 5 items to rate tremor during movement (part B) and 8 items to evaluate activities of daily living (part C). Another scale designed specifically for ET is termed as *Tremor Research Group Essential Tremor Rating Assessment Scale (TETRAS)*.<sup>80</sup> Its motor part has 9 items to rate tremor severity in 9 levels from 0 to 4 (0.5 intervals) and its second part has 12 items to evaluate activities of daily living. A third rating scale specially developed for ET is called the *Washington Heights-Inwood Genetic Study of Essential Tremor (WHIGET)*<sup>211</sup> rating scale. It is used to examine the upper extremities during rest and some other specific activities with a rating from 0 to 3 or 0 to 4.

<b>Tremor Guidelines:</b>				
1) at REST (in repose.) For head and trunk, when lying down.				
2) with posture holding (upper extremities (UE): arms outstretched, wrists mildly extended, fingers spread apart; lower extremities (LE): legs flexed at hips and knees, foot dorsiflexed; tongue: when protruded; head and trunk: when sitting or standing)				
3) with Action and Intention (upper extremities: finger to nose and other actions; lower extremities: toe to finger in a flexed posture)				
NA = Not applicable				
0 = None				
1 = Slight (amplitude <0.5 cm). May be intermittent.				
2 = Moderate amplitude (0.5 - 1 cm). May be intermittent.				
3 = Marked amplitude (1 - 2 cm)				
4 = Severe amplitude (> 2 cm)				
<b>Body Part</b>	Rest	Posture	Act./Int.	Total
Face tremor			NA	
Tongue tremor			NA	
Voice tremor	NA	NA		
Head tremor			NA	
Right upper extremity tremor				
Left upper extremity tremor				
Trunk tremor			NA	
Right lower extremity tremor				
Left lower extremity tremor				

**Figure 2.11:** The first 9 questions of the Fahn-Tolosa-Marin Tremor rating scale that is widely used to evaluate ET patients.

### 2.3.2 Pathology

Unlike PD, the pathology of ET has not been extensively researched and many questions remain unanswered.<sup>207,213</sup> Some postmortem studies in ET patients have identified differences in Purkinjee cells when compared to control samples like reduction in number of cells, thickening of the cell axon, etc.<sup>207</sup> These differences, however, are only seen in some of the ET patients and were not observed in other postmortem studies.<sup>285</sup> Nonetheless, researchers suggest that cerebellar abnormalities may be secondary pathology of ET.<sup>323</sup> Researchers investigated the presence of Lewy bodies in ET patients and did not find an increase unless patients had additional parkinsonism symptoms. Louis et al<sup>208</sup> performed postmortem study of ET patients and did find an increase in Lewy bodies in locus ceruleus in ET patients who did not later develop PD. However, the frequency of these patients mimics that of the incidental Lewy body disease cases in large autopsy series. Rajput et al.<sup>283</sup> showed in their study that there may be other reasons for ET patients that may be developing PD. Another hypothesis that has recently been proposed is that alterations in the LINGO-1 gene may alter the synaptic density in the cerebellum resulting in synchronization of its activity creating tremor.<sup>68</sup>

### Pathophysiology

Tremor physiology has been the center point of all discussion about the mechanisms of the disease<sup>61</sup> in most of the disease's research history. With the support from animal model of action tremor using harmaline (neurotoxin), it was proposed that a disturbance in the routine oscillatory-pacemaking properties of the inferior olivary nucleus would be the main reason behind ET.<sup>176,221</sup> However, unlike animal models, cortico-muscular coherence studies indicated presence of several rather than one central pacemaker in ET.<sup>196,281</sup> In addition, PET studies did not show any involvement of the inferior olivary nucleus in ET<sup>370</sup> and postmortem studies did not show any structural changes.<sup>200</sup> Thus, although physiological studies proposed the involvement of inferior olivary nucleus, empirical proof was not available. On the other hand, clinical research studies of ET indicated the involvement of cerebellum in ET. Symptoms like abnormalities in gait and balance, oculomotor deficits, etc. which are related to the cerebellum have been reported in ET patients.<sup>155,169,263,286,336</sup> Studies have also reported that unilateral cerebellar stroke abruptly terminates ipsilateral arm tremor in ET patients.<sup>79,284</sup> In addition, neuroimaging studies including functional magnetic resonance imaging (fMRI,<sup>41,375</sup> PET,<sup>370</sup> DTI<sup>170</sup>) of ET patients suggest functional, metabolic and structural abnormalities in cerebellar gray and white matter. Research thus far suggests that ET is a neurodegenerative disorder which involves oscillatory activity in many parts of the motor circuit and pathological changes in the cerebellum for some patients. However, extensive research is necessary to identify the primary pathogenesis of ET.

### 2.3.3 Treatments

Like PD, clinicians aim to suppress the symptoms with various treatments as there is no cure. Alcohol is known to reduce tremor for a limited time and may be used by patients with mild tremors before social events, but not for long term treatment. First approach to treat ET is using pharmacological drugs propranolol and primidone. Propranolol is one of the best beta blockers and suppresses tremor by antagonism of peripheral beta adrenergic receptors. It is effective against limb tremor and is known to reduce tremor amplitude by 50%. Primidone is a GABA agonist and suppresses tremor by enhancing GABAergic tones in the central nervous system. Studies show that it reduces tremor by at least 50%. Many patients have a strong feeling of being unwell and some even stop using it for this reason. Other drugs like topiramate (sodium channel blocker) gabapentine (calcium channel blocker), etc. are also used to treat ET patients.

When ET patients do not respond to pharmacological treatments, clinicians may also consider surgical options. Thalamotomy, surgical destruction of part of the thalamus, is known to suppress tremor in ET patients. Thalamotomy has till date been performed using stereotactical procedures to target and ablate the tissue. Newer techniques that are being investigated like Gamma knife therapy and Magnetic Resonance Imaging (MRI)-guided focused ultrasound allow for non-invasive thalamotomy. Currently, the most used surgical treatment for ET patients is DBS (Section 2.4). Electrodes are implanted in the ventro-intermediate nucleus (VIM) of the thalamus and stimulated continuously via a neurostimulator. Stimulation parameters can be adapted to worsening symptoms and, if needed, electrodes can be removed if severe adverse effects are observed. Adaptability and reversibility of DBS are two of its advantages over thalamotomy that make it the preferred clinical choice.

## 2.4 Deep Brain Stimulation (DBS)

DBS is a surgical procedure in which electrodes are implanted in the deep-seated structures of the brain and stimulated using a neurostimulator implanted in the thoracic cavity or the pelvic region. It is approved by the Food and Drug Administration (FDA) to treat PD and ET patients who do not respond to medications or are having severe adverse effects due to high drug dosage. It is also approved by the FDA under humanitarian device exemption rules for treating dystonia and obsessive compulsive disorder.<sup>75</sup> Since it was first performed in 1987, more than 150000 patients have been treated with this procedure worldwide.<sup>301</sup> Research is being carried out to use DBS to treat diseases like Alzheimer's, depression, epilepsy and other neurological disorders, but the adoption has been slow.

The roots of DBS can be found in ablative surgeries that were performed to treat PD and ET patients before the availability of pharmaceutical drugs. The

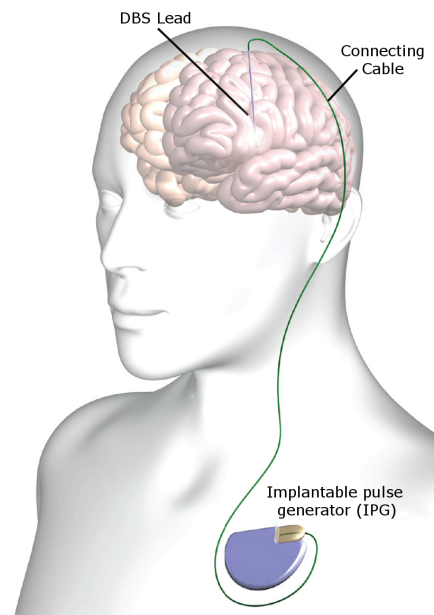


**Figure 2.12:** The components of a DBS system implanted in a patient. Adapted from Shamir et al.<sup>320</sup> under the CC BY license (<https://creativecommons.org/licenses/by/4.0/>).

ablative surgery of the thalamus (thalamotomy) was known to suppress motor symptoms of PD and ET. However, it was necessary to identify the exact location of ablation to avoid severe adverse effects to the patient. To do so, electrical stimulation in the thalamus allowed the clinicians to distinguish between the sensory and motor parts based on the response of stimulation. It was observed that high frequency electrical stimulation in the motor parts of the thalamus suppressed tremor. In 1991, Benabid et al.<sup>22</sup> published their study of 26 PD patients and 6 ET patients treated with chronic electrical stimulation in the thalamus and reported major improvement in PD and mild to major improvement in ET. This was followed by various clinical studies with similar promising results which began the steep rise of DBS surgeries since then.

From the hardware perspective, DBS consists of three components (**Figure 2.12**) that have to be implanted in the patient, DBS lead(s), connecting cables and the implantable pulse generator (IPG). The DBS leads (**Figure 2.13**) are flexible electrodes with variable number (4 or more) and type (non-directional and directional) of contacts on one end to deliver the stimulation in the desired target. The IPG has an inbuilt battery which makes it large and cannot be implanted in the skull region. It is therefore implanted in the thoracic (or pelvic) cavity and connected to the electrode via subcutaneous connecting cables. The stimulation parameters of the IPG are altered by an external programmer with wireless communication through the skin. Currently, DBS systems are manu-

factured by Medtronic, St Jude Medical (now Abbott) and Boston Scientific with variable regional availability.

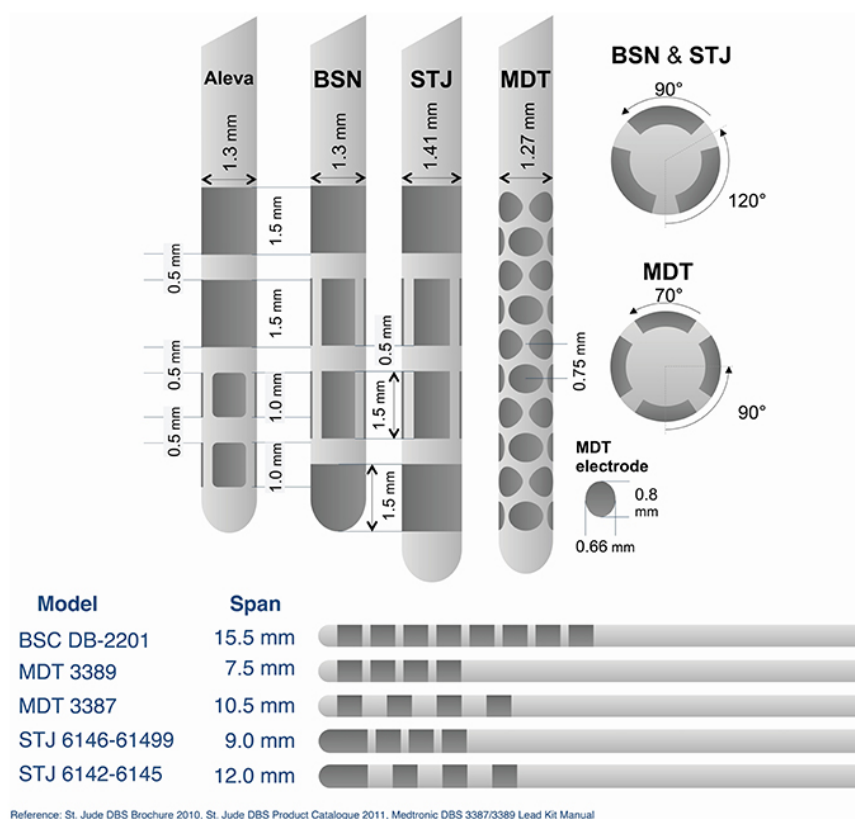


**Figure 2.13:** Commercially available DBS leads from various companies and their schematic. BSN: Boston Scientific, STJ: Saint Jude Medical (Now Abbott) and MDT: Medtronic. Reproduced with permission from Rossi et al.<sup>297</sup> under the CC BY license (<https://creativecommons.org/licenses/by/4.0/>).

The size of the electrode and the anatomical structures in which they are implanted is in the range of millimetres. Therefore, the optimal outcome of DBS depends heavily on the implant location of the electrode. Over the years, mostly through trial and error and through the results of ablative surgeries, different anatomical structures in the basal ganglia have been identified as regions of interest for DBS for different diseases. For example, stimulation in the STN is highly effective in reducing PD symptoms, while the stimulation of VIM in the thalamus has been used to treat ET patients. The commercially available DBS leads have a minimum of 4 contacts resulting in a tolerance in the infero-superior direction. However, no tolerance is available in the antero-posterior and latero-medial directions which makes lead implantation in the right region a complex task.

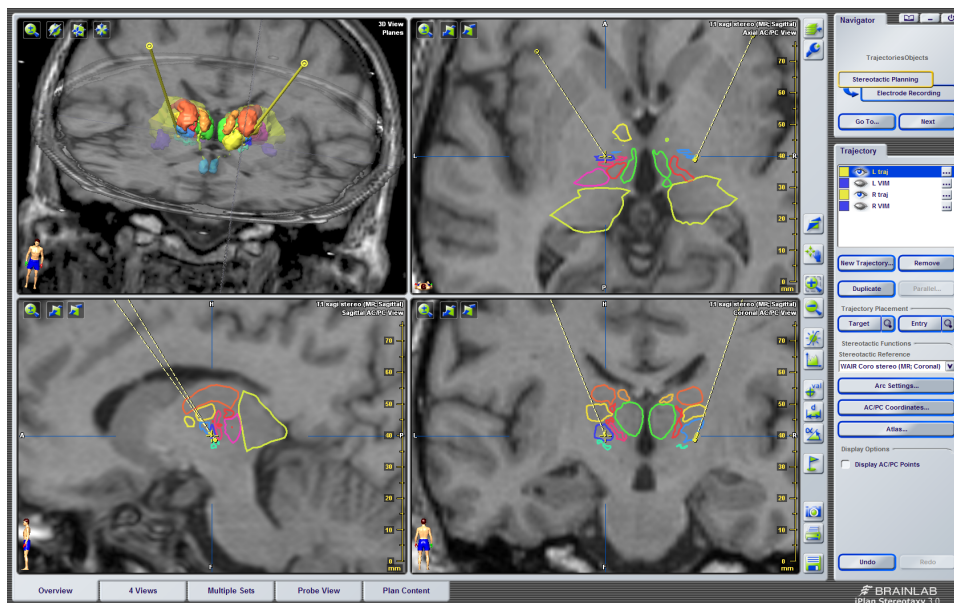


**Figure 2.14:** The iPlan Stereotaxy 3.0<sup>®</sup> from Brainlab, Munich, Germany is one of the many surgical planning software available for DBS. Figure shows the planning of patient operated in Centre Hospitalier Universitaire (CHU), Clermont-Ferrand.

The DBS therapy consists of two parts: a surgical intervention to implant the electrodes and the pulse-generator and post-operative control sessions to adapt the stimulation to symptom worsening due to increasing degeneration of neurons. The aim of the surgical intervention is to implant the DBS leads in the optimal location such that the patient's symptoms are alleviated with minimum stimulation energy and without inducing any adverse effects. While the aim of the surgery remains the same, the procedure followed for the surgery varies from center to center. A typical surgical procedure can be divided into 3 basic parts : a) Planning b) Lead implantation c) Implanted Pulse Generator (IPG) implantation.<sup>144</sup> Some centers perform the complete procedure on the same day while others may spread it out over 2 weeks. After the surgery, post-operative setup of the IPG (programming) is performed by a neurologist. The following sections describe the DBS procedure in general.

### 2.4.1 Surgical Procedure

#### Planning

The first step that clinicians perform to ensure that the lead is implanted in the optimal location is extensive surgical planning. Multiple radiological (CT and MRI) image sets of patients are acquired and imported into one of various commercial software systems (**Figure 2.14**) that are available to facilitate the planning process. The desired target may not always be discernible based on

spontaneous contrast alone and so, to localize the target in the patient images, clinicians use direct visualization targeting<sup>56,135</sup> or landmark based indirect targeting or a combination of both. Researchers have developed anatomical atlases of the sub-cortical region using the known landmarks of anterior commissure (AC) and the posterior commissure (PC). To identify the target area in patient images, clinicians identify the AC and PC points in these images and then scale the atlas in the antero-posterior direction using the AC-PC length and in medio-lateral direction using the distance to the edge of the thalamus. This method of identifying a target location is termed as "*indirect targeting*". In the "*direct visualization targeting*", clinicians first outline those sub-cortical structures that are easily identifiable using spontaneous contrast and/or specific MRI sequences. The desired target is then localized in relation to these structures alone or with the help of a commercial atlas or an in-house atlas. Some centers use a combination of both methods as well.

In order to be able to reach the desired target with least amount of damage to the brain, the surgery is performed stereotactically.<sup>333</sup> Commercial stereotactic frames are used to assign a 3D co-ordinate system to the human brain. To recognize this co-ordinate system in the digital images of the patient, a localizer box (**Figure 2.15**) is used which transfers the physical coordinates of the frame to a digital one. The planning software identifies various fiducials of this localizer



**Figure 2.15:** The Leksell Stereotactic System<sup>®</sup> and corresponding localizer box from Elekta, Stockholm, Sweden is an example of the commercially available stereotactic frames. Reproduced from their website([www.elekta.com](http://www.elekta.com)) for non-commercial purpose.

box in the images and can reconstruct the stereotactic frame's coordinate system in a digital form. The desired target structure is thus assigned coordinates in the stereotactic reference system. An entry point near the skull and the best path to reach the target are identified such that no critical anatomical structures or blood vessels are penetrated.

The surgical equipment allows insertion of up to 5 electrodes in parallel along the planned path; the number of electrodes used during the surgery depends on the surgical team. The planned trajectories of these electrodes (parallel to the best path) is verified to avoid penetration of blood vessels. The team then identifies a number of positions along these trajectories at different depths to



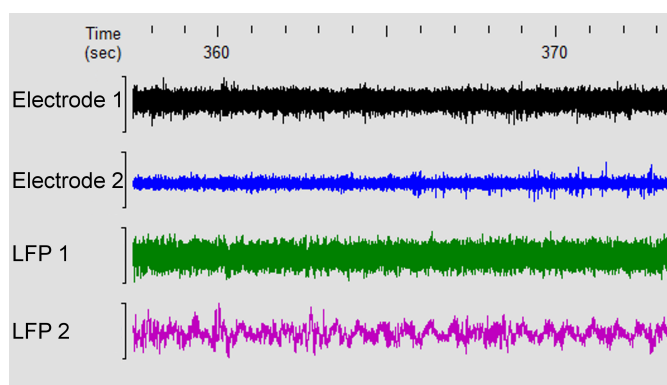
**Figure 2.16:** The neurosurgeon is inserting one of the intraoperative electrodes for recording electrophysiological activity and performing stimulation tests. Photo taken during a surgery at Inselspital Bern.

record neurophysiological data and to test the response to stimulation. For bilateral implantation, the procedure is repeated for the other hemisphere.

### Lead Implantation

The second step to DBS is the electrode implantation. The time between planning and surgery varies from center to center and can be from few minutes to few days. The implantation procedure can be performed using local or general anesthesia; the choice is dependent on the disease of the patient and the clinicians preference and expertise. On confirmation of the effect of anesthesia, the surgeon mounts the stereotactic frame on the patient using head-holding clamps. The frame is then adjusted to the co-ordinates provided by the planning system which aligns it to the planned entry point and trajectory. After opening the head tissue near the entry point, a burr-hole is drilled and electrodes are inserted as per the pre-determined number of trajectories (**Figure 2.16**).

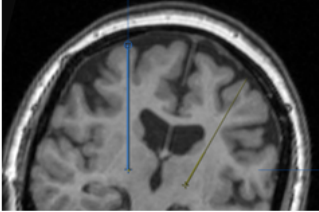
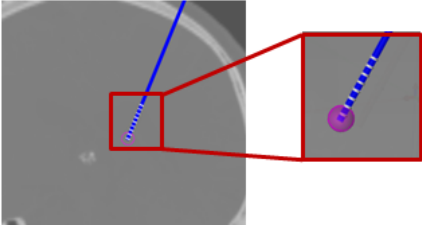
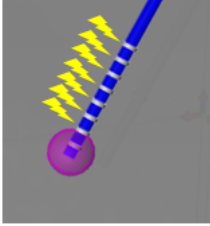
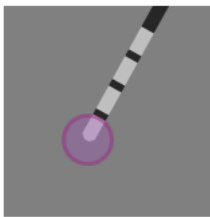
In order to confirm that the electrodes are inserted along the planned trajectories, some clinicians record electrophysiological activity using micro-electrodes at pre-determined positions.<sup>66,136</sup> The electrodes are pushed till the depth of the first planned Micro-Electrode Recording (MER) position. MER and Local Field Potential (LFP) (**Figure 2.17**) data is recorded and visualized using commercially available systems, some of which also perform real time analysis for checking neuronal response. Researchers have identified typical neuronal firing pattern for some of the structures which can be used to verify their presence along the trajectory.<sup>324</sup> A typical trajectory for Ventral Intermediate Nucleus (VIM) implantation would pass through the dorsal thalamus, into the ventrolateral nucleus including the VIM, followed by the caudal thalamus and ending in the Posterior Sub-thalamic Area (PSA)<sup>305</sup> containing the Zona Incerta (ZI),



**Figure 2.17:** An example of MER (Electrode 1 and 2) and LFP (LFP 1 and 2) data recorded during a DBS surgery along two parallel trajectories

Pre-Lemniscal Radiations (PLR) and the Fields of Forel (FF). Signal pattern changes when entering the VIM with an increase in firing rate compared to dorsal thalamus.<sup>282</sup> In some cases, tremor cells can be found firing at twice the tremor frequency.<sup>189</sup> Inferior to the VIM, an increase in firing rate and amplitude with altered background activity would suggest ventro-caudal thalamus which also responds to sensory phenomena.<sup>188</sup> A decrease in background activity would suggest exiting the thalamus and entering the ZI.<sup>106</sup> For STN implantation, a typical trajectory would pass through the thalamus, ZI and FF, STN and end in the SNr. MER firing rates are slow and asynchronous and background activity is less in ZI or FF compared to the thalamus, but the distinction is not always clear.<sup>324</sup> In the STN, cellular firing rate and background activity increase and sometimes tremor cells can be observed.<sup>247</sup> A significant rise in firing rates would indicate entrance into the SNr.<sup>247</sup>

Planning and MER (**Figure 2.18**) establish that the region being explored is right for treating the disease in question. Clinicians still need to decide where to implant the DBS lead. Therefore, stimulation tests are performed during the surgery either at all the predetermined positions or only some positions that are chosen based on MER data. Unlike MER, stimulation tests can be performed at only one position on one trajectory. Tests start at the highest position for a preferred trajectory, followed by the same position on the alternative trajectory/trajectories and then moving progressively deeper. During each test, one stimulation parameter (current or voltage) is stepwise increased from 0 to a fixed upper limit. Before the start of stimulation the severity of the patient's symptoms are noted (baseline). For each increment in the stimulation parameter, changes in the symptoms are evaluated (Section 2.5) compared to the baseline and the patient is observed for any noticeable adverse effects. Some clinical centers note the observed changes for all increments of stimulation parameter while others note only for the ones where the maximum improvement in symp-

Description	Representation
Step 1: Surgical planning and target selection	
Step 2: Micro-Electrode recording at different positions (in white)	
Step 3: Test stimulation positions (yellow identifiers)	
Step 4: DBS Lead placement (Stimulating contacts in silver)	

**Figure 2.18:** The steps that are taken to implant the DBS leads at the optimal location. After surgical planning and target selection, MER is performed to record brain activity. This is followed by stimulation tests to determine therapeutic and adverse effect inducing stimulation parameters. Finally DBS lead is placed at the location with the best results obtained from stimulation tests.

toms is observed (**Figure 2.19**). If severe adverse effects are observed at low values of stimulation current or voltage, stimulation tests are aborted.

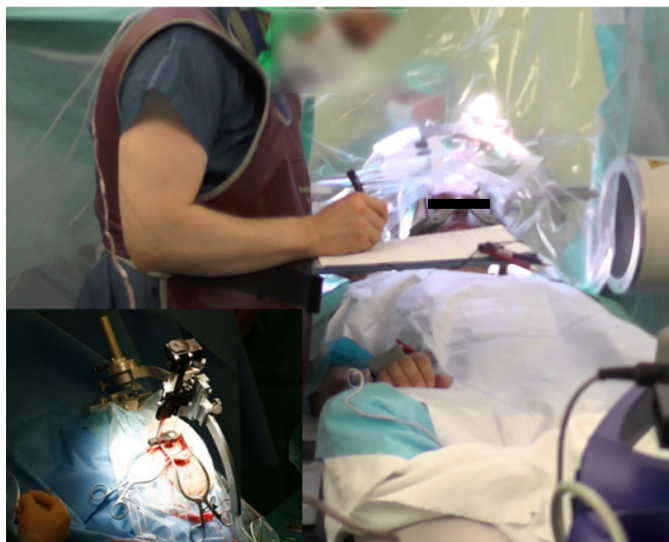


**Figure 2.19:** The observed changes in patient's symptoms and the corresponding stimulation test parameters are noted by the neurologist using pen and paper for later reference. Photo taken during a surgery in Inselspital Bern.

On completion of the stimulation tests, the surgical team must choose the trajectory and the position at which a particular contact of the electrode should be implanted. For each stimulation test position, the team mentally calculates the therapeutic window i.e. the difference between the stimulation parameter where largest therapeutic effects were observed and either the parameter where the first adverse effects were observed or the fixed upper limit of stimulation. To implant the DBS lead, clinicians choose the trajectory that has the most number of positions with large therapeutic window and is closer to the desired target structure. For lead placement, i.e. choosing the position and the contact of the lead for chronic stimulation, the surgical team tries to match most of the stimulation test positions with large therapeutic windows to the stimulating contact of the lead'. One of the many ways to achieve this is to implant the lowest (distal) contact of the DBS lead at the deepest position with a large therapeutic window. Any higher positions with large therapeutic windows can then be stimulated with proximal contacts. Once the decision is made, the neurosurgeon implants the DBS lead (**Figure 2.18**), secures it into position and places the connector between the skin and the skull to connect to the IPG.

### Implantation of Pulse Generator

Depending on unilateral or bilateral DBS, one or two IPGs are implanted in the subclavicular area in a subcutaneous pouch. The implantation is performed

under general anesthesia. Some clinical centers implant the IPG on the same day while others do it the next day or a few days after. The extension cables to connect the IPG to the DBS leads are implanted deep under the skin to prevent adhesion to the subdermal area. Once the IPG is connected to the DBS leads via the extension cables, tests are performed to ensure proper connections. All the incisions are then sutured to complete the procedure.

### 2.4.2 Risks and Complications

DBS is regarded to be a relatively safe and effective procedure, but it is not absolutely free of risks and complications.

#### Stimulation induced Adverse Effects

The complexity of the surgical procedure of DBS results in causing undesired effects of stimulation due to unplanned position of the DBS lead or due to stimulation spreading into tissue surrounding the planned target. Naturally these effects vary based on the planned target structure. The most common adverse effect of GPi DBS is dysarthria, perhaps due to stimulation of the cortico-bulbar tract in the internal capsule.<sup>342</sup> Other adverse effects of GPi DBS include headache, nausea, muscle contractions of face and limbs, numbness and abnormal eye movements. In case of STN DBS, adverse effects caused by the stimulation of third nerve or rostral interstitial nucleus like motor contractions and dysarthria, paresthesia and oculomotor effects are observed.<sup>21,344</sup> Other effects like nausea, heat sensation and sweating are also common.<sup>239</sup> Flora et al.<sup>60</sup> performed a systematic review for a collective of 430 patients of VIM DBS and found adverse effects like paraesthesia (18.84%), dysarthria (8.84%) and headache (7.21%) among others. These may be a result of stimulation spreading posteriorly into the Ventro-caudal (Vc) nucleus, medially into the medial lemniscus<sup>242</sup> or laterally into the internal capsule.<sup>16,102,344</sup> These symptoms are usually temporary, occurring during intraoperative stimulation tests or immediately after stimulation and wearing off with time. In case they persist afterwards, they can still be controlled by adjusting stimulation parameters.

Apart from these acute adverse effects of stimulation, reports of chronic adverse effects affecting the cognitive and psychiatric status of the patients have also been reported. Verbal fluency has been reported to decrease after STN-DBS.<sup>111,252,328</sup> Studies have compared cognitive function of PD patients after STN-DBS with GPi-DBS and have reported that STN-DBS patients showed greater decline.<sup>364</sup> This decline however, is not very large and it cannot be said for certain if it is an adverse effect of DBS or signs of worsening disease. Mood variations have also been reported in relation to STN-DBS, Berney et al.<sup>26</sup> reporting a decline while Daniele et al.<sup>58</sup> reporting an improvement. Takeshita et al.<sup>343</sup> have reported an incidence rate of mania between 4.2% and 8.1% as well as of depression between 2 and 33%. Depression is an important psychiatric

symptom in terms of patient management as it relates to suicide risks. Reported incidence rate of minor depression (31.4%) are much higher compared to major depression (1.6%).<sup>99</sup> History of depression and excessive tapering of levodopa after DBS have been reported as risk factors of depression.<sup>363,371</sup> In another study, Witt et al.<sup>372</sup> reported that STN-DBS effects on cognitive function could be avoided by ensuring that the stimulating contact is in the STN and the DBS lead does not pass through the head of the caudate nucleus.

Suicide risks have been reported in relation to DBS. In a multicentre study consisting of 5311 patients, 24 (0.45%) committed suicide while 48 attempted suicide (0.90%).<sup>360</sup> The researchers also identified 3 risk factors for suicide: i) relatively younger age, ii) early onset of PD and iii) a preoperative suicide attempt. Other studies have reported different incidence rates of suicide risks between 0 and 5%.<sup>42,99</sup> But, like adverse cognitive function, incidence rates of suicide are higher in PD patients than in the world population as reported by the World Health Organization.<sup>243</sup> In addition, PD patients who undergo DBS have higher severity of the disease and usually are on their limits for treatment through medication. Thus, in absence of any studies comparing the suicide risks between advance PD patients with and without DBS, it is not possible to attribute higher suicide rates to STN-DBS alone.

### **Other Complications**

A critical surgical complication of DBS is intracranial haemorrhage i.e. bursting of blood vessels due to insertion of DBS leads or microelectrodes. The reported incidence rate in clinical studies varies from 1 to 25%.<sup>94</sup> Older patients and patients with high blood pressure are at a higher risk of having haemorrhage during DBS. The use of multiple MER electrodes has also been associated with higher occurrence of haemorrhages, and studies have suggested to use few MER electrodes and only when necessary.<sup>383</sup> Another way to reduce chances of haemorrhages would be to use contrast based MRI images during the planning to identify the blood vessels and avoid them along the trajectory. Other surgical complications with lower incidence rates include confusion, anxiety and seizure as well as hypotension and arrhythmia.<sup>94</sup>

Continuous chronic stimulation may be halted due to hardware failures like cable breakage or malfunctioning IPG. Incidence rates for electro-mechanical failures including failure of IPG, electrode displacement and breakage as well as breakage of extension cords range from 4 to 9.7%.<sup>338</sup> One study also reported 2 patients having allergic reactions to DBS systems.<sup>259</sup> The connection area between the DBS lead and the extension cord is the most frequent place for breakage.<sup>95</sup> Chances of equipment failure can be reduced by avoiding wiring at sharp angles and not implanting the IPG in the pectoral region for patients with well-developed muscles in that region. Another hardware related adverse event is infection with incidence rates ranging from 2.9 to 7.7%<sup>338</sup> with an average

infection rate of 4.7%.<sup>29</sup> Risk factors include age of the patients (younger than 58 years or older than 65 years) among others.<sup>28</sup> Sugiyama<sup>338</sup> suggests extensive patient management (bathing, etc), precautionary handling of DBS device (using surgical instruments) and other surgical precautions to limit chances of infection during DBS surgeries.

### 2.4.3 Mechanism of Action

The widespread adoption of DBS for the treatment of diseases like PD and ET clearly indicate its success in suppressing the patient's symptoms. Nevertheless, the mechanisms that bring about these therapeutic (or adverse) effects in patients are still unclear. In order to clearly understand these mechanisms, information with respect to the following topics have to be obtained.<sup>164,237</sup>

**Effects on neurons** What happens to the soma of neurons (cell body, **Figure 2.20**) in the vicinity of the stimulating electrode? Are they excited and transmit signals or are they inhibited from performing their designated tasks?

**Effects on axons** What happens to axons (**Figure 2.20**) that are located in the vicinity of the stimulating electrode but have their soma outside of this region? do these axons get activated and transmit information towards (antidromic) or away (orthodromic) from the soma?

**Effect on functional circuit** The neurons and axons surrounding the stimulating electrode are part of a larger functional circuit performing a certain task. For example, the STN neurons are part of the cortico-basal ganglia-thalamic circuit which is responsible for various tasks including movement. With this regards, what changes are seen in this cortico-basal ganglia-thalamic circuit during STN DBS? In general, are the effects of DBS on neurons and axons changing the functional circuit?

**Acute and chronic effects** The amount of time between stimulation and its effect varies based on the different symptoms and the disease. For example, DBS for PD patients immediately improves tremor but gait improvements can take days.<sup>125,154</sup> Are these differences in time because of changes in the functional circuits fo the brain or because the brain adapts to stimulation through physical changes (plasticity)?

Researchers have performed various experiments studying the effects of DBS at the cellular, tissue and system levels to get more information about these topics. According to Udupa,<sup>349</sup> these experiments can be roughly classified into electrophysiological, imaging, biochemical and molecular methods. The initial hypothesis of the mechanisms of action of DBS was based on the similarities between therapeutic effects of DBS and ablative surgeries indicating that electrical stimulation inhibited the neurons in the vicinity of the electrode.

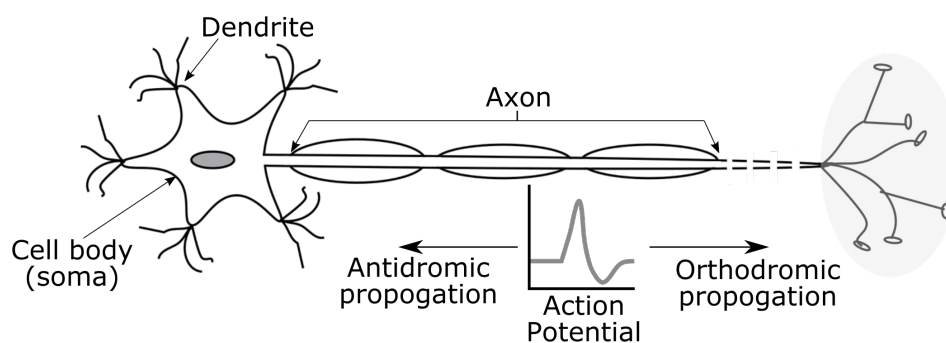


**Figure 2.20:** A rough representation of a neuron with its relevant parts

This hypothesis also supported the classical model of PD i.e. stimulation in the STN or GPi would decrease the GPi output to thalamus, in turn, promoting movement. In vitro experiments have shown that high frequency DBS prevents initiation and propagation of action potential through sustained depolarization of neuronal membranes<sup>218</sup> and perhaps through release of inhibitory neurotransmitters.<sup>76</sup> Experiments which recorded activity in the GPi<sup>76</sup> and STN<sup>367</sup> during stimulation provided further evidence in support of this hypothesis.

In animal model studies, Hashimoto et al.<sup>137</sup> found that during effective STN stimulation, neuronal activity in the GPe and GPi increased in contrast to expectations based on the inhibition hypothesis. Further research to understand the effect of stimulation on neurons revealed that the neuronal projections in the stimulated region were activated resulting in increased frequency of action potentials from the region.<sup>76, 226, 357</sup> Computational models revealed that high frequency stimulation affects the projections more than the soma because of their lower stimulation thresholds. Larger axons that are perpendicular to the electric field in the stimulated region are activated easily compared to others which may result in a neuron with its axon only in the stimulation region being activated.<sup>227</sup> Results of the optogenetic experiments by Gradinaru et. al.<sup>119</sup> further supported this idea as activation of fibers in STN of rat models resulted in therapeutic effects but inhibition of STN neurons did not. Experiments measuring the extracellular Cyclic guanosine monophosphate (cGMP) levels (an indirect marker for neuronal activity) in humans undergoing DBS showed increase in levels in putamen, GPi and SNr during effective stimulation in STN, concurring with the results of computational and animal models. Grill et. al.<sup>122</sup> argue that the increase in action potentials due to stimulation may restrict passing of information that is coded in the time-varying neuronal activity resulting in an "informational lesion." Some animal model studies have provided supporting results<sup>2, 51</sup> while others have suggested that information transfer decreases in parkinsonian state and is partially recovered through stimulation.<sup>74</sup>

Another hypothesis for the mechanisms of actions of DBS is the disruption of

oscillations. Experiments measuring LFP in PD patients and animal models have shown that, compared to healthy brains, beta band (12-30Hz) oscillations in PD become more coherent between different neuronal circuits, especially in the sensorimotor basal ganglia.<sup>77,194,257</sup> Additionally, while the beta oscillations in healthy brain disappear during movement, they persist for PD patients. In patients treated with levodopa, the beta-band power in STN and GPI decreases in correlation with the magnitude of clinical improvement in bradykinesia and rigidity.<sup>40</sup> Experimental evidence is available to support the idea that therapeutic effects of DBS are due to disruption in the beta-band oscillations.<sup>59</sup> Researchers have also found that stimulation in the STN at beta frequencies worsens bradykinesia.<sup>50</sup>

DBS also causes neurochemical changes in the vicinity of the electrode. Microdialysis studies in human brains<sup>222,384</sup> have shown that STN or GPi DBS can induce dopamine release. However, this may play no significant role or only a supportive role in the mechanisms of action<sup>269</sup> because tremor and dyskinesias worsen or do not change with dopamine medication, but respond to DBS. Nevertheless, for other diseases like cervical dystonia or OCD, these effects of DBS may be relevant.<sup>219,255</sup> Studies report only short term neurochemical effects of DBS, but with advancing technology, designs for long term experiments should be possible in the near future. The application of DBS to diseases other than PD and ET have led to the idea that only some therapeutic effects of DBS are due to neuromodulation. Based on the difference in time that symptoms take to respond to DBS, some effects may be also due to synaptic plasticity and network reorganization. The suppression of motor tics in Tourette's syndrome through DBS can take months.<sup>300,318</sup> While phasic dystonic movements improve immediately through GPi DBS, tonic symptoms require months. Imaging studies using fMRI, PET and Single-photon emission computed tomography (SPECT) have also shown that DBS causes global and long-term changes in the network activity.<sup>171</sup>

The above mentioned hypotheses of mechanisms of DBS were proposed based on research studying a particular pathology or target nuclei. It is clear that none of the hypotheses proposed for the mechanisms of DBS can explain all the observed effects in different pathologies and targets. Therefore, further research is necessary to obtain information about how the mechanisms of DBS vary between different pathologies and to find out if any similarities exist.

## 2.5 Symptom Evaluation During DBS Surgery

DBS for PD and ET is widely performed under local anaesthesia<sup>1</sup> to observe the effects of stimulation on the symptoms of the patient. During the intraoperative stimulation tests, the therapeutic effects of stimulation are evaluated based on these observed changes in the patient's symptoms. In case of ET patients or

PD patients with severe tremor, the baseline severity in tremor and any changes during stimulation are estimated by visual observation. When DBS is used to treat PD patients with rigidity, the therapeutic effects during intraoperative stimulation tests are evaluated by estimating changes in it. While tremor is an active symptom, rigidity is defined as a passive symptom and can only be observed through external intervention. Therefore, to estimate rigidity and its changes during the surgery, passive movements of the patient's arm or the wrist joint are performed (**Figure 2.21**). Other motor symptoms of PD patients like bradykinesia and akinesia also improve through DBS. But studies have shown that the latency for tremor and rigidity suppression after stimulation is within seconds while that for bradykinesia is longer. Therefore, during intraoperative stimulation tests, changes in these symptoms are either not evaluated or only evaluated after tremor and/or rigidity have been considerably suppressed. Thus, this section concentrates on tremor and rigidity evaluation.



**Figure 2.21:** A neurologist is performing passive movements to evaluate the changes in patient's rigidity with changing stimulation parameters. Photo taken during a surgery in Inselspital Bern.

In various DBS centers around the world, while the method of symptom evaluation remains the same, the rating scales used during intraoperative stimulation tests vary. In some centers, clinical rating scales like UPDRS are used to evaluate the baseline symptom and then again the changes at each step of varying stimulation parameter(s). In other centers, clinicians use a direct rating system where the baseline severity of the symptom is assigned 0 and any improvement is rated between 1 (low improvement) to 4 (symptom suppressed) in steps of 0.5. The method and rating system of symptom evaluation during intraoperative stimulation test are minor modifications of those used for routine clinical evaluation. The rating systems in particular were designed to be used to evalu-

ate symptoms over longer periods of time rather than continuous evaluation.<sup>10</sup> Hence, to adapt the rating system to intraoperative use, clinicians would introduce intermediate steps for each rating level<sup>177</sup> e.g. for UPDRS instead of just 0,1,2,3 and 4, they would use 0, 0+, 1-, 1, 1+,... 4. Studies have shown that these methods and rating systems have low inter-rater<sup>260,275</sup> and intra-rater reliability<sup>275</sup> as they depend significantly on the evaluator's experience.<sup>121</sup> Using these relatively subjective symptom evaluations during DBS thwarts other efforts to implant leads at the best possible location with millimeter precision.

In addition to the variations associated with the rating scales, the passive nature of rigidity evaluation introduces other challenges. Passive movements to estimate rigidity can be performed about the elbow or the wrist joint with movement patterns being extension-flexion, rotational or a combination of both. In routine clinical evaluation, neurologists tend to check rigidity for different joints and with different movements. Additionally, the evaluating neurologist may not be the same between different clinical visits. In contrast, rigidity evaluation during DBS is performed by only one neurologist and most often only about his/her preferred joint to reduce surgical time and in-turn patient stress.

The confinement of passive movements during DBS surgery to one neurologist and one joint is advantageous for the goal of this thesis as it limits the variations that have to be considered. Another advantage that is presented by the nature of intraoperative evaluation is the duration i.e. the movement pattern and its variations have to be analysed for the duration of a stimulation test at one position (1-5 minutes) independently of the previous stimulation test. In addition, as the passive movements are continuous for one stimulation test (from baseline to stimulation), the intra-rater variations are also reduced. Nevertheless, it is important that the evaluating neurologist has direct access to the patient's arm to perform passive movements as his experience plays an important role in the evaluation. Therefore, most centers ask experienced neurologists or movement disorder specialists to assist during the surgery for rigidity evaluation.

### 2.5.1 Quantitative tremor evaluation

Various techniques have been proposed by researchers to evaluate rigidity and tremor in a more quantitative fashion for the clinical assessment outside the operating room.<sup>84,139</sup> Tremor, for example, has been studied using various sensors like Electromyography (EMG),<sup>10,167,181,256,330</sup> spirometers,<sup>85,292</sup> gyroscopes<sup>238,294</sup> and accelerometers.<sup>233,291,337</sup> Some early propositions were based on mechanical setups which have largely been converted to electronic systems. Two of the most common techniques used to measure tremor are EMG and inertial sensors (**Figure 2.22**). EMG estimates muscle activity by measuring the electrical potential generated across them when they are activated using intramuscular electrodes (invasive) or surface electrodes (non-invasive). Researchers have used EMG to measure activity of tremor patients to characterize tremor in

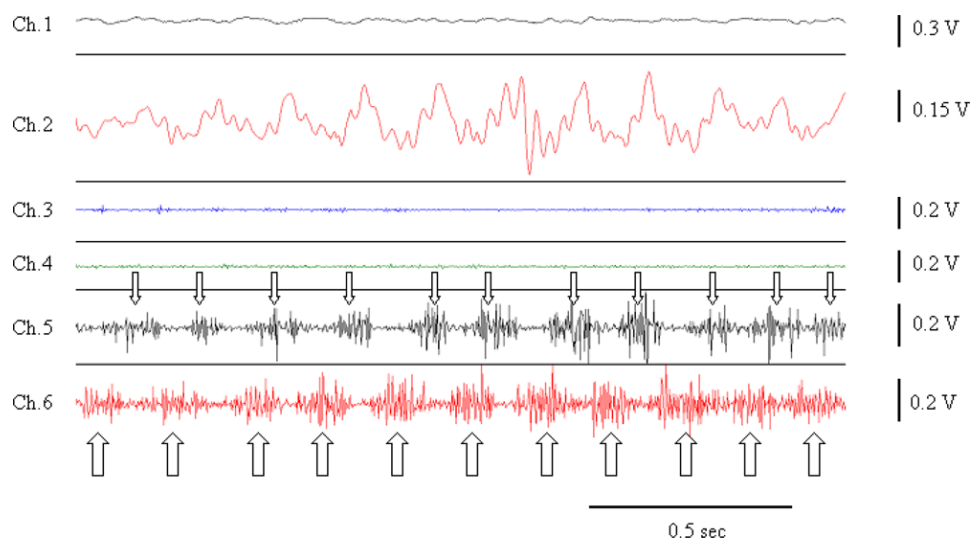


**Figure 2.22:** The figure shows tremor recorded by an accelerometer mounted to the extremity of the index finger on channel 2 and by surface EMG electrodes placed at the flexor and extensor muscles of the radial bone on channels 5 and 6 respectively. Reproduced from Grimaldi et al.<sup>123</sup> for non-commercial use under the CC BY-NC-SA 3.0 (<https://creativecommons.org/licenses/by-nc-sa/3.0/>) license.

terms of time-frequency parameters,<sup>256</sup> to distinguish between different types of tremor<sup>43, 153, 230</sup> and also to evaluate the therapeutic effect of drugs<sup>273</sup> and DBS.<sup>291, 337</sup> A major drawback of EMG is patient discomfort: intramuscular electrodes are invasive and surface electrodes require good contact with the skin to record good quality data.<sup>91</sup> This prevents the use of EMG to measure tremor for extended periods of time.

Inertial sensors (**Figure 2.23**) are a group of sensors that measure movement of a certain object by measuring its acceleration (accelerometer, **Figure 2.23a**), angular velocity (gyroscope, **Figure 2.23b**) or magnetic field (magnetometer, **Figure 2.23c**). Inertial sensors were designed to assist in the navigation of vehicles in areas where a Global Positioning System (GPS) signal was not available. Due to advancing technology, new inertial sensors are made using Micro Electro Mechanical Systems (MEMS) reducing their size to micrometers. These miniaturized sensors are now used in mobile devices, game controllers and fitness trackers to track movements of the user. These sensors provide an excellent opportunity to measure tremor. Early MEMS based inertial sensors were only able to measure acceleration along a single axis (uniaxial). Researchers used multiple uniaxial accelerometers to measure tremor in different directions and combined the signal to get an estimate of the tremor severity. Currently, MEMS units with triaxial accelerometers, triaxial gyroscopes and triaxial magnetometers are available providing the ability to track movements with 9 degrees of freedom. These advancements have made the inertial sensors a favourite among tremor

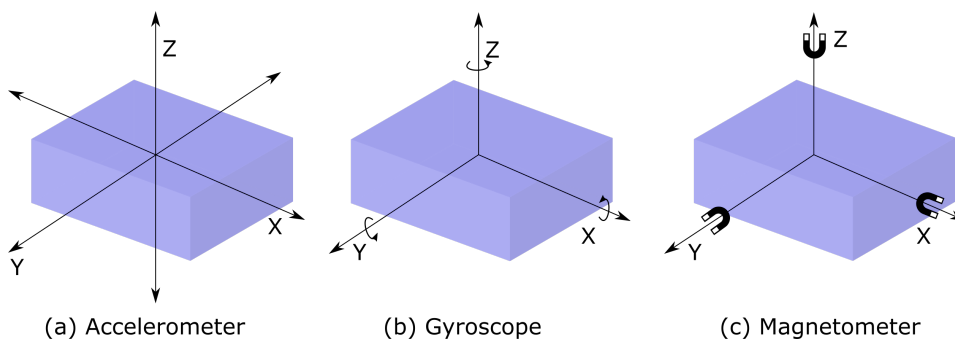


**Figure 2.23:** The three types of inertial sensors (a) Accelerometers measure the acceleration (b) Gyroscopes measure the angular velocity and (c) Magnetometers measure the magnetic field. New devices capable of measuring all three quantities are also available

investigators.

Over the years, many studies have been published where accelerometers have been used to measure tremor. Characterizing pathological tremor<sup>104,160</sup> and comparing it with physiological tremor,<sup>231,290,291</sup> measuring the changes in tremor with worsening disease<sup>262,266,316</sup> or to evaluate the effects of therapy on tremor<sup>233,291,337</sup> are few examples where accelerometers have been used. Accelerometers have also been used during post-operative programming for the IPG.<sup>233,280</sup> Apart from these research based uses of accelerometers, inertial sensors are also used in commercial systems to evaluate motor symptoms including tremor, bradykinesia and akinesia. The Kinesia system (Great Lakes Neurotechnologies, Cleveland, USA) can measure tremor, bradykinesia and dyskinesia in PD patients using an accelerometer mounted on a finger and transfer the data to the clinician providing a telemedicine tool to evaluate symptoms. The PKG system (Global Kinetics Corporation, Melbourne, Australia) is another similar telemedicine device which tracks the same symptoms through an accelerometer based wrist watch.

Despite these commercial and research systems mentioned above, intraoperative use of systems to quantify tremor has been very limited. To the best of my knowledge, there is no commercial system that allows for intraoperative evaluation of movement disorder symptoms. On the other hand, some researchers have proposed methods to quantitatively evaluate tremor during surgery. Effects of different temporal pattern of DBS signal on tremor was studied intraoperatively using an accelerometer.<sup>30</sup> MER signals were correlated to goniometer signals to identify the target structure.<sup>319</sup> An accelerometer was once used during thalamotomy as well.<sup>232</sup> Journee et. al.<sup>166</sup> used two uniaxial accelerometers during DBS surgery to evaluate tremor as well as finger tapping while stimulating through the DBS lead to identify the best contact. They however, used only spectral parameters to identify changes in tremor without applying any filters to

the raw data, thus not suppressing the influence of noise and gravity. They also only recorded the baseline before inserting the lead, thus unable to differentiate the effect of tissue damage due to lead insertion from the effect of stimulation on tremor. Another study used a commercial system designed for quantifying tremor called CATSYS 2000 (Danish Product Development Ltd, Snekkersten, Denmark) after implanting the DBS lead to identify the best stimulation parameters during the surgery.<sup>261</sup> This system uses a tremor pen containing a biaxial accelerometer which the patient has to hold in a certain position to record the best data. As patients were given time to familiarize themselves with the system, the surgical procedure was elongated and the data recorded was also affected by varying levels of familiarity. Neither of the two studies provided a detailed comparison of the accelerometer based results with the clinical evaluation. These inadequate and partial techniques gave the push to design a new technique to evaluate changes in tremor during intraoperative stimulation tests for DBS surgery and test it by applying it in more than one clinical center.

### 2.5.2 Quantitative rigidity evaluation

Rigidity evaluation has received less attention from researchers compared to tremor in terms of number of publications proposing methods for quantitative evaluation. Researchers have proposed methods using EMG to continuously monitor changes in rigidity,<sup>10</sup> to differentiate between PD rigidity and health subjects<sup>86,373</sup> and also to estimate changes in rigidity with and without DBS.<sup>191</sup> Others have used specially designed mechanical apparatus (**Figure 2.24**) to measure changes in rigidity by measuring parameters like angular impulse.<sup>101</sup> It has been shown that parameters representing viscous properties of rigidity correlate better with clinical scores than those measuring elastic properties.<sup>264,317</sup> Shapiro et. al<sup>321</sup> used a custom made mechanical setup to show that STN-DBS was better at reducing rigidity compared to drug therapy only.

The use of these techniques in the OR would be very cumbersome and could cause discomfort to the patient. At the beginning of this doctoral work, a literature search for rigidity evaluation during DBS surgery came up empty. The absence of any such literature motivated us to accommodate rigidity evaluation during DBS using an accelerometer. During the time-course of this work, to the best of my knowledge, only one other research group published a method to evaluate rigidity intraoperatively.<sup>177</sup> They used a mechanical setup which could only evaluate rigidity through the wrist joint. The use of their system during the surgery resulted in less number of stimulation tests than usual due to time constraints.

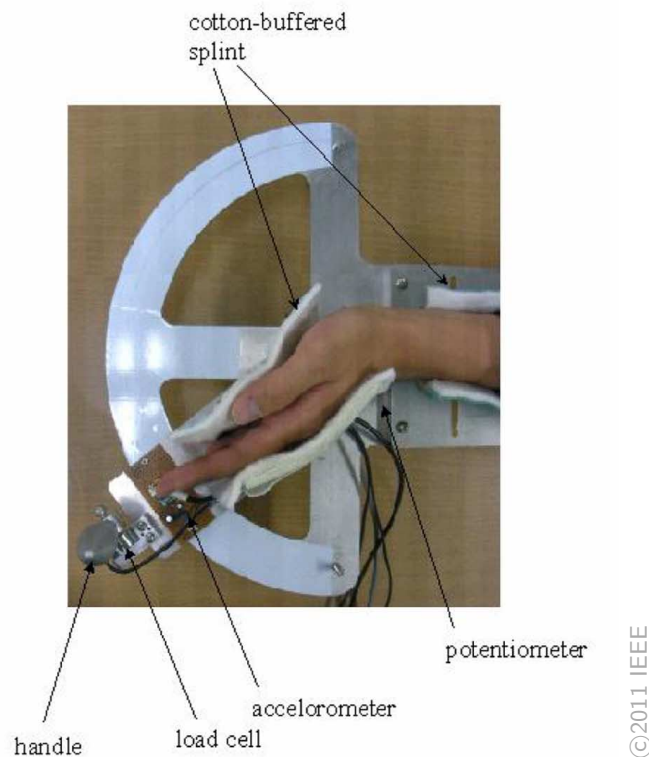


**Figure 2.24:** The mechanical setup used by Park et al.<sup>264</sup> to measure the viscoelastic properties of rigidity in Parkinsonian patients. Reproduced from their paper with permission ©2011 IEEE.

## 2.6 Anatomical Targets for DBS Lead Implantation

The current anatomical targets for PD (STN and GPi) and ET (VIM) were identified from lesioning surgeries. Various long term clinical studies have shown that stimulation through DBS leads in these structures suppresses the patients symptoms, albeit to a variable degree. But existing knowledge of the pathophysiology of the diseases and the mechanisms of action of DBS is limited and some contradictory reports have also been published where desired improvement was not achieved by stimulation of these structures. Therefore, further research is necessary to identify anatomical structures that are more efficient and reliable DBS targets.

### 2.6.1 Identifying structures

It is necessary to know the anatomical structures surrounding the intraoperative electrode or the DBS lead to analyse which structures play a role in the therapeutic effect of stimulation. In a recent review study, Caire et al.<sup>47</sup> identified many techniques with which this task can be achieved. These include projection

of active contact(s) on anatomical images,<sup>353</sup> on anatomical atlas<sup>302, 306</sup> or even probabilistic functional atlas.<sup>179</sup> MER results alone<sup>382</sup> or in combination with imaging<sup>366</sup> and white matter tracking<sup>54</sup> can also be used for this purpose.

## 2.6.2 STN implantation

The STN is surrounded by other structures like the ZI, SNr and the thalamus as well as fibre tracts like FF and Internal Capsule (IC) (**Figure 2.25**). Trajectories

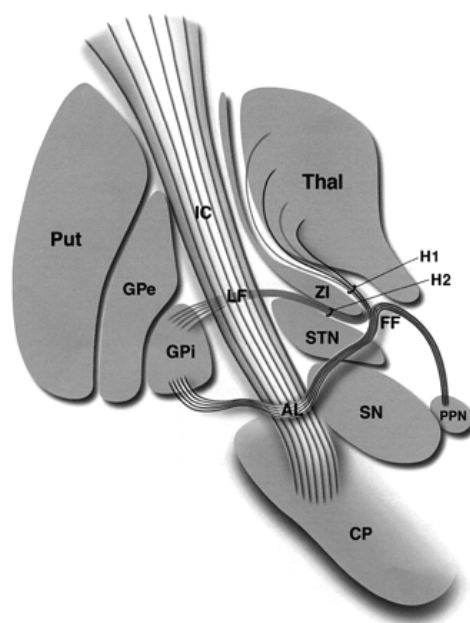


**Figure 2.25:** The structures surrounding the Subthalamic Nucleus (STN), some of which are along the trajectories used for STN-DBS implantation. AL = ansa lenticularis; CP = cerebral peduncle; FF = Fields of Forel; GPe = globus pallidus externus; GPi = globus pallidus internus; H1 = H1 Field of Forel (thalamic fasciculus); IC = internal capsule; LF = lenticular fasciculus (H2); PPN = pedunculopontine nucleus; Put = putamen; SN = substantia nigra; Thal = thalamus; ZI = zona incerta. Reproduced with permission from Hamani et al.<sup>131</sup>

to implant a lead in the STN will pass through some of the structures and stimulation in the STN at higher amplitudes will spread into these neighbouring structures. Zheng et. al.<sup>380</sup> analysed the position of the DBS lead in 40 cases using post-operative MR images in relation to the position of STN which was identified through a combination of intraoperative MER and post-operative MRI. He found that the most effective contact on the DBS lead was located in the sensorimotor region of the STN or dorsal to it in the ZI or FF. Other studies have also reported similar results.<sup>112, 132, 302</sup>

### 2.6.3 VIM implantation

In the vicinity of the VIM, apart from other thalamic nuclei (**Figure 2.26**), there are the fibre tracts like the Dentato-Rubro Thalamic Tract (DRTT) and PLR and other structures like the ZI. Other thalamic nuclei like the Intermediolateral (InL)<sup>150</sup> and the Ventro-Oral (VO)<sup>48,352</sup> have already been shown to have a role in the therapeutic effects of DBS. Lesioning studies have reported targeting the PLR<sup>241</sup> and some researchers have also implanted DBS leads close to it.<sup>331,352</sup> Others have targeted the DRTT<sup>124</sup> and some have suggested that ZI could also play a role for ET patients.<sup>103</sup>

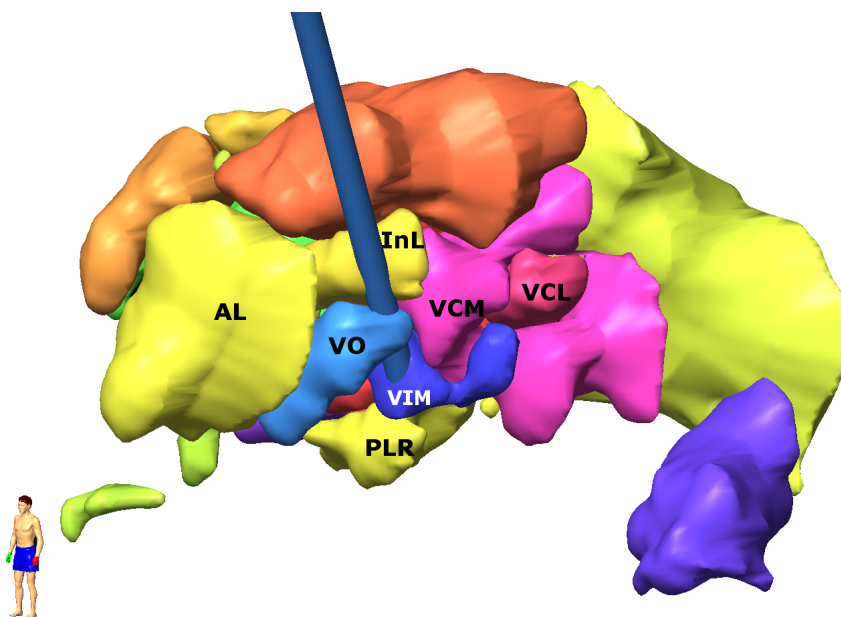


**Figure 2.26:** The different thalamic nuclei around the Ventral Intermediate Nucleus (VIM) which are traversed through during VIM-DBS implantations. AL = AnteroLateral; VO = Ventro-oral; InL = Intermediolateral; VCM = Ventrocaudal medial; VCL = Ventrocaudal lateral and PLR = prelemniscal radiations. For comparison to other nomenclatures of thalamic nuclei, refer to Lemaire et al.<sup>187</sup>

## 2.7 Data Management and Visualization for DBS Lead Placement

The use of software in the field of medicine has increased significantly in recent years. As computational power increases, the abilities of software to simplify tasks of clinicians has also increased. For DBS as well, software is used for all phases i.e. from planning to post-operative follow up. Nevertheless, one area where software can further assist the clinicians is at the time of placing the lead for optimal chronic stimulation. Stimulation at the optimal position should

have the maximal reduction in patient symptoms with minimal energy consumption without inducing any adverse effects. To achieve this, the team identifies positions with large therapeutic windows, mentally visualizes the anatomy surrounding these positions and identifies one as an optimal position. The surgical planning software can assist the team by visualizing the anatomy, but not all centres have access to it in the OR room.

During a typical DBS surgery, a large amount of data is collected from the patient to optimize DBS leads implantation viz. pre-operative CT and/or MR images, intraoperative MER and response to stimulation tests. In addition, the surgical team spends significant time during surgical planning generating more information by combining their anatomical knowledge and patient images. At the time of identifying the optimal position to implant the DBS lead, all of this information is considered. These data are however, either available on different computer systems or only in the form of paper based notes (**Figure 2.27**). Clearly, the decision making process can be simplified through a tool that would consolidate all the relevant information, process it and visualize it together. An absence of such a software provided the impetus to further investigate and develop a solution to fill up this void during this doctoral work.

There are a few commercial software systems available that surgical teams can use during a DBS surgery. Software designed to assist during surgical planning can import, register and visualize image data, localize stereotactic frames, outline and label anatomical structures, plan trajectories and generate co-ordinates for the frame. Systems designed for intraoperative use are able to record and analyse MER data in real time and assist during stimulation tests. But most of these single-purpose systems have proprietary data formats hindering data consolidation. While some planning systems accept MER and stimulation test results, these have to be entered manually. Doing so during the surgery would heavily burden the stressed surgical staff. Additionally, no commercial system exists that automatically calculates the results of intraoperative stimulation tests.

Scientific literature describing software for DBS are also plentiful, most of which aim to automate certain tasks related to DBS. D'Albis et al.<sup>57</sup> have developed a tool called PyDBS that allows identification of AC-PC points, automatically identifies the frame in stereotactic images and automatically segments and registers patient images (pre- and post-operative). Qualitative assessment showed its ability to assist clinicians in planning and post-operative phases. Another software called StimExplorer<sup>46</sup> allows manual alignment of patient images with anatomical atlas and place the post operative DBS leads. It predicts the Volume of Tissue Activated (VTA) in homogeneous tissue based on the stimulation parameters (not patient-specific) which can assist clinicians during postoperative IPG programming. However, neither of these systems were designed to be used during intraoperative stimulation tests.



Guo et al.<sup>128</sup> developed a tool to visualize a database of their previously operated patients consisting of electrophysiological information, segmented deep-brain nuclei and previously chosen targets on images of prospective patients using non-rigid registration. The results of their retrospective and prospective study showed that using their software system would reduce the duration of surgical planning and intraoperative exploration without affecting surgical outcome. However, their software was not patient-specific as it did not visualize the results of the intraoperative stimulation tests of the patient being operated. Cranial Vault is another repository of DBS patients which can be accessed through software modules called CRAVE.<sup>70</sup> This tool had various algorithms to automate image processing tasks to reduce duration of surgical planning. It could be used intraoperatively to visualize manually entered therapeutic and adverse effects of stimulation tests. On testing the system in a clinical study, it was observed that the task of manually entering information to be tedious for the surgical staff.

## Chapter 3

# Clinical Data Acquisition

An important aspect of this doctoral work is the acquisition of clinical data, i.e. acceleration data during DBS surgery. The approach to use acceleration sensors during a DBS surgery to evaluate tremor and rigidity may not seem complicated at first, but the restrictions and requirements of the surgical room act as significant deterrents. This chapter describes these requirements and the specifications of the equipment that was developed to satisfy them. It also provides the details of two clinical studies that were undertaken to acquire data, including the details of the participating patients.

### 3.1 Accelerometer Data Recording Setup

#### 3.1.1 Technical Requirements

A review of the published literature as described in Section 2.5 shows that an accelerometer would be a good option to evaluate changes in tremor and rigidity during DBS surgery. In order to choose an accelerometer, it is necessary to identify the parameters of the movement that have to be measured. Tremor is a rhythmic movement and thus can be modelled by a sinusoidal function described by the following equation:<sup>84</sup>

$$T = A \sin(2\pi ft) \quad (3.1)$$

where  $T$  is the tremor,  $A$  is the peak to peak distance moved by the tremulous limb,  $f$  is the frequency of tremor and  $t$  is the duration of time for which tremor is measured. The acceleration of tremor would be the second derivative of equation 3.1 and can be described by the equation:<sup>84</sup>

$$T_{acc} = -A(2\pi f)^2 \sin(2\pi ft) \quad (3.2)$$

where  $T_{acc}$  is the acceleration of tremor. This equation can be used to calculate the range that an acceleration sensor should have to successfully measure

tremor. For a tremor of 6 Hz having a peak to peak distance of 10 *cm*, the amplitude can be calculated using  $A(2\pi f)^2$  to be approximately 14212.23 *cm/s*<sup>2</sup> or 14.5 *g* ( $1g = 9.8m/s^2$  i.e. acceleration due to gravity). Therefore, a uniaxial accelerometer must have a range higher than this to measure tremor along its axis. Another factor to consider for choosing the acceleration sensor is the sampling frequency, which according to the Nyquist theorem, must be more than twice the frequency of the data that has to be measured.

Passive movements for rigidity evaluation (Section 2.2) are also rhythmic in nature and thus can also be modelled by the equation 3.1 and 3.2. The difference between the two however is that the peak to peak amplitude (*A*) can be significantly larger (upto 50 *cm*) while the frequency (*f*) of movement is lower (less than 2 *Hz*<sup>228, 278</sup>). Based on these values the required range for an accelerometer is 8*g*. Considering the definition of rigidity as the resistance to passive movement, any improvement in rigidity would decrease the resistance and instantaneously increase the speed of the movement. Combining this information with the scenario of intraoperative evaluation of rigidity described in Section 2.5.2, it can be hypothesized that any change in rigidity due to stimulation could be detected by using an acceleration sensor. Contrary to tremor evaluation though, the acceleration sensor should be attached to the evaluator's wrist (**Figure 3.1**) instead of the patient. This counter-intuitive approach is based on the thinking that such a setup would result in better recording of passive movements of the wrist joint.

The above estimation of accelerometer range assumes that tremor or passive movements are uniaxial, which in reality is not the case. Therefore, in practice, a triaxial accelerometer is necessary to record these movements. Commercial accelerometers record inertial acceleration and are influenced by the acceleration due to gravity (*1g*).<sup>83</sup> This influence will vary on individual axis based on the orientation of the accelerometer, but will appear as a constant on the vector magnitude of acceleration. Furthermore, accelerometers by design cannot measure rotations about their own axis. But the data they record will be influenced by the rotational component of pathological tremor as the rotational axis of a patient's limb does not match the axis of the accelerometer.

### 3.1.2 Clinical Requirements

Apart from the technical specifications necessary for evaluation of tremor and rigidity, certain constraints are imposed by the environment of the operating room in which the acceleration sensors would be used. The sensors must be attached to the patient or the evaluator to record data and therefore should not cause any allergic reactions. It should also not have electrical leakage or overheat after long periods of use. In addition, it should be possible to disinfect the sensor or its housing so as to prevent any hygienic hazards in the operating room. Sterilization of the equipment was not necessary as it was to be used



**Figure 3.1:** The accelerometer sensor mounted on the neurologist's wrist to measure the acceleration of passive movements to evaluate rigidity.

in the non-sterile area of the operating room. An additional requirement set by the setup for DBS surgery is in terms of electromagnetic noise. The MER equipment is very sensitive to external noise due to the small range of electrical activity that it measures in the patient's brain. For this purpose, before MER is performed, any devices that could potentially cause electromagnetic interference are turned off in the operating room. The chosen acceleration sensor should therefore not create any such interference. In case of unforeseen circumstances, it should be possible to stop the data recording and detach the acceleration sensors quickly.

Data collection using the acceleration sensor during DBS surgeries would have to be approved by the local ethics commission of the surgical center. In Switzerland, these commissions are governed by the Federal laws. Based on these laws, the clinical study for this doctoral work would fall under the Ordinance on Human Research with the Exception of Clinical Trials (HRO 810.301<sup>347</sup>). In order to be categorized as a study with minimal risks and burdens, it would be necessary to use a device certified by governing authority in Switzerland or bears the Conformité Européenne (CE) marking.<sup>346</sup> Thus, while it would be possible to acquire commercial sensor modules and connect them to a microcontroller in house, such a setup would present significant hurdles in attaining approval from the ethics commission. On the other hand, commercial accelerometer based devices which are approved for evaluating tremor use wireless communication



**Figure 3.2:** The photo shows the STEVAL-MKI022V1, ST, Geneva, Switzerland sensor evaluation board placed in a 3D printed case and a Velcro strap that is used to attach the sensor.

to transfer the data to the recording software. In addition, the analysis of the data would be done through proprietary algorithms which may or may not be valid for intraoperative evaluations. Rigidity evaluations with such a system would not be possible.

### 3.1.3 Hardware

With regards to all the requirements described above, the commercially available sensor evaluation board STEVAL-MKI022V1 based on the LIS331DLH accelerometer from ST, Geneva, Switzerland, was chosen. The LIS331DLH is a triaxial accelerometer with a maximum range of  $\pm 8g$  and is coupled with a ST7-USB microcontroller which can transfer data at a maximum sampling rate of 400 Hz. This is sufficient to record pathological tremor which is known to have a frequency of less than 10 Hz. It can be connected to a computer using a USB connection to record data using software from ST or custom made software. A case was designed for the board in-house at the Institute for Medical and Analytical Technologies (IMA) and 3D-printed using non-conductive biocompatible material (FullCure 830 VeroWhite, Stratasys, Eden Prairie, USA). The case could be attached to the patient or evaluator's arm using a hook-and-loop Velcro strap (**Figure 3.2**).

### 3.1.4 Software

Data collection during surgery needs a software tool to complement the dedicated hardware. The tool must be able to record acceleration data in quick succession and save them to allow post-operative analysis. In addition to the acceleration data, it should also be able to save information pertaining to each surgical procedure like the position of the electrode and the stimulation param-

ters corresponding to the acceleration data collected. Real-time visualization of the data is necessary to indicate proper functioning. The software provided by ST for recording the data is useful to test the range of the evaluation board, but does not satisfy all the above requirements. Therefore, a new software called LemurDBS (Fachhochschule Nordwestschweiz (FHNW), Muttenz, Switzerland) capable of recording accelerometer data from the evaluation board was developed in Java (Oracle, Redwood City, United States). The user interface was designed to be customized for each surgery based on the planning to simplify data recording (**Figure 3.3**). Provisions were made to input other data like the number of planned trajectories, distance of the stimulation position from the target, the stimulation current amplitude and therapeutic and adverse effects. These data were stored for each position in separate files to allow post-operative analysis. Apart from the modules necessary for accelerometer data recording, others were also added which could import patient images and visualize them, identify the stereotactic frame and visualize the planned target in 3D.

### 3.1.5 Synchronization

An important part of the recording setup was the synchronization with the equipment used for acquiring MER data and delivering current for stimulation tests. Such a synchronization between the two systems is necessary to precisely correlate changes in the symptoms to the stimulation parameters. Various commercial systems are available and can vary from center to center. Provisions for synchronization were developed for two such systems that were used in the two clinical centers from where data were acquired for this work: MicroGuide Pro (Alpha Omega Eng. Nazareth, Israel) and LeadPoint (Medtronic, Minneapolis, USA). For the MicroGuide Pro, a 5V pulse was sent to one of its input channels using a USB-TTL cable at the start of accelerometer data acquisition. This signal was saved by the system in its data which was exported after the surgery for post-operative analysis. Synchronization with the LeadPoint system was achieved by acquiring time-stamped analogue stimulation signal. These setups allowed synchronization of the accelerometer data with the stimulation signal within millisecond accuracy.

### 3.1.6 Laboratory tests

The above setup was tested in the laboratory environment for electrical leakage, temperature changes after prolonged periods of recording, disinfection capabilities and any other potential hazards. No electrical leakage was found in the hardware setup and, as an additional precaution, a portable computer powered by its battery only was used to record the accelerometer data during surgery. Accelerometer data was acquired continuously for 5 hours which slightly raised the temperature of the sensor by 2.5 °C. This increase does not pose a severe risk because the maximum duration of a recording during the surgery would be

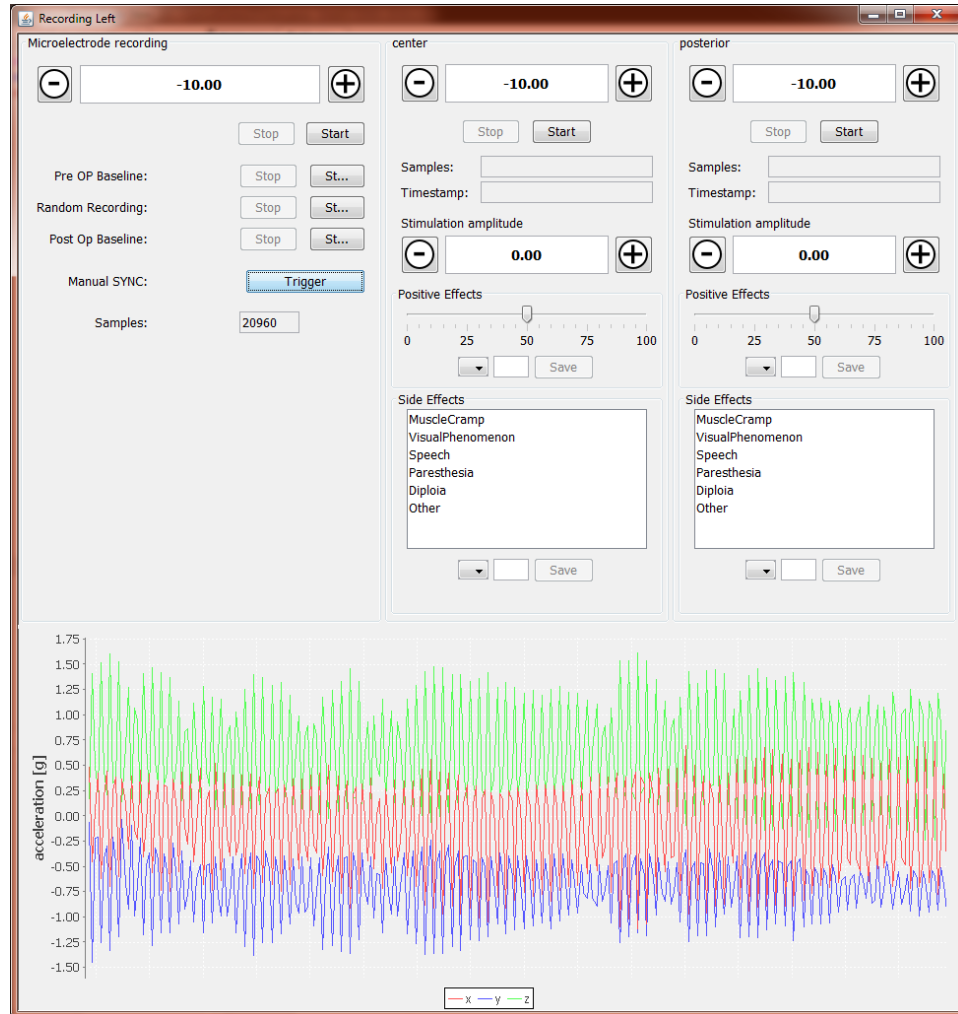


**Figure 3.3:** Image of the software LemurDBS (FHNW, Muttentz, Switzerland) designed to record acceleration data during DBS surgery. The first panel is used to record pre-op and post-op baseline and during MER. The other two panels are for recording during stimulation. The stimulation current amplitude and observed therapeutic and adverse effects can also be saved. The panel for trajectories are added based on the choices made during surgical planning. The panel below displays the acceleration data recorded in real-time.

15 minutes and the case for the board would insulate the patient from the heat. The case also made it possible to disinfect the hardware before every surgery. The Velcro strap simplified attaching and detaching the sensor to and from the patient; the patient could also remove it by his/herself if he/she felt uncomfortable wearing it. Apart from these tests, as we aimed to answer a basic research question and as the sensor evaluation board had CE markings, it was possible to categorize the study as bearing minimum risks and burdens to the patient and consequently simplify acquiring approval from the ethics commission.

## 3.2 Clinical Studies

The accelerometer data recording setup described above had to be used during DBS surgeries to acquire data. The DBS surgical procedure varies from center to center and, thus, to test the versatility of the system, two clinical studies were set up. In comparison to setting up one large multinational multi-center study, two studies in different countries were easier to set up from an administrative point of view.

### 3.2.1 Study 1: Clermont-Ferrand

One clinical study was set up at the neurosurgery department of CHU, Clermont-Ferrand lead by Prof. Jean-Jacques Lemaire. He was the principle investigator of this study which aimed to use the setup described above as a quantitative tool to estimate changes in *rigidity and tremor* and to compare the results to currently used methods. Other aims include studying the influence of quantitative symptom evaluation on lead placement, comparing efficiency of different anatomical structures in suppressing symptoms and use the data to collect more information about the mechanisms of action of DBS. The study was designed to last for 2 years and to collect data from 20 DBS surgeries. The criteria for selecting patients were:

- age between 18 and 70 years
- absence of cognitive deterioration
- absence of depression
- PD patients with levodopa sensitivity more than 50% in the 6 months preceding the surgery and presence of disabling adverse effects of levodopa
- ET patients with more than a year old disabling pathology that is refractory to medical treatment
- absence of lesions of basal ganglia on MRI
- absence of neurosurgical or anaesthetic counter indications to surgery.

- presence of tremor and/or rigidity
- written consent of patient

The exclusion criteria for the study were:

- patients with cognitive impairment, progressive psychiatric conditions or at high risk for surgery
- patients whose medical or surgical history is deemed to be incompatible with the test by the investigator
- pregnant women.

The details of the 20 patients that were recruited in the study are presented in **Table 3.1**. To summarize, 6 ET patients underwent VIM-DBS implantation, 2 PD patients underwent VIM-DBS implantation and 12 PD patients underwent STN-DBS implantation. Data collected from two surgeries were not usable because one patient took the regular medication before surgery which suppressed the symptoms and another patient had no tremor during the surgery.

### 3.2.2 Study 2: Basel and Bern

A multicentre clinical study was undertaken in Switzerland at the Universitätsspital Basel and Inselspital Bern with Dr. Ethan Taub and Dr. med Michael Schüpbach as the primary investigators respectively. The pilot study was undertaken with the aim to use accelerometry to quantitatively evaluate *tremor* during DBS surgery to compare the efficiency of different structures and identify the one that significantly alleviates tremor. The planned duration of the study was 2 years with the goal to include 10 patients. The inclusion criteria for the study were:

- age 18 or above
- medically intractable tremor
- well-documented clinical diagnosis of PD or ET
- clinical determination by the interdisciplinary DBS team that tremor treatment using DBS is indicated
- informed consent to surgery and to participation in the study

The exclusion criteria for the study were:

- cognitive or emotional impairment that would render the subject unable to give informed consent to DBS or to participation in the study (this had to be explicitly assessed by the psychiatrist and neuropsychologist in the interdisciplinary DBS team)

Patient Number	Disease	Symptom Evaluated	DBS Target
1	PD	Tremor	STN
2	ET	Tremor	VIM
3	PD	Rigidity	STN
4	ET	Tremor	VIM
5	PD	Tremor	STN
6	ET	Tremor	VIM
7	ET	Tremor	VIM
8	PD	Rigidity	STN
9	PD	Tremor	VIM
10	ET	Tremor	VIM
11	PD	Rigidity	STN
12	PD	Tremor	VIM
13	PD	Rigidity	STN
14	PD	Rigidity	STN
15	PD	Rigidity	STN
16	PD	Rigidity	STN
17	PD	Rigidity	STN
18	PD	Tremor	STN
19	PD	Rigidity	STN
20	ET	Tremor	VIM

**Table 3.1:** The details of the patients that were recruited as a part of the clinical study in CHU, Clermont-Ferrand, France. The "Symptom Evaluated" columns shows which symptom was evaluated quantitatively during the surgery. Tremor was evaluated for tremor-dominant PD and ET patients. Rigidity was evaluated for the PD patients that presented severe rigidity.

- lessened communicative ability (because of deafness, lack of a common language with DBS team, or other reasons) that would render the subject unable to give informed consent or to cooperate with the clinicians and investigators during the DBS procedure
- major pathological findings on brain MRI unrelated to PD or ET
- bleeding disorders, therapeutic anticoagulation, infectious conditions, or other medical factors that would contraindicate surgery because of increased risk

- pregnancy (which is a temporary contraindication to DBS surgery in general, regardless of study participation)
- lack of informed consent to surgery or to participation in the study

**Table 3.2** lists the details of the 10 patients that were included in the study. Seven PD patients underwent STN-DBS while one PD and two ET patients underwent VIM-DBS. Data collected from 3 surgeries could not be used for analysis due to suppression of tremor during surgery or failure of synchronization between LemurDBS and the MER system. For another 3 patients, data was recorded only during one implantation as this led to severe suppression of symptoms on the ipsilateral side.

Patient Number	Disease	Symptom Evaluated	DBS Target
1	PD	Tremor	STN
2	PD	Tremor	STN
3	PD	Tremor	STN
4	ET	Tremor	VIM
5	PD	Tremor	STN
6	PD	Tremor	STN
7	PD	Tremor	STN
8	ET	Tremor	VIM
9	PD	Tremor	STN
10	PD	Tremor	VIM

**Table 3.2:** The details of the patients that were recruited as a part of the multicenter study in Universitätsspital Basel and Inselspital Bern in Switzerland

### 3.2.3 Data Recording Protocol

Data recording during the surgery has to be consistent among patients to perform a collective analysis. Therefore, data recording protocols were defined for tremor and rigidity evaluation. In general, recording must be started before the stimulation is delivered in order to establish a baseline state of the symptom severity for every stimulation test. However, the protocol had to be modified to accommodate variations in tremor and rigidity evaluation as well as evaluation at different clinical centers. The specifics of data recording protocols are available in the relevant sections: Section 4.2 for tremor evaluation and Section 5.1 for rigidity.

## **Chapter 4**

# **Quantitative Tremor Evaluation during DBS Surgery**

The details of our method to evaluate tremor during DBS surgery using accelerometer have been published in two peer-reviewed papers attached in the following sections. The first publication (Section 4.1) is a case-study describing the method and its application to 2 patients which was presented at the 6th Annual International IEEE EMBS Conference on Neural Engineering. The second publication (Section 4.2) contains the exhaustive details about the method and its use in two clinical studies.

## 4.1 A method to quantitatively evaluate changes in tremor during deep brain stimulation surgery

**Authors:** Ashesh Shah, Jérôme Coste, Jean-Jacques Lemaire, Erik Schkommodau, and Simone Hemm-Ode

This paper was submitted to the 6th Annual IEEE EMBS conference on neural engineering which was held in San Diego, California, United States of America from 6th to 8th November, 2013. The aim of this paper is to demonstrate the feasibility and advantages of using quantitative tremor evaluation during DBS surgery.

The paper is available at the address :  
<https://doi.org/10.1109/NER.2013.6696155>

Copyright Notice: ©2013 IEEE. Reprinted, with permission, from Ashesh Shah, Jérôme Coste, Jean-Jacques Lemaire, Erik Schkommodau, and Simone Hemm-Ode, A method to quantitatively evaluate changes in tremor during deep brain stimulation surgery, 2013 6th International IEEE/EMBS Conference on Neural Engineering (NER), November, 2013.

In reference to IEEE copyrighted material which is used with permission in this thesis, the IEEE does not endorse any of Universität Basel's products or services. Internal or personal use of this material is permitted. If interested in reprinting/republishing IEEE copyrighted material for advertising or promotional purposes or for creating new collective works for resale or redistribution, please go to [http://www.ieee.org/publications\\_standards/publications/rights/rights\\_link.html](http://www.ieee.org/publications_standards/publications/rights/rights_link.html) to learn how to obtain a License from RightsLink.

## A Method to Quantitatively Evaluate Changes in Tremor During Deep Brain Stimulation Surgery\*

Ashesh Shah, Jerome Coste, Jean-Jacques Lemaire, Erik Schkommodau, *Member, IEEE*, and Simone Hemm-Ode

**Abstract**— Deep Brain Stimulation (DBS) surgery is used increasingly as a symptomatic treatment for patients with movement related neuro-degenerative disorders. However, the method of intraoperative symptom evaluation is subjective. This paper proposes a method to quantitatively evaluate tremor by measuring the acceleration of the patient's wrist during the surgery. The results of applying the method to 2 patients suggest that the acceleration measurements are very sensitive to the change in the tremor and that they can be used to identify clinically effective stimulation amplitudes. By collecting acceleration data from DBS surgeries for many patients, we hope to add more knowledge to the mechanisms of deep brain stimulation.

### I. INTRODUCTION

Essential tremor and particularly Parkinson's disease are among the most prevalent neuro-degenerative movement related disorders [1]. Although, there are drugs which can be used to treat the symptoms, Deep Brain Stimulation (DBS) surgery is used as the alternative symptomatic treatment as well. For 25 years, DBS has become a commonly performed operation for the treatment of such disorders. Nevertheless, the mechanism of action of this therapy is so far only incompletely understood.

DBS is a complex surgical treatment in which electrodes are implanted in the deep brain structures which are stimulated using a neuro-stimulator implanted in the chest. Careful planning is done on anatomical images of the patient's brain to map out a path to implant the electrodes. In order to locate the best position of the electrodes to control the symptoms, most centers perform the surgery under local anesthesia. Micro-electrodes are used to record the electrical activity at previously planned positions to identify the location of the deep brain structures (Micro-electrode recording MER). This is followed by test stimulation at some or all of those locations and changes in the patient's symptoms and occurring side effects are observed visually and by clinical examination. The electrode is finally implanted at the location with the best effect on the symptoms and the least side effects.

One aspect of DBS which needs to be improved is the symptom evaluation during the surgery[2]. The current

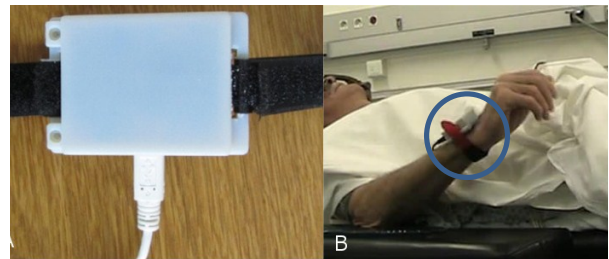


Figure 1. A) Accelerometer case B) Accelerometer mounted to patient during surgery

methods are semi-quantitative and the judgment is largely based on the experience of the neurologist. Various methods to quantitatively evaluate tremor have been proposed using different methods like accelerometry, use of gyro meters, and EMG recording [3-7]. However, very few methods [8-10] are designed to be used in the operating room (OR), while none of them have become a part of the routine surgical procedure. The method proposed in this paper uses accelerometer to quantify the change in the tremor of the patient. Compared to the existing methods based on accelerometers [11], this method is designed specifically for usage during the DBS surgery.

### II. METHOD

#### A. Equipment

The quantitative evaluation of tremor is achieved using an accelerometer attached to the patient's wrist. A commercial accelerometer system evaluation board (STEVAL-MKI022V1, ST Micro, Geneva, Switzerland) is used for this purpose. The sampling frequency used in this method is 400 Hz. This evaluation board is placed inside an in-house developed, non-conductive printed plastic case (FullCure 830 Vero White, Objet Geometries Ltd - Belgium) and tied behind the wrist using a Velcro strap (Fig. 1). An USB cable (along with an extension) is used to interface this board with a laptop computer to record data.

An in-house application (Lemur DBS) has been developed using Java (Oracle Corporation, California, USA) to record the data during the surgery. The software is initialized by interfacing it with the accelerometer board and defining the recording protocol (see below). The software then opens a recording window tweaked for the defined protocol. The software also allows the user to select the different parameters (like stimulation position or amplitude, for example) during an acceleration recording and stores these parameters for referencing at the time of data analysis. The recorded acceleration data is also displayed in graphical manner in real-time. The software creates a new data file for each acceleration recording to simplify the data analysis.

\*Research supported by Swiss National Science Foundation.

A. Shah, E. Schkommodau and S. Hemm-Ode are with the Institute of Medical and Analytical Technologies, University of Applied Sciences and Arts Northwestern Switzerland (phone: 0041 (0)61-467-4413; e-mail: ashesh.shah@fnw.ch).

J.-J. Lemaire and J. Coste are with the Centre Hospitalier Universitaire de Clermont-Ferrand, Image-Guided Clinical Neurosciences and Connectomics (EA 7292, IGCNC), Université d'Auvergne, France (email: jerome.coste@udamail.fr).

In order to synchronize the data between acceleration measurements and the intraoperative electrophysiological system (MicroGuide; Alpha Omega Eng., Israel), an USB-TTL cable is used. When an acceleration recording is started, a TTL signal is sent to the electrophysiology system, which stores the signal according to the time, the position, the trajectory and the stimulation amplitude.

A video recording is also made during the surgery for the interpretation of unexpected signals.

### C. Surgical Procedure

The routine surgical procedure at the University Hospital in Clermont-Ferrand is distributed over 2 days, planning and surgical procedure. For the planning, a stereotactic frame (Leksell G frame, Elekta, Sweden), with its repositioning kit, is mounted on the patient under the local anesthesia, and stereotactic images (CT and MRI) are obtained. The frame is then removed during the planning phase and remounted just before the surgery. Using the stereotactic planning software (Iplan 3, Brainlab, Feldkirchen, Germany) the deep brain structures are carefully identified and manually outlined on the patient's MRI. The labeling of the different structures is performed based on surgical anatomical knowledge and in-house 3D 4.7-Tesla MRI anatomy software [12]. After identifying the target structures, trajectories are planned for the patient in a manner to avoid blood vessels and the caudate nucleus. On these trajectories, test stimulation locations are identified from maximum 10 mm, in steps of 1mm in the region of interest.

The actual DBS surgery is performed on the next day of the planning. Before performing test stimulations, micro-electrode recording (MER) is done at the planned locations to confirm the position of the deep brain structures. MER is followed by test stimulations at all or most of the planned locations. At each location, the neurosurgeon changes the stimulation current from 0 to 3mA in steps of 0.2mA and identifies the stimulation amplitude at which a considerable change is observed in the patient's tremor (subjective threshold). The decrease in the tremor amplitude is identified in 5 levels (0, 25%, 50%, 75%, and 100%) and is noted along with the amplitude. The neurosurgeon also checks for side-effects of stimulation and the amplitudes at which they are first observed (side effect threshold).

After completion of test stimulation for all the positions, the neurosurgeon, mentally visualizes the subjective and the side-effect thresholds with reference to the anatomy. The final implant location for the optimized DBS electrode contact will be the position with the lowest subjective threshold on tremor, with the largest difference between the latter and side-effect threshold. In the case of bilateral implantation, the above procedure is repeated for the second brain hemisphere.

### D. Data Recording Protocol

In order to maximize the acceleration data recording and minimize the obstruction to routine surgery, a recording protocol has been defined. Before the start of the surgery, a baseline recording is performed. The acceleration sensor is then disconnected during the remounting of the frame and surgical preparations. Acceleration data recording is resumed during MER for every pre-planned position. The

acceleration data recording is started after the start of MER recording in the electrophysiological system. After completion of MER for all the positions, test stimulations are performed at those locations to observe the effects and the side-effects. Contrary to MER, acceleration data recording is started a few seconds before the test stimulation and is continued till the end of test stimulation for every position. The data recorded without any stimulation is used as a baseline data during the analysis to identify changes in the patient's tremor.

On completion of the surgery, another acceleration recording is performed to use as a post-operative baseline.

### E. Data Analysis

The accelerometer data analysis involves many different steps. The data recorded in the electrophysiology system is analyzed using Neuroexplorer (Nex Technologies, Madison, Alabama, USA). The synchronization time stamps and the stimulation amplitude are transferred to Matlab (Mathwork Inc., Massachusetts, USA) for further analysis. A Matlab function has been developed to analyze the data recorded for one side of the brain.

As a first step, the synchronization points and the stimulation amplitude are extracted from the electrophysiology data. This is followed by importing the acceleration recording into Matlab. The accelerometer data is then synchronized to the time stamps from the electrophysiology system and this synchronization is visually verified. The data from the 3 different axes of the accelerometer, stored in separate columns at first, are combined by calculating the RMS value for every sample. In case when rigidity and tremor were both present but the clinician decided to mainly observe stimulation effects on tremor, the data corresponding to the rigidity evaluations within the acceleration data were removed. A time varying high-pass filter (cut-off 2 Hz) called smoothness priors method [13] was used to remove the low-frequency trends and acceleration due to gravity. Another low pass Butterworth filter (cut-off 10 Hz) is used to filter the noise and then statistical features are extracted in a windowed manner (Fig 2).

A non-overlapping window of 2 seconds (795 samples on

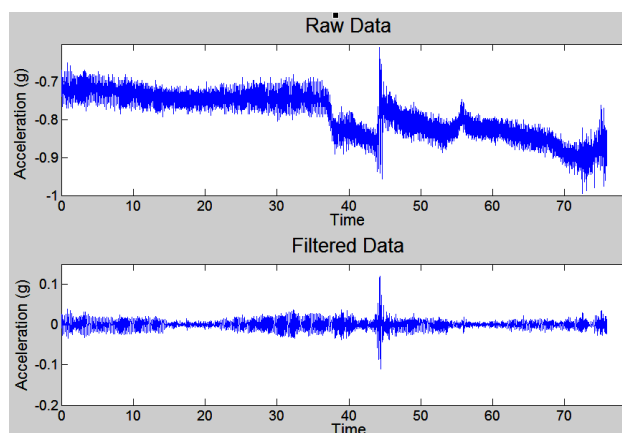


Figure 2. A. Raw signal including arm movement in addition to tremor (see arrows). B) The signal after application of smoothness priors and Butterworth filter.

average) is chosen for optimum analysis based on factors like average duration of one stimulation amplitude, sampling rate, etc. From the windowed data, the standard deviation, signal energy, signal entropy, peak frequency and peak frequency amplitude (standard fft function in Matlab) are extracted. Thereafter, the baseline data recorded just before the corresponding test stimulation is imported into Matlab and statistical features are extracted from it in the same way as from the test stimulation acceleration data. These statistical features are then plotted on a graph and the best baseline features are selected for further analysis.

The statistical features extracted from the acceleration data are then normalized to the baseline value. These normalized features are used to extract the stimulation amplitude at which a change in the tremor is observed, referred as acceleration threshold. Three such acceleration thresholds are calculated from the normalized parameters corresponding to their change as compared to the baseline - 25% reduced, 50% reduced, and 75% reduced. Such acceleration thresholds are extracted for every position on each trajectory. These acceleration thresholds are represented graphically along with the side-effect thresholds and a final implant site is decided as the position which has the lowest acceleration threshold and the largest difference between the that and the side-effect threshold for every brain side.

#### F. Case studies

Under an ongoing clinical study at the University Hospital in Clermont-Ferrand, France, data was recorded following the above described protocol on 2 patients being good candidates for DBS surgery following the international guidelines [14]. No alterations were made to the routine surgical procedure. Both patients showed high amplitudes of tremor.

Patient 1 included in the study underwent a bilateral DBS implantation in the subthalamic nucleus (STN) for the treatment of Parkinson's disease. For the left hemisphere, 11 positions were explored for test stimulation starting from the zona incerta to the subthalamic nucleus on two parallel trajectories (6 on central and 5 on 2mm-posterior). For the right hemisphere, 18 positions were explored from the thalamus to the subthalamic nucleus via the zona incerta on the same two trajectories (9 each). Along with high tremor patient 1 showed rigidity.

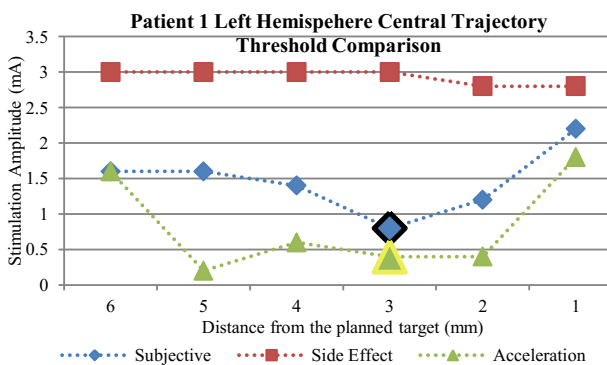


Figure 3. Comparison of different thresholds for left hemisphere, central trajectory of patient 1. The highlighted markers indicate the final implant location chosen based on subjective data (blue with black border) and acceleration data (green with yellow border).

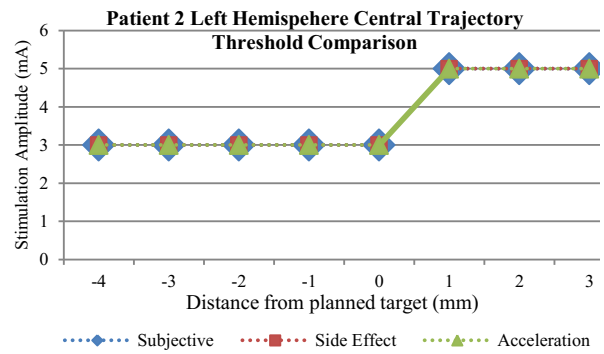


Figure 4. Comparison of thresholds for central trajectory of left hemisphere of patient 2. Since the stimulation did not cause any effect, no thresholds were found.

Patient 2 underwent bilateral DBS implantation in the ventralis intermedius nucleus (Vim) for the treatment of Essential tremor. Sixteen test stimulation locations were explored for central (8) and posterior (8) trajectories for the left hemisphere, while 14 locations were explored for the same trajectories (7 each) for the right hemisphere. Both trajectories were planned to explore different thalamic regions involved in tremor. Patient 2 presented high amplitudes of tremor and the neurosurgeon had to stimulate till 5.0 mA to observe an effect on the tremor.

### III. RESULTS

A total of 59 recordings were made during the test stimulations for the two patients. Out of the different acceleration thresholds identified, 80% of the 75% thresholds are lower than the subjective threshold, 90% of the 50% threshold are lower than the subjective threshold and 99% of the 25% threshold are lower the subjective threshold.

All of the 3 different acceleration thresholds for patient 1 are equal to or lower than the subjective threshold suggesting that the stimulation location was very effective. Fig 3 shows the comparison between different thresholds for right hemisphere, central trajectory. The 75% acceleration threshold corresponded well with the subjective thresholds. The final implant site determined based on acceleration thresholds (Fig 3 for left hemisphere only) for both the brain sides are the same as the one decided based on the surgery (Fig 3 for the left hemisphere only).

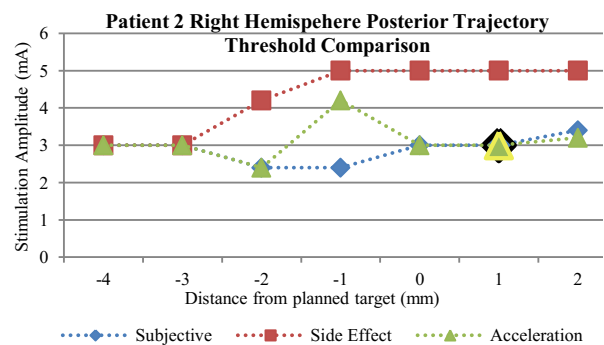


Figure 5. Comparison of thresholds for the posterior trajectory of the right hemisphere of patient 2. The highlighted markers indicate the final implant location chosen based on subjective data (blue with black border) and acceleration data (green with yellow border).

In the case of patient 2, at 14 of the 30 stimulation locations the acceleration features changed by less than 50%. This suggests that the stimulation effect at this location was not very effective. This was also confirmed for the central trajectory of the left hemisphere (Fig 4), where 75% acceleration thresholds and subjective thresholds could both not be found for any position. For the other trajectories, the 75% acceleration threshold corresponded well with the subjective threshold. The final implant site determined based on acceleration thresholds (Fig 5 for the right hemisphere only) for both the brain sides are the same as the one decided based on the surgery (Fig 5 for the right hemisphere only)

#### IV. DISCUSSION

The method described in the paper demonstrates that by using acceleration measurements of the patient's wrist it is possible to quantify the changes in tremor during DBS surgeries without hindering the existing surgical procedure. Simple statistical features like standard deviation can be used to quantify the changes in the tremor of the patient. From the results of the two patients, it is clear that the acceleration measurements are very sensitive to the changes in tremor. The differences between the subjective and the acceleration threshold suggest that by objectively evaluating tremor, target selection in DBS can be improved.

One of the main factors that influence the objective evaluation using acceleration data is the baseline data. It is very important that during the baseline data recording, the patient is in a state of high tremor.

Although this method can objectively evaluate tremor, it has so far only been used for post-operative analysis and not yet in the operating room during the target selection procedure. Thus, our next step is to implement the data analysis in our recording software to extract the statistical features in real-time. We intend to visualize these features and other information about the surgery on the patient's anatomical images so as to support the neurosurgeon during target selection. Furthermore, we are also working on a method to evaluate rigidity during DBS surgery.

In addition to the optimization of the targeting procedure, the collected acceleration data will be correlated with the anatomical structures and electrophysiological signal to get more knowledge about the mechanism of action of DBS. This is the primary intention why to record acceleration data during MER in the clinical study. By collecting data in many surgeries and correlating them to different information about the deep brain, new information related to the mechanisms of DBS may come to light.

#### V. CONCLUSION

The current paper presents a methodology allowing intraoperative acceleration measurements for tremor evaluation during DBS electrode implantation. First results are encouraging but have to be confirmed in further patients included in the clinical study. The objectively obtained data in correlation with the patient's anatomy might represent an interesting approach to further elucidate the mechanism of action of DBS.

#### ACKNOWLEDGMENT

The authors would like to thank Germaine De Stael for providing the travel funds to collect data during the surgery.

#### REFERENCES

- [1] M. Stacy, "Medical Treatment of Parkinson Disease," *Neurologic Clinics*, vol. 27, no. 3, pp. 605–631, 2009.
- [2] S. Hemm and K. Wårdell, "Stereotactic implantation of deep brain stimulation electrodes: a review of technical systems, methods and emerging tools," *Med Biol Eng Comput*, vol. 48, no. 7, pp. 611–624, 2010.
- [3] G. Rigas, A. Tzallas, D. Tsalikakis, S. Konitsiotis, and D. Fotiadis, "Real-time quantification of resting tremor in the Parkinson's disease," pp. 1306–1309.
- [4] S. M. Rissanen, M. Kankaanpää, M. P. Tarvainen, V. Novak, P. Novak, Kun Hu, B. Manor, O. Airaksinen, and P. A. Karjalainen, "Analysis of EMG and Acceleration Signals for Quantifying the Effects of Deep Brain Stimulation in Parkinson's Disease," *IEEE Trans. Biomed. Eng.*, vol. 58, no. 9, pp. 2545–2553, 2011.
- [5] L. M. Gil, T. P. Nunes, F. H. S. Silva, A. C. D. Faria, and P. L. Melo, "Analysis of human tremor in patients with Parkinson disease using entropy measures of signal complexity," (eng), *Conf Proc IEEE Eng Med Biol Soc*, vol. 2010, pp. 2786–2789, 2010.
- [6] H. Jeon, S. K. Kim, B. Jeon, and K. S. Park, "Distance estimation from acceleration for quantitative evaluation of Parkinson tremor," (eng), *Conf Proc IEEE Eng Med Biol Soc*, vol. 2011, pp. 393–396, 2011.
- [7] P. H. G. Mansur, L. K. P. Cury, A. O. Andrade, A. A. Pereira, G. A. A. Miotto, A. B. Soares, and E. L. M. Naves, "A review on techniques for tremor recording and quantification," (eng), *Crit Rev Biomed Eng*, vol. 35, no. 5, pp. 343–362, 2007.
- [8] M. M. Koop, A. Andrzejewski, B. C. Hill, G. Heit, and H. M. Bronte-Stewart, "Improvement in a quantitative measure of bradykinesia after microelectrode recording in patients with Parkinson's disease during deep brain stimulation surgery," (eng), *Mov Disord*, vol. 21, no. 5, pp. 673–678, 2006.
- [9] M. J. Birdno, A. M. Kuncel, A. D. Dorval, D. A. Tumer, and W. M. Grill, "Tremor varies as a function of the temporal regularity of deep brain stimulation," (eng), *Neuroreport*, vol. 19, no. 5, pp. 599–602, 2008.
- [10] S. D. Tabbal, F. J. Revilla, J. W. Mink, P. Schneider-Gibson, A. R. Wernle, G. A. de Erausquin, J. S. Perlmutter, K. M. Rich, and J. L. Dowling, "Safety and efficacy of subthalamic nucleus deep brain stimulation performed with limited intraoperative mapping for treatment of Parkinson's disease," (eng), *Neurosurgery*, vol. 61, no. 3 Suppl, pp. 119-27; discussion 127-9, 2007.
- [11] H. L. Journee, A. A. Postma, and M. J. Staal, "Intraoperative neurophysiological assessment of disabling symptoms in DBS surgery," (eng), *Neurophysiol Clin*, vol. 37, no. 6, pp. 467–475, 2007.
- [12] J. J. Lemaire, F. Caire, J. M. Bonny, J. Kemeny, A. Villeger, and J. Chazal, "Contribution of 4.7-Tesla MRI in the analysis of the MRI anatomy of the human subthalamic area," *Acta Neurochir (Wien)*, vol. 146, pp. 906–907, 2004.
- [13] M. Tarvainen, P. Ranta-aho, and P. Karjalainen, "An advanced detrending method with application to HRV analysis," *IEEE Trans. Biomed. Eng.*, vol. 49, no. 2, pp. 172–175, 2002.
- [14] A. E. Lang and H. Widner, "Deep brain stimulation for Parkinson's disease: Patient selection and evaluation," *Mov Disord*, vol. 17, no. S3, pp. S94, 2002.

## 4.2 Intraoperative acceleration measurements to quantify improvement in tremor during deep brain stimulation surgery

**Authors:** Ashesh Shah, Jérôme Coste, Jean-Jacques Lemaire, Ethan Taub, W. M. Michael Schüpbach, Claudio Pollo, Erik Schkommodau, Raphael Guzman and Simone Hemm-Ode.

This paper is published in the journal titled *Medical & Biological Engineering & Computing*. The aim of this paper is to evaluate tremor quantitatively during stimulation tests for DBS surgery in two observational clinical studies and compare the results with current clinical practice of visual tremor evaluation.

The paper is available at the address:

<https://doi.org/10.1007/s11517-016-1559-9>

Copyright Notice: Reprinted by permission from Springer Nature: *Springer Medical & Biological Engineering & Computing*, Shah, Ashesh, Jérôme Coste, Jean-Jacques Lemaire, Ethan Taub, W. M. Michael Schüpbach, Claudio Pollo, Erik Schkommodau, Raphael Guzman, and Simone Hemm-Ode. 2016. "Intraoperative acceleration measurements to quantify improvement in tremor during deep brain stimulation surgery." *Med Biol Eng Comput.* doi:10.1007/s11517-016-1559-9. ©2016.

# Intraoperative acceleration measurements to quantify improvement in tremor during deep brain stimulation surgery

Ashesh Shah<sup>1</sup> · Jérôme Coste<sup>2,3</sup> · Jean-Jacques Lemaire<sup>2,3</sup> · Ethan Taub<sup>4</sup> ·  
W. M. Michael Schüpbach<sup>5,6</sup> · Claudio Pollo<sup>7</sup> · Erik Schkommodau<sup>1</sup> ·  
Raphael Guzman<sup>4</sup> · Simone Hemm-Ode<sup>1</sup>

Received: 13 March 2016 / Accepted: 8 August 2016  
© International Federation for Medical and Biological Engineering 2016

**Abstract** Deep brain stimulation (DBS) surgery is extensively used in the treatment of movement disorders. Nevertheless, methods to evaluate the clinical response during intraoperative stimulation tests to identify the optimal position for the implantation of the chronic DBS lead remain subjective. In this paper, we describe a new, versatile method for quantitative intraoperative evaluation of improvement in tremor with an acceleration sensor that is mounted on the patient's wrist during surgery. At each anatomical test position, the improvement in tremor compared to the initial tremor is estimated on the basis of extracted outcome measures. This method was tested on 15 tremor patients undergoing DBS surgery in two centers. Data from

359 stimulation tests were acquired. Our results suggest that accelerometric evaluation detects tremor changes more sensitively than subjective visual ratings. The effective stimulation current amplitudes identified from the quantitative data ( $1.1 \pm 0.8$  mA) are lower than those identified by visual evaluation ( $1.7 \pm 0.8$  mA) for similar improvement in tremor. Additionally, if these data had been used to choose the chronic implant position of the DBS lead, 15 of the 26 choices would have been different. These results show that our method of accelerometric evaluation can potentially improve DBS targeting.

**Keywords** Deep brain stimulation · Intraoperative monitoring · Acceleration · Tremor · Parkinson's disease · Essential tremor

✉ Simone Hemm-Ode  
simone.hemm@fhnw.ch

- <sup>1</sup> Institute for Medical and Analytical Technologies, University of Applied Sciences and Arts Northwestern Switzerland, Gruendenstrasse 40, 4132 Muttenz, Switzerland
- <sup>2</sup> Image-Guided Clinical Neuroscience and Connectomics (EA 7282), Université Clermont Auvergne, Clermont-Ferrand, France
- <sup>3</sup> Service de Neurochirurgie, CHU Clermont-Ferrand, Clermont-Ferrand, France
- <sup>4</sup> Departments of Neurosurgery and Biomedicine, University of Basel, Basel, Switzerland
- <sup>5</sup> Department of Neurology, University Hospital Bern and University of Bern, Bern, Switzerland
- <sup>6</sup> Assistance Publique Hôpitaux de Paris, Institut National de Santé et en Recherche Médicale, Institut du Cerveau et de la Moelle Epinière, Centre d'Investigation Clinique 1422, Département de Neurologie, Hôpital Pitié-Salpêtrière, 75013 Paris, France
- <sup>7</sup> Department of Neurosurgery, University Hospital Bern, Bern, Switzerland

## 1 Introduction

Parkinson's disease (PD) and essential tremor (ET) are common movement disorders [46]. Deep brain stimulation (DBS), in which electrical leads are surgically implanted in the thalamic, subthalamic, or pallidal region of the brain, is a highly effective symptomatic treatment of these conditions [12]. The leads are connected to a subcutaneously implanted impulse generator (neurostimulator). Unlike ablative surgery, DBS is reversible and adaptable in the setting of progressively worsening disease. Over the past three decades, more than 100,000 patients have been treated with DBS around the world [39].

In many centers, DBS surgery is performed under local anesthesia to enable intraoperative stimulation tests [1] mostly through a specific exploration electrode, for direct observation of the therapeutic effect of stimulation and of side effects. The therapeutic effects induced by stimulation

tests are visually evaluated and rated in different ways by different centers, but always with the same underlying concept: either the observer directly rates the improvement of a symptom (e.g., tremor) in response to stimulation, or the observer rates the severity of the symptom both without and with stimulation using a clinical scale such as the Unified Parkinson's Disease Rating Scale (UPDRS [9]). Previous studies have revealed that such ratings have a low inter-rater [26, 33] and intra-rater [33] reliability because of their subjectivity and their high dependence on the experience of the evaluating neurologist [11]. Moreover, pen and paper are used to note down the subjective ratings of the therapeutic effects and side effects that are observed at varying stimulation parameters and positions; retrospective comparisons once the testing is completed are difficult and dependent on human memory. If the measurement and evaluation of changes in tremor were performed quantitatively, these limitations could be overcome.

Numerous methods with different sensors, including EMG [2, 15, 17, 25, 44], spiograms [7, 37], and gyroscopes [23, 32, 38], have been used to quantify tremor. Accelerometers have been applied outside the operating room (OR) for a wide variety of purposes, e.g., to characterize pathological tremor [8, 13], to compare it with physiological tremor [20, 35, 36], and to evaluate the severity and evolution of tremor [28, 29, 40] and the tremor-alleviating effect of drugs or DBS [22, 36, 47]. Pulliam et al. [34] used motion sensors during postoperative DBS pulse generator programming to develop automated programming algorithms and concluded that objective assessment can improve patients' outcomes. These methods, however, were developed to evaluate tremor outside the OR and cannot be used in their current form during surgery, for multiple reasons. The patient has only limited freedom of movement during surgery, compared to preoperative or postoperative examination; to be useful, intraoperative tremor assessment must be performed at many different positions of the test electrode and at a variety of stimulation current amplitudes; and the surgical team's access to the patient and the level of patient comfort are especially important considerations in the design of systems for intraoperative use.

For these reasons, unlike the numerous methods mentioned above for tremor assessment outside the OR, intraoperative quantitative tremor assessment has only rarely been described in the literature. These descriptions were mostly for research purposes, for example the one-time use of inertial sensors during a thalamotomy [21], the evaluation of the effect of non-constant inter-pulse intervals of DBS stimulation on tremor [4], or the identification of a target structure by spectral correlation of a tremor signal from goniometers with the electrophysiological signal from microelectrode recording [43]. To our knowledge, only Journee et al. [14] and Papapetropoulos et al. [27] evaluated

tremor intraoperatively in a relatively large patient cohort. Their tests, however, seem to have been performed by stimulating through the *chronic DBS lead* in order to ascertain the optimal stimulation parameters, rather than through exploratory test electrodes of the type used in most centers to find the optimal target site for stimulation. None of these methods were used to help determine the best site for DBS lead implantation, nor were any of them implemented in more than a single surgical center or as a part of the regular surgical protocol for DBS. Additionally, to the best of our knowledge, the correlation between the intraoperative visual (subjective) and quantitative evaluations has not yet been thoroughly investigated.

This study presents a method designed for the specific purpose of quantitatively estimating changes in tremor during intraoperative stimulation tests through an *exploratory electrode* to identify the optimal position for implantation of the chronic lead in routine DBS surgery. It tries to overcome the limitations of previous methods by recording data in parallel to conventional subjective visual evaluation, by recording baseline activity before each stimulation test, and by synchronizing the data with the electrophysiology system. The aim of the present study was to evaluate the feasibility and adaptability of the method by applying it to 15 patients undergoing DBS surgery in two clinical centers. Furthermore, the correlations between the recorded accelerometer data and the visual evaluations during surgery were studied to better understand the similarities and differences of the two evaluation methods.

## 2 Materials and methods

### 2.1 Surgical protocol

In order to design a method for intraoperative use, the DBS surgical procedure has to be understood, which, in most centers, can be summarized in 4 steps as follows: (1) the anatomical target and the best path to reach it are defined on the patient images during pre-surgical planning. An electrode trajectory or, in many cases, multiple closely spaced parallel trajectories through the target region are selected for intraoperative testing. (2) At surgery, intraoperative exploratory electrodes are inserted along the chosen trajectory or trajectories, and the target region is electrophysiologically mapped with microelectrode recording (MER). (3) After MER, stimulation test is administered at various locations, and the therapeutic effects and side effects are observed. The visually observed improvement in tremor ( $I_V$ ), the amplitude of the stimulating current that brought about this improvement ( $A_V$ ), and the lowest stimulation current amplitude at which a side effect is observed (side-effect threshold) are noted for each site of stimulation. (4)

**Table 1** Details of the configuration and execution of surgical steps in the two clinical centers that were considered when designing the adaptable accelerometer recording system

Surgical step	Center 1	Center 2
<b>Pre-surgical planning</b>	Direct visual targeting	Combination of AC/PC based and direct visual targeting
<b>Number of trajectories per hemisphere</b>	2	1 to 2
<b>Intraoperative MER</b>	Yes	Yes
No. of explored positions per trajectory	5–10	15 or more
Distance of first position from target (=0 mm)	Based on pre-surgical planning	10 mm
Distance between positions	1 mm	1 mm (5–10 mm) 0.5 mm (4.5 mm to target)
<b>Intraoperative stimulation tests through exploration electrode</b>	Yes	Yes
Test positions	All MER positions	Chosen based on MER data (2 to 6 per hemisphere)
<b>Stimulation pattern</b>	Current-controlled	Current-controlled
Range (mA)	0–3	0–4
Step size (mA)	0.2	0.5 or 1
<b>Visual evaluation of baseline tremor</b>	At every position just before start of test stimulation	Before starting test stimulation of each hemisphere.
<b>Documentation of findings of intraoperative test stimulation</b>	For each position of test stimulation	For each position and amplitude of test stimulation
Level of improvement	Maximum degree of improvement and the stimulation amplitude that induced it	The degree of improvement with stimulation at that position and amplitude
Side effects	Type and amplitude	Type
<b>Rating scale for tremor evaluation</b>	Direct relative improvement rating; 0–4 scale, worst (0) to best (4)	Absolute rating based on UPDRS; 0–4 scale, best (0) to worst (4)
Before stimulation	Baseline tremor defined as 0	Tremor severity based on UPDRS scale
Tremor arrest	4	0
Number of intermediate levels (indicated using underlining)	1 level (0, <u>0.5</u> , 1, <u>1.5</u> ...)	2 levels (4, <u>4-</u> , <u>3+</u> , 3, <u>3-</u> ...)
<b>Choice of chronic implant position for DBS lead</b>	Stimulation test position among a group of adjacently located positions all having a large therapeutic window	Deepest stimulation test position with a large therapeutic window
Stimulating contact	Based on the adjacent positions having large therapeutic windows	Distal contact (number 0)
Contact border		Distal border

The site for implantation of the chronic DBS lead is chosen to be one with low  $A_V$  and a large difference (“therapeutic window”) between  $A_V$  and the side-effect threshold. Optimally, the target site should be one among a group of adjacently located sites that all have a large therapeutic window.

We aimed to design the acceleration recording system to be usable in multiple clinical centers with few or no modifications. Patients from two different clinical centers were included: from the University Hospital in Clermont-Ferrand, France (Center 1), and from the Inselspital in Bern, Switzerland (Center 2). Although the basic surgical steps in these centers correspond to the ones described above, there are significant differences in how these steps are configured and executed. Table 1 lists the various surgical steps and the configuration used in the two centers which were

considered when developing the quantitative symptom evaluation system. In Center 1, stimulation tests are performed at various preoperatively chosen positions on the trajectories (between 10 and 18 per hemisphere) and only the highest improvement in tremor and the corresponding stimulation current amplitude are noted for each stimulation position (one improvement noted per position). In Center 2, stimulation tests are performed only at a few positions (between 2 and 6 per hemisphere) chosen on the basis of the electrophysiological activity observed during MER, but the improvement in tremor is noted for each stimulation current amplitude (between 4 and 8 improvements noted per position). In addition, in Center 1, the stimulation current is varied from 0 to 3 mA in steps of 0.2 mA for each stimulation test position, whereas, in Center 2, the stimulation current

range goes up to 4 mA and the step size is decided based on the observed response of the patient. These differences significantly influence the data recording procedure.

The analysis of the acquired data is also altered because of some of the differences in the surgical procedure like the rating scales for tremor evaluation and the method used for choosing the chronic implant position of the DBS lead. In Center 1, the chronically stimulating lead is implanted at the position having a large therapeutic window itself as well as its adjacent positions, and the contact and its border are chosen in a manner permitting chronic stimulation at these adjacent positions if needed. In Center 2, the distal border of the distal contact is implanted at the deepest effective stimulation position making it possible to chronically stimulate other effective positions located proximally. Such differences should be considered when designing a method for intraoperative use in multiple clinical centers.

## 2.2 Acceleration data recording

A commercially available 3-axis acceleration sensor evaluation board (STEVAL-MKI022V1,<sup>1</sup> ST Micro, Geneva, Switzerland), with a sampling rate of 400 Hz and a range of 8 g, was used to quantify changes in tremor. To facilitate its use in the OR, it was placed in an in-house-developed, non-conductive printed plastic case (FullCure 830 Vero White, Stratasys, Eden Prairie, USA) that can be attached to the patient's wrist with a Velcro strap (Fig. 1). The sensor evaluation board was interfaced with and powered by a laptop via a USB connection.

The data recording setup was approved for use in clinical studies after multiple tests revealed its harmlessness to patients: The chosen 3D printing material was biocompatible. Heating tests performed by continuously recording acceleration data for 5 h marginally raised the temperature of the case by 2.5 °C; the maximum duration of continuous intraoperative recording was 15 min, which would not lead to any degree of heating that would be appreciable by the patient. Nevertheless, the Velcro strap made it possible to remove the sensor at any time at the patient's request in case wearing it was uncomfortable. All the equipment was cleaned with disinfectant wipes before and after each use, and a new Velcro strap was used for each patient, to minimize potential sources of infection. To lessen the risk of leakage currents, the laptop was powered by battery only, rather than by line current.

<sup>1</sup> STEVAL-MKI022V1 (data sheet: <https://www.arrow.com/en/products/steval-mki022v1/stmicroelectronics> or at authors) is no longer produced by the manufacturer. It has been replaced by STEVAL-MKI089V1 evaluation board (data sheet: [http://www.st.com/content/st\\_com/en/products/evaluation-tools/product-evaluation-tools/mems-motion-sensor-eval-boards/steval-mki089v1.html](http://www.st.com/content/st_com/en/products/evaluation-tools/product-evaluation-tools/mems-motion-sensor-eval-boards/steval-mki089v1.html)) which uses the same accelerometer (LIS331DLH) as in the present study.

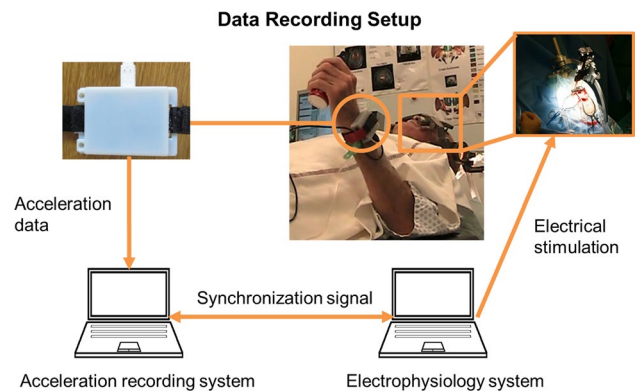


**Fig. 1** Intraoperative data recording setup. The acceleration sensor is inside a plastic case (top left), which is mounted on the patient's wrist with a Velcro strap. The sensor is connected to our recording system (bottom left), which is also connected to the DBS system (bottom right) so that data from the two sources can be synchronized

For data recording and visualization, a computer application (LemurDBS) has been developed in our laboratory in Java (Oracle Corporation, California, USA). In order to make the system adaptable to the varying DBS procedures in different clinical centers, software profiles can be made for individual centers to customize LemurDBS during the initiation phase to adapt it to the center's surgical procedure. In addition, the software can be further adapted for individual operations by providing certain details of the operation, such as the number of trajectories or number of positions at which stimulation tests would be performed. The important information to be obtained intraoperatively, for example the position and amplitude of the stimulation test, any observed side effects, and the threshold amplitudes at which they arose, can be entered manually. During data recording, the acceleration data and extracted outcome measures (for details, see data analysis section) are visualized online to check the correct functioning of the system and to identify any fluctuation of the pre-stimulation baseline tremor. All data are stored for offline analysis.

For data synchronization, the acceleration data recording software was connected to the MicroGuide Pro (Alpha Omega Eng., Nazareth, Israel) or LeadPoint (Medtronic, Minneapolis, USA) electrophysiology systems that were used in the two centers for MER and stimulation tests (Fig. 1). A PhidgetInterfaceKit 2/2/2 board (Phidgets Inc. Calgary, Alberta, Canada) was used for this purpose. A 5 V CMOS signal was sent from LemurDBS to the MicroGuide Pro system at the beginning and end of each acceleration data recording. For the LeadPoint system, synchronization was obtained by acquiring time-stamped analog stimulation signal as measured by the non-stimulating electrode 2 mm away from the stimulating one.

**Table 2** Details of the included patients and their surgical procedures

Patient	Surgical Center	Disease	Target structure	Trajectory position (number of stimulation test positions on this trajectory)	
				Left side	Right side
1	Center 1	PD	STN	Central (6) Posterolateral (5)	Central (9) Posterior (9)
2	Center 1	ET	VIM	Central (8) Posterolateral (8)	Central (7) Posterolateral (8)
3	Center 1	ET	VIM	Central (6) Posterior (6)	Central (7) Posterior (6)
4	Center 1	ET	VIM	Central (5) Posterior (5)	Central (7) Posterior (7)
5	Center 1	ET	VIM	Central (8) Posterior (8)	Central (8) Posterior (8)
6	Center 1	ET	VIM	Central (9) Posterior (9)	Central (5) Posterior (5)
7	Center 1	PD	VIM	Central (7) Posterior (7)	Central (7) Posterior (7)
8	Center 1	PD	STN	Central (7) Posterolateral (7)	Central (6) Posterolateral (6)
9	Center 1	ET	VIM	Central (8) Posterior (8)	Central (8) Posterior (8)
10	Center 2	PD	STN	Central (2)	Central (1) Lateral (1)
11	Center 2	PD	STN	Central (2)	Central (2) Medial (2)
12	Center 2	PD	STN	Central (2) Lateral (1)	Central (2) Lateral (1)
13	Center 2	PD	STN	Central (2) Medial (2) Posterior (1)	Central (4) Medial (4) Posterior (2)
14	Center 2	ET	VIM	Central (2) Medial (2)	Central (2) Medial (2)
15	Center 2	PD	STN	Central (3)	Central (2)

*STN* subthalamic nucleus, *VIM* ventral intermediate nucleus of the thalamus

As MER recording systems are very sensitive to noise, wired connections were used between the laptop, the acceleration sensor, and the electrophysiology system. The wireless system on the laptop was disabled to ensure that no wireless signals were emitted from our recording setup that could interfere with other systems in the OR.

No specific instructions were given to the patient or the surgical team for the data recording, which did not require any conscious effort or participation on their part and therefore did not prolong the operations.

### 2.3 Clinical application

Quantitative evaluation of change in tremor was carried out during DBS implantations of 15 patients, 9 in Center 1 and

6 in Center 2. All patients were good candidates for DBS according to the international guidelines [16]. They gave written informed consent before surgery, and the experimental procedures were approved by the respective Institutional Ethics Committee (Center 1: 2011-A00774-37/AU905; Center 2: 2365—multicenter study together with the University Hospital in Basel). The details of surgery for each patient, including the number of trajectories explored and the number of stimulation tests on each trajectory, are provided in Table 2.

In Center 1, for patient 1, rigidity was also evaluated by the neurologist for short periods of 2–5 s and subsequently recorded during stimulation tests by moving the patient’s forearm. However, rigidity was only evaluated at stimulation amplitudes at which the tremor was suppressed by

stimulation. Patient 7 also exhibited rigidity as a symptom. However, during surgery, only the tremor was evaluated. Because of a software error during the implantation of the left hemisphere of patient 7, no synchronization signal was sent to the electrophysiology system. Hence, data from the left hemisphere could not be analyzed. The problem had no influence on the operation itself and was resolved before the neurosurgeons proceeded to the right hemisphere.

In Center 2, for patient 10, during the stimulation of the right hemisphere, no tremor was observed and rigidity was evaluated by a neurologist during the surgery. Patient 12 had more tremor in the left lower limb than in the left hand; therefore, to test the versatility of the method, the acceleration sensor was mounted on the foot in the distal metatarsal region. The visual evaluation was also based on rest tremor reduction in the patient's foot. During implantation in the right hemisphere of patient 11, the acceleration sensor was unintentionally disconnected from the recording software, and for the right hemisphere of patient 13, no acceleration data were recorded because of waning battery power in the recording laptop.

## 2.4 Data analysis

The raw data recorded during DBS surgery as well as a first analysis were visualized in real time in LemurDBS during surgery. For ethical reasons, the results of the acceleration data analysis were not considered when the chronic implant position for the DBS lead was chosen (the study had been declared a purely observational study of the potential usefulness of a new method, and any influence of the intraoperative accelerometric findings on surgical decision making was explicitly ruled out). An exhaustive data analysis was performed postoperatively in MATLAB (Mathwork Inc., Massachusetts, USA) including a comparison between results of the accelerometric and visual evaluations. Statistical analysis was performed with SOFA Statistics (Paton-Simpson & Associates Ltd, Auckland, New Zealand) and OriginPro (OriginLab Corporation, Massachusetts, USA).

### 2.4.1 Preprocessing

As a first step, the magnitude (square root of sum of squares) of every sample of the 3 different axes of acceleration data was calculated. In general, acceleration signals corresponding to movements other than tremor were also present in the recorded data and could be clearly identified visually. Large movements, like those corresponding to rigidity evaluations, were ignored for real-time analysis and were manually eliminated from the data sets during postoperative evaluation [48]. It was necessary to filter the acceleration data to extract the tremor signal while suppressing the effect of gravity and

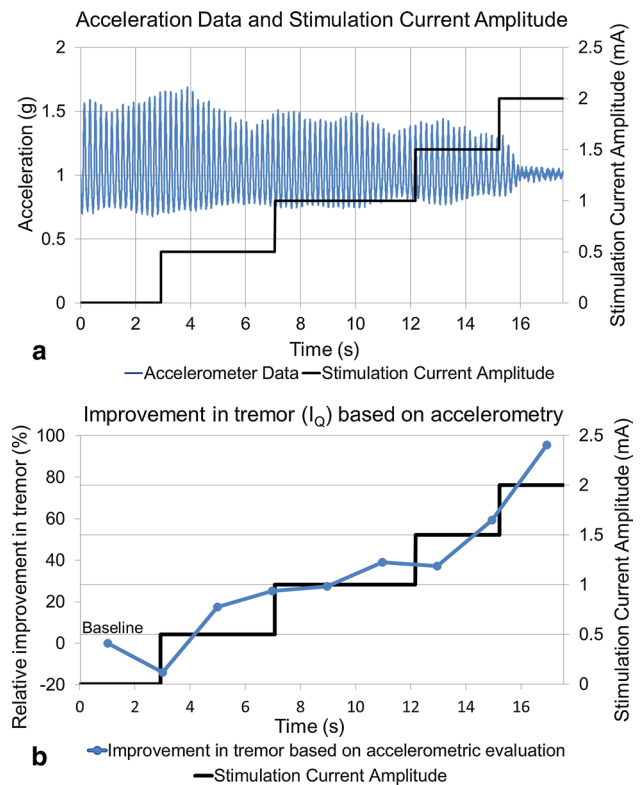


**Fig. 2** a Raw acceleration data (blue signal) recorded in synchronization with the stimulation amplitude (black stepped line). b Improvement in tremor estimated from the outcome measures extracted from accelerometer data ( $I_Q$ ) for the different stimulation current amplitudes (color figure online)

higher-order spectral harmonics. In addition, the filters had to be optimized for low computation time to allow for real-time evaluation. While previous studies have shown that PD and ET have a dominant frequency between 3 and 12 Hz [18], our data showed a range of 3–6 Hz. Based on this, a 2-step process was employed to filter the data. (1) A time-varying high-pass filter called “smoothness priors” [48], with a cutoff frequency of 2 Hz [20], was used to remove low-frequency trends and the effect of gravity. (2) A second-order Butterworth low-pass filter was tested with cutoff frequencies from 10 to 30 Hz in steps of 5 Hz. In the present study, a cutoff frequency of 10 Hz was used because of adequate suppression of higher-order (2 and more) harmonics and digital noise without altering the outcome measures or the calculated improvement in tremor. Nevertheless, the cutoff frequency can be adapted to accommodate unexpected variations in tremor frequency. For postoperative analysis, synchronization markers and stimulation amplitude from the data for each stimulation test position were imported into MATLAB. For data coming from the Alpha Omega system, Neuroexplorer (Nex Technologies, Madison, Alabama, USA) was used to read the proprietary format. Acceleration data were imported

and synchronized with the stimulation amplitude (Fig. 2, top). Correct synchronization was verified by visual inspection.

### 2.4.2 Outcome measures

To estimate the changes in tremor during intraoperative stimulation tests, the accelerometer data were analyzed in a windowed manner. Various factors such as the average duration per stimulation amplitude, the sampling rate, and the range of tremor frequency had to be taken into account in choosing the window length. Based on these factors, windows of 1–4 s of time length and 0–50 % overlap were tested, and a non-overlapping window of 2 s was found to be optimal for data analysis. For each measurement position, outcome measures (standard deviation (1), signal energy (2), entropy (3), dominant frequency (4), and spectral amplitude of the dominant frequency (5)) were extracted from data recorded during baseline and stimulation periods:

$$\text{Standard deviation} = \sqrt{\frac{1}{N-1} \sum_{n=1}^N |x_n - \mu|^2}$$

$$\text{with } \mu = \frac{1}{N} \sum_{n=1}^N x_n \tag{1}$$

and  $N =$  Total number of samples

$$\text{Signal energy} = \sum_{n=1}^N |x_i|^2 \tag{2}$$

$$\text{Entropy} = - \sum_{n=1}^N p_n \log_2 p_n \text{ where } p \text{ is}$$

the probability density function

$$\tag{3}$$

Dominant frequency =  $k$  such that  $\max(X_k)$  where

$$X_k = \sum_{n=0}^{N-1} x_n e^{-i2\pi k \frac{n}{N}} \tag{4}$$

and  $k = 0, \dots, N - 1$

Spectral amplitude of dominant frequency =  $\max(X_k)$

$$\text{where } X_k = \sum_{n=0}^{N-1} x_n e^{-i2\pi k \frac{n}{N}} \text{ and } k = 0, \dots, N - 1 \tag{5}$$

However, statistical tests showed that 3 outcome measures (standard deviation, signal energy, and spectral amplitude of the dominant frequency) were more sensitive

toward changes in tremor [41], and only they were retained for further analysis. The extracted measures were graphically presented along with the stimulation current amplitude for visual analysis. Once the stimulation test was completed, the time window representing the highest tremor in the baseline data was identified and selected. The measures (a set of all three) extracted from this baseline window were used to normalize (6) the respective measures extracted for the following windows obtained during the stimulation test.

Normalized outcome measure

$$= \left( \frac{\text{Baseline value} - \text{current value}}{\text{Baseline value}} \right) \times 100 \% \tag{6}$$

Such normalization permitted a relative evaluation of tremor with changing stimulation current amplitude. The mean (7) of the normalized standard deviation, signal energy, and spectral amplitude of dominant frequency for any given window was termed as quantitatively calculated improvement in tremor or  $I_Q$  (Fig. 2, bottom).

$$I_Q = \frac{1}{3} \times \left( \begin{array}{l} \text{Normalized} \\ \text{standard deviation} \end{array} + \begin{array}{l} \text{Normalized} \\ \text{signal energy} \end{array} + \begin{array}{l} \text{Normalized spectral} \\ \text{amplitude of dominant frequency} \end{array} \right) \tag{7}$$

### 2.4.3 Comparative postoperative analysis

To establish the benefits of accelerometric tremor evaluation during DBS over visual evaluation, the first step was to compare the improvement in tremor identified by the two methods. To compare the discrete levels of the rating scales used for visual evaluations to the continuous values of accelerometric evaluation and to eliminate the difference between the rating scales used by the two different centers, the improvement values were classified in 5 categories as described in Table 3. Since in Center 1 the relative improvement in tremor was directly visually rated, the categories were easy to assign. In Center 2, tremor severity was rated on the UPDRS scale, i.e., in absolute rather than relative terms (see Table 1 for details). In consequence, the baseline severity had to be considered to determine the corresponding improvement values. Table 3 shows the baseline-dependent classification. As no patient had a baseline rating of 1, it is not listed in the table.

The classification of improvement values from visual evaluation ( $I_V$ ) was straightforward, as only one  $I_V$  value was

**Table 3** Categories used for classification of tremor improvement for the different rating scales used for visual- and accelerometer-based evaluations

Category	Descriptive evaluation in tremor	Quantitative accelerometry-based evaluation ( $I_Q$ ) (%)	Visual evaluation ( $I_V$ ) <sup>a</sup>			
			Center 1: Direct rating	Center 2: Rating using absolute UPDRS		
				Baseline = 4	Baseline = 3	Baseline = 2
A	Tremor arrest	>87.5	4	0	0	0
B	High improvement	75 ± 12.5	3, 3.5	1+,1,1-, 0+	1-,0+	0+
C	Average improvement	50 ± 12.5	2, 2.5	2+,2,2-	2-,1+,1	1+,1,1-
D	Limited improvement	25 ± 12.5	0.5, 1, 1.5	4-,3+, 3, 3-	3-,2+,2	2-
E	No improvement/tremor worsening	<12.5	0	4	3	2

<sup>a</sup> Details about the two different clinical scales are given in Table 1

available for each stimulation current amplitude. Because the quantitative improvement values ( $I_Q$ ) were calculated in a windowed fashion, multiple values were available depending on the number of windows that were completely enclosed in the period of a given stimulation current amplitude. Therefore, for the classification as well as for the comparison with  $I_V$  at any given stimulation current amplitude, the  $I_Q$  values for the same stimulation current amplitude were averaged. To study the distribution (pairwise) of  $I_V$  and  $I_Q$  values, the Wilcoxon two-sided signed rank test [50] was used to compare their population mean ranks. Also, as  $I_V$  and  $I_Q$  are both tremor improvement values, a positive linear correlation should exist between these two data sets. To check statistically for such a correlation, Spearman's test [45] was used.

In addition to comparing the improvement in tremor identified by the different methods, the  $I_Q$  values were also used to identify effective stimulation current amplitudes. For every stimulation test position, the lowest stimulation current amplitude (mA) at which the  $I_Q$  value was similar to the  $I_V$  value (highest  $I_V$  value for Center 2) was identified and termed as the quantitatively identified effective stimulation current amplitude ( $A_Q$ ). The Wilcoxon two-sided signed rank test was used to compare  $A_Q$  values to the visually identified effective amplitude ( $A_V$ ) values. To study the effect of using accelerometric evaluation of tremor on the implant position of the permanent DBS lead, the clinical staff was given the  $A_Q$  values after implantation and asked to state where they would have implanted the permanent DBS lead on the basis of these values rather than  $A_V$  values.

### 3 Results

The presented setup and method were successfully applied to the intraoperative stimulation tests in both the clinical centers. The data recording setup had certain failures during the surgery of 4 patients. While the synchronization failure for patient 6 was due to a software error, the loss of battery

power for patient 13 was due to human error. The disconnection between the sensor and the software during the surgery for patient 11 was rectified after the surgery with the use of a cable loop on the plastic case of the sensor board. Also, the synchronization with the LeadPoint system highlighted problems of signal saturation. On the other hand, the data analysis techniques were successful in eliminating noise and in extracting relevant information from the raw acceleration data.

In total, from all 15 patients, accelerometry data for 359 stimulation current amplitudes (223 in Center 1; 136 in Center 2) and the respective visually observed improvement values in tremor were acquired and analyzed offline. The Wilcoxon two-sided signed rank test ( $p = 0.041$ ) showed that for any given improvement in tremor, the  $I_V$  and  $I_Q$  values are not significantly different. The result of the Spearman's test confirmed that for increasing improvement in tremor,  $I_Q$  and  $I_V$  values increase in a correlated manner ( $R = 0.661$ ,  $p < 0.001$ ).

Figure 3a shows the counts of the quantitatively evaluated improvement  $I_Q$  as a function of the corresponding visually assessed improvement  $I_V$  in terms of categories as defined in Table 3. For example, if for one stimulation current amplitude, the change in tremor was visually assessed as average improvement (category C) and quantitatively as 70 % improvement (category B), then this evaluation would fall in the group CB (column 3, row 2) in Fig. 3. Ideally, all the evaluations would fall in one of the groups on the 45° diagonal, implying that both methods identify similar improvement in tremor for all the ranges. In fact, only 156 (43.5 %) evaluation pairs fell in the same category for both evaluation methods (Fig. 3b). Of the remaining 203 evaluations,  $I_Q$  values were lower than  $I_V$  values for 93 (26 %) (Fig. 3b, groups below the diagonal) and  $I_Q$  values were higher for 110 (30.5 %) (Fig. 3b, groups above the diagonal). Further, 296 (82.5 %) of the evaluations fell in the same or adjacent categories (neighborhood, Fig. 3c), while the remaining 63 (17.5 %) evaluations showed differences of at least 2 categories between the two values

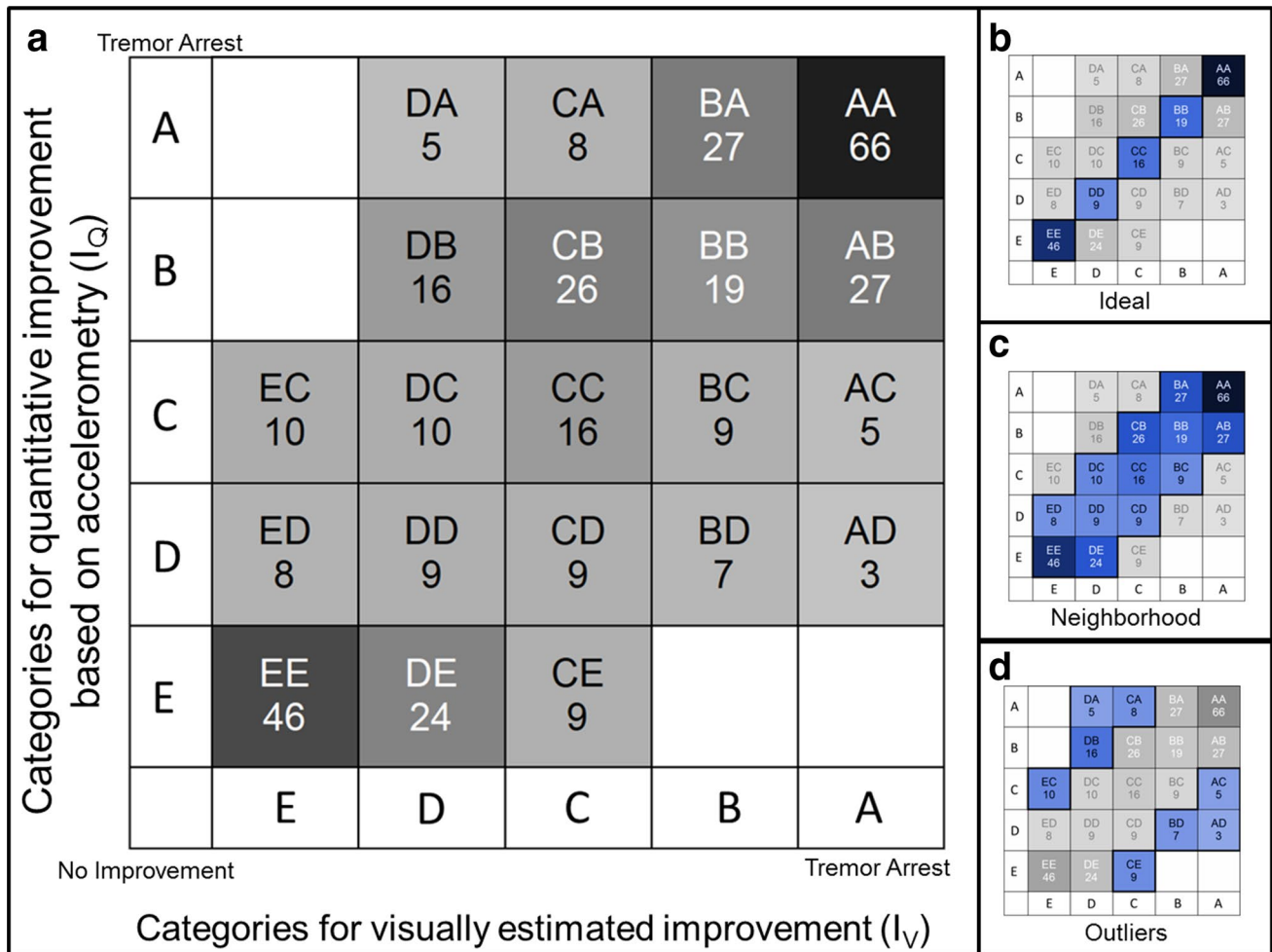


**Fig. 3** a  $5 \times 5$  Heatmap illustrating the number of evaluations falling in each category pair, based on Table 3. The intensity of gray is proportional to the number of evaluations. (Right) Subdivision of the heatmap of the left into 3 scenarios: **b** the ideal scenario would be that all the evaluations fall along the diagonal meaning that visual

and quantitative evaluation are equal; **c** inclusion of the neighborhood around the diagonal, i.e., taking account as well variations of one category between the two evaluation methods; **d** considering the outliers where the difference between the visual improvement and the quantitative improvement is of at least two categories (color figure online)

(outliers, Fig. 3d). As mentioned in Table 1, in Center 1, only the maximum improvement in tremor was noted for every stimulation test. This, along with the higher number of patients from Center 1, creates a bias in the results as evident from the number of evaluations in category A for both  $I_V$  and  $I_Q$  values (Fig. 3a).

The comparison between effective stimulation current amplitudes  $A_V$  and  $A_Q$  is depicted in Fig. 4.  $A_Q$  values (mean  $\pm$  SD:  $1.1 \pm 0.8$  mA) were significantly lower ( $p < 0.001$ ) than  $A_V$  values ( $1.7 \pm 0.8$  mA). The consideration of the acceleration data instead of the visual evaluations would have affected the choice of the chronic implant position for the DBS lead. Out of the 26 (Center 1: 18, Center 2: 8) choices, 15 (Center 1: 15, Center 2: 0) would have been different, and for 2 implantations (Center 1: 2, Center 2: 0), a position on a different trajectory would have been chosen.

#### 4 Discussion

The aim of this study was to provide an assistive tool supporting the neurologists in their tremor assessment during DBS surgery normally performed by visual inspection (the method now used in most centers). With the versatile system based on accelerometry, improvement in tremor can be measured quantitatively and any evaluation performed during DBS surgery can be revisited and visualized. The system was specifically designed to be used in the operating room during stimulation tests through exploration electrodes in different clinical centers, without impeding or prolonging the surgical procedure.

Some researchers have performed intraoperative quantitative evaluations to identify the best stimulation parameters for stimulating through the chronically implanted

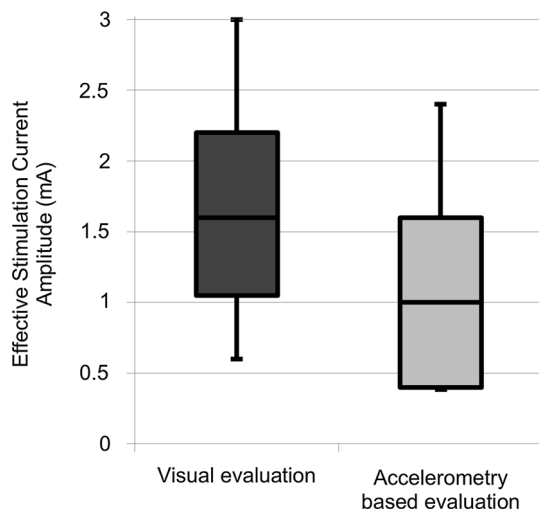


**Fig. 4** Box plot comparing the effective stimulation current amplitudes identified from visual evaluation ( $A_V$ ) and quantitative evaluation ( $A_Q$ ). The lower whiskers indicate 5th and the upper whiskers 95th percentile of the values

DBS lead. Journee et al. [14] performed intraoperative neurophysiological measurements with multiple sensors, including two uniaxial accelerometers, on a large patient cohort. They evaluated tremor by comparing it with a common baseline recorded before any incision. This method of comparison ignores the improvement in tremor that is often observed after insertion of the electrode but before any stimulating current is turned on (the so-called micro-lesional effect [24]). A baseline recording performed before each stimulation test, as in the current method, is necessary to have an accurate objective evaluation of improvement in tremor. Papapetropoulos et al. [27] used the commercially available CATSYS system (Danish Product Development Ltd., Snekkersten, Denmark) to evaluate the best stimulation parameters for PD patients undergoing DBS immediately after the DBS lead was placed in the brain. However, their method required the active participation of the patient by holding the tremor pen in a certain position, and the patients were given practice time to familiarize themselves with the testing procedure. Varying levels of familiarity with the system increase the subjectivity of such evaluations. In the method presented here, the acceleration data were recorded passively and in parallel to the routine visual evaluation.

Quantitative evaluation of improvement in tremor with accelerometers depends heavily on the filtering parameters used and the outcome measures extracted from the data. Gravity also has an effect on the data measured by the accelerometer [30] and therefore has to be corrected for before any outcome measures are extracted. In contrast to previously proposed methods, in which the effect of gravity was not suppressed, our method uses a cutoff frequency

of 2 Hz for the smoothness-priors detrending method which has been shown to suppress the effect of gravitational acceleration on the raw data [20]. With regard to the outcome measures, as Papapetropoulos et al. [27] used a commercial system; they were restricted to the outcome measures available from it, i.e., tremor intensity, center frequency, its standard deviation, and harmonic index. Journee et al. [14] relied on spectral outcome measures without any filtering of the data. Additionally, they extracted temporal outcome measures from displacement estimated from the accelerometer data after double integration, which also significantly amplifies the noise in the accelerometer data [49]. In contrast, the linear outcome measures (temporal and spectral) like the ones proposed in this study have been shown to correlate with the UPDRS tremor scores during routine non-surgical clinical evaluation [20].

The use of our method in 15 patients in 2 different centers has already revealed some of its benefits and limitations. The complete setup was initially designed for use with the MicroGuide Pro system and later adapted for use with the LeadPoint system. Imperfect adaptation might underlie the signal saturation that was initially observed during synchronization with LeadPoint system but subsequently eliminated after the present study was conducted by modification of certain parameters in LemurDBS. This experience only underscores the need to test any quantitative symptom evaluation method in multiple clinical centers. A clear advantage of the method is the absence of any patient discomfort. The acceleration sensor is easy to attach to the patient's affected (usually upper) limb and to remove from it afterward; aside from patient comfort, this also ensures that the device does not block the surgical team's access to any part of the patient's body if needed (for insertion of new intravenous lines, etc.).

The comparison of improvement in tremor identified visually ( $I_V$ ) with that calculated from the acceleration data ( $I_Q$ ) is shown in Fig. 3. It must be noted, however, that a categorization of evaluations based on Table 3 results in loss of information, partly because of the large ranges of quantitative improvement values for each category and also because any worsening in tremor is also categorized in E, i.e., "No change/tremor worsening." Despite this loss of information, the number of evaluations in each category provides a better understanding of the similarities and differences between the two tremor evaluation methods. The results show that for 43.5 % of the evaluations, both the methods identified similar improvement in tremor, i.e.,  $I_V$  and  $I_Q$  values fell in the same category (Fig. 3b). In practice, however, minor changes in tremor are difficult to estimate visually, especially when the baseline tremor is small. Therefore, it is plausible that  $I_Q$  values would be in the same category as the  $I_V$  values, or at least in a neighboring category. In this scenario, 82.5 % of the evaluations are

either in the same or neighboring categories (Fig. 3c). The remaining 17.5 % of evaluations show very large differences between the visual evaluation and the accelerometric evaluation (Fig. 3d).

One of the primary objectives of intraoperative stimulation tests is to identify sites where stimulation suppresses tremor. The high number of evaluations in the AA group would indicate that both methods can be used for this purpose. However, considering that the total number of the evaluations where only one of the methods indicated tremor arrest (AB, AC, AD, BA, CA, and DA) is 76, it seems that a small residual tremor might not always be visually identified. As both methods estimate change in tremor compared to a baseline condition, the difference in estimation by the two methods may be a result of different choices of baseline. The visual evaluation is based on the complete baseline activity before test stimulation, whereas the accelerometric evaluation is based on the worst tremor (2 s long) in the whole baseline recording. Further, it may be possible that in case of very low baseline tremor, it was considered as suppressed by visual estimation, while the accelerometric evaluation only measured 50 % improvement. Another possible reason for such differences might be that the evaluator did not retain an accurate memory of the observed baseline tremor while performing the evaluation. This emphasizes the need of an evaluation system that lets the evaluator re-check the severity of tremor at any time during the surgery. Previous studies proposing quantitative evaluation methods have shown similar findings [14, 27, 36] suggesting that the limitations of current visual evaluation methods could be overcome by supplementing them with quantitative methods.

The impact of quantitative tremor evaluation on the DBS surgery can be gauged by its influence on surgical decision making, i.e., the choice of the site where the chronic DBS lead is finally implanted. One of the factors that influence this choice is the therapeutic window, i.e., the difference between the amplitude of stimulating current that results in an appreciable clinical effect and the side-effect threshold. As evident from Fig. 4, the quantitatively identified amplitude for effective stimulation ( $A_Q$ ) tends to be lower than the corresponding value obtained by visual evaluation ( $A_V$ ) and is thus associated with a wider therapeutic window. The evidence of this expansion in range affecting the choice of chronic implant position is provided by the results of comparison between clinical choices and choices based on quantitative data for the chronic implant position. The results show a stark difference in the choices between Center 1 and Center 2 because of the differences in the method of choosing the chronic implant position (Table 1). In Center 1, the stimulation test position among a group of adjacently located positions with large therapeutic window is chosen as opposed to Center 2, where the deepest

effective stimulation test position is chosen. Also, as the number of stimulation tests per hemisphere is lower in Center 2, the choice of chronic implant position of the DBS lead would be less influenced by the accelerometer-based improvement values. A clinical study would be needed to determine the impact of different methods of choosing the chronic implant site on the ultimate clinical efficacy of stimulation.

We infer from our data analysis that the recording of a sufficient amount of baseline data is important. In the case of insufficient baseline data (<5 s) at a position, the analysis has to be done with the baseline from the previous position. However, this scenario does not significantly limit the method. Additionally, as the data analysis is performed with windows of 2 s, each stimulation tests at any particular amplitude should be longer than that to increase the reliability of the result. A shorter duration might result in an incorrect identification of the effective amplitude of the stimulating current. Such errors will be smaller if the current is raised in smaller increments.

The results of this study show that our quantitative tremor evaluation method can help improve the placement of the chronic DBS lead. As a next step, a visualization tool will also be added to the software to allow the surgical team to see the results superimposed on the patients' brain scans (MRI or CT). To allow automatic identification of effective stimulation current amplitudes, thresholds for the quantitatively calculated improvement in tremor will be identified. For patients with Parkinson's disease, the quantification of tremor alone may not be sufficient. Rigidity is also present in these patients and is clinically evaluated during DBS surgery. Moreover, rigidity seems to be less affected by other factors like psychological stress, pain, alertness, microlesioning effects. Thus, in patients with Parkinson's disease a quantitative evaluation of rigidity is also needed for a comprehensive quantification of stimulation test results. Rigidity can be measured with intraoperative accelerometry as well [42].

Recent years have seen the development and marketing of new types of DBS leads. The idea of directional stimulation [5, 19] has been extensively researched, and new leads [6, 31] are already undergoing clinical trials. With the aid of quantitative methods as proposed in the current study, a more robust comparison can be made between different stimulation parameters and positions, and the time needed for testing may be shortened. Another area of increasing research is closed-loop DBS. Closed-loop systems have been proposed that are based not only on electrophysiological signals [10], but also on EMG and acceleration signals of tremor [3]. For such technologies to be practically useful and rapidly applicable, intraoperative quantitative evaluations of disease manifestations such as tremor and rigidity might play an important role.

## 5 Conclusion

In this paper, we describe a new method in which an acceleration sensor is used for the quantitative evaluation of improvement in tremor in patients undergoing DBS for movement disorders. The method can be used in different surgical centers with little or no change of the system setup. It improves upon the previously proposed methods by using better filtering techniques and outcome measures that correlate with tremor severity. Accelerometry-based tremor evaluation widens the apparent therapeutic window of stimulation for tremor; it can therefore alter the exploratory test stimulation results and thus affect the choice of site for chronic DBS lead implantation. In the present study, the site of chronic lead implantation would have been different in 60 % of cases if the surgeons had been allowed to consider the accelerometric evaluations instead of the subjective visual evaluations of tremor. Our preliminary results suggest that the limitations of the current clinical rating methods can be overcome by supplementing them with objective evaluation methods and, in turn, improve the determination of the optimum site for lead placement. To confirm the present findings, the method will have to be used in more patients undergoing DBS surgery.

**Acknowledgments** This research was funded by the Swiss National Science Foundation and partly by the Germaine de Staël program of the Swiss Academy of Engineering Sciences. The authors acknowledge the contribution of Ms. Katrin Petermann in the programming of the connection of the LeadPoint system for synchronization with the acceleration data recording system.

## References

- Abosch A, Timmermann L, Bartley S, Rietkerk HG, Whiting D, Connolly PJ et al (2013) An international survey of deep brain stimulation procedural steps. *Stereotact Funct Neurosurg* 91(1):1–11. doi:[10.1159/000343207](https://doi.org/10.1159/000343207)
- Askari S, Zhang M, Won DS (2010) An EMG-based system for continuous monitoring of clinical efficacy of Parkinson's disease treatments. In: Conference proceedings: Annual international conference of the IEEE engineering in medicine and biology society. IEEE engineering in medicine and biology society. Conference, 2010, pp 98–101. doi:[10.1109/IEMBS.2010.5626133](https://doi.org/10.1109/IEMBS.2010.5626133)
- Basu I, Graupe D, Tuninetti D, Shukla P, Slavin KV, Metman LV et al (2013) Pathological tremor prediction using surface electromyogram and acceleration: potential use in 'ON-OFF' demand driven deep brain stimulator design. *J Neural Eng* 10(3):36019. doi:[10.1088/1741-2560/10/3/036019](https://doi.org/10.1088/1741-2560/10/3/036019)
- Birdno MJ, Kuncel AM, Dorval AD, Turner DA, Grill WM (2008) Tremor varies as a function of the temporal regularity of deep brain stimulation. *NeuroReport* 19(5):599–602
- Chaturvedi A, Foutz TJ, McIntyre CC (2012) Current steering to activate targeted neural pathways during deep brain stimulation of the subthalamic region. *Brain Stimul* 5(3):369–377. doi:[10.1016/j.brs.2011.05.002](https://doi.org/10.1016/j.brs.2011.05.002)
- Contarino MF, Lo Bour J, Verhagen R, Lourens MAJ, de Bie Rob M A, van den Munckhof P et al (2014) Directional steering: a novel approach to deep brain stimulation. *Neurology* 83(13):1163–1169. doi:[10.1212/WNL.0000000000000823](https://doi.org/10.1212/WNL.0000000000000823)
- Elble RJ, Pullman SL, Matsumoto JY, Raethjen J, Deuschl G, Tintner R (2006) Tremor amplitude is logarithmically related to 4- and 5-point tremor rating scales. *Brain J Neurol* 129(Pt 10):2660–2666. doi:[10.1093/brain/awl190](https://doi.org/10.1093/brain/awl190)
- Gantert C, Honerkamp J, Timmer J (1992) Analyzing the dynamics of hand tremor time series. *Biol Cybern* 66(6):479–484
- Goetz CG, Tilley BC, Shaftman SR, Stebbins GT, Fahn S, Martinez-Martin P et al (2008) Movement disorder society-sponsored revision of the unified Parkinson's disease rating scale (MDS-UPDRS): scale presentation and clinimetric testing results. *Mov Disord Off J Mov Disord Soc* 23(15):2129–2170. doi:[10.1002/mds.22340](https://doi.org/10.1002/mds.22340)
- Greenwald E, Masters MR, Thakor NV (2016) Implantable neurotechnologies: bidirectional neural interfaces-applications and VLSI circuit implementations. *Med Biol Eng Comput* 54(1):1–17. doi:[10.1007/s11517-015-1429-x](https://doi.org/10.1007/s11517-015-1429-x)
- Griffiths RI, Kotschet K, Arfon S, Xu ZM, Johnson W, Drago J et al (2012) Automated assessment of bradykinesia and dyskinesia in Parkinson's disease. *J Parkinson's Dis* 2(1):47–55. doi:[10.3233/JPD-2012-11071](https://doi.org/10.3233/JPD-2012-11071)
- Hemm S, Wårdell K (2010) Stereotactic implantation of deep brain stimulation electrodes: a review of technical systems, methods and emerging tools. *Med Biol Eng Comput* 48(7):611–624. doi:[10.1007/s11517-010-0633-y](https://doi.org/10.1007/s11517-010-0633-y)
- Jankovic J, Frost JD (1981) Quantitative assessment of parkinsonian and essential tremor: clinical application of triaxial accelerometry. *Neurology* 31(10):1235. doi:[10.1212/WNL.31.10.1235](https://doi.org/10.1212/WNL.31.10.1235)
- Journée HL, Postma AA, Staal MJ (2007) Intraoperative neurophysiological assessment of disabling symptoms in DBS surgery. *Neurophysiol Clin Clin Neurophysiol* 37(6):467–475. doi:[10.1016/j.neucli.2007.10.006](https://doi.org/10.1016/j.neucli.2007.10.006)
- Journée HL, Postma AA, Sun M, Staal MJ (2008) Detection of tremor bursts by a running second order moment function and analysis using interburst histograms. *Med Eng Phys* 30(1):75–83. doi:[10.1016/j.medengphy.2006.12.005](https://doi.org/10.1016/j.medengphy.2006.12.005)
- Lang AE, Widner H (2002) Deep brain stimulation for Parkinson's disease: patient selection and evaluation. *Mov Disord* 17(S3):S94–S101. doi:[10.1002/mds.10149](https://doi.org/10.1002/mds.10149)
- Lauk M, Timmer J, Guschlbauer B, Hellwig B, Lücking CH (2001) Variability of frequency and phase between antagonistic muscle pairs in pathological human tremors. *Muscle Nerve* 24(10):1365–1370
- Mansur PHG, Cury LKP, Andrade AO, Pereira AA, Miotto GAA, Soares AB et al (2007) A review on techniques for tremor recording and quantification. *Crit Rev Biomed Eng* 35(5):343–362
- Martens HCF, Toader E, Decré MMJ, Anderson DJ, Vetter R, Kipke DR et al (2011) Spatial steering of deep brain stimulation volumes using a novel lead design. *Clin Neurophysiol Off J Int Fed Clin Neurophysiol* 122(3):558–566. doi:[10.1016/j.clinph.2010.07.026](https://doi.org/10.1016/j.clinph.2010.07.026)
- Meigal AY, Rissanen SM, Tarvainen MP, Georgiadis SD, Karjalainen PA, Airaksinen O et al (2012) Linear and nonlinear tremor acceleration characteristics in patients with Parkinson's disease. *Physiol Meas* 33(3):395–412. doi:[10.1088/0967-3334/33/3/395](https://doi.org/10.1088/0967-3334/33/3/395)
- Meldrum SJ, Watson BW (1970) Tremor recording in Parkinson's disease. *Phys Med Biol* 15(2):249–254. doi:[10.1088/0031-9155/15/2/302](https://doi.org/10.1088/0031-9155/15/2/302)

22. Mera T, Vitek JL, Alberts JL, Giuffrida JP (2011) Kinematic optimization of deep brain stimulation across multiple motor symptoms in Parkinson's disease. *J Neurosci Methods* 198(2):280–286. doi:[10.1016/j.jneumeth.2011.03.019](https://doi.org/10.1016/j.jneumeth.2011.03.019)
23. Moore GP, Ding L, Bronte-Stewart HM (2000) Concurrent Parkinson tremors. *J Physiol* 529(Pt 1):273–281
24. Morishita T, Foote KD, Wu SS, Jacobson CE, Rodriguez RL, Haq IU et al (2010) Brain penetration effects of microelectrodes and deep brain stimulation leads in ventral intermediate nucleus stimulation for essential tremor. *J Neurosurg* 112(3):491–496. doi:[10.3171/2009.7.JNS09150](https://doi.org/10.3171/2009.7.JNS09150)
25. O'Suilleabhain PE, Matsumoto JY (1998) Time-frequency analysis of tremors. *Brain J Neurol* 121(Pt 11):2127–2134
26. Palmer JL, Coats MA, Roe CM, Hanks SM, Xiong C, Morris JC (2010) Unified Parkinson's disease rating scale-motor exam: inter-rater reliability of advanced practice nurse and neurologist assessments. *J Adv Nurs* 66(6):1382–1387. doi:[10.1111/j.1365-2648.2010.05313.x](https://doi.org/10.1111/j.1365-2648.2010.05313.x)
27. Papapetropoulos S, Jagid JR, Sengun C, Singer C, Gallo BV (2008) Objective monitoring of tremor and bradykinesia during DBS surgery for Parkinson disease. *Neurology* 70(15):1244–1249. doi:[10.1212/01.wnl.0000308936.27780.94](https://doi.org/10.1212/01.wnl.0000308936.27780.94)
28. Papapetropoulos S, Katzen HL, Scanlon BK, Guevara A, Singer C, Levin BE (2010) Objective quantification of neuromotor symptoms in Parkinson's disease: implementation of a portable, computerized measurement tool. *Parkinson's Dis* 2010:760196. doi:[10.4061/2010/760196](https://doi.org/10.4061/2010/760196)
29. Patel S, Lorincz K, Hughes R, Huggins N, Growdon J, Standaert D et al (2009) Monitoring motor fluctuations in patients with Parkinson's disease using wearable sensors. *IEEE Trans Inf Technol Biomed Publ IEEE Eng Med Biol Soc* 13(6):864–873. doi:[10.1109/TITB.2009.2033471](https://doi.org/10.1109/TITB.2009.2033471)
30. Perera T, Yohanandan SAC, McDermott HJ (2015) A simple and inexpensive test-rig for evaluating the performance of motion sensors used in movement disorders research. *Med Biol Eng Comput* 54(2–3):333–339. doi:[10.1007/s11517-015-1314-7](https://doi.org/10.1007/s11517-015-1314-7)
31. Pollo C, Kaelin-Lang A, Oertel MF, Stieglitz L, Taub E, Fuhr P et al (2014) Directional deep brain stimulation: an intraoperative double-blind pilot study. *Brain J Neurol* 137(Pt 7):2015–2026. doi:[10.1093/brain/awu102](https://doi.org/10.1093/brain/awu102)
32. Popović Maneski L, Jorgovanović N, Ilić V, Došen S, Keller T, Popović MB et al (2011) Electrical stimulation for the suppression of pathological tremor. *Med Biol Eng Comput* 49(10):1187–1193. doi:[10.1007/s11517-011-0803-6](https://doi.org/10.1007/s11517-011-0803-6)
33. Post B, Merkus MP, de Bie Rob M A, de Haan Rob J, Speelman JD (2005) Unified Parkinson's disease rating scale motor examination: are ratings of nurses, residents in neurology, and movement disorders specialists interchangeable? *Mov Disord Off J Mov Disord Soc* 20(12):1577–1584. doi:[10.1002/mds.20640](https://doi.org/10.1002/mds.20640)
34. Pulliam CL, Heldman DA, Orcutt TH, Mera TO, Giuffrida JP, Vitek JL (2015) Motion sensor strategies for automated optimization of deep brain stimulation in Parkinson's disease. *Parkinsonism Rel Disord* 21(4):378–382. doi:[10.1016/j.parkreldis.2015.01.018](https://doi.org/10.1016/j.parkreldis.2015.01.018)
35. Rissanen SM, Kankaanpää M, Meigal A, Tarvainen MP, Nuutinen J, Tarkka IM et al (2008) Surface EMG and acceleration signals in Parkinson's disease: feature extraction and cluster analysis. *Med Biol Eng Comput* 46(9):849–858. doi:[10.1007/s11517-008-0369-0](https://doi.org/10.1007/s11517-008-0369-0)
36. Rissanen SM, Kankaanpää M, Tarvainen MP, Novak V, Novak P, Hu K et al (2011) Analysis of EMG and acceleration signals for quantifying the effects of deep brain stimulation in Parkinson's disease. *IEEE Trans Biomed Eng* 58(9):2545–2553. doi:[10.1109/TBME.2011.2159380](https://doi.org/10.1109/TBME.2011.2159380)
37. Riviere CN, Reich SG, Thakor NV (1997) Adaptive Fourier modeling for quantification of tremor. *J Neurosci Methods* 74(1):77–87
38. Rocon E, Pons JL, Andrade AO, Nasuto SJ (2006) Application of EMD as a novel technique for the study of tremor time series. In: Conference proceedings: annual international conference of the IEEE engineering in medicine and biology society. IEEE engineering in medicine and biology society. Annual conference, Supplementary, pp 6533–6536. doi:[10.1109/IEMBS.2006.260871](https://doi.org/10.1109/IEMBS.2006.260871)
39. Sarem-Aslani A, Mullett K (2011) Industrial perspective on deep brain stimulation: history, current state, and future developments. *Front Integr Neurosci*. doi:[10.3389/fnint.2011.00046](https://doi.org/10.3389/fnint.2011.00046)
40. Senova S, Querlioz D, Thiriez C, Jedynak P, Jarraya B, Palfi S (2015) Using the accelerometers integrated in smartphones to evaluate essential tremor. *Stereotact Funct Neurosurg* 93(2):94–101. doi:[10.1159/000369354](https://doi.org/10.1159/000369354)
41. Shah A, Coste J, Lemaire J-J, Schkommodau E, Hemm-Ode S (2013) A method to quantitatively evaluate changes in tremor during deep brain stimulation surgery. In: 6th international IEEE/EMBS conference on neural engineering, pp 1202–1205. doi:[10.1109/NER.2013.6696155](https://doi.org/10.1109/NER.2013.6696155)
42. Shah AA, Coste J, Lemaire J-J, Ulla M, Schkommodau E, Hemm-Ode S (2014) Using acceleration sensors to quantify symptoms during deep brain stimulation surgery: poster presentations. *Mov Disord* 29(S1):30. doi:[10.1002/mds.25914](https://doi.org/10.1002/mds.25914)
43. Shamir RR, Eitan R, Sheffer S, Marmor-Levin O, Valsky D, Moshel S et al (2013). Intra-operative identification of the subthalamic nucleus motor zone using goniometers. In Hutchison D, Kanade T, Kittler J, Kleinberg JM, Mattern F, Mitchell JC et al (eds) Information processing in computer-assisted interventions, vol 7915. Lecture notes in computer science). Springer, Berlin, pp 21–29
44. Sowman PF, Türker KS (2005) Methods of time and frequency domain examination of physiological tremor in the human jaw. *Hum Mov Sci* 24(5–6):657–666. doi:[10.1016/j.humov.2005.09.003](https://doi.org/10.1016/j.humov.2005.09.003)
45. Spearman C (1904) The Proof and measurement of association between two things. *Am J Psychol* 15(1):72. doi:[10.2307/1412159](https://doi.org/10.2307/1412159)
46. Stacy M (2009) Medical treatment of Parkinson disease. *Neurol Clin* 27(3):605–631. doi:[10.1016/j.ncl.2009.04.009](https://doi.org/10.1016/j.ncl.2009.04.009)
47. Sturman MM, Vaillancourt DE, Metman LV, Bakay RAE, Corcos DM (2004) Effects of subthalamic nucleus stimulation and medication on resting and postural tremor in Parkinson's disease. *Brain J Neurol* 127(Pt 9):2131–2143. doi:[10.1093/brain/awh237](https://doi.org/10.1093/brain/awh237)
48. Tarvainen M, Ranta-aho P, Karjalainen P (2002) An advanced detrending method with application to HRV analysis. *IEEE Trans Biomed Eng* 49(2):172–175. doi:[10.1109/10.979357](https://doi.org/10.1109/10.979357)
49. Veluvolu KC, Ang WT (2011) Estimation of physiological tremor from accelerometers for real-time applications. *Sensors* 11(12):3020–3036. doi:[10.3390/s110303020](https://doi.org/10.3390/s110303020)
50. Wilcoxon F (1945) Individual comparisons by ranking methods. *Biom Bull* 1(6):80–83



**Ashesh Shah** obtained his B.E. in Biomedical Engineering at the Gujarat University in 2008 and M.Sc. in Medical Physics at the Heidelberg University in 2011. He is a Ph.D. student at the University of Basel.



**Jérôme Coste** completed his Ph.D. study in Neuroscience in 2006 (Auvergne University) and is electrophysiologist in the Neurosurgery Department of the Clermont-Ferrand University Hospital, France.



**Claudio Pollo** is responsible for the stereotactic and functional neurosurgery, surgery for Epilepsy and Radiosurgery Programs at the Inselspital in Bern, Switzerland.



**Jean-Jacques Lemaire MD, PhD**, professor of Neurosurgery, is the head of the department of Neurosurgery at the University Hospital of Clermont-Ferrand, and the Head of the Image-Guided Clinical Neurosciences and Connectomics at the Clermont Auvergne University, France.



**Erik Schkommodau** is Head of the Institute for Medical and Analytical Technologies at the University of Applied Sciences and Arts Northwestern Switzerland.



**Ethan Taub** is the Head of Functional Neurosurgery at the Department of Neurosurgery, University Hospital Basel, Switzerland.



**Raphael Guzman MD**, is a Professor of Neurosurgery and Neurosciences and the Vice Chair of the Department of Neurosurgery at the University Hospital in Basel, Switzerland.



**W. M. Michael Schüpbach MD**, is the Head of the Movement Disorders Center and Deep Brain Stimulation Unit at the Department of Neurology, University Hospital Bern, Switzerland.



**Simone Hemm-Ode Ph.D.**, is Professor at the University of Applied Sciences and Arts Northwestern Switzerland and Guest Researcher and Docent at the Technical Faculty at Linköping University, Sweden.

## **Chapter 5**

# **Assistive Rigidity Evaluation during DBS Surgery**

## 5.1 A novel assistive method for rigidity evaluation during deep brain stimulation surgery using acceleration sensors

**Authors:** Ashesh Shah, Jérôme Coste, Jean-Jacques Lemaire, Erik Schkommodau, Ethan Taub, Raphael Guzman, Philippe Derost, Simone Hemm.

This paper is published in the Journal of Neurosurgery. It contains the details about the method to evaluate rigidity during DBS and the clinical study undertaken to test the method. A supplementary document describing the tests conducted in a controlled environment with 3 patients and 3 evaluators to test the reliability of the method was provided to the reviewers of the paper only and is not available through the publisher. This supplementary document is attached here in addition to the paper.

The paper is available at the address:

<https://thejns.org/doi/abs/10.3171/2016.8.JNS152770>

Copyright Notice: Reprinted by permission from Journal of Neurosurgery, JNS Publishing Group, American Association of Neurological Surgeons. Ashesh Shah, Jérôme Coste, Jean-Jacques Lemaire, Erik Schkommodau, Ethan Taub, Raphael Guzman, Philippe Derost, Simone Hemm, 2017. "A novel assistive method for rigidity evaluation during deep brain stimulation surgery using acceleration sensors" Journal of Neurosurgery 127, no. 3 (September 2017): 602–12. <https://doi.org/10.3171/2016.8.JNS152770>. ©2017

## A novel assistive method for rigidity evaluation during deep brain stimulation surgery using acceleration sensors

Ashesh Shah, MSc,<sup>1</sup> Jérôme Coste, PhD,<sup>2,3</sup> Jean-Jacques Lemaire, MD, PhD,<sup>2,3</sup>  
Erik Schkommodau, PhD,<sup>1</sup> Ethan Taub, MD,<sup>4</sup> Raphael Guzman, MD,<sup>4</sup> Philippe Derost, MD,<sup>5,6</sup> and  
Simone Hemm, PhD<sup>1</sup>

<sup>1</sup>Institute for Medical and Analytical Technologies, School of Life Sciences, University of Applied Sciences and Arts Northwestern Switzerland, Muttenz; <sup>2</sup>Departments of Neurosurgery and Biomedicine, University Hospital of Basel, Switzerland; <sup>3</sup>Image-Guided Clinical Neuroscience and Connectomics, and <sup>4</sup>Neuro-Psycho-Pharmacologie des Systèmes Dopaminergiques Sous-Corticaux, Université Clermont Auvergne, Université d'Auvergne; and <sup>5</sup>Service de Neurochirurgie and <sup>6</sup>Service de Neurologie, CHU Clermont-Ferrand, France

**OBJECTIVE** Despite the widespread use of deep brain stimulation (DBS) for movement disorders such as Parkinson's disease (PD), the exact anatomical target responsible for the therapeutic effect is still a subject of research. Intraoperative stimulation tests by experts consist of performing passive movements of the patient's arm or wrist while the amplitude of the stimulation current is increased. At each position, the amplitude that best alleviates rigidity is identified. Intra-rater and interrater variations due to the subjective and semiquantitative nature of such evaluations have been reported. The aim of the present study was to evaluate the use of an acceleration sensor attached to the evaluator's wrist to assess the change in rigidity, hypothesizing that such a change will alter the speed of the passive movements. Furthermore, the combined analysis of such quantitative results with anatomy would generate a more reproducible description of the most effective stimulation sites.

**METHODS** To test the reliability of the method, it was applied during postoperative follow-up examinations of 3 patients. To study the feasibility of intraoperative use, it was used during 9 bilateral DBS operations in patients suffering from PD. Changes in rigidity were calculated by extracting relevant outcome measures from the accelerometer data. These values were used to identify rigidity-suppressing stimulation current amplitudes, which were statistically compared with the amplitudes identified by the neurologist. Positions for the chronic DBS lead implantation that would have been chosen based on the acceleration data were compared with clinical choices. The data were also analyzed with respect to the anatomical location of the stimulating electrode.

**RESULTS** Outcome measures extracted from the accelerometer data were reproducible for the same evaluator, thus providing a reliable assessment of rigidity changes during intraoperative stimulation tests. Of the 188 stimulation sites analyzed, the number of sites where rigidity-suppressing amplitudes were found increased from 144 to 170 when the accelerometer evaluations were considered. In general, rigidity release could be observed at significantly lower amplitudes with accelerometer evaluation (mean  $0.9 \pm 0.6$  mA) than with subjective evaluation (mean  $1.4 \pm 0.6$  mA) ( $p < 0.001$ ). Of 14 choices for the implant location of the DBS lead, only 2 were the same for acceleration-based and subjective evaluations. The comparison across anatomical locations showed that stimulation in the fields of Forel ameliorates rigidity at similar amplitudes as stimulation in the subthalamic nucleus, but with fewer side effects.

**CONCLUSIONS** This article describes and validates a new assistive method for assessing rigidity with acceleration sensors during intraoperative stimulation tests in DBS procedures. The initial results indicate that the proposed method may be a clinically useful aid for optimal DBS lead placement as well as a new tool in the ongoing scientific search for the optimal DBS target for PD.

<https://thejns.org/doi/abs/10.3171/2016.8.JNS152770>

**KEY WORDS** deep brain stimulation; Parkinson's disease; rigidity; acceleration sensor; quantification; intraoperative; subthalamic nucleus; fields of Forel; functional neurosurgery

**ABBREVIATIONS** AmpQ = quantitatively identified rigidity-suppressing amplitude; AmpS = subjectively assessed amplitude; DBS = deep brain stimulation; FF = fields of Forel; MER = microelectrode recording; OR = operating room; PD = Parkinson's disease; QC = quantitatively assessed change; S-EMG = surface electromyography; STN = subthalamic nucleus; USB = Universal Serial Bus; ZI = zona incerta.

**SUBMITTED** December 1, 2015. **ACCEPTED** August 24, 2016.

**INCLUDE WHEN CITING** Published online December 16, 2016; DOI: 10.3171/2016.8.JNS152770.

**D**EEP brain stimulation (DBS) is a neurosurgical technique in which electrodes are implanted in deep-seated brain structures (e.g., the subthalamic nucleus [STN], globus pallidus, or thalamus) so that these structures can be stimulated with electrical pulses generated in an attached, extracranially implanted neurostimulator device. DBS is a highly effective symptomatic treatment for Parkinson's disease (PD) and other movement disorders.<sup>25</sup> More than 100,000 patients have been treated with DBS in the past 3 decades.<sup>23</sup>

The current incomplete understanding of the mechanisms of action of DBS and interindividual variation of brain anatomy necessitate patient-specific planning. Most centers also perform intraoperative stimulation tests under local anesthesia at multiple anatomical locations in the vicinity of a preoperatively chosen target<sup>1</sup> to evaluate the therapeutic effects and side effects of stimulation before the DBS lead (permanent electrode) is definitively fixed in place. For some patients with PD, the therapeutic effects of stimulation tests are estimated by assessing the changes in rigidity as the stimulation current is increased. Expert evaluators (generally a neurologist) perform passive movements of the patient's arm continuously to assess the changes in rigidity. When either a reduction in rigidity or a side effect is observed, the amplitude and the effect of stimulation are noted. After completion of all stimulation tests, the results are compared to identify the best implant position, that is, the one that yields the best improvement with the fewest side effects.

Different evaluators assess rigidity during surgery in different ways,<sup>5</sup> but with the same basic concept: the baseline rigidity is rated before any stimulation, and the changes in rigidity are assessed in comparison with this baseline value. Intraoperatively used rating scales for PD are based on those commonly used outside the operating room (OR), mainly the Unified Parkinson's Disease Rating Scale<sup>7</sup> and the Hoehn and Yahr staging scale.<sup>10</sup> Previous studies have shown that such rating scales have low interrater<sup>16,18</sup> and intrarater<sup>18</sup> reliability, because they are subjective and depend highly on the experience of the evaluating neurologist.<sup>8</sup> Additionally, these scales have only discrete levels and were not designed for continuous rigidity evaluation.<sup>2</sup> To increase the sensitivity for intraoperative use, some neurologists add intermediate levels to the existing rating scales.<sup>12</sup> An alternative way to increase sensitivity is to measure movement parameters during passive movement with sensors and thereby quantify the change in rigidity.

Various methods have been proposed for quantifying the absolute level of rigidity in patients with PD by measuring responses to passive movement.<sup>11,17,19</sup> Some researchers have used surface electromyography (S-EMG) to measure muscle activity and have shown that the signals differ between healthy subjects and patients with PD.<sup>15,26</sup> Other techniques have also been proposed, which use a torque-motor setup to perform precise movements of a patient's arm or wrist while measuring joint angle and resistance.<sup>2,5,21</sup> These studies showed that the features extracted from such precise movements are more strongly correlated with rating scales than those extracted from S-EMG signals.<sup>4</sup> However, the intraoperative use of such techniques to quantify rigidity would be excessively cum-

bersome or impossible. Usable signals from S-EMG electrodes can only be obtained when they are in close contact with the skin; the prolonged use of such electrodes might cause discomfort. In addition, the mechanical torque-motor setup limits the evaluation of rigidity to a single joint, and the apparatus is typically too large for use in the OR.

Rigidity is defined as the resistance to passive movement; thus, it can be presumed that during stimulation tests, the speed of the movement would increase with a reduction in rigidity. To the best of our knowledge, no such method has been proposed, in which the change in rigidity is assessed by measuring the change in speed (acceleration) of the passive movement. One reason for the lack of such a method could be the variations associated with the passive movements. In general, each expert evaluator has a preferred joint (arm/wrist) to perform passive movements to evaluate rigidity. Each expert can also choose the pattern of passive movement (extension, flexion, or circular) to be performed during a test. An expert may also stop and restart passive movements to prevent the patient's active participation in the movements. Therefore, any method for assessing rigidity that is based on the speed of movement should have robust outcome measures that are not influenced by the intrarater and interrater variability associated with passive movement.

We previously published a method<sup>22</sup> for evaluating tremor during DBS surgery by using acceleration sensors. In the current study, we present various modifications of this method, with the aim of helping the neurologist assess the effect of stimulation on rigidity during intraoperative stimulation tests. Our hypothesis is that the relative change in rigidity can be assessed by measuring the acceleration of the evaluator's wrist during passive movement. To validate our approach, we studied the intra- and interrater variability of accelerometer measurements of passive movement in postoperative follow-up examinations of patients with PD treated with DBS. We evaluated the feasibility of intraoperative use of the system in a total of 9 DBS operations. The impact that this method would have had on the DBS surgery was studied by analyzing differences in the choice of position for the chronic DBS lead implantation (clinical choice vs choice based on accelerometry), a decision that is based on results of intraoperative stimulation tests. In addition, the accelerometry-based change in rigidity was correlated with the anatomical location of the stimulating electrode to identify the most effective stimulation sites.

## Methods

### Recording Equipment

A commercially available accelerometer sensor evaluation board (STEVAL-MKI022VI, STMicroelectronics) was used to measure the acceleration of the passive movements. It was housed inside a printed plastic case (Full-Cure 830 Vero White, Stratasys) that could be attached to the wrist with a Velcro strap (Fig. 1). The sensor board was connected through a Universal Serial Bus (USB) cable to the laptop running custom-made in-house software (LemurDBS). A wireless sensor system was not used to avoid any possible interference with the microelectrode record-

ing (MER) of the signal. Acceleration data were recorded and visualized with LemurDBS.

### Filtering and Outcome Measures

The acceleration data were processed with MATLAB version R2015b (MathWorks, Inc.). They were filtered with a smoothness priors<sup>24</sup> filter to remove the influence of gravity. To identify the changes in rigidity during intraoperative stimulation tests, the data were analyzed in a windowed manner. Various time lengths, ranging from 1 to 4 seconds with 0%–50% overlap, were tested. On the basis of the duration of a single passive movement (approximately 1 second), the duration of a single stimulation current amplitude, and the sampling frequency of the accelerometer, the 4-second window with 50% overlap was found to be optimal. To simplify the comparisons between various data sets, outcome measures were extracted from all windowed data. The measures previously found to be correlated with changes in tremor<sup>22</sup> (standard deviation, signal energy, and spectral amplitude of the dominant frequency) were used, along with others (entropy and primary frequency). For simplicity, these outcome measures will be referred to numerically as follows: 1) standard deviation, 2) signal energy, 3) spectral amplitude of the dominant frequency, 4) dominant frequency, and 5) entropy.

### Data Acquisition

#### Reliability Tests

To study the intra- and interrater variability of the outcome measures, it was necessary to collect data in a controlled environment. Such data collection during intraoperative stimulation tests would have prolonged the operations and put the patients under additional stress. Moreover, because of restrictions imposed by the OR environment, only 1 sensor could be used at a time to measure acceleration. Theoretically, acceleration of passive movements could be measured by attaching the sensor either to the patient or to the evaluator. We hypothesized that attaching the sensor to the evaluator would record higher-quality data than placing the sensor on the patient during passive movements of the wrist joint. To study this matter further and investigate the intra- and interrater variability of accelerometer data measured during passive movement, we performed special tests during the postoperative follow-up of patients with PD treated with DBS.

A specific protocol was set up to be followed by each evaluator when obtaining data from a patient. The evaluators were required to perform a set of 4 passive movements (left elbow, left wrist, right elbow, and right wrist) twice, with a short pause in between. Data from 2 acceleration sensors (1 attached to the patient and 1 attached to the evaluator) were recorded simultaneously and in a synchronized manner to test the quality of acceleration data obtained from the 2 fixation positions during different evaluations.

#### Feasibility of Intraoperative Use

To study the intraoperative feasibility of the system, it was used during DBS operations at the University Hospital in Clermont-Ferrand, France.

*Surgical Procedure.* The clinical team uses direct targeting on patient-specific imaging data as part of the surgical procedure.<sup>14</sup> During the planning session, with the aid of a brain atlas developed in-house<sup>13</sup> and multiple image sets of the patient (CT scans and MR images), including a specific white matter–attenuated inversion recovery sequence, the neurosurgeon identified and outlined the different deep brain structures in the subthalamic region with the iPlan Stereotaxy 3.0 planning software (Brainlab). Two trajectories per hemisphere were planned, from an entry point in the skull to the target structure, avoiding sensitive structures (blood vessels, cerebral ventricles). For stimulation tests, multiple positions were identified along these trajectories in the region of interest, in 1-mm steps.

The surgery was performed on awake patients. Two exploration electrodes (Alpha Omega) were inserted and electrophysiological mapping (MER) was performed at the preplanned positions in both trajectories simultaneously. After MER, stimulation tests were performed at the same positions: first in one trajectory, then in the other, moving progressively deeper into the brain tissue in steps of 1 mm. At each position, the stimulation current was increased from 0 to 3 mA in steps of 0.2 mA. To evaluate rigidity, the neurologist first passively moved the patient's arm/wrist to assess baseline rigidity, before any stimulation was delivered. Then, during stimulation, changes in rigidity compared with baseline were rated on a scale from 0 (no change) to 4 (complete suppression of rigidity). Rigidity could be rated multiple times in a single evaluation, but only the maximum reduction in rigidity was noted and used for comparison with the results at other stimulation positions. The evaluator continuously interacted with the patient to observe any side effects and to make sure that he or she was not actively moving the limb.

At each position, 2 stimulation amplitudes were identified: 1) the amplitude at which the highest reduction in rigidity was observed (subjectively assessed amplitude [AmpS]), and 2) the amplitude at which the first side effect occurred (side-effect threshold). When stimulation tests were completed, the surgical team determined the best implant position, according to the following criteria: 1) low AmpS value, 2) large difference (“therapeutic window”) between AmpS and the side-effect threshold, 3) neighboring positions having a comparatively large therapeutic window, and 4) anatomical position. Depending on the number of preoperatively chosen positions, stimulation tests in 1 cerebral hemisphere can take 15–30 minutes.

*Intraoperative Protocol for Data Recording.* To avoid prolonging the surgical procedure while maximizing the data recorded during all of the stimulation tests, a systematic data-recording procedure was followed. The acceleration sensor was mounted on the evaluator's wrist during the stimulation tests. The strap was tightened snugly, but not uncomfortably, to prevent slippage. Data recording was started during the baseline evaluation and continued until the stimulation test for 1 position was completed. A new recording was started in a similar manner for each position, and the data were saved in separate files for off-line analysis.

The stimulation current amplitude was varied in quick succession. To identify the exact amplitude responsible for

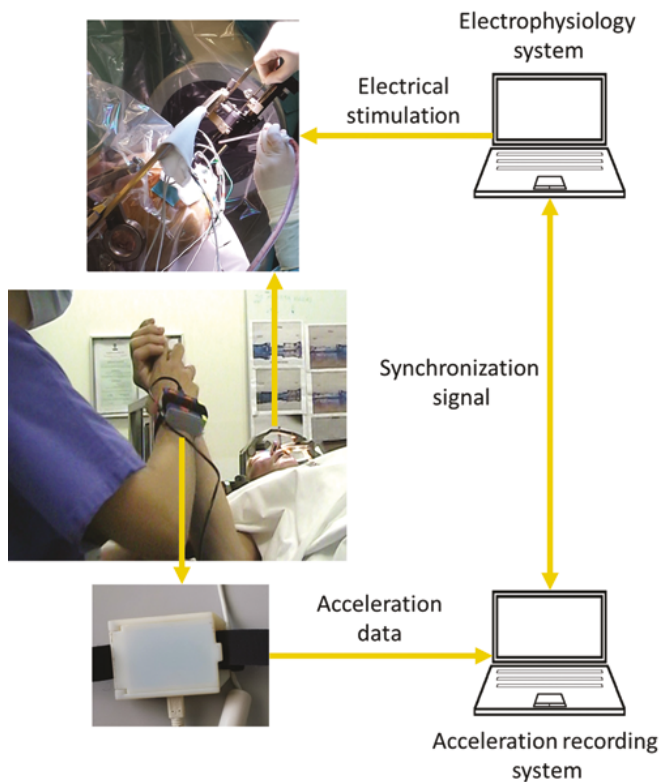


**FIG. 1.** Data recording setup used to assist rigidity evaluations performed during DBS surgery. Figure is available in color online only.

the therapeutic effects, recording of acceleration data was synchronized with the electrophysiological system. For this purpose, the electrophysiology system (Microguide Pro, Alpha Omega) was connected to a laptop running LemurDBS with a USB–Bayonet Neill–Concelman (USB–BNC) cable (Fig. 1).

**Clinical Application**

The clinical use of the afore-described data-recording system for the purpose of intraoperative and postoperative symptom evaluation in the framework of this study was approved by the institutional review boards of the Univer-

sity Hospital in Clermont-Ferrand (France) and the University Hospital of Basel (Switzerland).

For the tests of intra- and interrater reliability in post-operative follow-up, 3 different evaluators were asked to perform passive movements to assess rigidity in 3 patients with PD, according to a predefined protocol. To simulate OR conditions, the tests were done with the patients supine. Each evaluator completed 8 passive movements for each patient, yielding a total of 72 evaluations (3 patients × 3 evaluators × 2 sides × 2 joints × 2 evaluations).

To investigate the feasibility of using the system during intraoperative stimulation tests, the recording system was used during the DBS operations of 9 patients with PD, who had rigidity as their primary symptom. The patients gave their written informed consent to participate in the study (for details, see Table 1). Four different neurologists performed routine passive movements to evaluate rigidity while wearing the acceleration sensor on their wrist (each patient was evaluated intraoperatively by only 1 neurologist).

**Data Analysis Method**

The data were analyzed with MATLAB. Statistics were performed with SOFA Statistics version 1.4.5 (Patton-Simpson & Associates Ltd.) and OriginPro (Origin-Lab Corporation).

**Reliability Tests**

To validate the outcome measures, they were extracted from the acceleration sensors in both positions (attached to the patient and to the evaluator, respectively) with the MATLAB scripts after verification of synchronization. Because these measures were extracted in a windowed fashion, multiple sets of measures were available per evaluation. The outcome measures extracted from the sensors on the patient and on the evaluator would be expected to be strongly correlated with each other (pairwise) because of the simultaneous synchronized recording of data. An absence of correlation would indicate insufficient quality of acceleration data. For each evaluation, the multiple sets of outcome measures were averaged to create a pairwise data set. To confirm our presumption that the sensor on

**TABLE 1.** Details about patients participating in the clinical study and their surgical procedures

Patient No.	Age at Surgery (yrs)	Preop UPDRS-III Scores (medication off)	Evaluator ID	Tested Trajectories (no. of stimulation positions)	
				Lt	Rt
1	67	17	E1	<b>Central (9), posterolateral (9)</b>	Central (8), posterolateral (8)
2	60	26	E1	Central (8), posterior (8)	Central (3), posterior (3)
3	53	39.5	E1	<b>Central (4), posterior (4)</b>	Central (8), posterior (8)
4	61	26	E4	Central (8), posterior (8)	Central (6), posterior (6)
5	66	35	E3	Central (8), posterior (8)	Central (7), posterior (7)
6	69	45	E2	Central (6), posterior (6)	Central (6), posterior (6)
7	57	45	E4	<b>Central (8), posterior (8)</b>	Central (8), posterior (8)
8	69	27	E2	Central (7), posterior (7)	Central (7), posterior (7)
9	53	43	E2	Central (7), posterolateral (7)	Central (7), posterolateral (7)

UPDRS = Unified Parkinson's Disease Rating Scale.  
Acceleration data were unavailable for the stimulation tests in boldface type.

**TABLE 2. Categorization, comparison, and statistical tests used for analysis of data collected during reliability tests**

Purpose	Data Constraints & Groups	Comparison	Test	Result
Patient sensor vs evaluator sensor	Test 1: elbow movements; Test 2: wrist movements	Pairwise correlation of outcome measures from patient's sensor & evaluator's sensor	Spearman's correlation test	Correlation for elbow movements (Test 1): outcome measures 1, 2, & 3; correlation for wrist movements (Test 2): none
Intrarater variability	Data only from evaluator's sensor	Pairwise comparison btwn outcome measures of repeated evaluation of the same joint	Paired-sample Wilcoxon signed-rank test	No change in outcome measures 1, 2, & 3
Interrater variability	Data only from evaluator's sensor. Comparison per patient, side, & joint	Comparison of outcome measures 1, 2, & 3 btwn different evaluators	Kruskal-Wallis ANOVA	Interrater variability in outcome measures 1, 2, & 3

the patient would not be sensitive enough to detect wrist movements, the pairwise correlation of the outcome measures from the patient's and the evaluator's sensors was tested for wrist and elbow evaluations separately with the Spearman correlation test.

For reliable assessment of changes in rigidity, the outcome measures of the evaluator's sensor were checked for intrarater variability by comparing data from evaluations 1 and 2 of each evaluation type. From the data set of averaged outcome measures, only those for the evaluator's sensor were separated into data from evaluations 1 and 2 for pairwise comparison. The Wilcoxon signed-rank test was used to verify similarity between the outcome measures of these 2 groups.

To study interrater variability, the multiple outcome measures per evaluation were compared independently for the different evaluators and patients. The data were grouped for the 4 different joints (left elbow, left wrist, right elbow, and right wrist). The Kruskal-Wallis ANOVA test was used for each patient to check for interrater variations.

The different groupings and statistical tests described above are summarized in Table 2.

#### Feasibility of Intraoperative Use

The intraoperatively recorded acceleration data were synchronized with the stimulation current amplitude according to the time-stamped synchronization signal (Fig. 2, upper). The repetitive nature of passive movements facilitated the identification and removal of data corresponding to other movements of the evaluator's arm. The data corresponding to 1 stimulation test were divided into 2 parts as follows: 1) the data recorded during passive movements without any stimulation were called baseline data, and 2) the remaining data were called stimulation data. These data were then filtered and outcome measures were extracted with the MATLAB scripts as described above. Further, to perform comparative analysis in a manner similar to the neurologists' evaluations, the extracted outcome measures from the stimulation data were normalized to the highest outcome measures at baseline (Fig. 2, lower).

To investigate the pairwise correlation between normalized outcome measures and clinical ratings, Spearman's correlation test was used. Because a neurologist's assessment of change in rigidity was only noted once for each stimulation position (change at AmpS), the subjective ratings were compared with the normalized outcome mea-

asures at AmpS. Furthermore, the mean of the normalized outcome measures that were well correlated was called the quantitatively assessed change (QC) in rigidity.

#### Identification of Rigidity Release Threshold

During subjective evaluations, the AmpS (that is, the stimulation current amplitude for the highest change in rigidity) was determined by the evaluator for each stimulation position. In addition, the amplitude inducing a QC similar to the subjectively assessed reduction at AmpS was identified and designated as quantitatively identified rigidity-suppressing amplitude (AmpQ). The Wilcoxon 2-sided signed-rank test was used to compare AmpS and

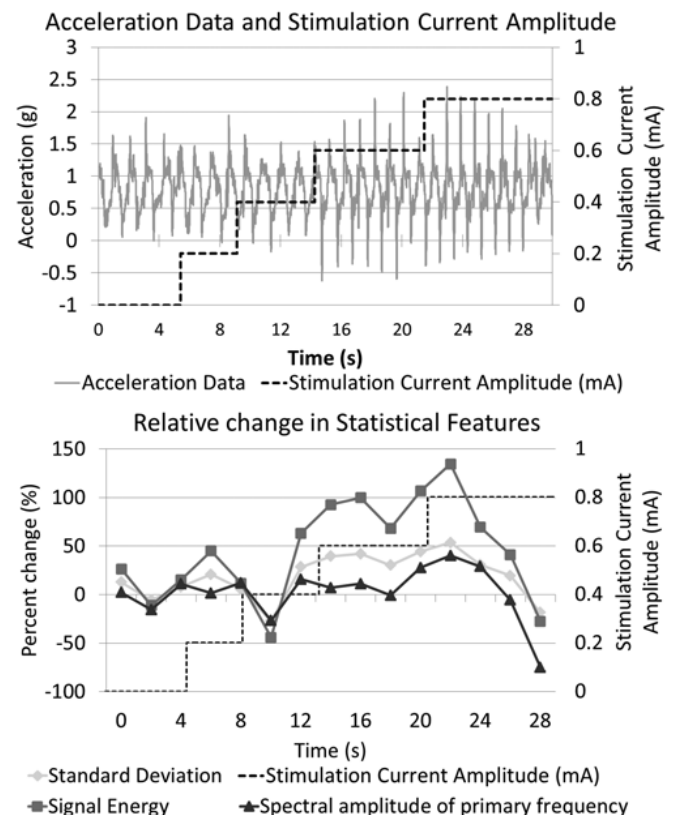


**FIG. 2.** Graphical representation of the recorded acceleration data synchronized with the stimulation current amplitude (upper) for 1 stimulation test, and outcome measures extracted in a windowed manner from the recorded signal along with the stimulation current amplitude (lower).

AmpQ for stimulation tests where both the AmpQ and the AmpS were identified.

#### Impact on Surgical Decision Making

During the routine procedure, the surgical team would determine the best implant position of the DBS lead on the basis of the AmpS, the side-effect threshold, and the anatomy, as described above. To study the effect of accelerometry-based rigidity change assessment on the final implant position chosen, the clinical staff was asked which final implant position they would have chosen if they had considered the AmpQ rather than the AmpS values. These choices were compared with the actual best implant positions chosen after intraoperative stimulation testing for each patient.

#### Anatomical Analysis

The intraoperative accelerometric assessment of change in rigidity was used to study the efficacy of stimulation in different anatomical structures as targets for the reduction of rigidity. On the basis of the planning data, the surgical team postoperatively identified the anatomical structure present at the center of the stimulating contact for every stimulation position and verified it with the MER data. To compare the efficacy of the different anatomical locations on the basis of the accelerometric measurements, at each stimulation test position the lowest stimulation current amplitude at which the QC value increased to more than 75% was identified, if it existed (Amp75). The threshold value of 75% was chosen to identify only the structures responsible for high reduction of rigidity. We also compared the side-effect thresholds and the number of stimulation tests where side effects were observed as a percentage of the total number of stimulation tests in a particular structure. These data sets, composed of Amp75, occurrence of side effects, and side-effect thresholds, were used to compare the efficacies of different anatomical structures.

## Results

The accelerometric method could be successfully applied in the postoperative validation tests and in 9 DBS operations without prolonging the procedures. All evaluators and patients were comfortable with wearing the acceleration sensor while performing the rigidity evaluations. Routine evaluations and routine surgical procedures took place as usual, without any interruptions. During implantation in the left hemisphere of Patient 1, the sensor was mounted on the patient's wrist and not on the evaluator's. Data recorded during these stimulation tests were not included in the analysis. No electrophysiological data were available for implantation in the left hemisphere of Patient 3. For Patient 7, due to the absence of rigidity, akinesia was evaluated during stimulation tests in the left hemisphere.

#### Reliability Tests

Figure 3 shows an example of a comparison between data sets acquired with acceleration sensors mounted on the patient and on the evaluator for elbow and wrist movements. For the elbow tests, of the 5 outcome measures, 3 showed a strong correlation (outcome measure 1:  $R = 0.766$ ,  $p < 0.001$ ; outcome measure 2:  $R = 0.756$ ,  $p < 0.001$ ;

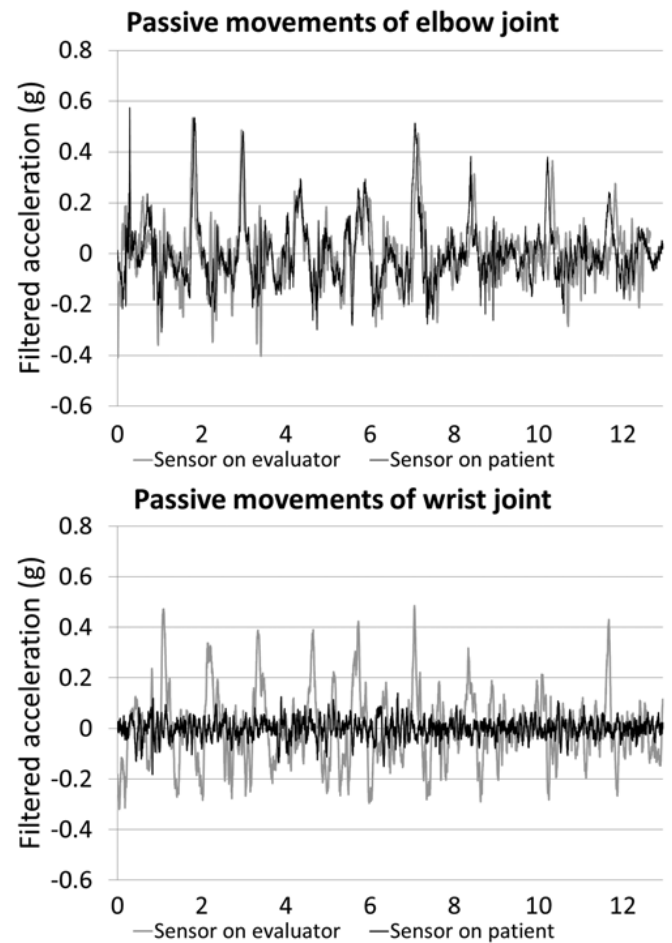


**FIG. 3.** Filtered acceleration data from the sensors mounted on the evaluator (solid gray line) and on the patient (solid black line). The graphs show data from the passive movements of the elbow (upper) and wrist joint (lower).

and outcome measure 3:  $R = 0.697$ ,  $p < 0.001$ ) between the 2 sensors, whereas the remaining outcome measures (4 and 5) showed a weak or no correlation. In contrast, none of the features exhibited a correlation between patient-derived and evaluator-derived measurements of passive movement of the wrist.

In the analysis of intrarater variability, the results of the paired-sample Wilcoxon signed-rank tests showed that 3 outcome measures did not change (outcome measures 1, 2, and 3;  $p < 0.001$ ) between repeated evaluations of the same joint. Therefore, only these 3 outcome measures were retained in the further analysis.

The interrater variability analysis (Kruskal-Wallis ANOVA test) for the different joints and for each patient showed that outcome measures 1, 2, and 3 were significantly different ( $p < 0.05$ ) among the 3 evaluators. Box plots in Fig. 4 represent the interrater variations in outcome measure 1. They show that for some evaluations (left elbow, right elbow, and right wrist of Patient 3), the interrater variability was very low, but for others (left and right elbow of Patient 1, and right wrist of Patient 3) there were significant interrater differences. Outcome measures 2 and 3 have similar distributions.

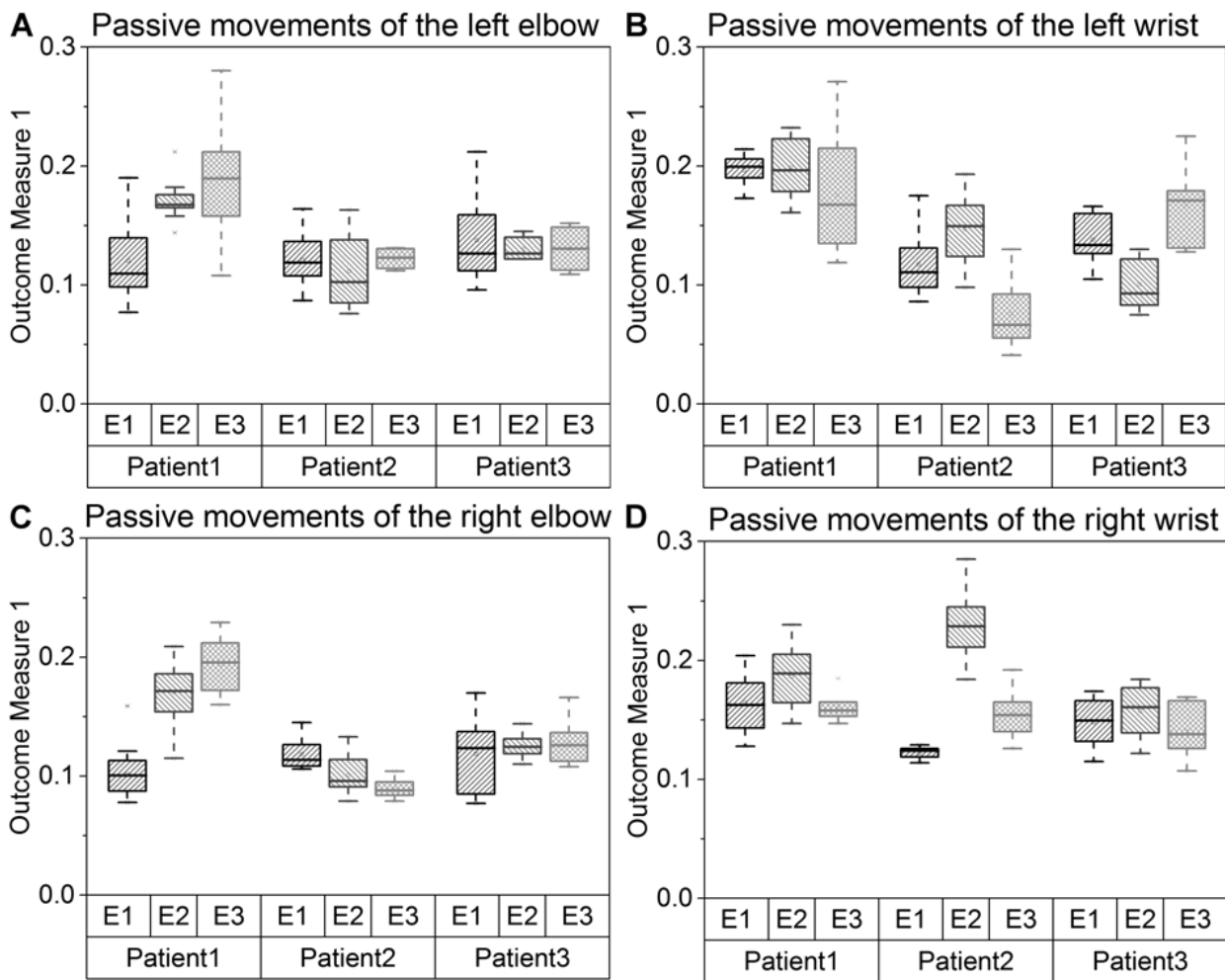


FIG. 4. Box plots showing the interrater variations (E1, E2, E3) for outcome measure 1 for passive movements of the left elbow (A), left wrist (B), right elbow (C), and right wrist (D).

The statistical results of the above tests are summarized in Table 2.

#### Feasibility of Intraoperative Use

The comparison between the normalized outcome measures and the subjectively rated change in rigidity during intraoperative stimulation tests indicates a strong correlation for outcome measures 1 ( $R = 0.308$ ,  $p < 0.001$ ), 2 ( $R = 0.313$ ,  $p < 0.001$ ), and 3 ( $R = 0.237$ ,  $p < 0.05$ ). Therefore, QC (the quantitatively assessed change in rigidity) was calculated as the mean of the normalized values of these outcome measures.

#### Identification of Rigidity Release Threshold

Of 188 stimulation tests during which acceleration data were recorded, AmpS and AmpQ were available and could be compared for 140 stimulation tests. The other 48 were composed of 14 evaluations where neither method identified any reduction in rigidity, 30 evaluations where the subjective evaluation did not find any threshold, and 4 evaluations where the accelerometric evaluation did not identify a threshold. The mean value of AmpQ ( $0.9 \pm 0.6$  mA) was lower than AmpS ( $1.4 \pm 0.6$  mA), and the results of the

Wilcoxon 2-sided signed-rank test confirmed inequality between AmpQ and AmpS values (Fig. 5,  $p < 0.001$ ). For stimulation tests where the value for AmpQ was lower than for AmpS, it was observed that the value of QC during stimulation was uniform between these 2 amplitudes.

#### Impact on Surgical Decision Making

The comparison of choices of the final implant position is shown in Table 3. Because of error in the synchronization setup, only 2 stimulation tests were analyzed for the left implantation in Patient 5, for which data were insufficient to identify the best implant position for this hemisphere. Of the remaining 14 implantations, for only 2 positions (rows in boldface type in Table 3), the choice was the same when made with AmpS or AmpQ. In 4 cases, a position on another trajectory was chosen on the basis of the AmpQ compared with the AmpS values.

#### Anatomical Analysis

For this analysis, 125 stimulation tests were used for which QC values were higher than 75%. Furthermore, the number of stimulation tests in the substantia nigra (1 test) and thalamus (4 tests) were not large enough to pro-

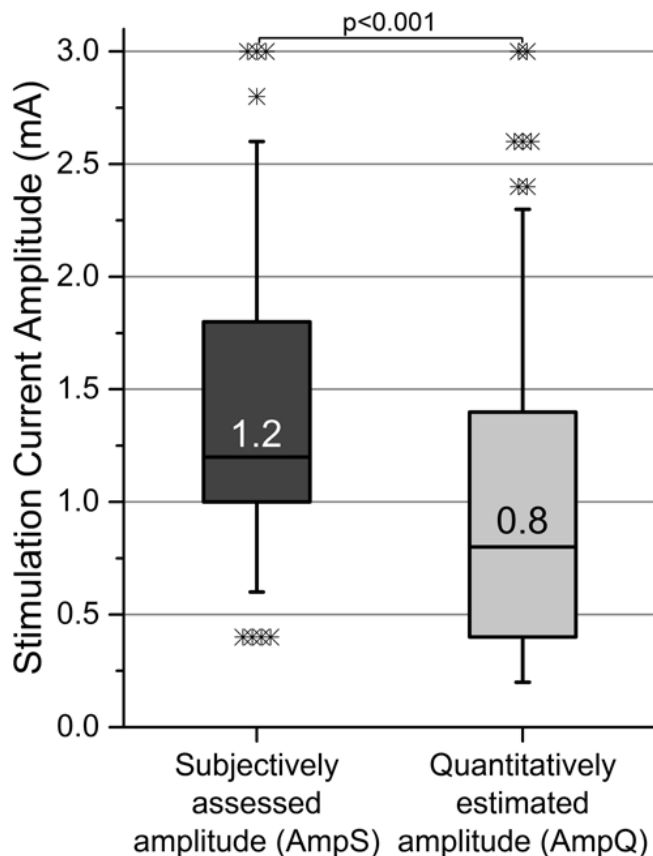


**FIG. 5.** Box plot comparing the rigidity-suppressing stimulation current amplitudes ( $n = 140$ ) identified with subjective evaluation (AmpS) and from the quantitative data (AmpQ). *Upper whiskers* are at the 95th percentile and *lower whiskers* are at the 5th percentile. Asterisks represent outliers.

vide statistically significant results. Of the remaining 120 stimulation tests, 64 were in the STN, 35 were in the zona incerta (ZI), and 21 were found in the fields of Forel (FF). The results depicted on the left in Fig. 6 show that the STN requires lower stimulation current amplitudes than the ZI and FF to reduce rigidity by at least 75%. The average values of side-effect thresholds were similar for all 3 structures (STN  $2.68 \pm 0.36$  mA, ZI  $2.72 \pm 0.17$  mA, and FF  $2.5 \pm 0.22$  mA), but the STN had a significantly higher occurrence of side effects (Fig. 6, right).

## Discussion

This article describes a novel method of recording and analyzing rigidity evaluation during DBS surgery by means of an acceleration sensor strapped on the evaluator's wrist. The aim was to test the hypothesis that changes in the patient's rigidity can be assessed by measuring acceleration during passive movement. Validation tests were performed to confirm the optimal mounting position of the acceleration sensor, to check for low intrarater variability of the outcome measures, and to assess interrater variability, before using the system intraoperatively.

### Reliability Tests

The comparison between the data of the sensor on the

patient's wrist and the sensor on the evaluator's wrist (Fig. 3) and the Spearman's correlation test confirmed our hypothesis that a fixation on the evaluator's wrist is more robust for measuring passive movements of both joints. Therefore, for an intraoperative use without altering the existing surgical procedure, the sensor should be mounted on the wrist of the evaluator, as done in the current study.

The low intrarater variability in 3 of the 5 outcome measures shows that these outcome measures are sufficiently robust for use in the intraoperative environment. During our intraoperative stimulation tests, intrarater variability would not have been relevant because the evaluator performs no other activity than passive movement, pausing only between stimulation test positions. In any case, even if the evaluator has to stop and then resume passive movements, the current method will be able to reliably assess the change in rigidity.

As mentioned previously, the performed passive movements vary between evaluators,<sup>27</sup> so interrater variations are expected in the accelerometer data. These variations also influence the outcome measures, as depicted in the box plots in Fig. 4 and as statistically confirmed. It must be borne in mind that the results of the Kruskal-Wallis ANOVA test are based on a small sample size, thus reducing their power. Because of the high inherent interrater variability of passive movements, the determination of the absolute level of rigidity in patients by measuring the acceleration is not possible. Thus, the aim of the current study was to develop a method for the determination of relative changes compared with baseline evaluations.

### Feasibility of Intraoperative Use

The method proposed in this article is designed to assist the neurologist in estimating the changes in rigidity during intraoperative stimulation tests of DBS surgery. Considering that in most centers only 1 evaluator is present to perform the passive movements, the current method will produce reliable results because of the high intrarater reliability. Additionally, the technique of normalization of the outcome measures used in the current method not only mimics the subjective evaluation method (that is, assess changes compared with baseline values), but also minimizes the effect of any residual intrarater variability between different stimulation test positions. The evidence is provided by the results of the Spearman's correlation tests between the 3 normalized outcome measures and the clinically rated changes in rigidity.

Moreover, such an evaluation is superior to absolute evaluation, because the rigidity of the patient may also change due to other factors such as microlesional effects, patient stress, and so on. However, it was also noted during the data analysis that a minimum recording of 5 seconds of baseline evaluation is needed to obtain evaluable results. When such data were unavailable, the baseline data from the previous stimulation test position (a maximum of 3 minutes before) were used. The results of the application of this method in 9 DBS operations support its future use in the OR.

Quantitative rigidity evaluations have rarely been performed during DBS surgery. To our knowledge, only Kwon et al.<sup>12</sup> have used a mechanical setup to measure parameters of rigidity in the wrist joint while the patient

TABLE 3. Choice of best implant position for the DBS lead

Patient No.	Hemisphere	Choice Based on Clinical Evaluation		Choice Based on Thresholds Extracted From Acceleration Data	
		Trajectory	Distance to Target (mm)	Trajectory	Distance to Target (mm)
1	Lt	Central	0	NA	NA
1	Rt	Central	-1	Central	-3
2	Lt	Central	0	Posterior	-1
2	Rt	Central	-3.5	Posterior	-4
3	Lt	Central	-4	NA	NA
<b>3</b>	<b>Rt</b>	<b>Central</b>	<b>-3</b>	<b>Central</b>	<b>-3</b>
4	Lt	Central	-1	Central	-3
4	Rt	Central	-2	Central	-3
5	Lt	Central	-4.5	NA	NA
<b>5</b>	<b>Rt</b>	<b>Central</b>	<b>-1</b>	<b>Central</b>	<b>-1</b>
6	Lt	Central	-3.5	Central	-3
6	Rt	Central	-3.5	Posterolateral	-3
7	Rt	Central	-2	Posterolateral	-5
8	Lt	Central	-2	Central	-1
8	Rt	Central	-2	Central	-6
9	Lt	Central	-2.5	Central	-1
9	Rt	Central	-3.5	Central	-8

NA = not available (that is, for stimulation tests in the left hemisphere of Patients 1, 3, and 5, acceleration data were insufficient to make a choice). The choice of the best implant position was the same for the rows in boldface type.

underwent surgery. An expert evaluator passively moved the patient's wrist around the joint through a handle while the input force of the evaluator and the inertia of the movement were measured. Mechanical parameters such as work, impulse impedance, and so on were extracted. In contrast to our method, their setup enables the measurement of multiple variables simultaneously, but is restricted to evaluation of the wrist joint. Moreover, for proper functioning, instructions were given to the evaluator to perform a specific movement, which resulted in longer evaluations. In addition, the evaluator had to change his or her routine evaluation protocol. In order not to prolong the surgical

procedure, fewer evaluations were performed when their setup was used.<sup>12</sup> Our system was specifically designed for use in routine evaluation; no instructions were given to the patient or the evaluator. Because the evaluator could follow his or her usual evaluation protocol, the duration of the routine surgery was unaltered.

#### Identification of Rigidity Release Threshold

One of the advantages of using our method rather than subjective evaluation is in the identification of rigidity release thresholds. Twenty-six more thresholds were found with our data analysis technique. Also, the results of the

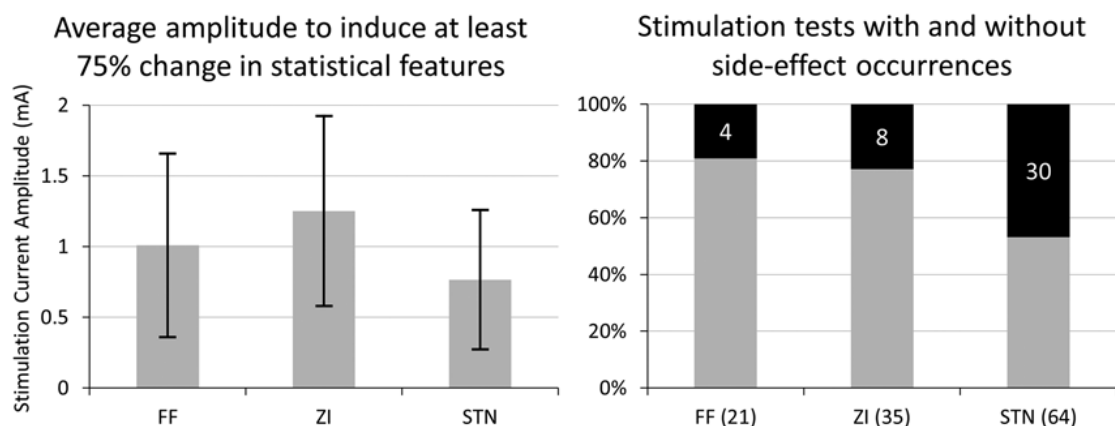


FIG. 6. **Left:** Column charts comparing the average stimulation current amplitude required to observe at least a 75% reduction in the mean of the 3 outcome measures (standard deviation, signal energy, and spectral amplitude of the primary frequency). **Right:** Stacked 100% column charts present the number of stimulation tests where side effects were observed (black) as a percentage of the total number of stimulation tests in the corresponding structure. The numbers inside the black part of the bars indicate the actual count of the side-effect occurrences; the numbers below the bars indicate the total number of stimulation tests.

Wilcoxon 2-sided signed-rank test and the box plot show that values tend to be lower for AmpQ than for AmpS. We believe that the human evaluator, on observing the change in rigidity, may need a few seconds to verify and assess the amount of reduction. During this time, the amplitude may have already been increased, resulting in higher AmpS values. This result suggests that the current setup enhances the sensitivity of the subjective rigidity evaluation. On the other hand, there were 4 positions where AmpS values, but no AmpQ values, were found. On inspection of these 4 positions, it was observed that the baseline data were insufficient to extract outcome measures for normalization. Because they were the first positions tested, baseline evaluations of previous positions were unavailable to use the workaround. This underscores the need for sufficient baseline recording for data analysis.

### Impact on Surgical Decision Making

The differences in the rigidity release amplitudes identified by the 2 methods significantly influenced the choice of the best implant position. Only 2 of the 12 choices would have been at the same position. This clearly shows the potential of using an assistive method during intraoperative symptom evaluation for DBS surgery. From the current data, it is not possible to judge which of the 2 choices was better. One possible way would be to compare the choice of best implant position with the choice of postoperative contact; the relative closeness of one or the other choice may help to judge whether the assistive evaluation system can identify better implant positions. However, such an analysis would need a very large data set to result in statistically significant conclusions.

### Anatomical Analysis

The anatomical analysis gives interesting insight into the target selection procedure of DBS. It shows that stimulation in the STN requires the lowest current amplitude to achieve a 75% reduction in rigidity. However, in view of the fact that side effects were observed in nearly 50% of stimulations in the STN, it may not be the optimum target structure. The FF require an additional 0.3 mA, on average, to achieve a comparable reduction in rigidity, but have significantly fewer side-effect occurrences. Hence, to achieve a better outcome of DBS for patients with rigidity, the DBS lead might be placed closer to the FF or the ZI and not inside the STN, to avoid side effects. This would be in accordance with reported findings<sup>3,6,9,20,28</sup> implying that the FF and the ZI may also be responsible for the therapeutic effects of DBS. However, this analysis has a limitation. It only considers the center of the electrode when associating a structure with a stimulation test position. Because the effect of stimulation spreads beyond the center, electric-field simulations would be a helpful tool to deepen the analysis of the available intraoperative data.

### Future Work

In its current state, the method proposed in this study has various advantages over the existing subjective ratings used in the OR. It provides a reproducible assessment of the change in rigidity, which can be reviewed at any time dur-

ing surgery without any discomfort to the patient or evaluator, and without prolonging the operation. Nevertheless, because the changes in rigidity are assessed indirectly, the results produced are only semiquantitative. In the future, to make the method a comprehensive evaluation system for use in DBS surgery, the current setup will be modified to enable data recording and analysis from 2 smaller acceleration sensors simultaneously. By mounting one sensor on the evaluator and the other on the patient,<sup>23</sup> it will be possible to evaluate rigidity and tremor at the same time. We intend to use the system in more operations (optimally, in additional clinical centers as well) so that we can continue to adapt it to physicians' needs. The long-term aim is to integrate this method in commercially available and currently used intraoperative stimulation systems to facilitate visualization of the symptom improvement in real time, along with other stimulation parameters and anatomical data. Such a system would enable the surgical team to interpret the results of intraoperative stimulation tests more easily and thus facilitate surgical decision making.

### Conclusions

We have described a new way to assess changes in rigidity by measuring the acceleration of the examiner's wrist during passive movement while the patient is undergoing intraoperative stimulation testing in DBS surgery. Outcome measures are reproducible over time but are influenced by variations in the passive movements of different evaluators. The intraoperatively assessed change in rigidity is reliable and is correlated with the subjective ratings. The quantitatively identified effective stimulation amplitudes show the potential of the method to optimize surgical decision making. Moreover, our findings concerning the thresholds for effective stimulation at different anatomical sites suggest that the optimal DBS target may, in fact, lie closer to the FF, just dorsal to the STN. The proposed method may be a clinically and scientifically useful aid to optimal targeting in DBS.

### Acknowledgments

This research was funded by the Swiss National Science Foundation as a part of the project 205321\_135285 and partly by the Germaine de Stael program of the Swiss Academy of Engineering Sciences. We acknowledge and thank Prof. F. Durif, Dr. M. Ulla, and Dr. A. Marques of the Department of Neurology at the CHU Clermont-Ferrand, France, and Ms. Bianca Raffaelli and Prof. Dr. Peter Fuhr of the Department of Neurology at the University Hospital of Basel, Switzerland, for performing the routine passive movements for rigidity evaluations.

### References

1. Abosch A, Timmermann L, Bartley S, Rietkerk HG, Whiting D, Connolly PJ, et al: An international survey of deep brain stimulation procedural steps. *Stereotact Funct Neurosurg* **91**:1–11, 2013
2. Askari S, Zhang M, Won DS: An EMG-based system for continuous monitoring of clinical efficacy of Parkinson's disease treatments. *Conf Proc IEEE Eng Med Biol Soc* **2010**:98–101, 2010
3. Aström M, Tripoliti E, Hariz MI, Zrinzo LU, Martinez-Torres I, Limousin P, et al: Patient-specific model-based investiga-

- tion of speech intelligibility and movement during deep brain stimulation. **Stereotact Funct Neurosurg** 88:224–233, 2010
4. Endo T, Okuno R, Yokoe M, Akazawa K, Sakoda S: A novel method for systematic analysis of rigidity in Parkinson's disease. **Mov Disord** 24:2218–2224, 2009
  5. Fung VS, Burne JA, Morris JG: Objective quantification of resting and activated parkinsonian rigidity: a comparison of angular impulse and work scores. **Mov Disord** 15:48–55, 2000
  6. Godinho F, Thobois S, Magnin M, Guenot M, Polo G, Benartru I, et al: Subthalamic nucleus stimulation in Parkinson's disease: anatomical and electrophysiological localization of active contacts. **J Neurol** 253:1347–1355, 2006
  7. Goetz CG, Tilley BC, Shaftman SR, Stebbins GT, Fahn S, Martinez-Martin P, et al: Movement Disorder Society-sponsored revision of the Unified Parkinson's Disease Rating Scale (MDS-UPDRS): scale presentation and clinimetric testing results. **Mov Disord** 23:2129–2170, 2008
  8. Griffiths RI, Kotschet K, Arfon S, Xu ZM, Johnson W, Drago J, et al: Automated assessment of bradykinesia and dyskinesia in Parkinson's disease. **J Parkinsons Dis** 2:47–55, 2012
  9. Hamel W, Fietzek U, Morsnowski A, Schrader B, Herzog J, Weinert D, et al: Deep brain stimulation of the subthalamic nucleus in Parkinson's disease: evaluation of active electrode contacts. **J Neurol Neurosurg Psychiatry** 74:1036–1046, 2003
  10. Hoehn MM, Yahr MD: Parkinsonism: onset, progression and mortality. **Neurology** 17:427–442, 1967
  11. Kirolos C, Charlett A, O'Neill CJ, Kosik R, Mozol K, Purkiss AG, et al: Objective measurement of activation of rigidity: diagnostic, pathogenetic and therapeutic implications in parkinsonism. **Br J Clin Pharmacol** 41:557–564, 1996
  12. Kwon Y, Park SH, Kim JW, Ho Y, Jeon HM, Bang MJ, et al: Quantitative evaluation of parkinsonian rigidity during intra-operative deep brain stimulation. **Biomed Mater Eng** 24:2273–2281, 2014
  13. Lemaire JJ, Caire F, Bony JM, Kemeny JL, Villeger A, Chazal J: Contribution of 4.7 Tesla MRI in the analysis of the MRI anatomy of the human subthalamic area. **Acta Neurochir (Wien)** 146:906–907, 2004
  14. Lemaire JJ, Coste J, Ouchchane L, Hemm S, Derost P, Ulla M, et al: MRI anatomical mapping and direct stereotactic targeting in the subthalamic region: functional and anatomical correspondence in Parkinson's disease. **Int J Comput Assist Radiol Surg** 2:75–85, 2007
  15. Levin J, Krafczyk S, Valkovic P, Eggert T, Claassen J, Bötzel K: Objective measurement of muscle rigidity in Parkinsonian patients treated with subthalamic stimulation. **Mov Disord** 24:57–63, 2009
  16. Palmer JL, Coats MA, Roe CM, Hanco SM, Xiong C, Morris JC: Unified Parkinson's Disease Rating Scale-Motor Exam: inter-rater reliability of advanced practice nurse and neurologist assessments. **J Adv Nurs** 66:1382–1387, 2010
  17. Park BK, Kwon Y, Kim JW, Lee JH, Eom GM, Koh SB, et al: Analysis of viscoelastic properties of wrist joint for quantification of parkinsonian rigidity. **IEEE Trans Neural Syst Rehabil Eng** 19:167–176, 2011
  18. Post B, Merkus MP, de Bie RM, de Haan RJ, Speelman JD: Unified Parkinson's disease rating scale motor examination: are ratings of nurses, residents in neurology, and movement disorders specialists interchangeable? **Mov Disord** 20:1577–1584, 2005
  19. Prochazka A, Bennett DJ, Stephens MJ, Patrick SK, Sears-Duru R, Roberts T, et al: Measurement of rigidity in Parkinson's disease. **Mov Disord** 12:24–32, 1997
  20. Saint-Cyr JA, Hoque T, Pereira LCM, Dostrovsky JO, Hutchison WD, Mikulis DJ, et al: Localization of clinically effective stimulating electrodes in the human subthalamic nucleus on magnetic resonance imaging. **J Neurosurg** 97:1152–1166, 2002
  21. Sepehri B, Esteki A, Ebrahimi-Takamjani E, Shahidi GA, Khamseh F, Moinodin M: Quantification of rigidity in Parkinson's disease. **Ann Biomed Eng** 35:2196–2203, 2007
  22. Shah A, Coste J, Lemaire JJ, Schkommodau E, Hemm-Ode S: A method to quantitatively evaluate changes in tremor during deep brain stimulation surgery, in **6th Annual International IEEE EMBS Conference on Neural Engineering**, San Diego, 2013 (<http://ieeexplore.ieee.org/abstract/document/6696155/>) [Accessed November 30, 2016]
  23. Strauss I, Kalia SK, Lozano AM: Where are we with surgical therapies for Parkinson's disease? **Parkinsonism Relat Disord** 20 (Suppl 1):S187–S191, 2014
  24. Tarvainen MP, Ranta-Aho PO, Karjalainen PA: An advanced detrending method with application to HRV analysis. **IEEE Trans Biomed Eng** 49:172–175, 2002
  25. Wichmann T, Delong MR: Deep-brain stimulation for basal ganglia disorders. **Basal Ganglia** 1:65–77, 2011
  26. Wright D, Nakamura K, Maeda T, Kutsuzawa K, Miyawaki K, Nagata K: Research and development of a portable device to quantify muscle tone in patients with Parkinson's disease. **Conf Proc IEEE Eng Med Biol Soc** 2008:2825–2827, 2008
  27. Xia R: Physiological and biomechanical analyses of rigidity in Parkinson's disease, in Rana AQ (ed): **Etiology and Pathophysiology of Parkinson's Disease**. Rijeka, Croatia: InTech, 2011, pp 485–506
  28. Zheng Z, Zhang YQ, Li JY, Zhang XH, Zhuang P, Li YJ: Subthalamic deep brain stimulation for Parkinson's disease: correlation of active contacts and electrophysiologically mapped subthalamic nucleus. **Chin Med J (Engl)** 122:2419–2422, 2009

---

## Disclosures

The authors report no conflict of interest concerning the materials or methods used in this study or the findings specified in this paper.

## Author Contributions

Conception and design: Hemm, Lemaire, Schkommodau. Acquisition of data: Shah, Coste, Lemaire, Derost, Taub. Analysis and interpretation of data: Hemm, Shah, Coste, Schkommodau, Taub, Guzman. Drafting the article: Shah. Critically revising the article: Hemm, Shah. Reviewed submitted version of manuscript: all authors. Statistical analysis: Shah. Administrative/technical/material support: Hemm, Coste, Lemaire, Schkommodau, Taub, Derost. Study supervision: Hemm, Lemaire, Taub. Supervision of PhD research: Hemm, Guzman, Taub, Schkommodau.

## Supplemental Information

### Previous Presentations

Portions of this work have been presented in poster form at the following conferences: 7th International IEEE Engineering in Medicine and Biology Society (EMBS) Neural Engineering Conference, Montpellier, France, April 22, 2015; Joint Annual Meeting of the Swiss Societies of Neuroradiology and Neurosurgery, Lucerne, Switzerland, September 10, 2015; 18th International Congress of Parkinson's Disease and Movement Disorders, Stockholm, Sweden, June 8, 2014; 20th Congress of the European Society for Stereotactic and Functional Neurosurgery, Lisbon, Portugal, September 26, 2012; and 46th Annual Conference of the German Society for Biomedical Engineering, Jena, Germany, September 16, 2012.

## Correspondence

Simone Hemm, Institute of Medical and Analytical Technologies, University of Applied Sciences and Arts Northwestern Switzerland, Gruendenstrasse 40, Muttenz CH-4132, Switzerland. email: simone.hemm@fhnw.ch.

## **Results of reliability tests for validation of acceleration sensors as an assistive tool for rigidity evaluation.**

In the manuscript titled "A novel assistive method for rigidity evaluation during deep brain stimulation surgery using acceleration sensors," the authors were asked to add tests to validate their method of using acceleration sensors to evaluate rigidity. **The aim of these tests was to answer the following questions:**

- a) **Optimal mount position of the sensor:** The acceleration sensor can be attached to the patient's wrist or the evaluator's wrist. Which of the two mount positions provides the optimum data?
- b) **Test-retest reproducibility:** Are the outcome measures extracted from the acceleration data reproducible over time, i.e. if an evaluator evaluates rigidity of the same patient twice, with a brief interval in between?
- c) **Inter-rater variations:** Do the variations in the passive movements of different evaluators evaluating the same patient affect the outcome measures?

As described in the manuscript, to answer the above questions, the proposed method was applied to rigidity evaluations during the post-operative follow-up of 3 patients who had undergone STN-DBS surgery. During these sessions, the evaluators were asked to perform passive movements in a specific sequence of tests while the stimulators were turned off. To identify which of the mount positions of the sensor is better for analysis, data from 2 sensors were recorded simultaneously in a synchronized fashion during the passive movements. Each evaluator was asked to perform passive movements on the wrist and elbow joints of both arms. After evaluating the elbow joint, the evaluator paused for a short break and repeated the passive movements of the elbow joint for the retest. After another short break, passive movements of the wrist joint were performed twice. Each evaluator performed 8 tests (two times each for left elbow, left wrist, right elbow and right wrist) for each patient. This permitted the study of inter-rater variations in the outcome measure. **As only some of the results could be integrated in the manuscript because of restrictions on length and the number of figures, the results of these tests are described here for the reviewers in greater detail.**

### **Optimum mount position of the sensor:**

Figure 3 in the paper shows the differences of the acceleration data from the sensor mounted on the evaluator and the sensor mounted on the patient. For passive movements of the elbow joint, the data from the two sensors are similar. However, for passive movements of the wrist joint, the sensor on the patient does not register enough information. The outcome measures extracted from the two sensors were checked for correlation and it was noted that they were correlated between the sensors for elbow evaluation but not for wrist evaluation.

Figure A in the present document shows the 6 scatter plots comparing the 3 outcome measures (standard deviation, signal energy and spectral amplitude of dominant frequency) obtained from a sensor attached to the evaluator with those obtained from a sensor attached to the patient during passive elbow and wrist movement. The distribution of points along the 45° diagonal and their relative closeness to it in figures A1, A2 and A3, show that the outcome measures correlate across the different evaluators and the patients for passive movements of the elbow joint. Yet, as seen in Figures A4, A5 and A6, the measures obtained from a sensor attached to the patient's wrist have much lower values than the corresponding measures obtained from a sensor attached to the evaluator's wrist. The outcome measures are not correlated for the passive movements of the wrist joint. When the sensor is mounted on the patient's wrist, the movements of the wrist joint are not recorded; therefore, the extracted statistical features are not correlated with the passive movements of the evaluator's arm. One solution would be to mount the sensor on the back of the patient's hand, but this would tend to get in the way of the grip of the evaluator. We therefore decided to mount the sensor on the evaluator, rather than the patient, during the surgery.

**Test-retest reproducibility:**

The paired-sample Wilcoxon signed-rank test reported in the manuscript revealed that the outcome measures used to assess changes in rigidity are reproducible over time. Figure B shows the scatter plots of the outcome measures (test vs. retest) obtained with the sensor mounted on the evaluator. The type of marker indicates the patient, while the gray scale of the marker indi-

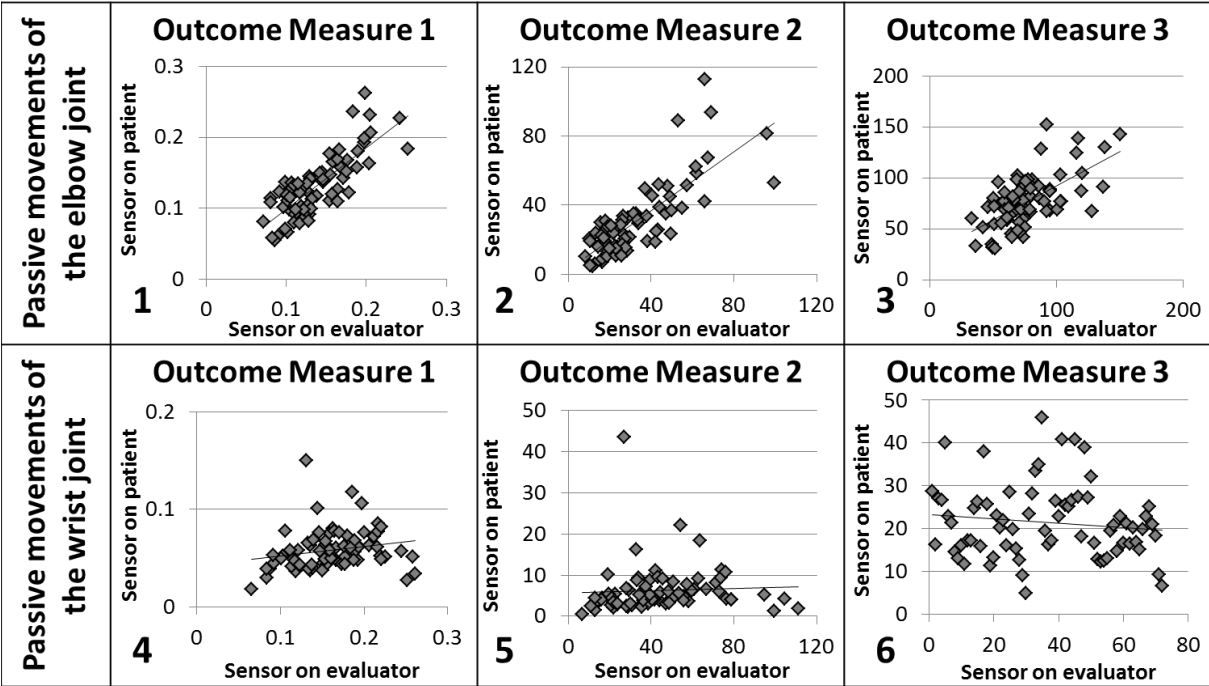


Figure A: Scatter plots for outcome measures extracted from passive movements of elbow (left column) and the wrist (right column) joints for all three evaluators together.

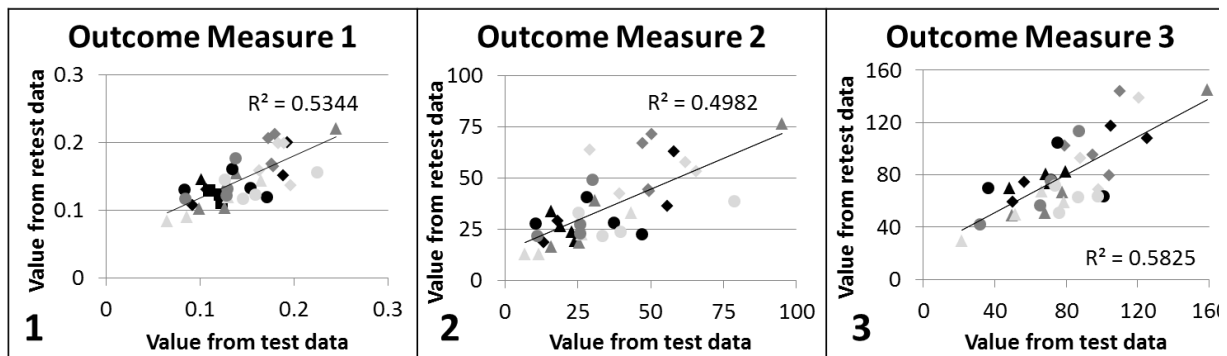


Figure B. Scatter plots showing pairwise comparison of outcome measures from test data against retest data 1) Standard deviation 2) Signal Energy and 3) Spectral amplitude of primary frequency.

Patient	Evaluator		
	1	2	3
1	◆	◇	◇
2	▲	▲	▲
3	●	●	●

icates the evaluator. The graph shows that the test and retest values are similar for nearly all evaluators and all patients, with only a few exceptions. Overall, for all the data combined, the three outcome measures (standard deviation, signal energy, and spectral amplitude of the primary frequency) are reproducible over time for each patient and evaluator. This is indicated by the angle of the trend-line (close to 45 degrees) and its  $r^2$  value (points do not lie too far away from the trend-line).

### Inter-rater variations:

The Kruskal-Wallis ANOVA test reported in the manuscript revealed variations between the outcome measures extracted from the same patient by different evaluators. As each evaluator has his/her specific pattern of passive movements to estimate rigidity, the signal recorded by the accelerometer will be different for each. As a result, the outcome measures will also vary. To suppress these variations, it would be necessary to instruct and train the evaluators to use a single, standardized type of passive movement, which might not be comfortable for and accepted by all the evaluators. More importantly, for intraoperative use of the system, these variations do not influence the result of the data analysis, because, in most clinical centers, one expert is responsible for all of the rigidity evaluations in each operation. Moreover, the purpose of the method is to identify the changes in rigidity by comparing passive movements of the same evaluator over different time periods, and not the absolute amount of rigidity in a patient.

In any case, in view of the inherently indirect nature of this technique for assessing changes in rigidity, and the observed inter-rater variability, the authors propose the method only as an assistive tool, rather than a quantitative one. The intention is to enable evaluators to assess changes in rigidity more reliably and confidently and to permit the review of any evaluation during the course of the operation or afterward.

## Chapter 6

# Quantitative Target Selection

The previously published efforts to improve target selection for DBS have relied on data collected from chronic stimulation through the DBS lead. In contrast, the large number of positions that are stimulated during the surgery may be better suited to study the efficiency of different structures. Planned surgical trajectories for a target structure traverse through neighbouring structures and in some cases, structures inferior to the target. In addition, use of intraoperative data also eliminates any effect of plasticity or post-operative adaptations in the patients brain that are observed for chronic stimulation. Furthermore, the setup of this study adds another benefit in terms of sensitivity to symptom changes due to the use of quantitative evaluation.

The surgical team in CHU, Clermont-Ferrand uses a direct targeting method with the help of an in-house developed microscopic 4.7 T 3D T1 MRI atlas.<sup>186</sup> For each patient, they carefully outline the anatomical structures (**Figure 6.1**) in the region of interest in the commercial surgical planning software called iPlan Stereotaxy (Brainlab, Munich, Germany). The necessary structures are identified based on the MRI tissue contrasts on 1.5T White Matter Attenuated Inversion Recovery (WAIR) images and the relative positions of these structures with respect to one another.<sup>379</sup> They use a previously published nomenclature<sup>187</sup> for the different thalamic nuclei for VIM-DBS implantations. In addition to the manual outlining and labelling, the surgical team also verifies the location of these structures with respect to the trajectory through MER.

In our clinical study in CHU, Clermont-Ferrand, a total of 20 patients had participated to use the quantitative symptom evaluation (**Table 3.1**). Out of these patients, 6 ET patients underwent VIM-DBS implantation, 2 PD patients underwent VIM-DBS implantation and 12 PD patients underwent STN-DBS implantation. These patients were categorized based on the disease, target and the symptom to analyze the data in terms of anatomy. This resulted in a group of 9 PD STN-DBS patients with rigidity, 3 PD STN-DBS patients with tremor,

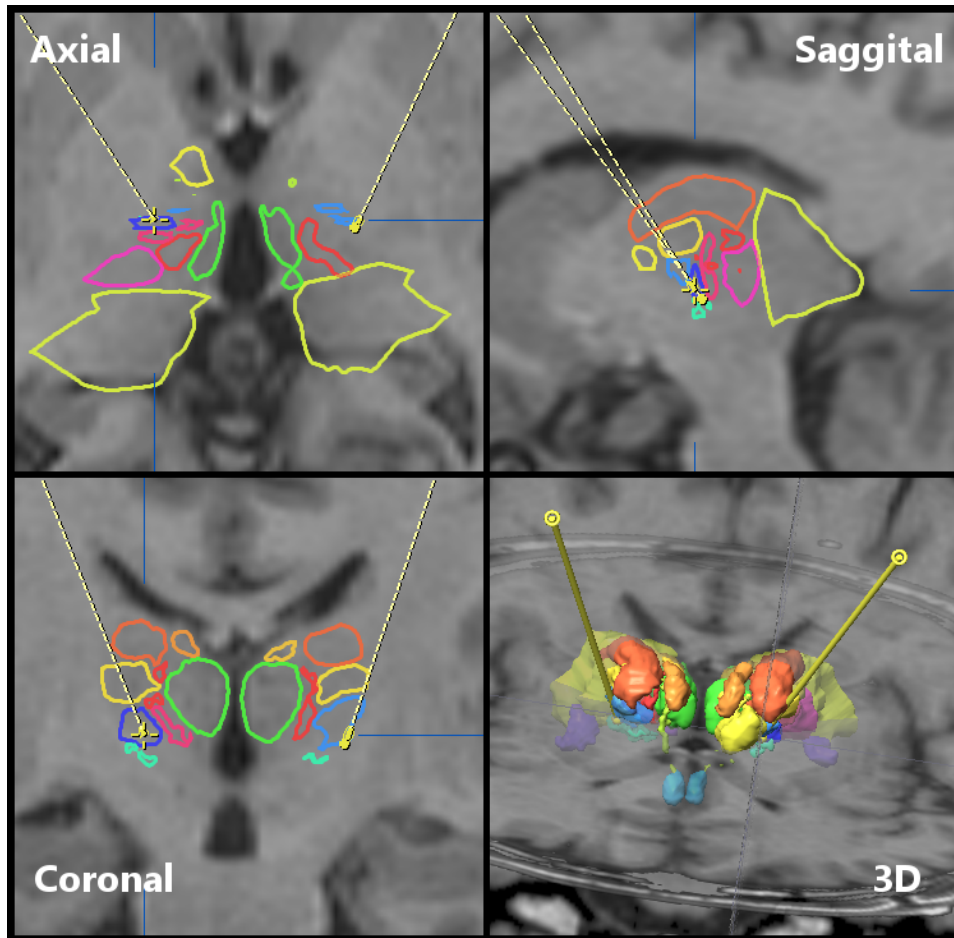


**Figure 6.1:** A screenshot of the iPlan Stereotaxy software showing the relevant structures for the DBS implantation. Courtesy of Prof. Jean-Jacques Lemaire, CHU, Clermont-Ferrand.

2 PD VIM-DBS patients with tremor and 6 ET VIM-DBS patients with tremor. One PD VIM-DBS patient took the regular medication before surgery which suppressed the symptoms and one PD STN-DBS patient had no tremor during the surgery. Due to these exclusions, anatomical analysis of the data was only possible for two groups - rigidity PD patients with STN-DBS implantation and ET patients with VIM-DBS implantation.

In accordance with the published literature, our first approach towards analysing intraoperative stimulation test data in terms of anatomy was to use the location of the stimulating contact of the electrode. For each stimulation test position, the anatomical structure surrounding the stimulating contact was identified using the pre-operative planning and verified using MER data. Using the accelerometer data, the stimulation current resulting in 75% improvement in the symptom was identified for each stimulation test. This data was classified based on the anatomical structures and compared. The details about the analysis, the results and the discussion for PD-rigidity patients with STN-DBS implantation can be found in the previous chapter (Section 5.1). Data collected from VIM-DBS implantations for ET patients are available below in the current chapter (Section 6.1).

## **6.1 Use of quantitative tremor evaluation to enhance target selection during deep brain stimulation surgery for essential tremor**

**Authors:** Ashesh Shah, Jérôme Coste, Jean-Jacques Lemaire, Erik Schkommodau, Simone Hemm-Ode.

This paper was submitted to the 49th Annual DGBMT conference which was held in Lübeck, Germany from 16th to 18th September, 2015. The aim of this paper is to identify the most effective stimulation target structure by comparing the accelerometer based tremor evaluation data. This paper is published in the journal titled "Current Directions in Biomedical Engineering".

The paper is available at the address:

<https://doi.org/10.1515/cdbme-2015-0117>

Copyright Notice: Reprinted by permission from Current Directions in Biomedical Engineering, Walter de Gruyter and Company. Shah, A., J. Coste, Jj. Lemaire, E. Schkommodau, and S. Hemm-Ode. "Use of Quantitative Tremor Evaluation to Enhance Target Selection during Deep Brain Stimulation Surgery for Essential Tremor." Current Directions in Biomedical Engineering 1, no. 1 (January 1, 2015). <https://doi.org/10.1515/cdbme-2015-0117>. ©2015.

A. Shah, J. Coste, J.J. Lemaire, E. Schkommodau, and S. Hemm-Ode\*

# Use of quantitative tremor evaluation to enhance target selection during deep brain stimulation surgery for essential tremor

**Abstract:** Deep brain stimulation (DBS), an effective surgical treatment for Essential Tremor (ET), requires test stimulations in the thalamus to find the optimum site for permanent electrode implantation. During these test stimulations, the changes in tremor are only visually evaluated. This, along with other parameters, increases the subjectivity when comparing the efficacy of different thalamic nuclei. We developed a method to quantitatively evaluate tremor during the test stimulations of DBS surgery and applied to 6 ET patients undergoing this treatment. From the quantitative data collected, we identified effective stimulation amplitudes for every test stimulation position and compared it with the ones identified visually during the surgery. We also classified the data based on the thalamic nuclei in which the center of the stimulating contact was present during test stimulations. Results indicate that, to achieve the same reduction in tremor, on average, the stimulation amplitude identified by our method was 0.6 mA lower than those identified by visual evaluation. The comparison of the different thalamic nuclei showed that stimulations in the Ventro-oral and the Intermediolateral nuclei of the thalamus result in higher reduction in tremor for similar stimulation amplitudes as the frequently targeted Ventrointermediate nucleus. We conclude that our quantitative tremor evaluation method is more sensitive than the widely used visual evaluation. Using such quantitative methods will aid in identifying the optimum target structure for patients undergoing DBS.

**Keywords:** deep brain stimulation; essential tremor; accelerometry; thalamus

DOI: 10.1515/CDBME-2015-0117

**\*Corresponding Author: S. Hemm-Ode:** Institute for Medical and Analytical Technologies, University of Applied Sciences and Arts Northwestern Switzerland, Gruendenstrasse 40, 4132 Muttenz, Switzerland, E-mail: simone.hemm@fhnw.ch; Phone: +41 61 467 4796; Fax: +41 61 467 4701

**A. Shah, J. Coste, J.J. Lemaire, E. Schkommodau:** Institute for Medical and Analytical Technologies, University of Applied Sciences and Arts Northwestern Switzerland, Gruendenstrasse 40, 4132 Muttenz, Switzerland

## 1 Background

Deep Brain Stimulation (DBS) is now a routinely used surgical treatment for movement disorders like Essential Tremor (ET) [1]. Electrical stimulation of certain brain structures is performed by implanting electrodes and connecting them to a subcutaneously implanted neurostimulator. Although the use of DBS is increasing, the optimum target structure is still debated. The limited knowledge of the mechanisms of action of DBS being one of the reasons, we believe the under-utilization of intraoperatively obtained data is another.

A typical DBS surgery is preceded by a planning session during which a trajectory is planned from an entry point in the skull to the target structure on the patient's anatomical images using stereotactic planning software. With the aid of stereotactic equipment, this trajectory is then explored during the surgery. In most of the surgeries, neuronal activity is recorded and test stimulations are performed at pre-planned positions on this trajectory while the patient is awake. The final implant position is decided after comparing the reduction in tremor, needed stimulation current for inducing those reductions and the side effects observed during the test stimulations.

In the routine clinical practice, the symptom evaluation methods are subjective [2]. Tremor is evaluated by a visual rating of the change compared to its level observed before stimulation. We have previously described the method of evaluating tremor during DBS quantitatively by using accelerometers [3]. We used this method to intraoperatively evaluate tremor from 6 ET patients who participated in a clinical study in the University Hospital in Clermont-Ferrand, France. In the current paper, we describe the result of the comparison between visual and quantitative evaluations. Further, we classified the results based on the anatomical location of the electrode and compared them to identify the target structure which is the most effective in reducing tremor.

## 2 Method

### 2.1 Surgical protocol

The primary goal of the DBS surgery remains the same for all surgical centres: to determine the optimal implantation position. However, the actual procedure may differ significantly. Lemaire et al have described, in detail, the routine surgical procedure at the University Hospital in Clermont-Ferrand [4]. For treating ET patients using DBS, the primary target structure is the Ventrointermedius nucleus (VIM) of the thalamus. At the University Hospital in Clermont-Ferrand, during the planning session on patient's images using a commercial stereotactic surgery planning software (iPlan Stereotaxy, Brainlab, Germany), the surgical team identifies and outlines different nuclei in the thalamus using MRI images of the patient [5]. After the definition of target and entry point, test stimulation positions are planned on the resulting trajectory. After performing micro-electrode recording (MER) at these positions, test stimulations are performed. For each test stimulation, the stimulation current is varied from 0 to 3 mA in steps of 0.2 mA and the changes in tremor are observed visually. The highest reduction in tremor (Visually identified Change, VC) and the corresponding stimulation amplitude (Visually identified Amplitude, VA) at which it was observed are noted for every test stimulation location. Along with these, the occurrence of side-effects, their type and their corresponding amplitudes are also noted. On completion of all test stimulations, these data are discussed upon by the surgical team and a position is determined as the "final implant location" for the chronic DBS electrode.

### 2.2 Acceleration data recording

Tremor was quantified during the surgery using a commercial acceleration sensor evaluation board (STEVAL-MKI022VI, ST Micro, Switzerland). Time-stamped acceleration values from 3 axes were obtained at a frequency of 400 Hz and a range of 8 g. The evaluation board was fixed in an in-house developed non-conductive printed plastic case which was attached to the patient's wrist using a Velcro strap. The acceleration data were recorded by in-house developed software installed on a laptop that was interfaced with the sensor via an USB cable. Furthermore, the recording software was also interfaced with the electrophysiology system to synchronize the acceleration data recording with the test stimulation data.

For the simplification of acceleration data recording and analysis, a data recording protocol was defined for all the surgeries. Acceleration data recording is started before the beginning of the test stimulation to record the data representing the baseline tremor for that test stimulation, and is continued till all the stimulation amplitudes are tested. The acceleration data and the related information about the test stimulation position and amplitude were saved in data files for offline analysis [3].

### 2.3 Post-operative data analysis

Acceleration data were analysed post-operatively using Matlab (Mathwork, USA). In brief, the resultant acceleration was calculated from the three axes and filtered to remove low frequency (2 Hz) movements and high frequency noise (10 Hz). Statistical features were extracted from these filtered acceleration data and the features from different stimulation amplitudes were normalized (%) using the features from the baseline data. These normalized features were used to identify a dataset of 2 values for each test stimulation: 1.) The change in acceleration features (Quantitatively identified Change, QC) at the visually identified best stimulation amplitude VA and 2.) The stimulation amplitude (Quantitatively equivalent Amplitude, QA) at which the quantitative change QC was similar to VC. These data were then statistically compared to the corresponding values from the visual evaluation (VC vs QC and VA vs QA) using the Wilcoxon two-sided signed rank test.

In order to analyse the correlation with the anatomical position of the electrode, the anatomical structure present at the centre of the stimulating electrode was determined. Data were then grouped based on the thalamic nucleus attributed to the test stimulation position. Furthermore, from the acceleration data of every test stimulation, we also calculated the minimum stimulation amplitude required to obtain a 75% reduction in the statistical features compared to baseline (Amp75). These data along with the occurrence of side-effects were used to compare the efficiency of different structures in reducing the patient's tremor by a fixed amount.

### 2.4 Patients

The above method was applied to 6 ET patients under a clinical study at the University Hospital in Clermont-Ferrand (2011-A00774-37 / AU905). Out of the 167 test stimulations that were performed, 148 positions were found

where both evaluation methods identified a reduction in tremor.

### 3 Results

The Wilcoxon signed rank test revealed a statistically significant difference between VA and QA ( $W=4256$ ,  $p < 0.001$ ,  $\alpha = 0.001$ ) which can also be observed in the box plot of the two data sets (Figure 1). On the other hand, the difference between VC and QC at the visually identified amplitude VA was not statistically significant ( $W = 3004$ ,  $p=0.72$ ,  $\alpha = 0.001$ ).

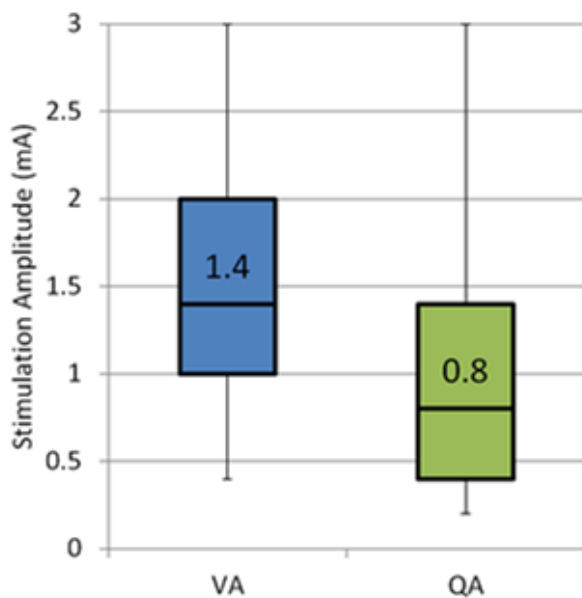


**Figure 1:** Box plot comparing visually identified effective stimulation amplitude VA to quantitatively identified effective stimulation amplitude QA for the same clinical improvement.

From the analysis of the electrode position during test stimulation, it was found that the positions were distributed in 7 thalamic nuclei: Center Median (CM), Intermedio-Lateral (InL), Ventrointermediate (VIM), Ventrocaudal lateral (VCL), Ventrocaudal medial (VCM), Ventro-Oral (VO) and also in Prelemniscal Radiations (PreR). Table 1 shows the average values of the different parameters extracted from the visual and the quantitative evaluations. The number of evaluations in the CM region (3) of the thalamus is small compared to the others and thus the significance of the results is very low. The values of QA are lower than VA for all the structures, the differ-

ence between them being the largest for InL, VO and the VIM.

Figure 2A shows the average minimum stimulation amplitude required to see 75% reduction in tremor quantitatively while 2B shows the number of test stimulations with and without side-effects (red and blue respectively). The VCL and the PreR achieve similar reductions in tremor at lower amplitudes. But these structures also have higher occurrence of side effects. The VCM require higher stimulation amplitudes than VCL and PreR, but also has high occurrence of side-effects. The InL and the VO require similar stimulation amplitudes as the VIM but have much lower occurrence of side effects. The VIM requires the highest stimulation amplitude to achieve 75% reduction, but also has high occurrence of side-effects.

### 4 Discussion

Various methods have been used previously to quantitatively evaluate tremor [6], but only a handful have been reported to be used during DBS surgery. Shamir et al. [7] used goniometers for Parkinson's patients undergoing DBS, but only during MER to identify borders of sub-thalamic nucleus and not to quantitatively evaluate tremor during test stimulations. Other quantitative evaluation techniques have been used to optimize the stimulation parameters of DBS but only after the implant position of the electrode was already decided [8, 9]. To the best of our knowledge, no other group has previously used quantitative tremor evaluation to compare the efficacy of different thalamic nuclei.

One of the observations of the application of our method to the current set of patients was that the use of quantitative evaluation during DBS surgery did not increase the duration of the surgery or cause any discomfort to the patient. Moreover, our results suggest that this quantitative method is more sensitive than the current visual evaluation methods used during the surgery. The significant difference (0.6 mA) between average values of VA and QA shows that stimulation parameters may be further optimized by using quantitative tremor evaluation.

The anatomical analysis of the data obtained using quantitative tremor evaluation suggests that the conventional target, VIM, may not be the most efficient target for ET patients undergoing DBS surgery. All other structures required stimulation amplitude equal to or lower than the VIM to reduce tremor by 75%. However, after looking at the number of positions with side effects, the VO and InL seem to be more efficient in reducing tremor and limit-

**Table 1:** Average visual and quantitative parameters for different thalamic nuclei

	CM	InL	VO	VIM	VCL	VCM	PreR
No. of Stimulations	3	19	18	52	13	24	15
No. of side-effect occurrence	0	1	1	10	2	6	2
Average VC (%)	50	45	63	60	65	72	67
Average QC (%)	76	66	65	57	76	66	57
Average VA (mA)	1.1	2.2	1.9	1.8	1.4	1.6	1
Average QA (mA)	0.4	1.3	1.1	1.3	1	1.5	0.7

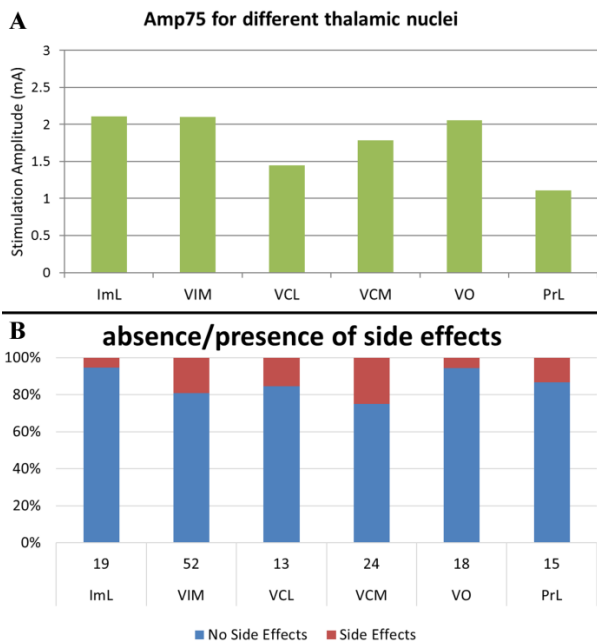


**Figure 2:** Comparison of efficacy of different thalamic nuclei. A) Average stimulation amplitude required to achieve 75% reduction in tremor. B) Stacked column plot of number of test stimulations with and without side-effects.

ing side-effects of the therapy. This seems to confirm published data [5] suggesting that parts of the ventro-oral nucleus (VO) could be appropriate targets as well.

The results have also indicated some limitations of the current method. One of the main factors that influences the proper functioning of the method is the recording of baseline data. A minimum baseline recording of 5 seconds is necessary to extract proper statistical features. However, in case a baseline recording is not available for the current position, the baseline data of the previous recording can be used to perform the analysis. Furthermore, the current analysis method is post-operative. The next step for this method will to perform real-time data analysis so that the results are available to the surgical team when they identify the final implant site.

## 5 Conclusion

The current paper presents the results of quantitative tremor evaluation during DBS surgery for ET patients. The results indicate that our method is more sensitive to changes in tremor than the current visual evaluation methods. Furthermore, the results of the anatomical analysis suggest that the thalamic sub-structures InL and VO are more efficient targets for DBS than the conventional and targeted VIM.

**Funding:** This work was supported by the Swiss National Science Foundation ([www.snf.ch](http://www.snf.ch)).

### Author's Statement

**Conflict of interest:** Authors state no conflict of interest. **Material and Methods:** Informed consent: Informed consent has been obtained from all individuals included in this study. **Ethical approval:** The research related to human use has been complied with all the relevant national regulations, institutional policies and in accordance the tenets of the Helsinki Declaration, and has been approved by the authors' institutional review board or equivalent committee.

## References

- [1] Sarem-Aslani A, Mullett K. Industrial Perspective on Deep Brain Stimulation: History, Current State, and Future Developments. *Front. Integr. Neurosci.* 2011;5.
- [2] Hemm S, Würdell K. [Stereotactic implantation of deep brain stimulation electrodes: a review of technical systems, methods and emerging tools.](#) *Med Biol Eng Comput* 2010;48:611–24.
- [3] Shah A, Coste J, Schkommodau E, Lemaire JJ, Hemm-Ode S. Using acceleration sensors to quantify symptoms during deep brain stimulation surgery. *Biomedical Engineering / Biomedizinische Technik* 2013.
- [4] Lemaire J, Coste J, Ouchchane L, Hemm S, Derost P, Ulla M, Siadoux S et al. MRI anatomical mapping and direct stereotactic targeting in the subthalamic region: functional and

- anatomical correspondence in Parkinson's disease. *Int J CARS* 2007;2:75–85.
- [5] Vassal F, Coste J, Derost P, Mendes V, Gabrillargues J, Nuti C, Durif F et al. Direct stereotactic targeting of the ventrointermediate nucleus of the thalamus based on anatomic 1.5-T MRI mapping with a white matter attenuated inversion recovery (WAIR) sequence. *Brain Stimul.* 2012;5:625–33
- [6] Mansur PHG, Cury LKP, Andrade AO, Pereira AA, Miotto GAA, Soares AB, Naves ELM. A review on techniques for tremor recording and quantification. *Crit Rev Biomed Eng* 2007;35:343–62.
- [7] Shamir RR, Eitan R, Sheffer S, Marmor-Levin O, Valsky D, Moshel S, Zaidel A et al. Intra-operative Identification of the Subthalamic Nucleus Motor Zone Using Goniometers. *Information Processing in Computer-Assisted Interventions*. Berlin, Heidelberg: Springer Berlin Heidelberg; 2013. p. 21–29.
- [8] Papapetropoulos S, Jagid JR, Sengun C, Singer C, Gallo BV. [Objective monitoring of tremor and bradykinesia during DBS surgery for Parkinson disease.](#) *Neurology* 2008;70:1244–9.
- [9] Journee HL, Postma AA, Staal MJ. Intraoperative neurophysiological assessment of disabling symptoms in DBS surgery. *Neurophysiol Clin* 2007;37:467–7

## Chapter 7

# Spatial Effects of Stimulation

The use of the electrode contact position only for anatomical analysis provides a preliminary idea but does not represent the full effects of DBS. The effects of stimulation are not confined to the location of the stimulating contact, but spread out in all directions depending on parameters and the surrounding tissue. Although technological limitations do not allow study of the true distribution of stimulation effect in human beings, a very good estimate can be obtained using computer simulations. On a microscopic level, this spatial effect of stimulation can be estimated by understanding its influence on the ion channels in the membrane of the surrounding neurons and neuronal projections (axons/dendrites). On the other hand, at a macroscopic level, stimulation effect can be estimated by understanding the electrical property of the neuronal tissue surrounding the electrode. Both these phenomena can be modelled using mathematical function and can be simulated using software.

A commonly used technique to simulate such mathematical models is known as the Finite Element Method (FEM) proposed by Olgierd Zienkiewicz in 1947.<sup>335</sup> In principle, the region in which a model has to be simulated is broken down into a mesh of tiny elements, each having its own variables for the mathematical model. The complete solution is obtained by calculating the values for all the variables in the mesh. In the field of DBS, FEM was first used by McIntyre<sup>226</sup> to study the effects of DBS on neurons. In general, the spatial effects of stimulation can be studied by simulations of different electrical quantities like electric potential,<sup>45</sup> electric field,<sup>143,351</sup> the second derivative of electric potential<sup>220</sup> or estimating the VTA by combining neuron models (mathematical representation of a neuron) with FEM.<sup>45,308</sup>

Until now, FEM modelling has been frequently used to study the effects of chronic stimulation through the DBS leads. We hypothesized that by simulating the effects of intraoperative stimulation tests and analysing the data in relation to the surrounding anatomy, more information about the different structures

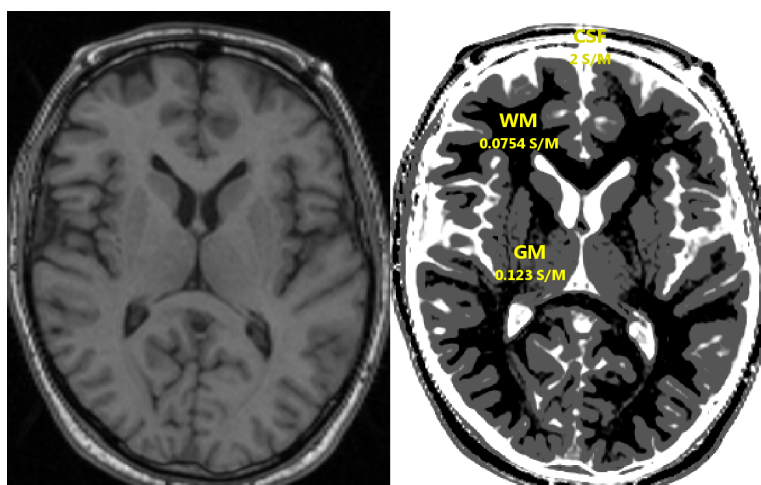


**Figure 7.1:** The MR image contrast is used to assign the conductivity values for the different voxels in the image volume and used to generate the patient-specific brain model. For details, refer to Åström et al.<sup>11</sup>

could be obtained. In order to do so, a patient-specific stimulation method that could be adapted to a model of the intraoperative electrode was required. Based on a published review comparing the different FEM simulation methods in DBS,<sup>12</sup> the method proposed by Åström<sup>14</sup> was identified to fit the criteria.

Extensive details of the patient-specific simulation method are available in the doctoral thesis of Mattias Åström.<sup>11</sup> The method simulates the distribution of Electric Field (EF) in the vicinity of the electrode during stimulation. To make it patient specific, MR images of the patient are used to estimate the tissue surrounding the electrode and assign electrical properties accordingly (**Figure 7.1**). The method was developed in the lab of Prof. Karin Wårdell at the Institutionen för medicinsk teknik (IMT) at the Linköping University (LiU), Sweden to simulate the effects of stimulation through the DBS lead. In collaboration with Prof. Wårdell and with Prof. Dr. Jean-Jacques Lemaire at the University Hospital in Clermont-Ferrand, this patient specific method was modified to simulate the effect of intraoperative stimulation tests and applied to 5 ET patients who underwent VIM-DBS. These simulations were combined with the results of intraoperative quantitative tremor evaluation and analysed in relation to the outline of anatomical structures extracted from the surgical planning software. Elaborate description about the method, the results of application and further discussion can be found in the publication titled "Patient-specific electric field simulations and acceleration measurements for objective analysis of intraoperative stimulation tests in the thalamus" attached in the current chapter (Section 7.1)

## **7.1 Patient-specific electric field simulations and acceleration measurements for objective analysis of intraoperative stimulation tests in the thalamus**

**Authors:** Simone Hemm, Daniela Pison, Fabiola Alonso, Ashesh Shah, Jérôme Coste, Jean-Jacques Lemaire, Karin Wårdell.

This paper is published in the *Frontiers in Human Neuroscience*. It contains the details about the method to simulate the effects of intraoperative stimulation tests in a patient specific manner. Data was analysed in relation to the anatomical structures surrounding the stimulating electrode to identify the role of the structures in therapeutic effects of stimulation.

The paper is available at the address:

<https://doi.org/10.3389/fnhum.2016.00577>

Copyright Notice: Reproduced from Hemm, Simone, Daniela Pison, Fabiola Alonso, Ashesh Shah, Jérôme Coste, Jean-Jacques Lemaire, and Karin Wårdell. "Patient-Specific Electric Field Simulations and Acceleration Measurements for Objective Analysis of Intraoperative Stimulation Tests in the Thalamus." *Frontiers in Human Neuroscience* 10 (November 25, 2016) <https://doi.org/10.3389/fnhum.2016.00577> under the CC BY license (<https://creativecommons.org/licenses/by/4.0/>)



# Patient-Specific Electric Field Simulations and Acceleration Measurements for Objective Analysis of Intraoperative Stimulation Tests in the Thalamus

Simone Hemm<sup>1,2\*</sup>, Daniela Pison<sup>1†</sup>, Fabiola Alonso<sup>2</sup>, Ashesh Shah<sup>1</sup>, Jérôme Coste<sup>3,4</sup>, Jean-Jacques Lemaire<sup>3,4</sup> and Karin Wårdell<sup>2</sup>

<sup>1</sup> Institute for Medical and Analytical Technologies, School of Life Sciences, University of Applied Sciences and Arts Northwestern Switzerland FHNW, Muttenz, Switzerland, <sup>2</sup> Department of Biomedical Engineering, Linköping University, Linköping, Sweden, <sup>3</sup> Université Clermont Auvergne, Université d'Auvergne, EA 7282, Image Guided Clinical Neurosciences and Connectomics (IGCNC), Clermont-Ferrand, France, <sup>4</sup> Service de Neurochirurgie, Hôpital Gabriel-Montpied, Centre Hospitalier Universitaire de Clermont-Ferrand, Clermont-Ferrand, France

## OPEN ACCESS

### Edited by:

Marcelo Merello,  
Fundación para la Lucha contra las  
Enfermedades Neurológicas de la  
Infancia, Argentina

### Reviewed by:

Aasef G. Shaikh,  
Case Western Reserve University,  
USA  
Hoon-Ki Min,  
Mayo Clinic, USA

### \*Correspondence:

Simone Hemm  
simone.hemm@fhnw.ch

†These authors have contributed  
equally to this work and should be  
considered as first authors.

**Received:** 25 July 2016

**Accepted:** 01 November 2016

**Published:** 25 November 2016

### Citation:

Hemm S, Pison D, Alonso F,  
Shah A, Coste J, Lemaire J-J and  
Wårdell K (2016) Patient-Specific  
Electric Field Simulations  
and Acceleration Measurements  
for Objective Analysis of Intraoperative  
Stimulation Tests in the Thalamus.  
*Front. Hum. Neurosci.* 10:577.  
doi: 10.3389/fnhum.2016.00577

Despite an increasing use of deep brain stimulation (DBS) the fundamental mechanisms of action remain largely unknown. Simulation of electric entities has previously been proposed for chronic DBS combined with subjective symptom evaluations, but not for intraoperative stimulation tests. The present paper introduces a method for an objective exploitation of intraoperative stimulation test data to identify the optimal implant position of the chronic DBS lead by relating the electric field (EF) simulations to the patient-specific anatomy and the clinical effects quantified by accelerometry. To illustrate the feasibility of this approach, it was applied to five patients with essential tremor bilaterally implanted in the ventral intermediate nucleus (VIM). The VIM and its neighborhood structures were preoperatively outlined in 3D on white matter attenuated inversion recovery MR images. Quantitative intraoperative clinical assessments were performed using accelerometry. EF simulations ( $n = 272$ ) for intraoperative stimulation test data performed along two trajectories per side were set-up using the finite element method for 143 stimulation test positions. The resulting EF isosurface of 0.2 V/mm was superimposed to the outlined anatomical structures. The percentage of volume of each structure's overlap was calculated and related to the corresponding clinical improvement. The proposed concept has been successfully applied to the five patients. For higher clinical improvements, not only the VIM but as well other neighboring structures were covered by the EF isosurfaces. The percentage of the volumes of the VIM, of the nucleus intermediate lateral of the thalamus and the prelemniscal radiations within the prerubral field of Forel increased for clinical improvements higher than 50% compared to improvements lower than 50%. The presented new concept allows a detailed and objective analysis of a high amount of intraoperative data to identify the optimal stimulation target. First results indicate agreement with published data hypothesizing that the stimulation of other structures than the VIM might be responsible for good clinical effects in essential tremor.

(Clinical trial reference number: Ref: 2011-A00774-37/AU905)

**Keywords:** deep brain stimulation (DBS), intraoperative stimulation tests, essential tremor, acceleration measurements, finite element method (FEM) simulations, ventral intermediate nucleus (VIM), patient-specific brain maps

## INTRODUCTION

Deep brain stimulation (DBS) is a common neurosurgical procedure for relieving movement disorders such as those observed in Parkinson's disease (PD) (Benabid et al., 1993, 2009; Hemm and Wårdell, 2010), essential tremor (ET) (Benabid et al., 1991) and dystonia (Coubes et al., 2000; Cif et al., 2010). Despite an increasing use and an extension of the indications (Hariz et al., 2013), the fundamental mechanisms underlying stimulation-induced effects, either therapeutic or adverse, remain largely unknown. The exact anatomical regions or white matter fibers responsible for these effects are still subject of discussion (Herrington et al., 2015). During a typical surgical planning, the optimal implantation position for a specific target is first approached based on anatomical images. Intraoperatively, the micro contact of an exploration electrode is often used for micro-electrode recordings (MER) (Coste et al., 2009) to evaluate the neuronal activity at previously planned positions of deep brain structures. In a further step, intraoperative stimulation tests are performed through the macro contact of the exploration electrode at different locations with help of the MER-system, and changes in the patient's symptoms are observed by clinical examination. The DBS electrode is finally implanted at the location with the highest therapeutic effect on the symptom with minimal stimulation amplitude and side effects, or with side effects occurring only for high stimulation amplitudes. This procedure is completely based on the physicians experience and will therefore vary depending on the clinical skills (Post et al., 2005).

A way to objectify this evaluation is to use accelerometer recordings of the movements. We have previously presented a method to support the physician's evaluation during surgery by quantifying intraoperatively obtained therapeutic effects on tremor (Shah et al., 2016b) and rigidity (Shah et al., 2016a) with the help of wrist acceleration measurements. These results suggest that mathematical parameters extracted from the acceleration signal are more sensitive to detect changes in tremor during intraoperative stimulation tests than the subjective neurologist's evaluation. An enhancement of this methodology would be to relate the wrist accelerometer measurements for the evaluation of intraoperative stimulation tests with the patient's own brain anatomy and patient-specific simulations of the EF around the stimulation electrode.

The finite element method (FEM) is commonly used to simulate the distribution of the EF around DBS electrodes often taking into account the individual patient's anatomical data (Åström et al., 2009; Chaturvedi et al., 2010; Wårdell et al., 2015). The established models have been applied to relate the results of long term chronic stimulation to anatomical structures surrounding the stimulating contact. However, the use of patient-specific models to simulate data acquired during intraoperative stimulation tests has not yet been proposed.

To support the patient-specific simulations and also the surgical planning, different brain atlases have been suggested over the years (Schaltenbrand and Bailey, 1959; Morel, 2007). This is especially important for brain nuclei generally not visible with current conventional magnetic resonance imaging (MRI).

With specific sequences it is possible to detail most common substructures of the thalamus and of other deep brain regions (Zerroug et al., 2016). Lemaire et al. (2010) introduced a high resolution atlas of the thalamus which makes extraction of such nuclei possible.

The aim of the present study was to introduce a new methodology combining different patient-specific data to identify the optimal implant position of the chronic DBS lead: thalamic patient-specific brain maps, EF simulations for intraoperative stimulation tests based on patient-specific simulation models and the corresponding therapeutic effects quantitatively evaluated by wrist accelerometer recordings. To illustrate the feasibility of this methodology, it was applied to five patients with ET who underwent stimulation tests during targeting of the ventral intermediate nucleus of the thalamus (VIM). An exemplary way of analysis is presented by comparing the extension of stimulation for no/low and intermediate/high improvements.

## MATERIALS AND METHODS

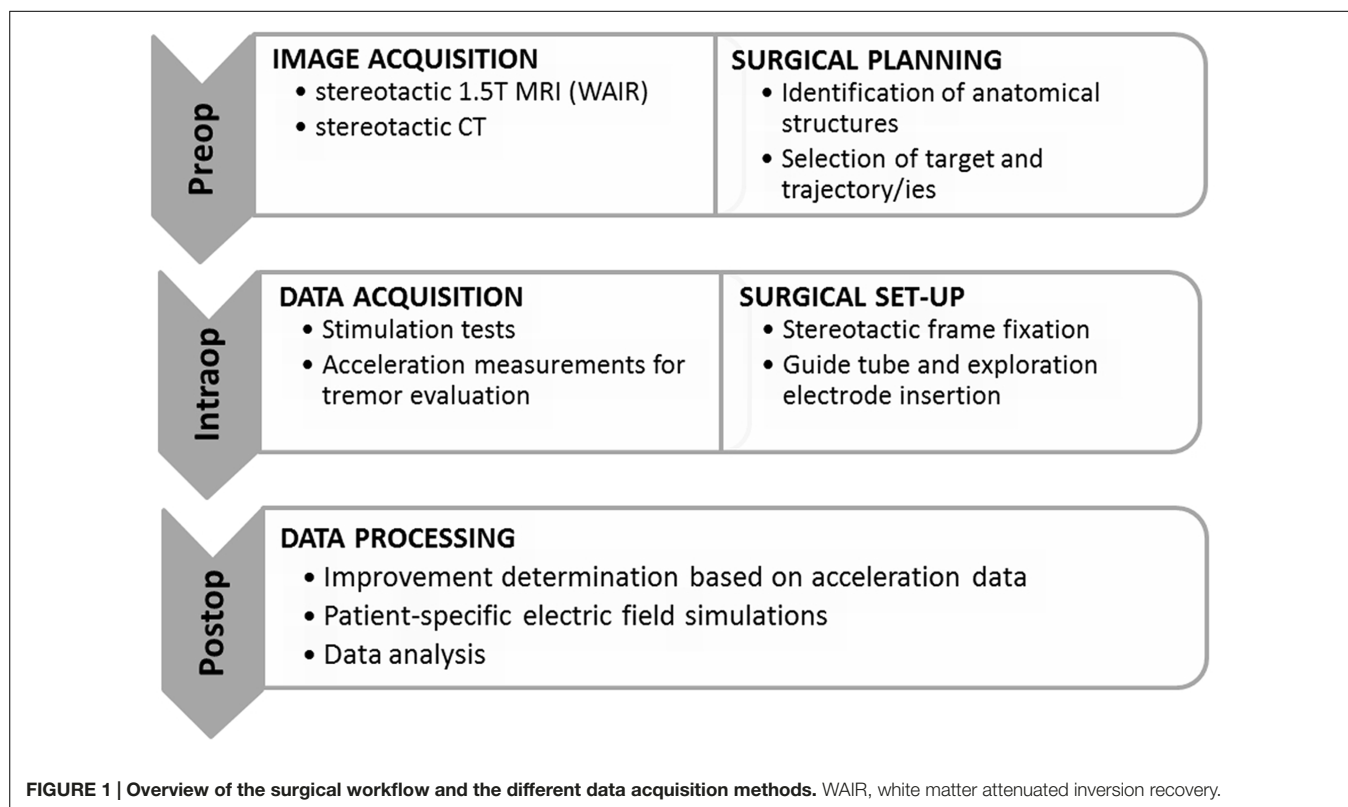
An overview of the methodology including imaging, generation of patient-specific maps of the thalamic region, surgical planning, surgical procedure, stimulation tests, accelerometer measurements, patient-specific EF simulations and data analysis is presented in **Figure 1**.

### Surgical Protocol

Stereotactic exploration and lead implantation were performed at the Department of Neurosurgery, Clermont-Ferrand University Hospital, France, under local anesthesia in a two-day procedure.

The first day, the stereotactic frame was mounted on the patient's head (Leksell® G frame, Elekta Instrument AB, Sweden) under local anesthesia. T1 MRI (0.63 mm × 0.63 mm × 1.30 mm) and white matter attenuated inversion recovery images (WAIR, 0.53 mm × 0.53 mm × 2.00 mm) (Magnotta et al., 2000; Lemaire et al., 2007) were acquired (Sonata, 1.5T, Siemens, Germany). Using a stereotactic planning software (iPlan 3, Brainlab, Feldkirchen, Germany), the VIM and its anatomic neighbors were carefully identified and manually outlined on the coronal plane of the WAIR sequence (Lemaire et al., 2010; Zerroug et al., 2016). The nuclei identification followed the previously published nomenclature (Lemaire et al., 2010; Vassal et al., 2012) based on their relative positions, intrinsic MRI tissue contrasts on 1.5T WAIR images (see **Figure 6** in Zerroug et al., 2016) and an in-house microscopic 4.7T 3D T1 MRI atlas (see **Figure 1** in Vassal et al., 2012). Target coordinates and two parallel trajectories were defined according to the stereotactic reference system, without AC-PC referencing. **Figure 2** shows a stereotactic planning including the patient-specific brain map and the planned trajectory.

The second day, after repositioning of the frame and stereotactic computed tomography (CT) acquisition (0.59 mm × 0.59 mm × 1.25 mm), the planned trajectories were checked and adjusted if necessary with the stereotactic reference system of the CT after rigid image fusion of WAIR and CT data sets. The target region was then explored intraoperatively



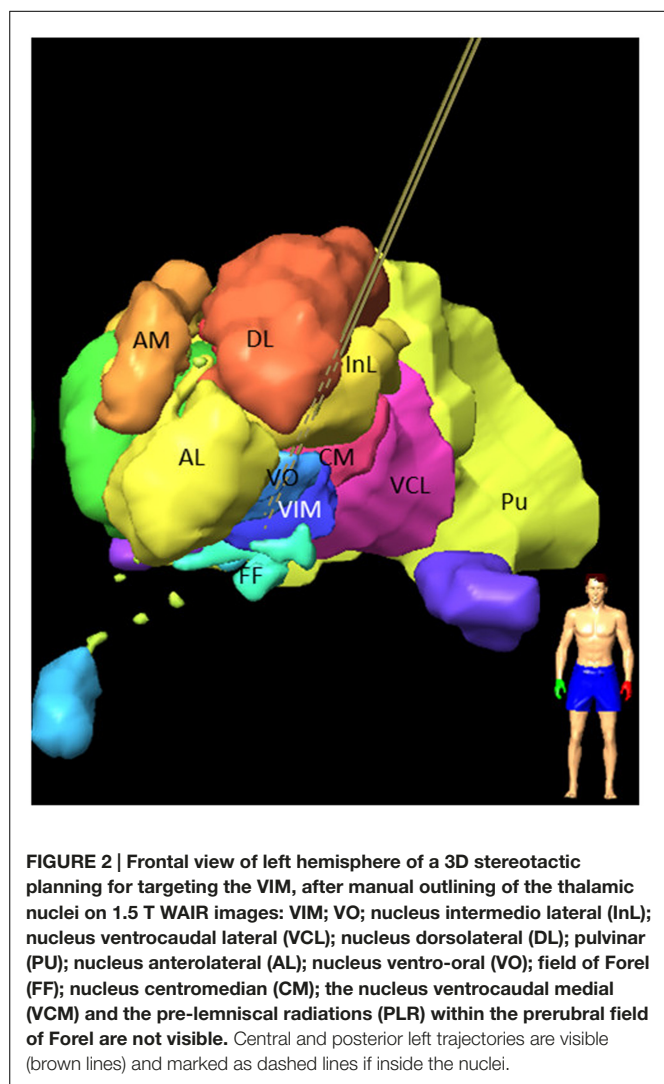
(MicroGuide Pro; Alpha Omega Engineering, Nazareth, Israel) (Slavin and Burchiel, 2002) under local anesthesia using two exploration electrodes (Neuroprobe 366-000024, Alpha Omega Engineering, Nazareth, Israel) that were steered by rigid guide tubes (ACS-7905/200-5, DIXI Microtechniques, Besançon, France): one for the planned track (named the central track) and one placed 2 mm in parallel, usually posterior or posterolateral to the central one. MER was acquired in millimeter steps using the micro contact of the electrode which was retracted before starting stimulation tests in order to avoid tissue damage. Gradual stimulation tests were performed at the same locations through a macro contact to assess clinical benefit and adverse effects and to identify the optimal target. For each stimulation test, the surgical team identified and noted the maximum change in the patient’s tremor relative to the initial state of the patient (baseline), and the corresponding stimulation amplitude as well as the occurrence of side effects. MER and stimulation tests were in general performed in a range starting some millimeters in front of the target point and going slightly below depending on the anatomical location. In addition to this routine assessment of tremor, wrist accelerometer measurements and video recordings were performed. Following the stimulation tests, a quadripolar DBS-lead (Lead 3389, Medtronic Inc., USA) was implanted at the optimal stimulation spot for chronic stimulation.

### Acceleration Measurements

To perform intraoperative acceleration measurements, a 3-axis accelerometer, placed inside an in-house developed plastic case, was tied to the patient’s wrist on the opposite side of

the stimulated hemisphere. Via a USB cable, the device was connected to a laptop based data recorder using homemade software LemurDBS (Java 1.6, Oracle, USA) (Shah et al., 2013). Synchronization between acceleration data and test stimulation amplitudes was assured by a pulse sent from the laptop to the stimulating equipment. The sensor was always attached at the same position on the wrist of the patient, and at each position a baseline recording was acquired before initiation of each stimulation sequence.

In order to quantify the clinical improvement for each stimulation amplitude, a previously developed analysis method in Matlab (R2014b) was used (Shah et al., 2016b). As a first step, movements other than tremor were removed offline by using the smoothness priors method (Tarvainen et al., 2002) and thereafter a second order Butterworth low pass-filter was applied at 10 Hz in order to suppress noise. Statistical features (standard deviation, signal energy and the spectral amplitude of the dominant frequency, defined as the frequency of the signal with maximum spectral power) were extracted by moving a 2 second-window over the data. These features were then normalized to the feature set representing the most intense tremor at baseline, i.e., during an initial off-stimulation period at the same position. For each stimulation amplitude the mean of the obtained quantitative clinical improvement was retained as a percentage value. An example is presented in **Figure 3A** where a typical acceleration signal in one position is presented together with the clinical improvement based on the calculated features. In the presented example, it can be seen that an improvement of 98.1% was obtained at a stimulation amplitude of 1.0 mA.



## Electric Field Simulations

In order to simulate the EF spatial distribution within the brain, a 3D FEM model of the exploration electrode with the surrounding brain tissue was built (Comsol Multiphysics, Version 4.4 Comsol AB, Sweden) for adapting an already established patient-specific modeling technique for DBS leads (Åström et al., 2010; Wårdell et al., 2015).

## Brain Tissue Model

The axial preoperative T1 MRI was registered and resampled to the stereotactic preoperative axial CT dataset. In a next step, it was imported into the in-house developed software (Matlab R2013) (Wårdell et al., 2012) modified for the creation of the brain tissue models. A separate filtered axial T1 image batch with enhanced region of interest was used to segment cerebrospinal fluid (CSF), gray matter and white matter (Alonso et al., 2016). The segmented image voxels were assigned with the corresponding electrical conductivities

( $\sigma$ ) (Gabriel et al., 1996)<sup>1</sup>. CSF and blood were set to 2.0 Siemens/meter (S/m) and 0.7 S/m, respectively. Considering the frequency (130 Hz) and pulse length (60  $\mu$ s) of the stimulation (Wårdell et al., 2013), to gray matter was assigned 0.123 S/m and to white matter 0.075 S/m. Interpolation was done for conductivity values in-between the thresholds used. In order to reduce the simulation time, a region of interest (a cuboid of approximately 100 mm per side) covering the thalamus and its surroundings was selected from the brain tissue model.

## Exploration Electrode and Guide Tube Model

A model of the stimulating contact of the exploration electrode and the guide tube was developed. **Figure 4A** presents the outer and inner dimensions of the exploration electrode and the guide tube, **Figure 4B** the corresponding model. The end of the guide tube was fixed 12 mm above the chosen target point, i.e., above the *a priori* optimal anatomic spot. A second exploration electrode and guide tube model was positioned in parallel at a distance of 2 mm. The distance between the guide tube and the center of the stimulating contact decreased or increased when the simulation site was ahead or beyond the target point, respectively. The center of the stimulating contact was placed at the different planned stimulation positions. The micro contact was not considered as it was retracted during the stimulation tests.

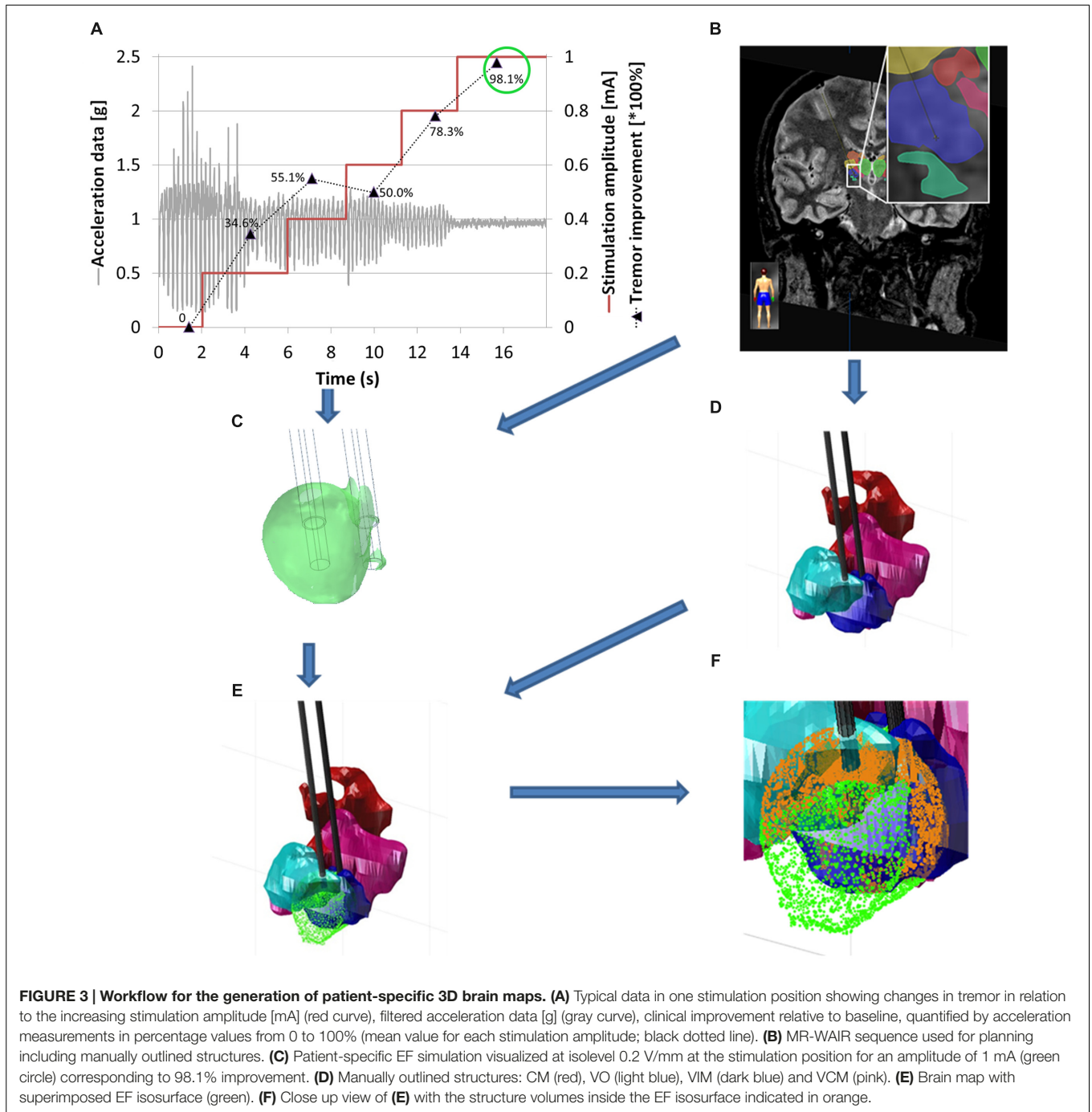
## Simulations

The EF was calculated by using the equation of continuity for steady current according to:

$$\nabla \cdot \vec{J} = \nabla \cdot (\sigma \nabla V) = 0$$

where  $J$  is the current density,  $\sigma$  a matrix containing the electrical conductivity values for the region of interest (thalamus and neighborhood) and  $V$  the electric potential. A monopolar configuration was conducted using the guide tube as the reference electrode setting it to ground, and the active electrode set to the same current as used during the stimulation tests. The non-active contact of the parallel lead was set to floating potential (Schmidt et al., 2013). The exterior boundaries of the tissue model were set to electrical insulation. The mesh density (consisting of about 250,000 tetrahedral elements) was defined by the built in physics-controlled mesh generator, where the smallest elements (0.204 mm) were located nearby the stimulating contacts in order to capture the strong EF gradients. The Cartesian coordinates of the points describing the surface of the simulated EF volume (**Figure 3C**) were exported for further analysis. In this study an EF isolevel of 0.2 V/mm was used in order to be able to perform relative comparisons between the simulations and to comply with approximate axon diameters in the thalamus (Kuncel et al., 2008; Åström et al., 2015; Alonso et al., 2016).

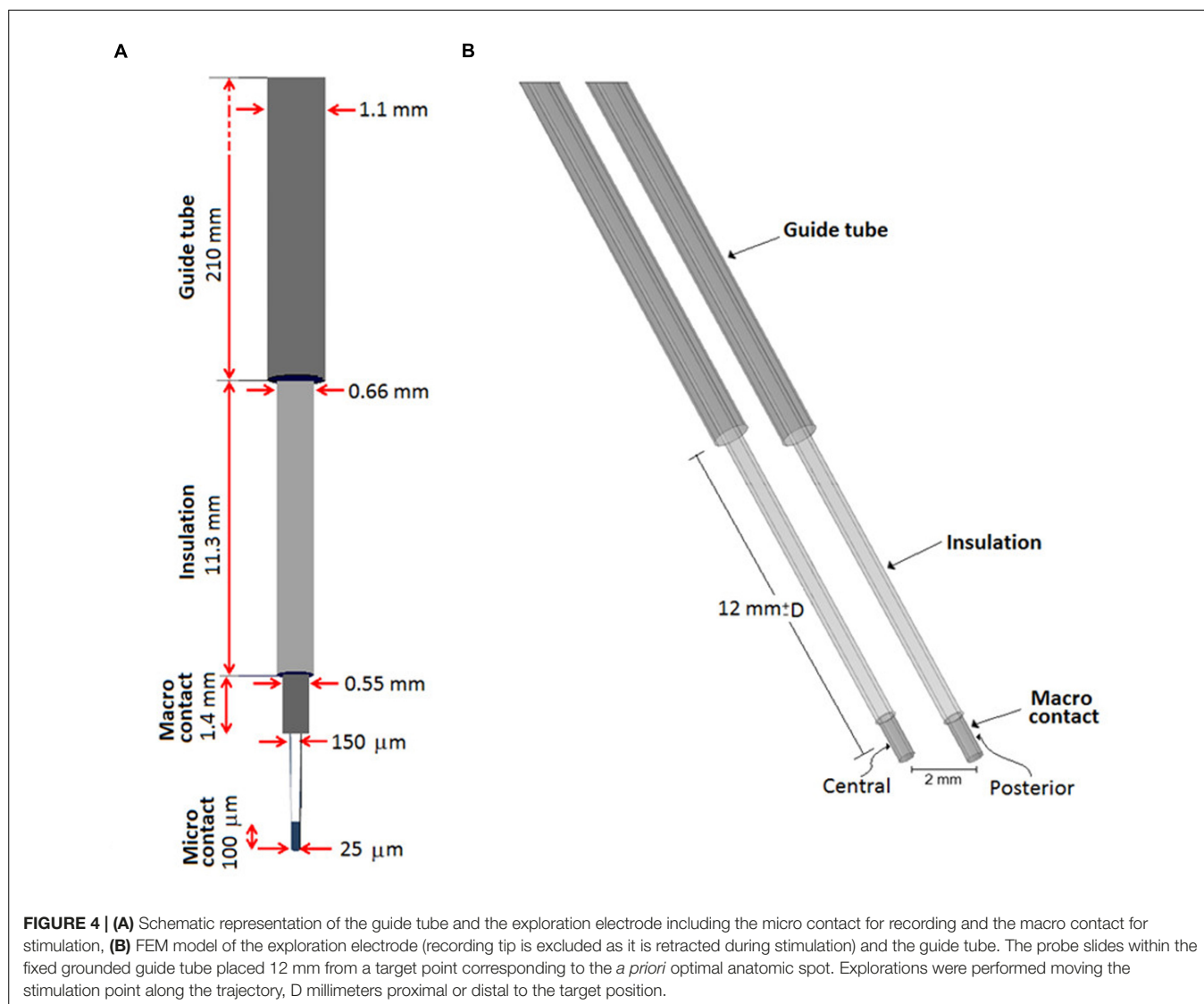
<sup>1</sup>Andreuccetti, D., R. Fossi and C. Petrucci, Florence, Italy. (2005). "Dielectric properties of the tissue." from <http://niremf.ifac.cnr.it/tissprop/>.



### Thalamic Brain Maps and Electric Field Visualization

The thalamic structures (Figures 2 and 3B) initially outlined on the WAIR weighted sequence in the iPlan software were exported in form of slices parallel to the stereotactic CT data set via an interface based on VVLink and VTK (VTK 5.2.0, Kitware Inc., Clifton Park, NY, USA). Target and trajectory coordinates were also exported in CT image coordinates by the same software interface. The CT data set was chosen

as it provides a higher resolution and no distortion of the stereotactic reference system compared to MR sequences. With the exported data a 3D thalamic brain map with trajectories was generated in Matlab (R2014b) (Figure 3D). For each stimulation test position and amplitude, the EF isosurface generated through FEM simulations was imported, superimposed to the 3D thalamic brain map and color-coded depending on the induced, quantitatively evaluated improvement (Figure 3E).



### Volumetric Analysis

An in-house algorithm developed by FHNW in Matlab (R2014b) was applied to detect and calculate the volume of the anatomical structures inside each EF isosurface. To reduce the computational time, a list of candidate structures (e.g., VIM, VO, and CM) was identified from the entire structure group by excluding the structures outside the coordinate's ranges of the EF volume. For each candidate structure, the points of the EF isosurface inside the structures' volume were detected by considering them as a concave or convex hull according to their shape. The obtained volume based on the selected point cloud was then calculated and associated with the respective clinical improvement. The algorithms then generated a list of the thalamic structures lying partially or completely inside the 0.2 V/mm EF isosurface, their volumes as well as the volume covered by the EF surface and the associated improvement value (Figure 3F).

### Clinical Application

The above presented protocol was applied to five ET patients (three male and two female) undergoing bilateral DBS electrode implantation in the VIM region and successively to both hemispheres. They gave their written informed consent to participate in the study (Ref: 2011-A00774-37/AU905, Comité de Protection des Personnes Sud-Est 6, Clermont-Ferrand, France). No alterations were made to the routine surgical procedure. In all patients a central and a posterior trajectory were chosen per hemisphere for MER and stimulation tests (stimulation parameters: amplitude = 0.2 to 3.0 mA in steps of 0.2 mA, pulse width = 60  $\mu$ s, frequency = 130 Hz). At each stimulation position stimulation lasted 1 to 3 min depending on the response of the patient and on side effect occurrence or not. Between all stimulation tests, a non-stimulation period was maintained to leave time to the symptoms to come back. The duration of this period depended on patient symptoms (minimum 2 min). Acceleration measurements were performed in parallel to the

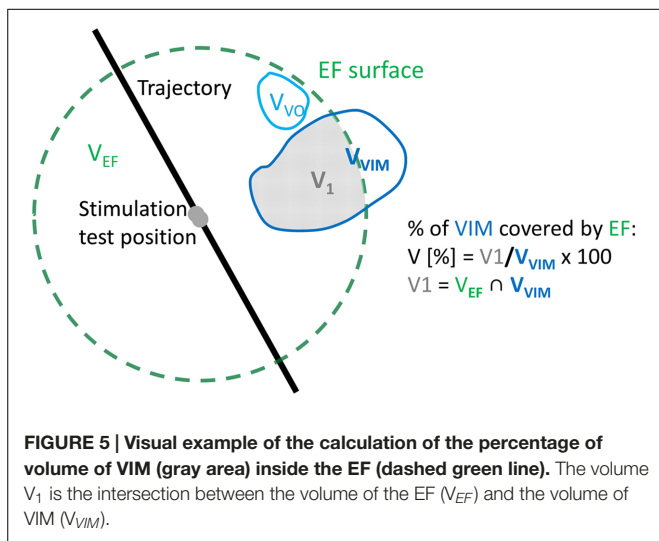


**FIGURE 5 |** Visual example of the calculation of the percentage of volume of VIM (gray area) inside the EF (dashed green line). The volume  $V_1$  is the intersection between the volume of the EF ( $V_{EF}$ ) and the volume of VIM ( $V_{VIM}$ ).

test stimulation in 31, 22, 30, 28, and 32 positions for Patient 1 to 5, respectively, mostly from 5 mm above the target point down to 4 mm below depending on the individual anatomical locations. The final electrode implantation site was based on clinical subjective evaluations.

Electric field simulations were performed for all stimulation test positions in both hemispheres of the five patients. At each position, up to four tested stimulation amplitudes were chosen for simulations using the following criteria based on the quantitatively evaluated symptom improvements ( $I_{acc}$ ): (1) The highest amplitude not resulting in any improvement in tremor compared to baseline; (2) the lowest amplitude at which a first improvement in tremor was measured; (3) The lowest amplitude resulting in at least 50% improvement in tremor; (4) The lowest amplitude resulting in at least 75% improvement. When the first improvement in tremor was more than 75%, criteria (2–4) gave the same amplitude. When the first improvement was identified already between 0.2 and 0.6 mA, no simulations were performed for the criterion 1. The extracted patient-specific 3D brain maps of the thalamus were superimposed with the four trajectories of each patient and with the simulated patient-specific EF isosurfaces. To make the data comparable between patients, the volume inside the isosurface was normalized to the size of the structure resulting in the percentage of the structure covered by the EF (Figure 5). For example, if the volume of VIM was  $10 \text{ mm}^3$  and only  $2 \text{ mm}^3$  of it was encompassed by an EF isosurface, the covered volume of VIM for that EF would have been  $(2/10) \times 100 = 20\%$ .

In order to identify structures responsible for the reduction in tremor, the results of all patients together were classified following the quantity of improvement detected by accelerometry ( $I_{acc}$ ). Data were divided into two groups considering no/low improvements ( $I_{acc} \leq 50\%$ ) and intermediate/high improvements ( $I_{acc} > 50\%$ ), respectively. The resulting data are presented in two different ways for comparison of these two improvement groups. Firstly, for each thalamic structure, the relative number of occurrences (the structure is at least partially

covered by the EF) was determined: the absolute number of occurrences of *each structure* in the considered improvement range was normalized to the total number of occurrences of *all structures* in this range. Second, the percentage volume of each structure covered by a specific EF isosurface was analyzed to see for example if the covered volume of some structures increases for higher improvements. These percentage volumes were graphically represented and visually analyzed together with the induced clinical improvement for all simulations. Furthermore, mean values and the standard error of the mean (SEM) were determined for each structure for the two improvement groups. The results for each structure in the two improvement ranges were statistically compared applying the Mann–Whitney  $U$  test. Mean stimulation amplitudes for 50% or less improvement and more than 50% improvement were determined.

## RESULTS

### Simulations

The proposed concept has been successfully applied to the five patients, resulting in 272 simulations at 143 different stimulation test positions. The detailed numbers of simulations for each patient and different improvement ranges are presented in Table 1.

### Visualization

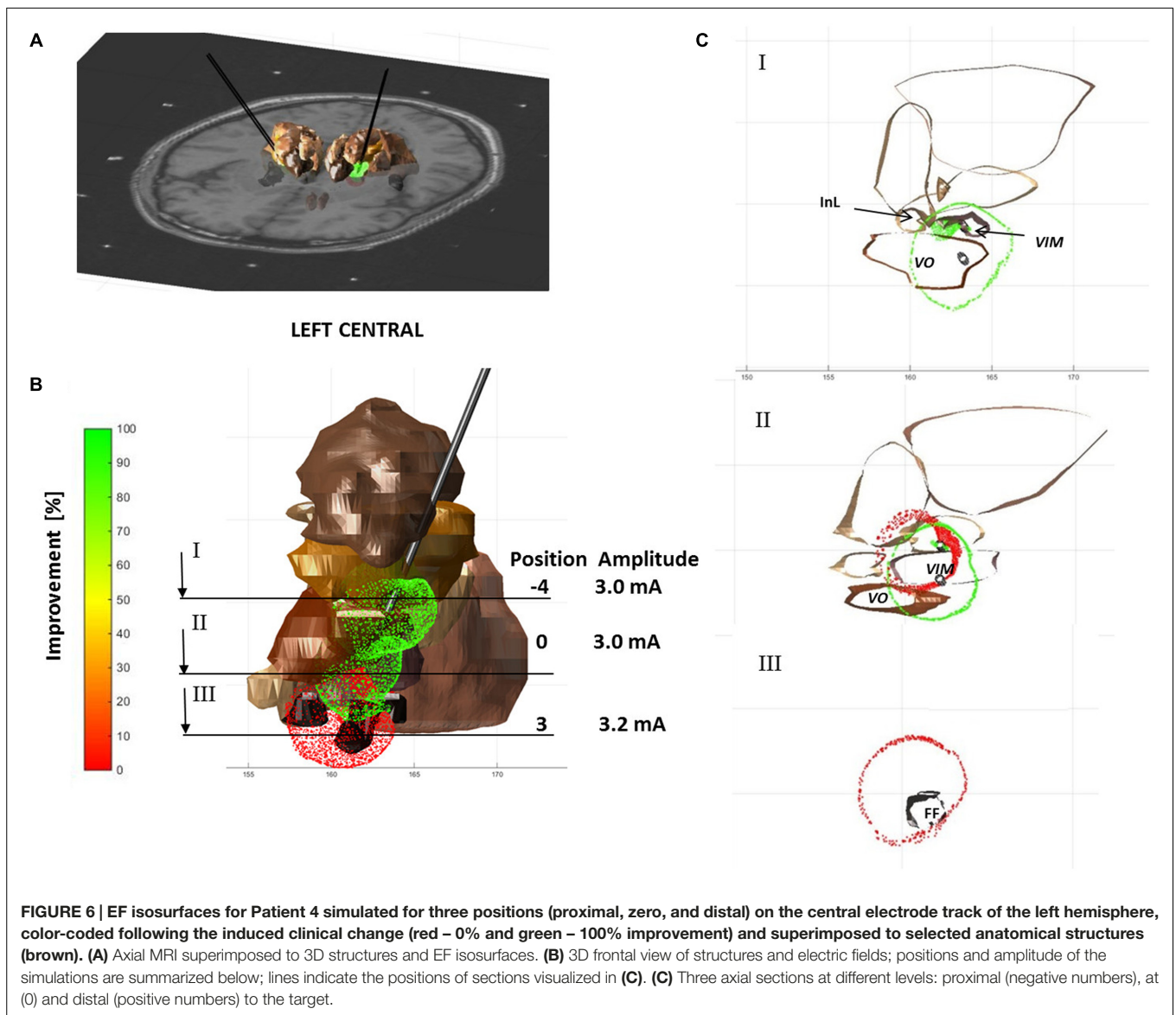
Figure 6 shows an example of visualization for Patient 4 with three simulated EF isosurfaces in the left hemisphere along the central tract. Each isosurface is superimposed to the extracted anatomical structures (seen in brown) and the patient-specific MRI (Figure 6A). At the target position or the *a priori* optimal anatomic spot for the left central trajectory an improvement of 90% was reached with a stimulation amplitude of 3 mA (Figure 6B). 3 mm below the target no improvement in tremor could be observed. The corresponding EF in red overlays the EF of 90% of improvement as can be seen at cross section II through the stimulation electrode as presented in Figure 6C.

### Involvement of Anatomical Structures

The relative occurrences of the different thalamic structures within the isosurfaces for improvements above and below 50% are presented in Figure 7. It shows that the percentage

**TABLE 1 |** Number of simulations per patient and clinical improvement range as recorded by accelerometry ( $I_{acc}$ ).

	$0 < I_{acc} \leq 25\%$	$25 < I_{acc} \leq 50\%$	$50 < I_{acc} \leq 75\%$	$75\% < I_{acc} \leq 100\%$	Total
Patient 1	3	13	17	12	45
Patient 2	3	11	20	10	44
Patient 3	1	23	15	22	61
Patient 4	2	9	23	18	52
Patient 5	2	15	23	30	70
Total	11	71	98	92	272

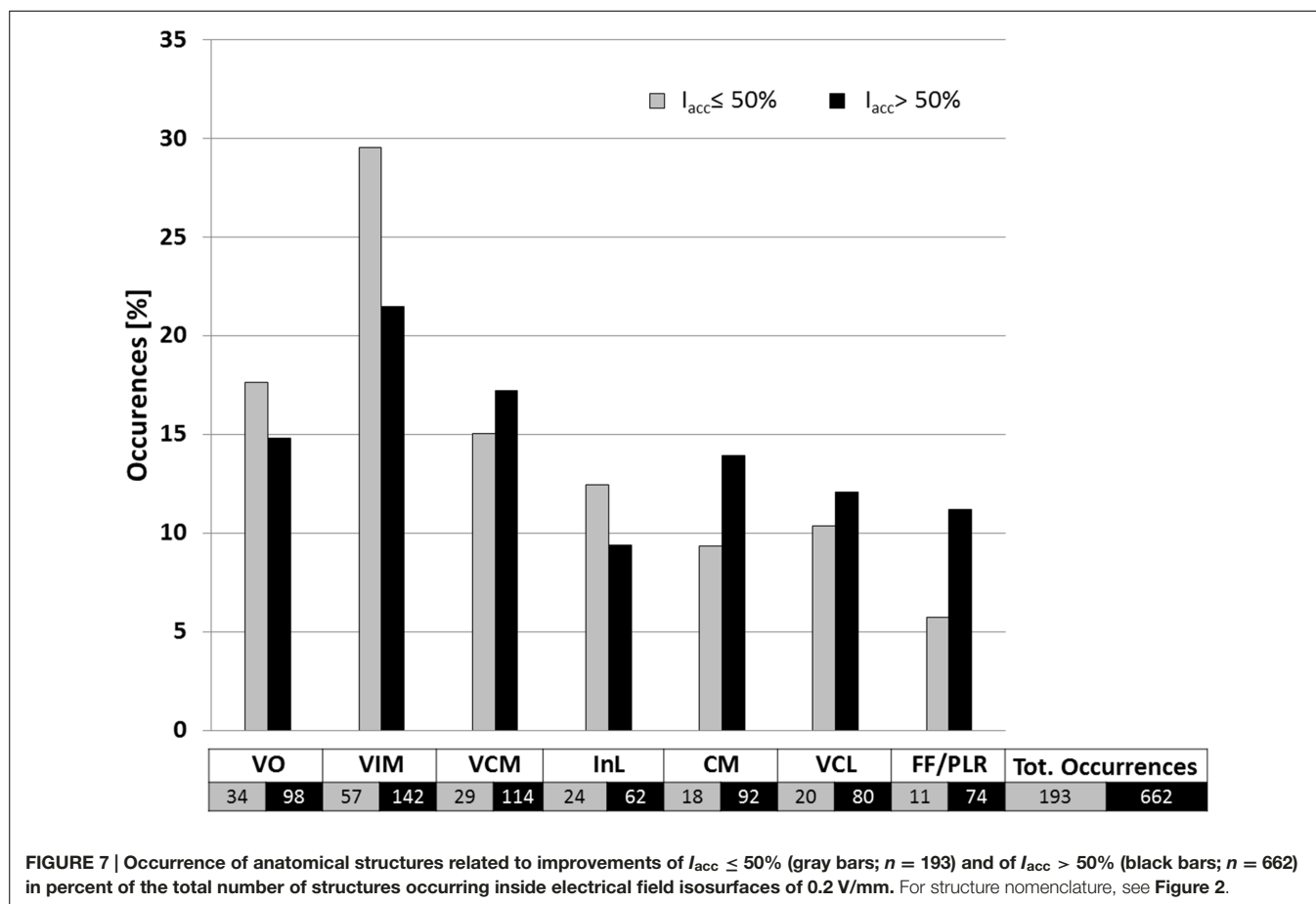


of occurrences of the different structures was always inferior or equal to 30%. The relative occurrence of InL, VO and especially VIM decreases for higher improvements. This means that their appearance does not as much increase as for CM, VCM, VCL and especially for FF/PLR. For all four structures the relative occurrence increases for higher improvements. Mean stimulation amplitudes for improvements  $I_{acc} \leq 50\%$  and  $I_{acc} > 50\%$  were  $0.9 \pm 1.1$  mA and  $1.5 \pm 1.2$  mA, respectively.

### Relation of Structure Occurrences, Clinical Improvement, and Volumes Covered by the Isosurfaces

A comparison between the clinical improvement and the volume of the structures included in the isosurface of the corresponding simulation is presented in **Figure 8**. While

**Figure 8A** shows all available data of the five patients, **Figures 8B,C** summarize the data in form of mean and SEM for improvements  $\leq 50\%$  and  $> 50\%$ . All SEM values remain below 3% except for the VO and the InL for the range  $I_{acc} \leq 50\%$  and the FF/PLR for both improvement ranges. A closer analysis of the volume of the different structures covered by the EF isosurface shows that the percentage volumes of the target structure VIM, of the InL and of the FF/PLR increase with significant clinical improvements. The difference for the VIM was statistically significant ( $p < 0001$ ). Only small volumes of CM and VCL are covered by the isosurface in both improvement ranges. Nevertheless the difference for the CM could be shown to be significant ( $p < 0.01$ ). The neighboring nuclei VIM and VCM appear together for nearly all simulations. FF/PLR and VO occur mostly in combination with VIM and VCM (same horizontal line) (**Figure 8A**).



## DISCUSSION

In the present study, a methodology is described that has the potential to give new insights into the efficacy of different anatomical structures in DBS. It consists in the combined analysis of intraoperatively acquired accelerometry data, patient-specific EF simulations for intraoperative stimulation tests and patient-specific anatomy. The method was successfully applied to five patients with ET and included more than 250 EF simulations. An exemplary way of analysis and preliminary results have been presented for the identification of the therapeutically effective anatomical region.

### Quantitative Symptom Evaluation

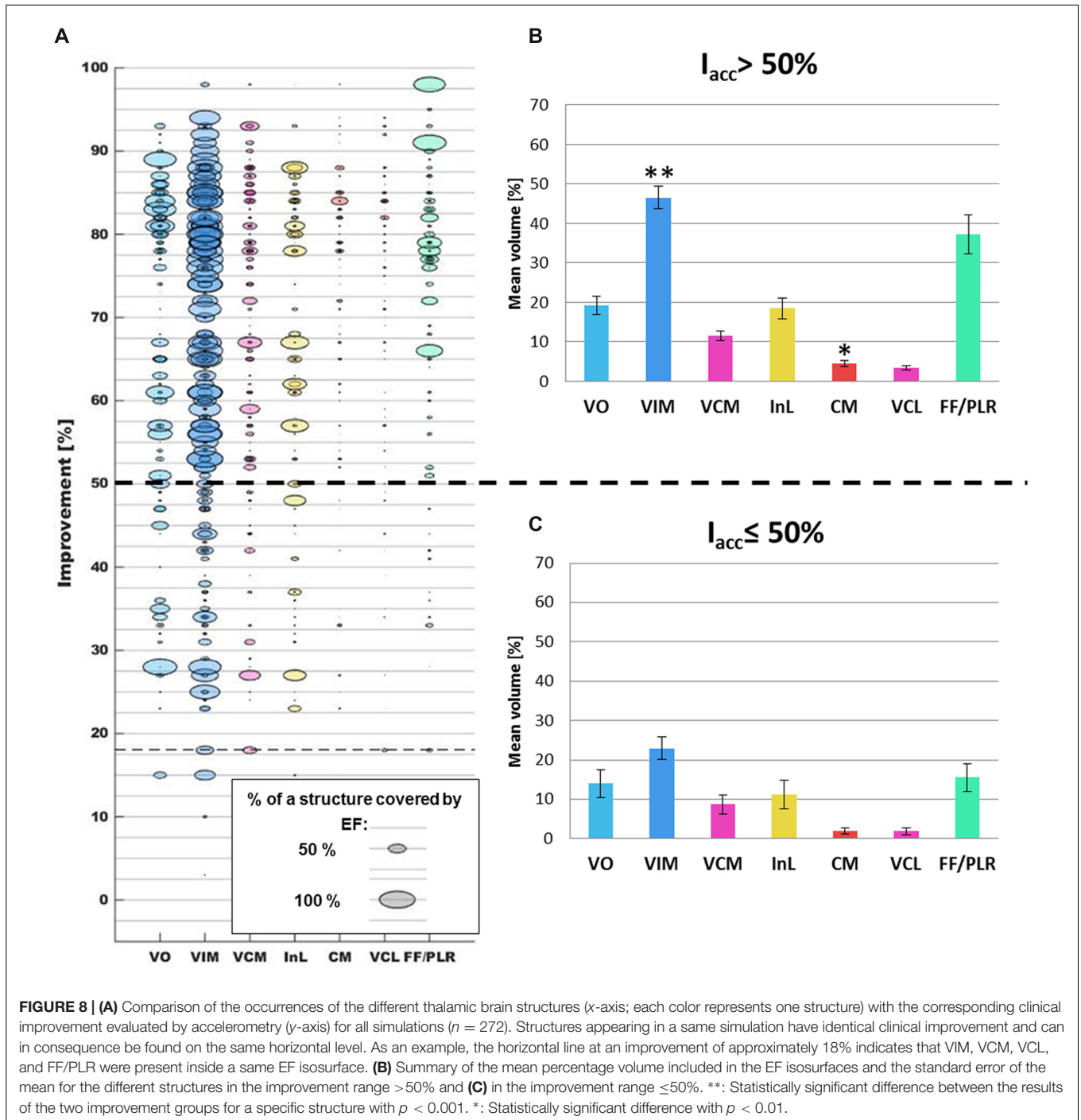
In order to overcome the limits of existing routinely used clinical rating scales, i.e., the inter- and intra-observer variability (Post et al., 2005; Palmer et al., 2010), the discrete evaluation levels and the high dependence on the experience of the evaluating neurologist (Griffiths et al., 2012), we have used accelerometry-based, quantitative tremor evaluations during intraoperative stimulation tests.

Tremor quantification outside the OR has been proposed since a long time by various authors (Mansur et al., 2007), many of whom have concluded that a quantitative evaluation method is more sensitive than the visually performed clinical evaluation.

Birdno et al. (2008) used an acceleration sensor to study the effects of temporal variations of the stimulation pulse during the replacement of the implantable pulse-generator. Journee et al. (2007) and Papapetropoulos et al. (2008) used quantitative tremor evaluation after the DBS lead was implanted, in order to compare the effects of stimulation through different contacts. But those systems were not designed to be used in different clinical centers or during stimulation tests performed through an exploration electrode. In a previous study, we have demonstrated the use of our system in 15 DBS surgeries in two different clinical centers, the possibility to visualize and revisit recorded data during surgery and the possible influences of quantitative evaluations on the choice of the final implant position of the lead for chronic stimulation (Shah et al., 2016b).

### Determination of the Therapeutically Implicated Structures

In the present clinical study, structures individually outlined by the neurosurgeon were available and could be used as anatomical reference. The use of the patient-specific MR-WAIR sequence together with a 4.7 T in-house atlas as reference and stereotactic books make an approximate identification of the structures possible (Zerroug et al., 2016). Other groups have proposed various approaches (Caire et al., 2013) among them projecting the position of the active contact(s) directly onto anatomical



images (Vayssiere et al., 2004), onto anatomical (Saint-Cyr et al., 2002; Sarnthein et al., 2013) or probabilistic functional atlases (Lalys et al., 2013), or linking them to MER results (Zonenshayn et al., 2004) sometimes combined with imaging data (Weise et al., 2013) and white matter tracking (Coenen et al., 2012). To analyze the relationship between the anatomical location of stimulating contacts and the clinical effectiveness of stimulation, we have decided to take into account the extent of stimulation by using EF simulations (Åström et al., 2012) as discussed in detail in the

next paragraph. Other published approaches consider either the anatomical position of the center of the contact (Starr et al., 2002; Voges et al., 2009; Garcia-Garcia et al., 2016) or of the whole contact taking into account its dimensions (Saint-Cyr et al., 2002; Zonenshayn et al., 2004; Herzog et al., 2007; Hemm et al., 2008).

### Electric Field Simulations

Finite element method models are commonly used to simulate and visualize the EF distribution around DBS electrodes and the

EF is one of the electrical entities that may be used to represent the stimulation field. In comparison with the electric potential or the second derivative of the electric potential with respect to the distance (activating function), EF has been shown to be the most stable and unchanged entity for different stimulation parameters (amplitude and pulse width) (Åström et al., 2015).

Today, FEM models have progressed from non-specific (McIntyre et al., 2004; Hemm et al., 2005; Åström et al., 2006) to patient-specific taking into account the individual's data (Åström et al., 2009; Chaturvedi et al., 2010; Wårdell et al., 2015). There is no consensus of the degree of complexity of the model to accurately simulate the neural response, however, many groups (Chaturvedi et al., 2010; Schmidt et al., 2013; Alonso et al., 2016; Howell and McIntyre, 2016) have shown that the inclusion of the heterogeneity and anisotropy of the brain tissue increases the model accuracy and prediction capability. For instance, Chaturvedi et al. (2010) and Åström et al. (2012) observed an overestimation of neural activation for homogeneous models. The present study relies on a brain model built upon the segmentation of the gray matter, white matter, CSF and blood from the patients' MRI and in consequence takes into consideration the inhomogeneity of brain tissue. An even more realistic model may be based on DTI which provides more anisotropic information, however, its resolution is lower than the one of MRI and may introduce other errors (Åström et al., 2012). The simulations in this study were performed for constant current while the dispersive components of the brain tissue have been considered by adjusting the conductivity values for gray and white matter to the particular stimulation frequency and pulse width (Wårdell et al., 2013).

According to previous studies where neuron activation distances were calculated using neuronal models (Åström et al., 2015), an isolevel of 0.2 V/mm represents an equivalent activation distance for neurons within 3–4  $\mu\text{m}$  of diameter (Alonso et al., 2016) and thus seems to comply with axon diameters in the thalamus as previously calculated by Åström et al. (Figure 6, 2015) based on Kuncel et al. (2008). The selection of a fixed EF isolevel allows then to compare the volume recruited for different amplitude settings and different positions.

## Transferability

The described methodology has been presented for an institution-specific surgical protocol but can be transferred to other clinical centers. The approach can be adapted to any kind of anatomical information. Instead of using manually outlined structures, it is possible to combine the generated data with anatomical atlases – with the limitations inherent to such an approach (Vayssiere et al., 2002; Wodarg et al., 2012; Anthofer et al., 2014) – or with fiber tracking data in order to analyze the implication of different fibers in the mechanism of action of DBS (Coenen et al., 2012). The MR image data (T1, T2) that are needed for the EF simulations are generally acquired in every institution for the surgical planning procedure. A modification of the developed model to the institution-specific stimulation test protocol in awake patients might be necessary: the characteristics of the stimulating electrode as well as the position of the guide tube during

stimulation have to be adapted. The acceleration data recording can relatively easily be added in the intraoperative phase without any changes in the surgical protocol, without lengthening surgery and most importantly, without any discomfort for the patient. Nevertheless, the correlation of the simulation results can be performed as well based on subjective visual evaluations.

## Clinical Application

The results of the present paper are described as relative occurrences and percentage volumes of the different anatomical structures covered by the EF isosurface. Even if the number of patients presenting ET in our clinical study was low and thus the confidence concerning the analysis of the mechanism of action of VIM-DBS is limited, we can present preliminary results thanks to the high number of stimulation test positions and EF simulations per patient. First results of these EF simulations in **Figure 7** show that the percentage of occurrence of VCM, CM, and FF/PLR increases for higher improvements while the percentage of VIM occurrences decreases. This can be explained by the fact that in 60 out of 143 measurement sites the center of the stimulation contact was already within the VIM. Furthermore, as shown, there is a tendency that higher improvements are linked to higher stimulation amplitudes leading in general to a larger distribution of EF for a same tissue type. When looking at the percentage of volume of the VIM covered by the isosurface between the two improvement groups (**Figures 8B,C**), a statically significant difference exists. Nevertheless, the size of the individual volumes varies inside each group. This result can be interpreted in two ways: either (I) a specific part of the VIM, for example the efferent fibers, has to be stimulated or (II) other structures than the VIM might at least partially be responsible for the therapeutic effect. Following our preliminary results such structures could be the InL or especially the fiber tracks FF/PLR. This hypothesis would confirm previously published data: parts of the InL have been earlier mentioned for tremor reduction (Hirai and Jones, 1989) and several authors (Spiegelmann et al., 2006; Vassal et al., 2012) have reported that chronic stimulation of PLR works very well. Some authors (Caparros-Lefebvre et al., 1999; Vassal et al., 2012) already suggested that parts of the VO or of the zona incerta (Fytaridis et al., 2012) could be appropriate targets as well. Recently Groppa et al. (2014) proposed the dentatohalamic tract as key therapeutic DBS target structure.

Following **Figure 7** our data suggest that parts of VCL and CM might be stimulated in some cases. However, **Figure 8** shows that the structure volumes included in the isosurface are below 5% in both improvement ranges. In order to avoid misinterpretation, either patient-specific improvement maps should be used for presentation or thresholds should be introduced to exclude insignificant volumes.

An optimal stimulation position and statistically significant clinical conclusions can only be provided after the analysis of more intraoperative data, the identification of occurring structure combinations and especially the side effect occurrences, which have a major influence on the choice of the final implant position of the chronic DBS lead.

## Limitations and Future Work

The suggested methodology allows a detailed interpretation of intraoperatively acquired data but one has to be aware of certain limitations. First of all, the substantial caveats of non-stimulation factors influencing tremor are undeniable and unfortunately inherent in the operating room conditions. Nevertheless, we have employed various signal analysis techniques to minimize the effect of such non-stimulation factors on the evaluation of tremor using accelerometer. Furthermore, the method was defined in a way trying to limit transformation and fusion errors as much as possible (Zrinzo, 2010). Nevertheless due to the available data, WAIR and T1 MRI data sets containing the anatomic information had to be fused to the stereotactic preoperative CT data set providing the reference for the targeting procedure. Concerning the position of the stimulating contact in relation to the structures, we assumed that the microelectrode was positioned exactly as planned. This seems to be a reasonable approach as the microelectrode was the first entering the brain, and it has been observed that brain shifts in the final electrode position and trajectory can appear when the exploration electrode is replaced by the DBS lead (unpublished data).

As the anatomical information is based on the structures manually outlined on the preoperative image data set, the approach does not consider the movement of the tissue due to the electrodes' insertion or brain shift between implantation sides. On the other hand, the use of these preoperative image data sets is common in analysis and simulation methods. The limitations are acceptable as postoperative image data sets present disturbing artifacts around the implanted DBS leads, in the region of interest. To increase the power of the statistic test performed in the present study, more data should be acquired from further patients and included in the analysis. A further limitation, specific to the anatomical information, concerns the availability of only some anatomical structures and the FF/PLR and that always part of the volume of the EF isosurface is outside any manually defined anatomical structure. In consequence, information from white matter fiber tracking would be helpful to define the region anterior to the VIM and the InL and for further investigating possible activation of fiber tracks (Coenen et al., 2012).

The method could in a next step also be complemented with the available MER data at the different positions including the analysis of time patterns describing the network dynamics as proposed by Andres et al. (2015).

The data analysis approach proposed in the present paper considers the percentage of the structure volume covered by the simulated EF isosurface and not which parts of the structure. Further data interpretation could consider the 3D position as well and should generate improvement maps taking into account stimulation positions of amplitudes as well as the occurrence of side effects.

## CONCLUSION

A new concept for the analysis of data acquired during DBS surgery has been proposed. A workflow and methodology

combining objective intraoperative tremor evaluation with patient-specific EF simulations on manually outlined anatomical structures has been defined and applied to five patients with ET undergoing DBS-implantation. This new approach is combined with an algorithm for detection of the volume of the anatomical structures involved during intraoperative microelectrode stimulation. It can be adapted to further surgical protocols, intraoperative set-ups and to other anatomical data. Its application will allow the analysis of intraoperative data obtained in clinical routine and will support the identification of anatomical structures, parts of them or white matter fibers responsible for the therapeutic effect. The analysis of more data and inclusion of occurrence of side effects are necessary to draw any final conclusions of the most efficient brain targets. The first results, however, indicate agreement with published data hypothesizing that the stimulation of structures other than the VIM might be responsible for good clinical effect in ET.

## AUTHOR CONTRIBUTIONS

All authors contributed in writing the manuscript and critically reviewed the last version. SH: Idea and conception of whole approach; design of protocols and clinical study, especially acceleration measurements; set-up of whole method; development of brain map extraction; participation in data analysis and interpretation; main drafting of manuscript. DP: Technical set-up and implementation of the defined workflow; final data analysis of all available multimodal data; participation in data interpretation; main drafting of manuscript. FA: Set-up of the EF simulation with its patient-specific models; performing all the simulations; data analysis. AS: Realization of acceleration measurements and their analysis; choice of parameters for simulation. JC: Set-up of clinical study and intraoperative realization of study; stimulation data acquisition. J-JL: Set-up of clinical study; patient selection and operation; data interpretation. KW: Set-up of initial e-field simulations; conception of work from simulation point of view; support and critical review of whole concept and especially patient-specific simulations.

## FUNDING

This research was financially supported by the Swiss National Science Foundation (CR3212\_153370), the Germaine de Staël program of the Swiss Academy of Engineering Sciences, the French Ministry of Health (2011-A00774-37), the Swedish Research Council (621-2013-6078) and the Parkinson Foundation at Linköping University.

## ACKNOWLEDGMENT

The authors acknowledge the contribution of Dr. Miguel Ulla for the neurological evaluation of the patients.

## REFERENCES

- Alonso, F., Latorre, M., Göransson, N., Zsigmond, P., and Wårdell, K. (2016). Investigation into deep brain stimulation lead designs: a patient-specific simulation study. *Brain Sci.* 6:39. doi: 10.3390/brainsci6030039
- Andres, D. S., Cerquetti, D., and Merello, M. (2015). Neural code alterations and abnormal time patterns in Parkinson's disease. *J. Neural. Eng.* 12:026004. doi: 10.1088/1741-2560/12/2/026004
- Anthofer, J., Steib, K., Fellner, C., Lange, M., Brawanski, A., and Schlaier, J. (2014). The variability of atlas-based targets in relation to surrounding major fibre tracts in thalamic deep brain stimulation. *Acta Neurochir. (Wien)* 156, 1497–1504. doi: 10.1007/s00701-014-2103-z
- Åström, M., Diczfalusy, E., Martens, H., and Wårdell, K. (2015). Relationship between neural activation and electric field distribution during deep brain stimulation. *IEEE Trans. Biomed. Eng.* 62, 664–672. doi: 10.1109/TBME.2014.2363494
- Åström, M., Johansson, J. D., Hariz, M. I., Eriksson, O., and Wårdell, K. (2006). The effect of cystic cavities on deep brain stimulation in the basal ganglia: a simulation-based study. *J. Neural. Eng.* 3, 132–138. doi: 10.1088/1741-2560/3/2/007
- Åström, M., Lemaire, J. J., and Wårdell, K. (2012). Influence of heterogeneous and anisotropic tissue conductivity on electric field distribution in deep brain stimulation. *Med. Biol. Eng. Comput.* 50, 23–32. doi: 10.1007/s11517-011-0842-z
- Åström, M., Tripoliti, E., Hariz, M. I., Zrinzo, L. U., Martinez-Torres, I., Limousin, P., et al. (2010). Patient-specific model-based investigation of speech intelligibility and movement during deep brain stimulation. *Stereotact. Funct. Neurosurg.* 88, 224–233. doi: 10.1159/000314357
- Åström, M., Zrinzo, L. U., Tisch, S., Tripoliti, E., Hariz, M. I., and Wårdell, K. (2009). Method for patient-specific finite element modeling and simulation of deep brain stimulation. *Med. Biol. Eng. Comput.* 47, 21–28. doi: 10.1007/s11517-008-0411-2
- Benabid, A. L., Chabardes, S., Mitrofanis, J., and Pollak, P. (2009). Deep brain stimulation of the subthalamic nucleus for the treatment of Parkinson's disease. *Lancet Neurol.* 8, 67–81. doi: 10.1016/S1474-4422(08)70291-6
- Benabid, A. L., Pollak, P., Gervason, C., Hoffmann, D., Gao, D. M., Hommel, M., et al. (1991). Long-term suppression of tremor by chronic stimulation of the ventral intermediate thalamic nucleus. *Lancet* 337, 403–406. doi: 10.1016/0140-6736(91)91175-T
- Benabid, A. L., Pollak, P., Seigneuret, E., Hoffmann, D., Gay, E., and Perret, J. (1993). Chronic VIM thalamic stimulation in Parkinson's disease, essential tremor and extra-pyramidal dyskinesias. *Acta Neurochir. Suppl. (Wien)* 58, 39–44.
- Birdno, M. J., Kuncel, A. M., Dorval, A. D., Turner, D. A., and Grill, W. M. (2008). Tremor varies as a function of the temporal regularity of deep brain stimulation. *Neuroreport* 19, 599–602. doi: 10.1097/WNR.0b013e3282f9e45e
- Caire, F., Ranoux, D., Guehl, D., Burbaud, P., and Cuny, E. (2013). A systematic review of studies on anatomical position of electrode contacts used for chronic subthalamic stimulation in Parkinson's disease. *Acta Neurochir. (Wien)* 155, 1647–1654. doi: 10.1007/s00701-013-1782-1
- Caparros-Lefebvre, D., Blond, S., Feltin, M. P., Pollak, P., and Benabid, A. L. (1999). Improvement of levodopa induced dyskinesias by thalamic deep brain stimulation is related to slight variation in electrode placement: possible involvement of the centre median and parafascicularis complex. *J. Neurol. Neurosurg. Psychiatry* 67, 308–314. doi: 10.1136/jnnp.67.3.308
- Chaturvedi, A., Butson, C. R., Lempka, S. F., Cooper, S. E., and McIntyre, C. C. (2010). Patient-specific models of deep brain stimulation: influence of field model complexity on neural activation predictions. *Brain Stimul.* 3, 65–67. doi: 10.1016/j.brs.2010.01.003
- Cif, L., Vasques, X., Gonzalez, V., Ravel, P., Biolsi, B., Collod-Beroud, G., et al. (2010). Long-term follow-up of DYT1 dystonia patients treated by deep brain stimulation: an open-label study. *Mov. Disord.* 25, 289–299. doi: 10.1002/mds.22802
- Coenen, V. A., Schlaepfer, T. E., Allert, N., and Madler, B. (2012). Diffusion tensor imaging and neuromodulation: DTI as key technology for deep brain stimulation. *Int. Rev. Neurobiol.* 107, 207–234. doi: 10.1016/B978-0-12-404706-8.00011-5
- Coste, J., Ouchchane, L., Sarry, L., Derost, P., Durif, F., Gabrillargues, J., et al. (2009). New electrophysiological mapping combined with MRI in parkinsonian's subthalamic region. *Eur. J. Neurosci.* 29, 1627–1633. doi: 10.1111/j.1460-9568.2009.06698.x
- Coubes, P., Roubertie, A., Vayssiere, N., Hemm, S., and Echenne, B. (2000). Treatment of DYT1-generalised dystonia by stimulation of the internal globus pallidus. *Lancet* 355, 2220–2221. doi: 10.1016/S0140-6736(00)02410-7
- Fyttagoridis, A., Sandvik, U., Astrom, M., Bergenheim, T., and Blomstedt, P. (2012). Long term follow-up of deep brain stimulation of the caudal zona incerta for essential tremor. *J. Neurol. Neurosurg. Psychiatry* 83, 258–262. doi: 10.1136/jnnp-2011-300765
- Gabriel, C., Gabriel, S., and Corthout, E. (1996). The dielectric properties of biological tissues: I. Literature survey. *Phys. Med. Biol.* 41, 2231–2249. doi: 10.1088/0031-9155/41/11/001
- Garcia-Garcia, D., Guridi, J., Toledo, J. B., Alegre, M., Obeso, J. A., and Rodriguez-Oroz, M. C. (2016). Stimulation sites in the subthalamic nucleus and clinical improvement in Parkinson's disease: a new approach for active contact localization. *J. Neurosurg.* 125, 1068–1079. doi: 10.3171/2015.9.JNS15868
- Griffiths, R. I., Kotschet, K., Arfon, S., Xu, Z. M., Johnson, W., Drago, J., et al. (2012). Automated assessment of bradykinesia and dyskinesia in Parkinson's disease. *J. Parkinsons Dis.* 2, 47–55. doi: 10.3233/JPD-2012-11071
- Groppa, S., Herzog, J., Falk, D., Riedel, C., Deuschl, G., and Volkmann, J. (2014). Physiological and anatomical decomposition of subthalamic neurostimulation effects in essential tremor. *Brain* 137(Pt 1), 109–121. doi: 10.1093/brain/awt304
- Hariz, M., Blomstedt, P., and Zrinzo, L. (2013). Future of brain stimulation: new targets, new indications, new technology. *Mov. Disord.* 28, 1784–1792. doi: 10.1002/mds.25665
- Hemm, S., Caire, F., Coste, J., Vassal, F., Nuti, C., Derost, P., et al. (2008). Postoperative control in deep brain stimulation of the subthalamic region: the contact membership concept. *Int. J. CARS* 3, 69–77. doi: 10.1007/s11548-008-0152-r6
- Hemm, S., Mennessier, G., Vayssiere, N., Cif, L., and Coubes, P. (2005). Co-registration of stereotactic MRI and isofieldlines during deep brain stimulation. *Brain Res. Bull.* 68, 59–61. doi: 10.1016/j.brainresbull.2005.08.024
- Hemm, S., and Wårdell, K. (2010). Stereotactic implantation of deep brain stimulation electrodes: a review of technical systems, methods and emerging tools. *Med. Biol. Eng. Comput.* 48, 611–624. doi: 10.1007/s11517-010-0633-y
- Herrington, T. M., Cheng, J. J., and Eskandar, E. N. (2015). Mechanisms of deep brain stimulation. *J. Neurophysiol.* 70, 163–171. doi: 10.1152/jn.00281.2015
- Herzog, J., Hamel, W., Wenzelburger, R., Potter, M., Pinsker, M. O., Bartussek, J., et al. (2007). Kinematic analysis of thalamic versus subthalamic neurostimulation in postural and intention tremor. *Brain* 130(Pt 6), 1608–1625. doi: 10.1093/brain/awm077
- Hirai, T., and Jones, E. G. (1989). A new parcellation of the human thalamus on the basis of histochemical staining. *Brain Res. Brain Res. Rev.* 14, 1–34. doi: 10.1016/0165-0173(89)90007-6
- Howell, B., and McIntyre, C. C. (2016). Analyzing the tradeoff between electrical complexity and accuracy in patient-specific computational models of deep brain stimulation. *J. Neural. Eng.* 13:036023. doi: 10.1088/1741-2560/13/3/036023
- Journee, H. L., Postma, A. A., and Staal, M. J. (2007). Intraoperative neurophysiological assessment of disabling symptoms in DBS surgery. *Neurophysiol. Clin.* 37, 467–475. doi: 10.1016/j.neucli.2007.10.006
- Kuncel, A. M., Cooper, S. E., and Grill, W. M. (2008). A method to estimate the spatial extent of activation in thalamic deep brain stimulation. *Clin. Neurophysiol.* 119, 2148–2158. doi: 10.1016/j.clinph.2008.02.025
- Lalys, F., Haegelen, C., Mehri, M., Drapier, S., Verin, M., and Jannin, P. (2013). Anatomico-clinical atlases correlate clinical data and electrode contact coordinates: application to subthalamic deep brain stimulation. *J. Neurosci. Methods* 212, 297–307. doi: 10.1016/j.jneumeth.2012.11.002
- Lemaire, J. J., Coste, J., Ouchchane, L., Hemm, S., Derost, P., Ulla, M., et al. (2007). MRI anatomical mapping and direct stereotactic targeting in the subthalamic region: functional and anatomical correspondence in Parkinson's disease. *Int. J. CARS* 2, 75–85. doi: 10.1007/s11548-007-0124-2
- Lemaire, J. J., Sakka, L., Ouchchane, L., Caire, F., Gabrillargues, J., and Bonny, J. M. (2010). Anatomy of the human thalamus based on spontaneous contrast and microscopic voxels in high-field magnetic resonance imaging. *Neurosurgery* 66(3 Suppl. Operative), 161–172.

- Magnotta, V. A., Gold, S., Andreasen, N. C., Ehrhardt, J. C., and Yuh, W. T. (2000). Visualization of subthalamic nuclei with cortex attenuated inversion recovery MR imaging. *Neuroimage* 11, 341–346. doi: 10.1006/nimg.2000.0552
- Mansur, P. H., Cury, L. K., Andrade, A. O., Pereira, A. A., Miotto, G. A., Soares, A. B., et al. (2007). A review on techniques for tremor recording and quantification. *Crit. Rev. Biomed. Eng.* 35, 343–362. doi: 10.1615/CritRevBiomedEng.v35.i5.10
- McIntyre, C. C., Mori, S., Sherman, D. L., Thakor, N. V., and Vitek, J. L. (2004). Electric field and stimulating influence generated by deep brain stimulation of the subthalamic nucleus. *Clin. Neurophysiol.* 115, 589–595. doi: 10.1016/j.clinph.2003.10.033
- Morel, A. (2007). *Stereotactic Atlas of the Human Thalamus and Basal Ganglia*. Boca Raton, FL: CRC Press.
- Palmer, J. L., Coats, M. A., Roe, C. M., Hanko, S. M., Xiong, C., and Morris, J. C. (2010). Unified Parkinson's Disease rating scale-motor exam: inter-rater reliability of advanced practice nurse and neurologist assessments. *J. Adv. Nurs.* 66, 1382–1387. doi: 10.1111/j.1365-2648.2010.05313.x
- Papapetropoulos, S., Jagid, J. R., Sengun, C., Singer, C., and Gallo, B. V. (2008). Objective monitoring of tremor and bradykinesia during DBS surgery for Parkinson disease. *Neurology* 70, 1244–1249. doi: 10.1212/01.wnl.0000308936.27780.94
- Post, B., Merkus, M. P., de Bie, R. M., de Haan, R. J., and Speelman, J. D. (2005). Unified Parkinson's disease rating scale motor examination: are ratings of nurses, residents in neurology, and movement disorders specialists interchangeable? *Mov. Disord.* 20, 1577–1584. doi: 10.1002/mds.20640
- Saint-Cyr, J. A., Hoque, T., Pereira, L. C., Dostrovsky, J. O., Hutchison, W. D., Mikulis, D. J., et al. (2002). Localization of clinically effective stimulating electrodes in the human subthalamic nucleus on magnetic resonance imaging. *J. Neurosurg.* 97, 1152–1166. doi: 10.3171/jns.2002.97.5.1152
- Sarnthein, J., Peus, D., Baumann-Vogel, H., Baumann, C. R., and Surucu, O. (2013). Stimulation sites in the subthalamic nucleus projected onto a mean 3-D atlas of the thalamus and basal ganglia. *Acta Neurochir. (Wien)* 155, 1655–1660. doi: 10.1007/s00701-013-1780-3
- Schaltenbrand, G., and Bailey, P. (1959). *Introduction to Stereotaxis with an Atlas of the Human Brain*. Stuttgart: Thieme Verlag.
- Schmidt, C., Grant, P., Lowery, M., and van Rienen, U. (2013). Influence of uncertainties in the material properties of brain tissue on the probabilistic volume of tissue activated. *IEEE Tran. Biomed. Eng.* 60, 1378–1387. doi: 10.1109/TBME.2012.2235835
- Shah, A., Coste, J., Lemaire, J., Schkommodau, E., Taub, E., Guzman, R., et al. (2016a). A novel assistive method for rigidity evaluation during deep brain stimulation surgery using acceleration sensors. *J. Neurosurg.*
- Shah, A., Coste, J., Lemaire, J. J., Schkommodau, E., and Hemm-Ode, S. (2013). "A method to quantitatively evaluate changes in tremor during deep brain stimulation surgery," in *Proceedings of the 6th International IEEE/EMBS Conference: Neural Engineering* (Rome: IEEE), 1202–1205.
- Shah, A., Coste, J., Lemaire, J., Taub, E., Schüpbach, M., Pollo, C., et al. (2016b). Intraoperative acceleration measurements to quantify tremor during deep brain stimulation surgery. *Med. Biol. Eng. Comput.* doi: 10.1007/s11517-016-1559-9 [Epub ahead of print].
- Slavin, K. V., and Burchiel, K. J. (2002). MicroGuide microelectrode recording system. *Neurosurgery* 51, 275–278. doi: 10.1097/00006123-200207000-00048
- Spiegelmann, R., Nissim, O., Daniels, D., Ocherashvilli, A., and Mardor, Y. (2006). Stereotactic targeting of the ventrointermediate nucleus of the thalamus by direct visualization with high-field MRI. *Stereotact. Funct. Neurosurg.* 84, 19–23. doi: 10.1159/000092683
- Starr, P. A., Christine, C. W., Theodosopoulos, P. V., Lindsey, N., Byrd, D., Mosley, A., et al. (2002). Implantation of deep brain stimulators into the subthalamic nucleus: technical approach and magnetic resonance imaging-verified lead locations. *J. Neurosurg.* 97, 370–387. doi: 10.3171/jns.2002.97.2.0370
- Tarvainen, M. P., Ranta-Aho, P. O., and Karjalainen, P. A. (2002). An advanced detrending method with application to HRV analysis. *IEEE Trans. Biomed. Eng.* 49, 172–175. doi: 10.1109/10.979357
- Vassal, F., Coste, J., Derost, P., Mendes, V., Gabrillagues, J., Nuti, C., et al. (2012). Direct stereotactic targeting of the ventrointermediate nucleus of the thalamus based on anatomic 1.5-T MRI mapping with a white matter attenuated inversion recovery (WAIR) sequence. *Brain Stimul.* 5, 625–633. doi: 10.1016/j.brs.2011.10.007
- Vayssiere, N., Hemm, S., Cif, L., Picot, M. C., Diakonova, N., El Fertit, H., et al. (2002). Comparison of atlas- and magnetic resonance imaging-based stereotactic targeting of the globus pallidus internus in the performance of deep brain stimulation for treatment of dystonia. *J. Neurosurg.* 96, 673–679. doi: 10.3171/jns.2002.96.4.0673
- Vayssiere, N., van der Gaag, N., Cif, L., Hemm, S., Verdier, R., Frerebeau, P., et al. (2004). Deep brain stimulation for dystonia confirming a somatotopic organization in the globus pallidus internus. *J. Neurosurg.* 101, 181–188. doi: 10.3171/jns.2004.101.2.0181
- Voges, J., Kiening, K., Krauss, J. K., Nikkhah, G., and Vesper, J. (2009). [Neurosurgical standards in deep brain stimulation : consensus recommendations of the German Deep Brain Stimulation Association]. *Nervenarzt* 80, 666–672. doi: 10.1007/s00115-009-2698-0
- Wårdell, K., Diczfalusy, E., and Åström, M. (2012). "Patient-Specific modeling and simulation of deep brain stimulation," in *Patient-Specific Modeling in Tomorrow's Medicine*, ed. A. Gefen (Berlin: Springer), 357–375.
- Wårdell, K., Kefalopoulou, Z., Diczfalusy, E., Andersson, M., Astrom, M., Limousin, P., et al. (2015). Deep brain stimulation of the pallidum internum for Gilles de la Tourette syndrome: a patient-specific model-based simulation study of the electric field. *Neuromodulation* 18, 90–96. doi: 10.1111/ner.12248
- Wårdell, K., Zrinzo, L., Hariz, M., and Andersson, M. (2013). "Patient-specific brain modelling for deep brain stimulation simulations," in *Proceedings of the 6th International IEEE/EMBS Conference: Neural Engineering* (Rome: IEEE), 148–151.
- Weise, L. M., Seifried, C., Eibach, S., Gasser, T., Roeper, J., Seifert, V., et al. (2013). Correlation of active contact positions with the electrophysiological and anatomical subdivisions of the subthalamic nucleus in deep brain stimulation. *Stereotact. Funct. Neurosurg.* 91, 298–305. doi: 10.1159/000345259
- Wodarg, F., Herzog, J., Reese, R., Falk, D., Pinsker, M. O., Steigerwald, F., et al. (2012). Stimulation site within the MRI-defined STN predicts postoperative motor outcome. *Mov. Disord.* 27, 874–879. doi: 10.1002/mds.25006
- Zerroug, A., Gabrillagues, J., Coll, G., Vassal, F., Jean, B., Chabert, E., et al. (2016). Personalized mapping of the deep brain with a white matter attenuated inversion recovery (WAIR) sequence at 1.5-tesla: experience based on a series of 156 patients. *Neurochirurgie* 62, 183–189. doi: 10.1016/j.neuchi.2016.01.009
- Zonenshayn, M., Sterio, D., Kelly, P. J., Rezai, A. R., and Beric, A. (2004). Location of the active contact within the subthalamic nucleus (STN) in the treatment of idiopathic Parkinson's disease. *Surg. Neurol.* 62, 216–225. doi: 10.1016/j.surneu.2003.09.039
- Zrinzo, L. (2010). The role of imaging in the surgical treatment of movement disorders. *Neuroimaging Clin. North Am.* 20, 125–140. doi: 10.1016/j.nic.2009.08.002

**Conflict of Interest Statement:** The authors declare that the research was conducted in the absence of any commercial or financial relationships that could be construed as a potential conflict of interest.

Copyright © 2016 Hemm, Pison, Alonso, Shah, Coste, Lemaire and Wårdell. This is an open-access article distributed under the terms of the Creative Commons Attribution License (CC BY). The use, distribution or reproduction in other forums is permitted, provided the original author(s) or licensor are credited and that the original publication in this journal is cited, in accordance with accepted academic practice. No use, distribution or reproduction is permitted which does not comply with these terms.

## Chapter 8

# Data Visualization during DBS Surgery

The existing pool of scientific work described in the background (Section 2.7) shows the potential that a software tool has to assist the surgical team during the important task of lead placement. The variety of data collected during our clinical study in CHU, Clermont-Ferrand as listed below, presented an excellent opportunity to develop such a tool to assist during the decision making process.

**Radiographical Images** Preoperative stereotactic CT, stereotactic T1 MR and stereotactic WAIR MR images are acquired to facilitate surgical planning.

**Expert-Labelled Anatomical Structures** Using the planning software, for each patient, all the relevant anatomical structures are outlined and labelled.

**Surgical Planning Data** The desired target is identified through the surgical planning software and trajectories are planned and saved.

**Electrophysiology** During the surgery, MER is performed at the planned positions to obtain electrophysiological data of the region of interest.

**Therapeutic and Adverse Effects of Stimulation** Stimulation tests are administered at the desired locations and the patient's response (therapeutic and adverse effects) are noted along with the stimulation parameters using pen and paper.

**Quantitative Symptom Evaluation** Analysis of acceleration data synchronized with the stimulation tests provide the quantitative improvement in symptoms for each stimulation current amplitude.

**Spatial Effects of Stimulation** The patient-specific FEM technique to simulate the electric field distribution based on the stimulation current amplitude provides information about the spatial effect of stimulation in the

brain tissue.

The consolidation of such variety of data into one visualization requires overcoming some hurdles. The image data sets, the labelled anatomical structures and the planned trajectories are stored on the planning software, the MER and test stimulation parameters are stored on the electrophysiology system, the accelerometer data are stored on our system and the simulations are performed at LiU. All this information has to be transferred to one system and then processed and visualized in a manner that retains the proper spatial position of each data set. The second hurdle is the amount of data that can be generated. During intraoperative stimulation tests, stimulation current amplitude is increased from 0 to 3 mA in steps of 0.2 mA at an average of 7 test stimulation positions each on two parallel trajectories. If all of the stimulation current amplitudes were simulated, it would result in an average of 210 ( $15 \times 7 \times 2$ ) simulations per patient implantation. Although visualizing all this data along with the anatomical structures and patient images would be possible, the resultant visualizations would contain redundant information and would also be difficult to analyse.

The adverse effects of stimulation are also considered when choosing the optimal place of the DBS lead. Therefore, adverse effects observed during intraoperative stimulation tests are also noted along with the corresponding current amplitude. In contrast to therapeutic effects which are noted for all stimulation test positions, adverse effects are only noted for the positions where they are observed. Additionally, in CHU, Clermont-Ferrand, the stimulation test at a given position is stopped at the first adverse effect occurrence. The visualization of this adverse effect dataset of one current amplitude per stimulation test position would depict the "no-go" zones for chronic stimulation. Out of the 5 ET patients that were used for the EF simulation study, adverse effects were observed during stimulation tests in 4 patients. EF simulations for the adverse effect inducing current amplitudes were analysed and visualized together with the patient images and outlines of the anatomical structures to create an "Adverse Effect Map". The details of the method, its application and results are described further in the recently accepted paper titled "Analysis of adverse effects of stimulation during DBS surgery by patient-specific FEM simulations" attached in the current chapter (Section 8.1).

The results of the adverse effect map study concur with the findings of other studies in terms of the anatomical structure that is responsible for a specific adverse effects. This demonstration of the utility of the maps gave the impetus to summarize and visualize all the data that are necessary for optimally placing the DBS lead. To reduce the redundancy of the data and to simplify the analysis, we propose a two-step technique. The first logical step is to simulate only selected stimulation current amplitudes per test position, i.e. those that significantly suppress the symptoms, which in turn, would reduce the number of simulations per implantation. Despite the reduction of simulations, there would

be many voxels in the stimulation test region which would be encompassed by more than one electric field simulation and in turn be associated to more than one value of improvement. Therefore, the next step to simplify analysis is to assign one improvement value to a voxel to divide the stimulation test region into smaller parts, each representing different levels of improvement in the symptom. The collective visualization of these improvement regions with the patient images and labelled anatomy is termed as "Improvement Maps."

The two important factors that would decide the shape and size of different regions in the improvement maps would be the choice of stimulation current amplitude that are simulated and the function used to assign one improvement value to each voxel. As our first approach, we simulated the lowest stimulation current amplitudes that resulted in the maximum improvement and also assigned the maximum improvement value to one voxel. This choice was based on the understanding that the aim of the DBS surgery is to place the lead at a position with maximum improvement in symptoms. This specific type of improvement maps were termed as "Maximum Improvement Maps" and were retrospectively created for 5 ET patients who underwent VIM-DBS at CHU, Clermont-Ferrand with the aim to gauge their utility. The resulting visualizations were analysed post-operatively by the surgical team at CHU, Clermont-Ferrand to choose the position for DBS lead placement. The following draft paper titled "Improvement Maps: a technique to visualize results of intraoperative stimulation tests for deep brain stimulation surgery" contains the detailed method of creating the maximum improvement maps, the results of application to 5 ET patients and the relevant discussion. The subsequent supplementary file contains the maximum improvement map figures for all implantations.

## 8.1 Analysis of adverse effects of stimulation during DBS surgery by patient-specific FEM simulations

**Authors:** Ashesh Shah, Fabiola Alonso, Dorian Vogel, Karin Wårdell, Jérôme Coste, Jean-Jacques Lemaire, Daniela Pison, Simone Hemm.

This paper was submitted to the 40th International Conference of the IEEE Engineering in Medicine and Biology Society which was held in Honolulu, Hawaii, United States of America from 18-21st July, 2018. It describes the method to visualize the spatial distribution of stimulation that induced adverse effects during intraoperative testing.

The paper is available at the address :  
<https://doi.org/10.1109/EMBC.2018.8512796>

Copyright Notice: ©2018 IEEE. Reprinted, with permission, from Ashesh Shah, Fabiola Alonso, Dorian Vogel, Karin Wårdell, Jérôme Coste, Jean-Jacques Lemaire, Daniela Pison, and Simone Hemm-Ode, Analysis of adverse effects of stimulation during DBS surgery by patient-specific FEM simulations, 2018 40th Annual International Conference of IEEE Engineering in Medicine and Biology Society (EMBC) July, 2018.

In reference to IEEE copyrighted material which is used with permission in this thesis, the IEEE does not endorse any of Universität Basel's products or services. Internal or personal use of this material is permitted. If interested in reprinting/republishing IEEE copyrighted material for advertising or promotional purposes or for creating new collective works for resale or redistribution, please go to [http://www.ieee.org/publications\\_standards/publications/rights/rights\\_link.html](http://www.ieee.org/publications_standards/publications/rights/rights_link.html) to learn how to obtain a License from RightsLink.

# Analysis of adverse effects of stimulation during DBS surgery by patient-specific FEM simulations

Ashesh A. Shah, Fabiola Alonso, Dorian Vogel, Karin Wårdell, *Member, IEEE*, Jérôme Coste, *Member, IEEE*, Jean-Jacques Lemaire, Daniela Pison and Simone Hemm, *Member, IEEE*

**Abstract**— Deep brain stimulation (DBS) represents today a well-established treatment for movement disorders. Nevertheless the exact mechanism of action of DBS remains incompletely known. During surgery, numerous stimulation tests are frequently performed in order to evaluate therapeutic and adverse effects before choosing the optimal implantation site for the DBS lead. Anatomical structures responsible for the induced adverse effects have been investigated previously, but only based on stimulation data obtained with the implanted DBS lead. The present study introduces a methodology to identify these anatomical structures during intraoperative stimulation tests based on patient-specific electric field simulations and visualization on the patient specific anatomy. The application to 4 patients undergoing DBS surgery and presenting dysarthria, paresthesia or pyramidal effects shows the different anatomical structures, which might be responsible for the adverse effects. Several of the identified structures have been previously described in the literature. To draw any statistically significant conclusions, the methodology has to be applied to further patients. Together with the visualization of the therapeutic effects, this new approach could assist the neurosurgeons in the future in choosing the optimal implant position.

## I. INTRODUCTION

DBS represents today a well-established therapy for the symptomatic treatment of movement disorders such as Parkinson's disease (PD) and essential tremor (ET) but as well for other diseases. Electrodes are implanted in the brain through which the surrounding structures are continuously stimulated. Before surgery, the brain target is chosen and the trajectory to reach it is planned on magnetic resonance images (MRI). During surgery, many centers perform microelectrode recording (MER) and stimulation tests on predefined positions on one or more parallel trajectories. Evaluations of therapeutic effects and adverse events are performed at these sites based on which the optimal stimulation position is chosen [1]. Despite the success of the therapy, the mechanism(s) of action

of DBS [2] and the exact structures or structure parts responsible for the therapeutic effect and certain adverse effects remain incompletely known. The aim of the present paper is to present a methodology to analyze the anatomical structures involved in inducing side effects during intraoperative stimulation tests based on patient-specific electric field simulations and visualization on the patient specific anatomy. The new approach is applied to intraoperatively obtained data in one clinical center in Clermont-Ferrand, France.

## II. METHOD

### A. Surgical procedure

At Clermont-Ferrand University hospital, the surgical procedure is defined as follows [3]: an extensive preoperative surgical planning is performed. Stereotactic CT, T1 MRI and white-matter attenuation inversion recovery sequences (WAIR) are acquired (Sonata 1.5T, Siemens, Germany). The different thalamic nuclei and the basal ganglia are then outlined by the neurosurgeon using a commercial planning software (iPlan stereotaxy 3.0, Brainlab, Munich, Germany) based on the spontaneous contrast of the WAIR sequence and with an in-house developed 4.7T brain atlas (Fig. 1). Based on these outlined structures, an anatomical target e.g. the ventral intermediate nucleus (VIM) for ET patients and an entry point are carefully chosen. Two parallel trajectories and positions for neuronal recording and stimulation tests are carefully identified within the volume of interest for the intraoperative testing. During surgery, MER is first performed followed by stimulation tests at the predefined positions. During stimulation tests the stimulation amplitude is increased from 0 to 3 mA in 0.2 mA steps and the symptom improvement is estimated. In addition, amplitudes and the kind of adverse effect are noted. The final implantation position of the DBS electrode is chosen where 1) the stimulation amplitude

A. Shah is with Institute for Medical and Analytical Technologies, School of Life Sciences, University of Applied Sciences and Arts Northwestern Switzerland FHNW, Muttentz, Switzerland (email: [ashesh.shah@fhnw.ch](mailto:ashesh.shah@fhnw.ch); phone: +41 61 228 56 89)

F. Alonso is with Department of Biomedical Engineering, Linköping University, Linköping, Sweden (email: [fabiola.alonso@liu.se](mailto:fabiola.alonso@liu.se))

D. Vogel is with Institute for Medical and Analytical Technologies, School of Life Sciences, University of Applied Sciences and Arts Northwestern Switzerland FHNW, Muttentz, Switzerland and Department of Biomedical Engineering, Linköping University, Linköping, Sweden (email: [dorian.vogel@fhnw.ch](mailto:dorian.vogel@fhnw.ch))

K. Wårdell is with Department of Biomedical Engineering, Linköping University, Linköping, Sweden (email: [karin.wardell@liu.se](mailto:karin.wardell@liu.se))

J. Coste is with the Université Clermont Auvergne, CNRS, Institut Pascal, UMR 6602, Image Guided Therapies (IGT), Image Guided Clinical Neurosciences and Connectomics (IGCNC), Clermont-Ferrand, France, and Service de Neurochirurgie, Hôpital Gabriel-Montpied, Centre Hospitalier

Universitaire de Clermont-Ferrand, Clermont-Ferrand, France (email: [jerome.coste@uca.fr](mailto:jerome.coste@uca.fr))

J.J. Lemaire is with the Université Clermont Auvergne, CNRS, Institut Pascal, UMR 6602, Image Guided Therapies (IGT), Image Guided Clinical Neurosciences and Connectomics (IGCNC), Clermont-Ferrand, France and Service de Neurochirurgie, Hôpital Gabriel-Montpied, Centre Hospitalier Universitaire de Clermont-Ferrand, Clermont-Ferrand, France (email: [jjlemaire@chu-clermontferrand.fr](mailto:jjlemaire@chu-clermontferrand.fr))

D. Pison is with Institute for Medical and Analytical Technologies, School of Life Sciences, University of Applied Sciences and Arts Northwestern Switzerland FHNW, Muttentz, Switzerland (email: [danielapison@yahoo.it](mailto:danielapison@yahoo.it))

S. Hemm is with Institute for Medical and Analytical Technologies, School of Life Sciences, University of Applied Sciences and Arts Northwestern Switzerland FHNW, Muttentz, Switzerland and Department of Biomedical Engineering, Linköping University, Linköping, Sweden (email: [simone.hemm@fhnw.ch](mailto:simone.hemm@fhnw.ch))

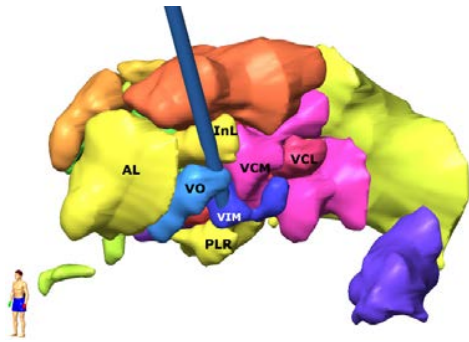


Figure 1. Example of outlined structures in the target area presented in 3D. AL: nucleus anterolateral; InL: nucleus intermedio lateral; VCL: nucleus ventrocaudal lateral; DL: nucleus dorsolateral; PU: pulvinar; VO: nucleus ventro-oral; FF: field of Forel; CM: nucleus centromedian; VCM: nucleus ventrocaudal medial; PLR: pre-llemniscal radiations. VIM: ventral intermediate nucleus

inducing significant therapeutic effects is very low; 2) therapeutically effective stimulation amplitudes at the neighboring positions are relatively low; 3) no adverse events are present or only at high stimulation amplitudes; 4) anatomical position is suitable.

#### B. Electric field simulations

To evaluate the spatial distribution of the stimulation, FEM simulations were performed as previously presented for implanted DBS leads [4]. In the present study, this simulation approach was adapted to the intraoperatively used electrode and electrical setup. An *electrode model* of the microelectrode (Neuroprobe, Alpha Omega Engineering, Nazareth, Israel) was generated. Like in clinical practice, two electrode models were positioned in parallel at a distance of 2 mm. The leading guide tubes were fixed 12 mm above the target. *Patient-specific brain models* were generated in the target area based on the patients' T1 MRI which was enhanced in the basal ganglia and thalamic area. Image voxels were classified into cerebrospinal fluid (CSF), gray matter and white matter and conductivity values were assigned to each voxel [5]: CSF - 2.0 Siemens/meter (S/m), blood - 0.7 S/m, gray matter 0.123 S/m and white matter 0.075 S/m. Between the selected thresholds, conductivity values were interpolated [4].

The *electric field* (EF) was calculated by using the equation of continuity for steady currents according to:

$$\nabla \cdot (\sigma \nabla V) = 0 \quad (1)$$

where  $\sigma$  is a matrix composed of the electrical conductivity values and  $V$  the electric potential. For each simulation, the electrodes were positioned at the clinically used electrode position. The active electrode contact was set to the clinically applied stimulation current while the non-active contact of the parallel lead was set to floating potential. The guide tube was set to ground and the boundaries of the tissue model to electrical insulation. The mesh density was set to about 250,000 tetrahedral elements using the in-built mesh generator (Comsol Multiphysics AB, Sweden), the smallest elements located close to the stimulating contacts to capture the strong EF gradients. For the points defining the surface of the simulated volume, the Cartesian coordinates were exported for further analysis. To perform relative comparisons between the

simulations, the EF isolevel was fixed at 0.2 V/mm as this magnitude is required to stimulate neurons with axons of around 3-4  $\mu\text{m}$  in diameter with a pulse width between 60 to 90  $\mu\text{s}$  [6, 7].

#### C. Anatomical data extraction

In order to be able to visualize the simulated electric field distributions on the patient-specific anatomy, a specifically designed interface based on VVLink and VTK (VTK 5.2.0, Kitware Inc. New York, USA) was used to extract the manually outlined anatomical structures from the stereotactic planning software [8]. To reduce error sources, to increase resolution and to remain in the same image coordinate reference system as the CT images, the outlined anatomical structures were exported in the CT reference space parallel to the CT images. Each anatomical structure was converted from slices to tabular list and saved as csv files (Matlab scripts).

#### D. Clinical Application

Four patients with ET, treated by bilateral DBS and presenting adverse effects during intraoperative stimulation tests were included in the current work (part of clinical study undertaken at the University Hospital; Ref: 2011-A00774-37/AU905, Comité de Protection des Personnes Sud-Est 6, Clermont-Ferrand, France). Trajectories towards the VIM vary from patient to patient due to the planning and individual anatomical differences but follow the path from the superior-anterior-lateral thalamus (ventro-oral nucleus, VO) towards the inferior-posterior-medial direction passing the VIM with the target at its inferior border. For each implantation, the stimulation test positions inducing adverse effects were identified. EF simulations were performed with the current amplitudes inducing the adverse effect. Three different types of adverse effects were observed: dysarthria (speech disturbances), paresthesia (abnormal sensations) and pyramidal effects (motor contractions mostly of the contralateral face and upper limb). Details of the implantations with adverse effects are presented in Table 1.

#### E. Data Processing and Analysis

The data generated through clinical application were processed for one implantation at a time. Using Matlab, the EF simulations for adverse effects were reconstructed as volumes. Union operations were applied when several domains were overlapping. For the visualization of the threshold on the patient-specific images the following data were imported in Paraview (Kitware) using Python (Python.org) scripts: 1) T1 MR and the WAIR MR image data sets, cropped to the region of interest; 2) csv files containing the coordinates of the thalamic nuclei and visualized as surface extracts of Delaunay triangulation of these coordinates; 3) adverse effect thresholds, visualized to depict them as boundary beyond which side effects were observed. The data were first visualized in 3D and then in orthographic slice view using a custom macro script.

The generated adverse effect maps were visually analyzed in axial, coronal and sagittal sections across all the visualized data for one implantation simultaneously in the orthographic slice view. For each side effect, the structures just at the limits

and beyond the adverse effect outline were noted together with the kind of side effect and listed in a table.

TABLE I. DETAILS OF THE SURGERIES FOR THE PATIENTS PARTICIPATING IN THE CLINICAL STUDY.

		Brain Hemisphere	Side Effects (N° of appearances)
Patient N°	1	Left	Paresthesia (4), Pyramidal (1)
		Right	Paresthesia (3)
	2	Right	Paresthesia (2)
	3	Right	Paresthesia (6), Pyramidal (2)
	4	Left	Dysarthria (1)
		Right	Dysarthria (1)

### III. RESULTS

The routine surgical procedure was not altered by application of this method in any way as the data were analyzed post-operatively. Adverse effect maps were analyzed for all six implantations. Table II lists the anatomical structures directly outside the adverse effect threshold outlines for the different types of adverse effects. Adverse effects induced due to *stimulation of the pyramidal tract* were observed during two implantations. The corresponding maps showed that the adverse effect outlines run through the internal capsula (Fig. 2, first row; Table II). *Paresthesia* was observed in three implantations. The adverse effect outlines in these maps were posterior to the VIM and penetrated the VCM, VCL and LaCM nuclei. In most cases, the outline was also inferior to the VIM, entering the posterior subthalamic area (Fig. 2, second row; Table II). For the right hemisphere of patient 4, on the posterior trajectory at the target position *dysarthria* was observed. From the axial and sagittal images, it could be observed that this outline penetrated the VCL, VCM and the LaCM nuclei of the thalamus (Fig. 2, third row; Table II). Stimulation tests in the left hemisphere of patient 4 also induced *dysarthria* at one position, and the adverse effect threshold outline was observed in a similar thalamic region.

### IV. DISCUSSION

This paper describes a new digital approach to assist clinicians in identifying the adverse effect region based on data acquired during intraoperative stimulation tests. In addition to learning more about the regions responsible for the different adverse effects, the combination of this information with the therapeutically effective regions would support the neurosurgeon in choosing the optimal implantation position. To the best of our knowledge, commercial software solutions for DBS do not offer visualization capabilities for intraoperative stimulation tests today. D'Haese et al. [9] developed a system visualizing therapeutic and adverse effects of stimulation in form of spherical balls without simulations. Miocinovic [10] proposes a software tool, Cicerone, estimating and visualizing the spatial distribution of stimulation for adverse effects. It visualizes patient images with brain atlas, MER, DBS leads and the volume of tissue activated (VTA) in three dimensions and can be used intraoperatively. However, the estimation of VTA is not patient specific and is based only on the model of the DBS

lead. In contrast to the existing literature, the approach described in the present paper was specifically designed for intraoperative use. It benefits from patient-specific electric field simulations to estimate the spatial effects of stimulation. Other groups tried as well to identify the structures linked to the occurrence of side effects. Baumgarten [11] introduced a method based on Artificial Neural networks to predict pyramidal tract side effects for postoperative programming of the DBS lead and showed that it was more effective than the calculation of the VTA based on simulations considering homogenous tissue. No comparison with patient-specific electric field simulations is available so far despite the fact that EF has been shown to be the most stable and unchanged entity for different stimulation parameters (amplitude and pulse width)[6]. We [12] have previously successfully applied the same patient-specific electric field simulations to visualize the extent of stimulation but to DBS leads and on atlases but not with patient-specific anatomical data. No study has so far used simulations for intraoperative exploration electrodes. The structures identified behind the outline of adverse effect thresholds presented in the present paper in different maps concur with the findings of other researchers. Adverse effects associated with the *stimulation of the pyramidal tract* were only observed when the threshold outline was very close to the internal capsula supero-lateral to the thalamus. Dowsey-Limousin reported similar effects during post-operative programming of the implanted pulse generator [13]. *Dysarthria* could be associated with the area posterior to the VIM where the VCL, VCM and the LaCM nuclei are located. Similar results were also observed by Reker's group [14] using post-operative stimulation tests. *Paresthesia* was observed for patients 1, 2 and 3. Few studies have associated paresthesia with the stimulation of medial lemniscal fibers that provide input to the VCM and VCL nuclei [15, 16] and to the zona incerta (ZI, [17]). The adverse effect outline in the adverse effect maps concur with results suggesting involvement of medial lemniscal fibers. To draw any statistically significant conclusions, these results have to be confirmed by the application of the method to further patients.

TABLE II. THALAMIC NUCLEI PENETRATED BY THE DIFFERENT ADVERSE EFFECT THRESHOLD OUTLINES

		Side-Effect							
		Pyramidal effect		Parasthesia			Dysarthr.		
Pat/Hemisph.		1/L	3/R	1/L	1/R	2/R	3/R	4/L	4/R
Anatomical structures	INL	X							
	VO	X					X		X
	VIM								X
	PLR					X		X	X
	VCL				X		X	X	X
	VCM			X		X	X		X
	LaCM	X				X		X	X
	IC*	X	X						

\* Internal Capsule (IC) is not outlined during the planning, but is distinguishable based on spontaneous MR contrast.

Lt: left; Rt: right; For structure names see Fig. 1.

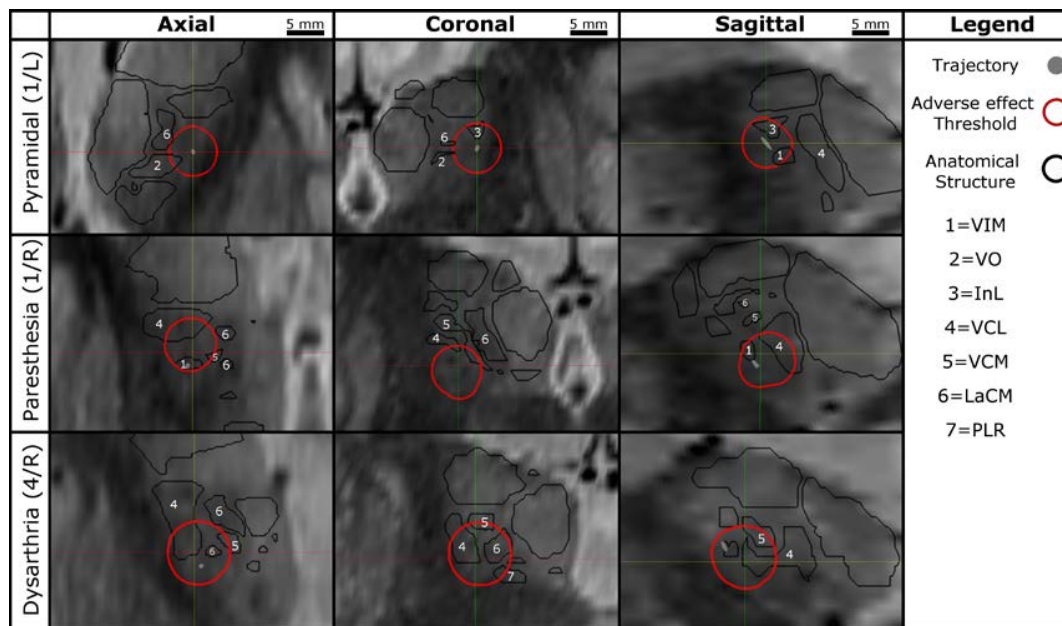


Figure 2. Example of Orthogonal sections across the electric field simulation for the different stimulation induced side effects. First row: Pyramidal effects, left hemisphere patient 1 - The internal capsule including the pyramidal tract can be seen as dark region at the edge of the thalamus (bright). Second row: Paresthesia effects, right hemisphere, patient 1 - VCL, VCM and LaCM nuclei may be involved. Third row: Dysarthria effect, right hemisphere, patient 4 - VCL, VCM, LaCM and the PLR might be involved.

## V. CONCLUSION

The current work presents a new approach how to identify anatomical regions that might be responsible for inducing adverse effects. Together with the visualization of the therapeutic effects, it could assist the neurosurgeons in the future in choosing the optimal implant position.

## ACKNOWLEDGMENT

The authors thank for the financial support of this research by the Swiss National Science Foundation (CR3212\_153370), the Germaine de Staël program of the Swiss Academy of Engineering Sciences, the French Ministry of Health (2011-A00774-37), the Swedish Research Council (2016-03564) and Swedish Foundation for Strategic Research (BD15-0032).

## REFERENCES

- [1] S. Hemm and K. Wårdell, "Stereotactic implantation of deep brain stimulation electrodes: a review of technical systems, methods and emerging tools," *Med Biol Eng Comput*, vol. 48, pp. 611-24, Jul 2010.
- [2] T. M. Herrington, J. J. Cheng, and E. N. Eskandar, "Mechanisms of deep brain stimulation," *J Neurophysiol*, vol. 115, pp. 19-38, 2015.
- [3] F. Vassal, J. Coste, P. Derost, V. Mendes, J. Gabrillargues, C. Nuti, *et al.*, "Direct stereotactic targeting of the ventrointermediate nucleus of the thalamus based on anatomic 1.5-T MRI mapping with a white matter attenuated inversion recovery (WAIR) sequence," *Brain Stimul*, vol. 5, pp. 625-33, Oct 2012.
- [4] K. Wårdell, Z. Kefalopoulou, E. Diczfalusy, M. Andersson, M. Astrom, P. Limousin, *et al.*, "Deep brain stimulation of the pallidum internum for Gilles de la Tourette syndrome: a patient-specific model-based simulation study of the electric field," *Neuromodulation*, vol. 18, pp. 90-6, Feb 2015.
- [5] F. Alonso, M. Latorre, N. Göransson, P. Zsigmond, and K. Wårdell, "Investigation into Deep Brain Stimulation Lead Designs: A Patient-Specific Simulation Study," *Brain Sci*, vol. 6, 2016.
- [6] M. Åström, E. Diczfalusy, H. Martens, and K. Wårdell, "Relationship between Neural Activation and Electric Field Distribution during Deep Brain Stimulation," *IEEE Trans Biomed Eng*, vol. 62, pp. 664-72, 2015.
- [7] A. M. Kuncel, S. E. Cooper, and W. M. Grill, "A method to estimate the spatial extent of activation in thalamic deep brain stimulation," *Clin Neurophysiol*, vol. 119, pp. 2148-58, Sep 2008.
- [8] S. Hemm-Ode, D. Pison, F. Alonso, A. Shah, J. Coste, J.-J. Lemaire, *et al.*, "Patient-specific electric field simulations and acceleration measurements for objective analysis of intraoperative stimulation tests in the thalamus," *Frontiers in Human Neuroscience*, vol. 10, 2016.
- [9] P. F. D'Haese, S. Pallavaram, R. Li, M. S. Remple, C. Kao, J. S. Neimat, *et al.*, "CranialVault and its CRAVE tools: a clinical computer assistance system for deep brain stimulation (DBS) therapy," *Med Image Anal*, vol. 16, pp. 744-53, Apr 2012.
- [10] S. Miocinovic, A. M. Noecker, C. B. Maks, C. R. Butson, and C. C. McIntyre, "Cicerone: stereotactic neurophysiological recording and deep brain stimulation electrode placement software system," *Acta Neurochir Suppl*, vol. 97, pp. 561-7, 2007.
- [11] C. Baumgarten, Y. Zhao, P. Sauleau, C. Malrain, P. Jannin, and C. Haegelen, "Improvement of Pyramidal Tract Side Effect Prediction Using a Data-Driven Method in Subthalamic Stimulation," *IEEE Trans Biomed Eng*, vol. 64, pp. 2134-2141, Sep 2017.
- [12] M. Åström, E. Tripoliti, M. I. Hariz, L. U. Zrinzo, I. Martinez-Torres, P. Limousin, *et al.*, "Patient-specific model-based investigation of speech intelligibility and movement during deep brain stimulation," *Stereotact Funct Neurosurg*, vol. 88, pp. 224-33, 2010.
- [13] P. Dowsey-Limousin, "Postoperative Management of Vim DBS for Tremor," *Mov Disord*, vol. 17, pp. S208-11, 2002.
- [14] P. Reker, T. A. Dembek, J. Becker, V. Visser-Vandewalle, and L. Timmermann, "Directional deep brain stimulation: A case of avoiding dysarthria with bipolar directional current steering," *Parkinsonism Relat Disord*, vol. 31, pp. 156-158, Oct 2016.
- [15] P. Krack, V. Fraix, A. Mendes, A. Benabid, and P. Pollak, "Postoperative Management of Subthalamic Nucleus Stimulation for Parkinson's Disease," *Mov Disord*, vol. 17, pp. S188-97, 2002.
- [16] F. Tamma, E. Caputo, V. Chiesa, M. Egidi, M. Locatelli, P. Rampini, *et al.*, "Anatomical-clinical correlation of intraoperative stimulation-induced side-effects during HF-DBS of the subthalamic nucleus," *Neurol Sci*, vol. 23 Suppl 2, pp. S109-10, Sep 2002.
- [17] T. A. Dembek, M. T. Barbe, M. Astrom, M. Hoevens, V. Visser-Vandewalle, G. R. Fink, *et al.*, "Probabilistic mapping of deep brain stimulation effects in essential tremor," *Neuroimage Clin*, vol. 13, pp. 164-173, 2017.

## **8.2 Improvement Maps: a technique to visualize results of intraoperative stimulation tests for deep brain stimulation surgery**

**Authors:** Ashesh Shah, Fabiola Alonso, Jean-Jacques Lemaire, Daniela Pison, Jérôme Coste, Karin Wårdell, Erik Schkommodau, Simone Hemm.

This manuscript is submitted to the Brain Imaging and Behavior journal. It describes the method of creating the improvement maps by combining delineated thalamic nuclei, accelerometer based tremor evaluation and electric field simulations to visualize the effects of stimulation on the patients brain. These visualizations are meant to assist the clinicians in optimizing lead placement.

The manuscript is currently under review.

# Improvement Maps: Visualization of results of intraoperative stimulation tests for deep brain stimulation surgery.

Ashesh Shah

Institute of Medical Technologies and Medical Informatics,  
School of Life Sciences,  
University of Applied Sciences and Arts Northwestern Switzerland,  
Hofackerstrasse 24,  
4132 Muttenz, Switzerland

Dorian Vogel

Institute of Medical Technologies and Medical Informatics,  
School of Life Sciences,  
University of Applied Sciences and Arts Northwestern Switzerland,  
Hofackerstrasse 24,  
4132 Muttenz, Switzerland

Department of Biomedical Engineering,  
Linköping University,  
Campus US  
SE-581 83 Linköping, Sweden

Fabiola Alonso

Department of Biomedical Engineering, Linköping University,  
Campus US  
SE-581 83 Linköping, Sweden

Jean-Jacques Lemaire

CNRS, Institut Pascal, UMR 6602, Image Guided Therapies (IGT), Image Guided Clinical Neurosciences and Connectomics (IGCNC),  
Université Clermont Auvergne,  
49 bd François Mitterrand,  
CS 60032  
63001 Clermont-Ferrand, France

Service de Neurochirurgie,  
Hôpital Gabriel-Montpied,  
Centre Hospitalier Universitaire de Clermont-Ferrand,  
58, Rue Montalembert,  
63003 CLERMONT FERRAND CEDEX 1,  
France

Daniela Pison

Institute of Medical Technologies and Medical Informatics,  
School of Life Sciences,  
University of Applied Sciences and Arts Northwestern Switzerland,  
Hofackerstrasse 24,  
4132 Muttenz, Switzerland

Jérôme Coste,

CNRS, Institut Pascal, UMR 6602, Image Guided  
Therapies (IGT), Image Guided Clinical  
Neurosciences and Connectomics (IGCNC),  
Université Clermont Auvergne,  
49 bd François Mitterrand,  
CS 60032  
63001 Clermont-Ferrand, France

Service de Neurochirurgie,  
Hôpital Gabriel-Montpied,  
Centre Hospitalier Universitaire de Clermont-  
Ferrand,  
58, Rue Montalembert,  
63003 CLERMONT FERRAND CEDEX 1,  
France

Karin Wårdell

Department of Biomedical Engineering, Linköping University,  
Campus US  
SE-581 83 Linköping, Sweden

Erik Schkommodau

Institute of Medical Technologies and Medical Informatics,  
School of Life Sciences,  
University of Applied Sciences and Arts Northwestern Switzerland,  
Hofackerstrasse 24,  
4132 Muttenz, Switzerland

Simone Hemm-Ode

Institute of Medical Technologies and Medical  
Informatics,  
School of Life Sciences,  
University of Applied Sciences and Arts  
Northwestern Switzerland,  
Hofackerstrasse 24,  
4132 Muttenz, Switzerland

Department of Biomedical Engineering,  
Linköping University,  
Campus US  
SE-581 83 Linköping, Sweden

Corresponding Author: Prof. Dr. Simone Hemm-Ode

Email: [simone.hemm@fhnw.ch](mailto:simone.hemm@fhnw.ch)

Phone: +41 61 228 56 89

## **Acknowledgements:**

This research was jointly funded by the Swiss National Science Foundation (CR3212\_153370), the Germaine de Staël program of the Swiss Academy of Engineering Sciences, the French Ministry of Health (2011-A00774-37), the Swedish Research Council (2016-03564) and Swedish Foundation for Strategic Research (BD15-0032).

## **Abstract:**

Deep brain stimulation (DBS) is an established therapy for movement disorders such as Parkinson's disease, but mechanisms of action remain incompletely known and the optimal target position is still subject of discussion. Positioning the DBS lead in the patient's brain is crucial for effective treatment. Extensive evaluations of improvement and adverse effects of stimulation at different positions for various stimulation amplitudes are performed intraoperatively. However, to choose the optimal position of the lead, the information has to be "mentally" visualized and analyzed. This paper introduces a new technique called Improvement Maps, which summarizes and visualizes the high amount of relevant data with the aim to assist in identifying the optimal DBS lead position. It combines three methods: a) direct visual surgical planning with outlines of the relevant anatomical structures, b) quantitative symptom evaluation during intraoperative stimulation tests and c) patient-specific electric field simulations to estimate the spatial distribution of stimulation. Through this combination, each voxel in the stimulation region is assigned one value of symptom improvement, resulting in the division of stimulation region into areas with different improvement levels. This technique was applied to five Essential Tremor (ET) patients who participated in a clinical study in the University Hospital in Clermont-Ferrand, France. Apart from identifying the optimal implant position, the resultant nine improvement maps show that the highest improvement region is frequently in the posterior sub-thalamic area. The results demonstrate the two fold utility of the improvement maps: identify the optimal implant position and improve DBS target selection.

Keywords: deep brain stimulation, electric field simulations, accelerometry, data visualization, essential tremor

# 1 Introduction

Deep brain stimulation (DBS) is a neurosurgical treatment for movement disorders like Essential Tremor (ET). Patients undergo a complex surgical procedure to implant leads in the brain, which are continuously stimulated through an implanted pulse generator (IPG) in the thoracic or the pelvic cavity. The outcome significantly depends on the location of the DBS lead in the brain. Over the years of DBS usage, clinicians have established few specific target regions in the brain based on the disease being treated, e.g. the ventro-intermedius nucleus (VIM) of the thalamus for ET. However, as these targets have a size in the range of millimeters and as the exact mechanisms behind the functioning of DBS are unknown (Herrington et al. 2016), clinicians implant the DBS lead after testing various positions on a locally anesthetized patient during surgery (Abosch et al. 2013; Hemm and Wårdell 2010).

Before the actual surgery, clinicians perform planning using specially designed software to identify the target structure on the patient images and the best path to reach it from an entry point in the skull. During the surgery, one or more parallel test electrodes are inserted along the planned path and neuronal recording and stimulation tests are performed at pre-determined positions. Therapeutic and adverse effects are evaluated at these stimulation test positions. The details of the surgical procedure may vary between centers, but certain limitations are observed in all centers: The therapeutic effects of stimulation tests for example, are evaluated visually or through passive movements using subjective clinical scales (Post et al. 2005; Palmer et al. 2010; Griffiths et al. 2012). Further, after completing stimulation tests for one hemisphere, the surgical team has to "mentally" visualize the results in relation to the anatomy to identify the optimal implant position.

To limit the subjectivity associated with the clinical ratings used for therapeutic evaluation, researchers have proposed methods to use quantitative tools to estimate the changes in symptoms. We have previously published a method (Shah et al. 2016b) using accelerometers to quantitatively evaluate improvement in tremor during intraoperative stimulation tests. By synchronizing the accelerometer recordings with the electrical stimulation, the improvement in tremor induced by the different stimulation current amplitudes could be quantitatively evaluated. The application of this method to clinical routine showed that such quantitative techniques might be able to improve DBS targeting. The data collected from DBS for ET patients were classified based on the position of the electrode with respect to the nuclei. The results suggested that the ventro-oral nuclei of the thalamus can be as efficient in reducing tremor as the VIM (Shah et al. 2015).

In the previous study, the location of the electrode contact's center was considered with respect to the anatomy. However, the effect of stimulation spreads farther in the region surrounding the electrode depending on the brain tissue. Various researchers have used computational models based on finite-element modelling (FEM) to simulate the distribution of electrical entities in the brain tissue for DBS (McIntyre et al. 2004; Hemm et al. 2005; Aström et al. 2006). Recent advancements in such techniques have made them patient-specific (Aström et al. 2009; Chaturvedi et al. 2010; Wårdell et al. 2015) where the patient's MR images are used to determine the tissue surrounding the electrode (white matter, gray matter or cerebro-spinal fluid) and assign electrical properties accordingly. We have developed a technique to simulate the electric field (EF) distribution during intraoperative stimulation tests using patient-specific computational models (Hemm et al. 2016). We applied this technique to 5 ET patients to simulate the EF distribution for multiple current amplitudes per stimulation test position. The aim of this previous study was to collectively analyze the data to study the role of different anatomical structures in reducing tremor. The resultant 272 simulations were classified based on the improvement in tremor (low or high) as measured by the accelerometer for the corresponding stimulation current amplitude. The data of the two groups was analyzed to identify 1) the difference in appearance of the

different anatomical structures covered by the EF and 2) the relative volume covered of a particular structure.

In the current study, we propose a methodology allowing the individual analysis of the high amount of data per patient. The aim is to combine electric field simulations with tremor improvement quantified by accelerometry and then visually present in form of so-called improvement maps superimposed to the patient specific anatomy to assist in surgical decision making i.e. choosing the optimal implant position for the chronic DBS lead. This improvement map approach has been applied post-operatively to 9 implantations from Clermont-Ferrand university hospital.

## **2 Method**

### **2.1 Surgical procedure**

The routine surgical procedure at the University Hospital in Clermont-Ferrand begins with a meticulous pre-surgical planning. A brief description of the procedure is given here while a complete description can be found elsewhere (Vassal et al. 2012). Numerous radiographic images including a stereotactic CT (0.59 mm x 0.59 mm x 1.25mm), stereotactic T1 MRI (0.63 mm x 0.63mm x 1.30mm) and white-matter attenuation inversion recovery (WAIR, 0.54 mm x 0,53 mm x 2.0 mm) sequence are acquired (Sonata 1.5T, Siemens, Germany) to be used for the planning. Based on the spontaneous contrast observed on the WAIR sequence and an in-house developed high field (4.7 Tesla) brain atlas, the neurosurgeon carefully outlines various thalamic nuclei and basal ganglia structures using a commercial planning software iPlan stereotaxy 3.0 (Brainlab). After delineating the desired target structure viz. the VIM for ET patients, two parallel trajectories are planned from an entry point in the skull. The trajectories usually follow the path from the superior-anterior-lateral thalamus (ventro-oral nucleus, VO) towards the inferior-posterior-medial direction passing the VIM with a target at its inferior border. Various test stimulation positions (between 5 to 10) are planned along each trajectory spanning the whole region of interest.

During surgery, the stereotactic co-ordinates of the planned trajectories obtained from the planning software are set up on the Leksell Stereotactic System (Elekta, Stockholm, Sweden) using the repositioning kit. After drilling the burr hole at the desired entry point, two intraoperative exploratory electrodes are inserted along the previously identified trajectories. Micro-electrode recording (MER) is performed at all the planned test-stimulation positions along both the trajectories simultaneously to confirm the location of the trajectories in relation to the surrounding anatomical structures (Coste et al. 2009). Stimulation tests are then administered at these positions, with stimulation current varied in most cases from 0 to 3 mA in steps of 0.2 mA. The highest visually observed improvement in tremor is noted along with the corresponding stimulation current amplitude for every test position. The amplitudes resulting in adverse effects, if any, are also noted.

After completion of stimulation tests for one brain hemisphere, the surgical team compares the results (current amplitudes improving tremor and/or inducing adverse effect) and mentally visualizes the information in relation to the patient's anatomy. The DBS lead (Medtronic 3389, Medtronic, Minneapolis, USA) is implanted at a position fulfilling the following conditions:

- a) Low therapeutic stimulation current amplitude
- b) High adverse effect inducing stimulation current amplitude
- c) Neighboring test positions having relatively low therapeutic stimulation current amplitudes
- d) Anatomical position

## 2.2 Accelerometric tremor evaluation

The changes in tremor during surgery were evaluated applying a previously published method using an accelerometer (Shah et al. 2016b). In short, a 3-axis acceleration sensor evaluation board (STEVAL-MKI022V1, ST Micro, Geneva, Switzerland) was attached to the patient's wrist with a Velcro strap and data were recorded with a sampling rate of 400 Hz and a range of 8 g using a computer application (LemurDBS) developed in Java (Oracle Corporation, California, USA). All data were stored for offline analysis. Data recording was synchronized with the MicroGuide Pro (Alpha Omega Eng., Nazareth, Israel) electrophysiology system that was used for MER and stimulation tests. For every stimulation test, changes in tremor were determined compared to the data recorded immediately before the start of the test. By using such a protocol, changes in tremor due to brain tissue damage caused by introducing the electrode would not influence the quantitative assessment.

Accelerometer data were analysed post-operatively using Matlab. The magnitude of acceleration was calculated and filtered to extract the tremor signal. This data was then divided into two: data recorded before the start of the stimulation was called "baseline" and data recorded during stimulation was called "stimulation data". Outcome measures (standard deviation, signal energy, and amplitude of dominant frequency) which have been shown to correlate with clinical changes (Shah et al. 2016b) were extracted from both the data sets in a windowed manner (time length of 2 seconds). The outcome measures for the stimulation data were normalized to the corresponding outcome measures of the baseline. The quantitative improvement in tremor was expressed by the mean of the three normalized outcome measures for each window and the average improvement per stimulation current amplitude was determined.

## 2.3 Spatial distribution of stimulation

The effects of electrical stimulation in the brain are not confined to the location of the electrode, but spread farther into the brain in all directions depending on the stimulation parameters and the brain tissue surrounding the contact. To understand these spatial effects of the stimulation, the distribution of the EF around the electrodes within the brain was simulated using an established patient-specific FEM-modeling technique for DBS leads (Aström et al. 2009; Aström et al. 2010; Wårdell et al. 2015) which has been adapted to the conditions and set-up of intraoperative stimulation tests. Details about the simulation method can be found in the previous publication (Hemm et al. 2016).

### 2.3.1 Microelectrode model

A model of the microelectrode (Neuroprobe, Alpha Omega Engineering) used in Clermont-Ferrand University Hospital was generated with its specific dimensions. As electrophysiological evaluations were performed through two parallel electrodes, a second model of the MER-electrode was positioned at a distance of 2 mm. The end of the grounded guide tubes were fixed at 12 mm above the target point, i.e. the a priori optimal anatomic spot. In consequence, the distance ( $d$ ) between the guide tube and the middle of the stimulating contact decreased or increased respectively when the simulation site was before or after the target ( $12 \text{ mm} \pm d$ ) along the trajectory.

### 2.3.2 Patient specific brain model

The patient specific simulation of EF distribution necessitates a patient-specific brain model. For this purpose, the T1 MRI was used after registration and resampling to the stereotactic preoperative CT having higher resolution. This data was imported into the in-house developed software (Matlab) for creating brain tissue models. The T1 images were filtered and enhanced in the region of interest to

segment it into cerebrospinal fluid (CSF), gray matter and white matter (Alonso 2016). The segmented image voxels were assigned electrical conductivity values ( $\sigma$ ) based on published literature (Gabriel et al. 1996): CSF - 2.0 Siemens/meter (S/m), blood - 0.7 S/m, gray matter 0.123 S/m and white matter 0.075 S/m. Conductivity values for voxels between the thresholds were interpolated. Simulation time was considerably reduced by selecting a cuboid region of interest of approximately 100 mm in each dimension encompassing the thalamus.

### 2.3.3 Patient specific stimulation data

For each patient, the planned trajectory to reach the target structure and the stimulation test positions along the trajectory were different. These data were extracted from the planning software (iPlan stereotaxy) and converted to the co-ordinate system of the brain model using Matlab. The target co-ordinates and the trajectory angles were used to calculate and position the stimulating contact and the parallel electrode in the brain model for the different stimulation test positions. In addition, to simulate the EF, the stimulation current amplitude has to be provided as input. Although it would be possible to simulate all the stimulation current amplitudes (15) per position, the resultant data set would have redundant information and would be tedious to analyze. Therefore, for each stimulation test position, we decided to simulate the EF distribution for the stimulation current amplitudes with 1) the first appearance of highest change in tremor (between 0.2 mA to 3 mA) and 2) the first adverse effects were observed (between 1 mA to 5 mA).

### 2.3.4 Electric field simulations

The spatial distribution of EF was simulated by using the equation of continuity for steady state current:

$$\nabla \cdot \vec{J} = \nabla \cdot (\sigma \nabla V) = 0$$

where  $J$  is the current density,  $\sigma$  is a matrix containing the electrical conductivity values for the region of interest (thalamus and its neighborhood) and  $V$  the electric potential. After placing the electrodes at a desired stimulation test position, the active contact was set to the stimulation current amplitude described in 2.3.3 and the guide tube was set to ground, resulting in a monopolar configuration. The inactive contact of the parallel lead was set to floating potential and the exterior boundaries of the tissue model were set to electrical insulation. The in-built mesh generator (Comsol Multiphysics) defined the mesh density (approximately 250,000 tetrahedral elements) where the smallest elements (0.03 mm) were located close to the stimulating contacts in order to capture the strong EF gradients. Previous research has shown that the EF isolevel of 0.2 V/mm represents the neuronal activation for the thalamic region. Therefore the Cartesian co-ordinates of the surface of EF volume for 0.2 V/mm were exported for further analysis.

### 2.3.5 Surgical planning data

In addition to the planned trajectory and target information, the manually outlined anatomical structures were extracted from the iPlan software via a specifically designed interface based on VVLink and VTK (VTK 5.2.0, Kitware Inc. New York, USA). In order to reduce error sources, only the CT data set was used as reference for the outlined anatomical structures and the target coordinates. In consequence, the structures initially outlined on the WAIR weighted sequence were transferred to the stereotactic CT data set providing a higher resolution and minimal distortion of the stereotactic reference system. The structures were exported in form of slices parallel to the CT data set in order to remain in the same image coordinate reference system. Using Matlab scripts the co-ordinates of each of the anatomical structure were converted from slices to tabular list and saved as csv files.

## 2.4 Clinical application

A clinical study was undertaken at the University Hospital in Clermont-Ferrand, France (Ref: 2011-A00774-37/AU905, Comité de Protection des Personnes Sud-Est 6, Clermont-Ferrand, France) and 5 patients who were treated for ET using DBS were included for the current work (Table 1). The number of stimulation tests varied from patient to patient based on the size of the region of interest and the occurrence of side effects during the stimulation tests. Three types of adverse effects were observed for different patients viz. pyramidal effects, paresthesia and dysarthria. Accelerometer data were recorded during the surgery following the above presented protocol to evaluate the changes in tremor induced

**Table 1: Details of the surgeries for the patients that participated in the clinical study.**

Pat. No	Brain Side	AC-PC length (mm)	Target Coordinates with respect to AC (mm)			Trajectory	No. of test positions	No. of electric field simulations	Side Effects
			Lat	Post	Inf				
1	Rt	30.37	18.24	13.22	3.04	Central	7	7	
						Posterior	8	8	
2	Lt	24.17	15.24	19.86	3.69	Central	5	8	Paresthesia Pyramidal
						Posterior	5	7	
2	Rt	24.17	15.2	16.33	2.06	Central	7	8	Paresthesia
						Posterior	7	8	
3	Lt	26.23	16.04	16.11	2.52	Central	8	8	
						Posterior	8	8	
3	Rt	26.23	13.47	15.52	2.4	Central	8	8	Paresthesia
						Posterior	8	10	
4	Lt	26.99	12.77	17.4	2.42	Central	9	9	
						Posterior	9	9	
4	Rt	26.99	15.72	18.59	1.1	Central	5	9	Paresthesia Pyramidal
						Posterior	5	9	
5	Lt	27.98	15.75	19.04	4.23	Central	8	8	Dysarthria
						Posterior	8	9	
5	Rt	27.98	16.23	16.71	3.23	Central	8	8	Dysarthria
						Posterior	8	9	

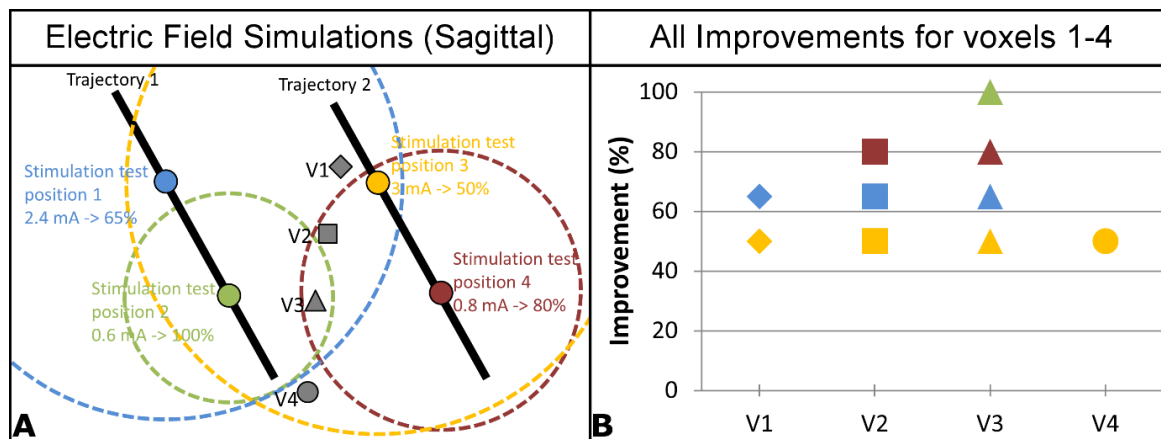


Figure 1: Diagrammatic representation of electric field simulations for the intraoperative stimulation tests in one hemisphere. Left: Sagittal view of the two electrodes with two stimulation test positions each. Each circle represents the electric field around one stimulation position generated by a specific current amplitude (mA) and inducing a specific clinical improvement (%). Four different voxels V1 to V4 have been picked between the two electrodes. Right: Graphical representation of the improvements induced by the different electric fields at the four voxels V1 to V4.

by varying stimulation current amplitudes. The procedure described above was applied to generate improvement maps for 9 brain hemispheres. For Patient 1, data acquired during the implantation of the left hemisphere were excluded from the analysis due to lack of synchronization with the electrophysiological data (recording software error).

## 2.5 Improvement Maps

### 2.5.1 Concept

The setup for EF simulations for intraoperative stimulation tests resulted in a large number of simulations per hemisphere. For one hemisphere, on average, there were 2 trajectories with 7 different positions (Table 1) simulated with their respective current. Figure 1A is a diagrammatic representation of EF simulations for intraoperative stimulation tests at different positions along the two trajectories. Each EF corresponds to one stimulation amplitude, each of them inducing a specific clinical improvement. The EFs overlap and many voxels can be encompassed in more than one EF simulation. Figure 1B illustrates with four examples how different improvements can be associated to a voxel in the stimulation test region. To summarize the data and to facilitate analysis, only one improvement value was directly linked to one voxel to create an "Improvement Map".

### 2.5.2 Creation

From the EF simulations, the Improvement Map is generated using Matlab scripts as presented in Figure 2. All the EF simulation files from COMSOL (refer section 2.3.4) are imported in Matlab and the extent of the stimulation test region in a given hemisphere is calculated (Figure 2, Step 1). A 3D mesh-grid with a resolution 4 times the resolution of the CT images is created (Figure 2, Step 2). Using the Delaunay Triangulation (Boris Delaunay 1934) and location-query function, the position of each EF in this mesh-grid is identified and a mask is created. The mask is multiplied with the improvement associated with the EF i.e. the mesh voxels of the EF hold the improvement value and are zero otherwise. All such

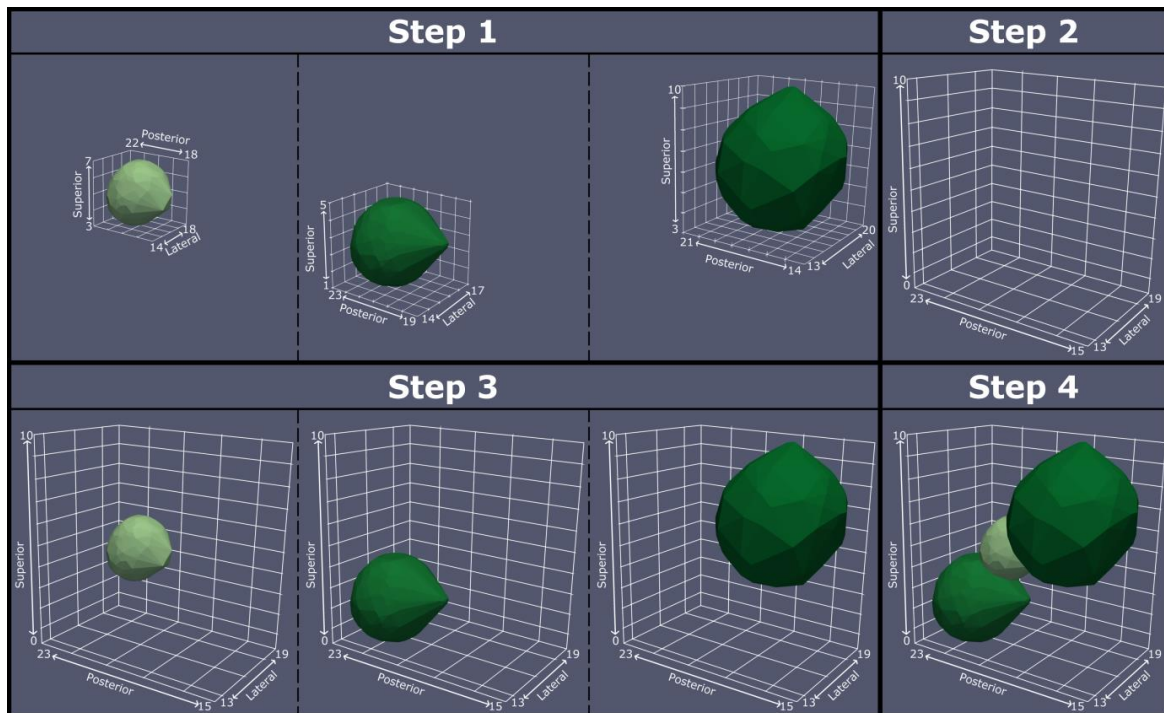


Figure 2: A diagrammatic representation of the steps to generate the Improvement Maps. The individual EF simulations are imported and the size of the stimulation test region is calculated (Step 1). A mesh grid of this size with 4 times the resolution of the MR data is created (Step 2). The location of each EF simulation in this mesh grid is determined (Step 3). Each voxel in the improvement map is then assigned the improvement value based on the chosen mathematical function (Step 4).

improvement masks have the same dimensions and are therefore appended together to create a 4D matrix (Figure 2, Step 3). By using a many to one function (e.g. minimum, mean, maximum etc.) on the 4<sup>th</sup> dimension, a 3D matrix is obtained having the same dimensions as the mesh-grid, and each voxel holding only one improvement out of all the EF simulations that encompassed it (Figure 2, Step 4). After identifying the different levels of improvement in this 3D matrix and using the location-query function, the X, Y and Z co-ordinates of each improvement level are obtained and exported. For the EF of adverse effect thresholds, their co-ordinates in the mesh-grid are identified and exported as csv files without any additional processing.

### 2.5.3 Visualization

For visual analysis of the improvement map, data were imported in Paraview (Kitware) using Python (Python) scripts in the following order: 1) The T1 MR and the WAIR MR image data sets were imported and cropped to the region of interest. 2) The csv files containing the co-ordinates of the thalamic nuclei (see section 2.3.5) were imported one by one, and visualized as surface extracts of Delaunay triangulation of these co-ordinates. 3) The csv files containing the improvement map were imported and visualized as Delaunay triangulations. 4) The simulations for adverse effect thresholds were imported and visualized as surface extracts of Delaunay triangulations to depict them as boundary beyond which adverse effects were observed. The data were first visualized in the 3D view and then loaded into the orthographic slice view using a custom macro script.

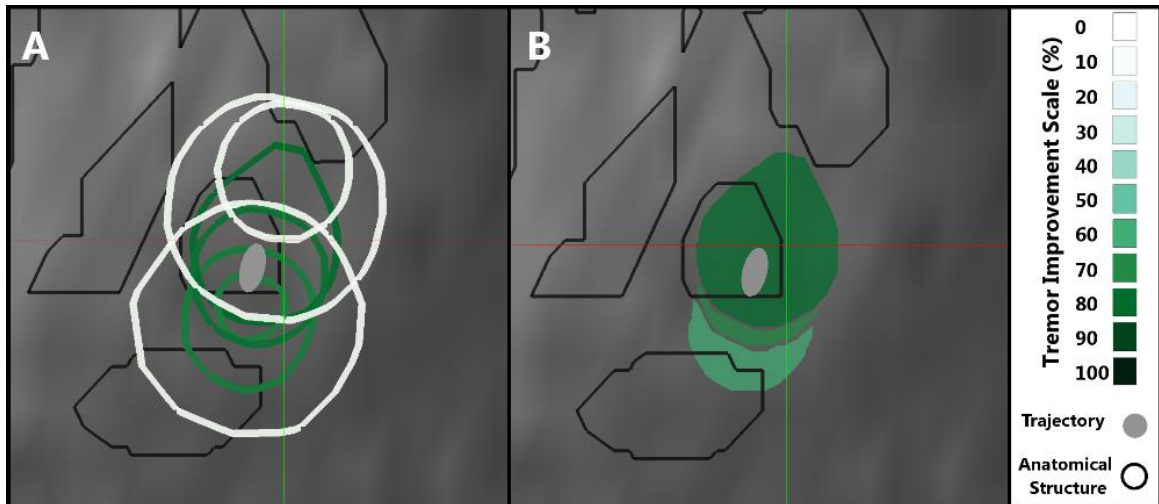


Figure 3: A) Sagittal view of 8 electric field simulations for left hemisphere of patient 5. The color of the border represents the improvement in tremor. It underlines the need to summarize the information using improvement maps. B) The maximum improvement map of the EFs seen in A. The shade of green corresponds to the improvement associated with the region based on the scale in the legend. The black outline represents different thalamic nuclei and the grey ovals represent the trajectory of the electrode.

#### 2.5.4 Maximum Improvement Maps

The improvement maps represent a summary of many EF simulations based on the mathematical function used to associate one improvement value to a voxel. In order to choose this function, we visualized EF simulations of the patients using Paraview. For some instances, the EF simulations of small stimulation amplitudes resulting in high improvement were encompassed by simulations of larger stimulation amplitudes of neighboring positions but with lower improvement (Figure 3A). Considering that the aim of the intraoperative tests is to identify regions, which are more effective with lowest stimulation current amplitude, we decided to assign the maximum improvement value to each voxel to create a "maximum improvement map". Figure 4A shows the maximum improvement map of the diagrammatic representation in Figure 1A with the maximum improvements for the selected voxels in

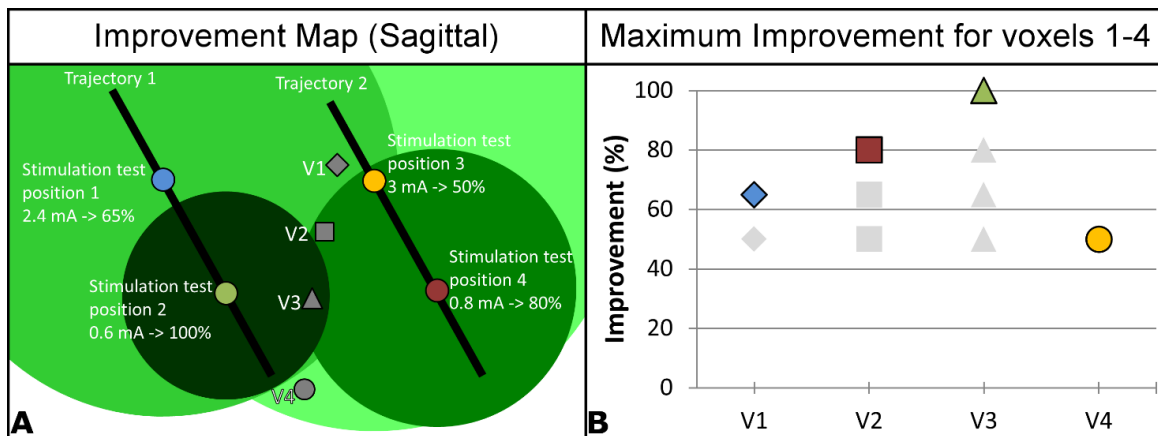


Figure 4: Diagrammatic representation of maximum improvement map of the representation in figure 1. Left: Sagittal view of the maximum improvement map. The shade of green represents the level of improvement measured using the accelerometer (darker shade corresponds to higher improvement). Four different voxels V1 to V4 have been picked between the two electrodes. Right: Graphical representation of maximum improvement associated with the four voxels V1 to V4.

Figure 4B. The maximum improvement map for the EFs shown in Figure 3A is shown in Figure 3B where the smallest region with the highest improvement is clearly identifiable.

## 2.6 Data Analysis

The improvement maps were analyzed individually by simultaneously moving the axial, coronal and sagittal sections across all the visualized data in the orthographic slice view. For each map, the location of the region showing the highest improvement was identified and carefully studied with respect to the outlined anatomical structures and the adverse effect threshold outline. The optimal depth along the trajectory to implant the permanent lead was determined using the criteria defined earlier (Section 2.1) and it was listed for all implantations. In addition, in each map, the interaction of various anatomical structures with the induced clinical effects were meticulously examined. In the highest improvement regions, structures partially or completely covered were identified while for adverse effects, structures externally touching the adverse effect threshold outlines and external to any improvement region were noted. Finally, recurring structures were studied for their interaction with the highest improvement region and the adverse effect threshold outline across all the implantations.

## 3 Results

Through the clinical study in University Hospital in Clermont-Ferrand, accelerometer data was recorded for a total of 129 test stimulation positions from the 5 DBS surgeries. Using the FEM based technique, 148 simulations (129 therapeutic + 19 adverse effects) were performed based on these stimulation tests and summarized in 9 improvement maps. These maps vary from patient to patient depending on the planned trajectory and the test stimulation positions along it. The analysis of one improvement map is provided in the following paragraph. The remaining 8 improvement maps and their analysis is provided in a supplementary file. The analysis of the variations in different maps is described in the final paragraph of this section.

Figure 5 shows a typical improvement map of the right hemisphere of patient 5. The inferolateral part of the thalamus was explored during the stimulation tests (Fig 5A to 5C) with the planned target at the inferior border of the VIM (Fig 5D to 5F). The highest improvement region (95%) can be seen further along the trajectory from +1 mm to +3 mm in front of the target (Fig 5E, 5F and 5J to 5L) shaped like a drop with its peak in the posterior direction. The region starts just below the VIM, touches the medial edge of the ventrocaudal lateral nucleus (VCL), lateral edge of the Center median nucleus (LaCM) and penetrates the supero-lateral part of the PLR. On the other hand, the spherical adverse effect (dysarthria) outline (red) interacts with VO, VCL, VCM, LaCM and PLR (Fig 5D to 5K) outside of the different improvement regions. It does not interact with the highest improvement region but is the closest near the inferior, anterior medial edge (Fig 5K and 5L). Based on this improvement map, the position +2 (Fig 5K) on the central trajectory would be optimal to implant the lead for chronic stimulation.

The procedure described above was applied to all the 9 implantations and the results were summarized. Table 2 lists the optimal position along the trajectory for all improvement maps. The interactions between the anatomical structures and the highest improvement region and the adverse effect threshold outline respectively are listed in Table 3.

In the 9 improvement maps, seven anatomical structures were identified that interacted with the highest improvement region: INL, VO, VIM, PLR, VCL, VCM and LaCM. The VIM, the planned target for all the patients, occurs the most frequently. It appears in 8 out of the 9 maps, with a complete coverage in 4 cases. In 6 of the 9 improvement maps, the highest improvement region encompassed

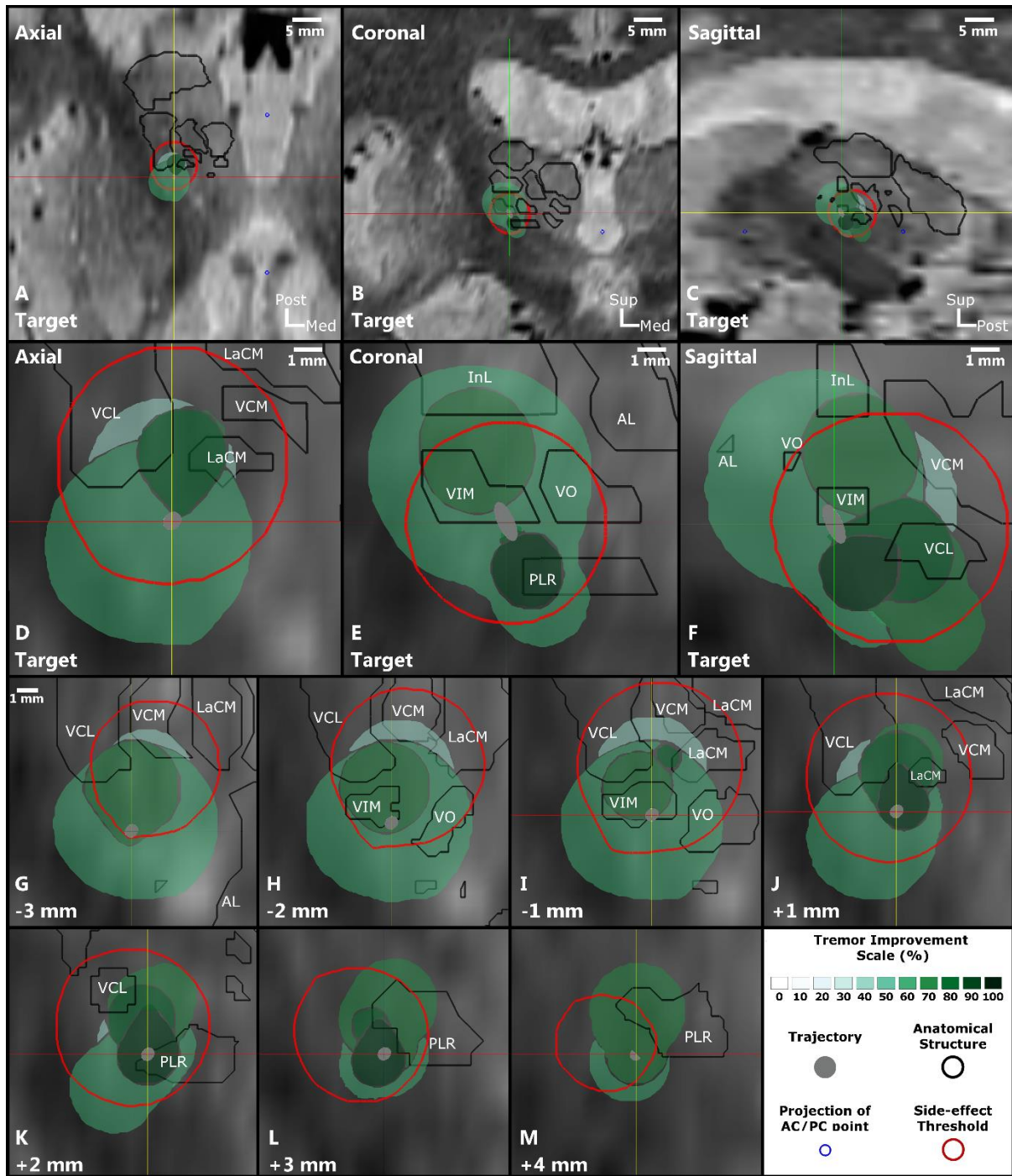


Figure 5: Images of the improvement map for the right hemisphere of patient 5. Parts A to C show the overview of the explored region in relation to the patient's brain in form of orthogonal slices at the target position. Parts D to F show a close-up (magnification of 5) of the improvement maps at the same position. Parts G to M are axial slices at the different stimulation test positions from -3 to + 4 mm. The bottom right part of the figure shows the legend containing the improvement scale in shades of green, representation of the trajectory in gray, anatomical structures in black, side-effect outline in red and projection of AC/PC point in blue. The names of the relevant thalamic nuclei are abbreviated based on the nomenclature in (Lemaire et al. 2010) as follows: VIM: Ventrointermediate VCL: ventrocaudal lateral, VCM: ventrocaudal medial, LaCM : laminar caudal medial, VO: ventro oral, PLR: prelemniscal radiations.

**Table 2: The choice of depth along the trajectory where the permanent DBS lead should be implanted based on improvement maps and their coordinates with respect to the AC.**

Patient Number	Hemisphere	Optimum implantation depth of permanent lead based on improvement maps
1	Right	+3mm
2	Left	-1mm
2	Right	+1mm
3	Left	-+1mm
3	Right	+2mm
4	Left	+4mm
4	Right	+1mm
5	Left	+2mm
5	Right	+2mm

the area inferior and posterior to the VIM (posterior sub-thalamic area, PSA) and included at least partially the PLR. This area was not explored in the other three maps as adverse effects were observed in this position at low stimulation current amplitudes. In addition the anterolateral part of the LaCM was partially enclosed in 6 maps, lateral parts of the ventrocaudal medial nucleus (VCM) in 5 maps, the VO was encompassed in 4 maps (2 partially, 2 fully), the inferomedial part of the VCL in 4 maps, and the inferior part of intermedialateral nucleus (InL) was partially included in 3 maps.

Three different types of adverse effects were observed during 6 out of the 9 implantations as described in Table 3: dysarthria, paresthesia and pyramidal effects. Dysarthria was observed in both implantations of patient 5 and the outline in the two maps (Figure 5 and Figure S8) is posterior and slightly lateral compared to the different therapeutic regions. Adverse effects induced due to stimulation of pyramidal tract were also observed during 2 implantations (Patient 2 Left and Patient 4 Right). The improvement maps of these implantations showed that the adverse effect outlines were superior and lateral to the thalamus (Figures S2 and S7). Paresthesia was also observed in 4 implantations (Patient 2 Left and Right, Patient 3 Right and Patient 4 Right). The adverse effect outline for these improvement maps (Figures S2, S3, S5 and S7) was posterior to the VIM and penetrated the VCM, VCL and LaCM nuclei.

The interaction of recurring structures and adverse effects across multiple implantations can be seen in Table 3. In case of paresthesia and dysarthria, VO and PLR are touching the adverse effect threshold outline for some implantations while, in others they are completely enclosed by the highest improvement region without inducing any adverse effects. , .

## 4 Discussion

This paper describes a new digital approach to assist the clinicians in identifying the optimal region to implant the chronic DBS lead after intraoperative stimulation tests: a task currently performed by evaluating handwritten notes taken during surgery. The approach combines the outline of the relevant

**Table 3: Table summarizing the results of the different improvement maps. The interaction of 7 structures with the highest improvement region and the adverse effect threshold outline for each implantation is listed. The improvement maps used to generate this table can be found in the supplementary material. ● indicates full coverage, ◐ indicates partial coverage and ○ indicates no coverage. Pyr is Pyramidal effect, Par is paresthesia and Dys is Dysarthria.**

Patient/ Hemisphere	Max Improvement/ Adverse Effect*	Structures						
		INL	VO	VIM	PLR	VCL	VCM	LaCM
1/R	90%	○	●	●	◐	○	○	◐
	Adverse Effect							
2/L	85%	◐	◐	◐	○	◐	◐	◐
	Adverse Effect	Pyr	Pyr				Par	Pyr
2/R	85%	○	○	●	◐	◐	◐	◐
	Adverse Effect					Par		
3/L	90%	◐	◐	●	○	◐	◐	◐
	Adverse Effect							
3/R	85%	◐	●	●	○	○	○	○
	Adverse Effect				Par		Par	Par
4/L	100%	○	○	◐	●	○	◐	◐
	Adverse Effect							
4/R	95%	○	○	◐	◐	◐	◐	○
	Adverse Effect		Par			Par	Par	
5/L	95%	○	○	◐	◐	◐	○	◐
	Adverse Effect				Dys	Dys		Dys
5/R	95%	○	○	○	◐	○	○	○
	Adverse Effect		Dys		Dys	Dys	Dys	Dys

\* For the interaction with adverse effect threshold outline, only the anatomical structures which were penetrated by different adverse-effect threshold outlines *outside of the therapeutic improvement regions* are considered.

anatomical structures with a novel technique to quantitatively evaluate the therapeutic effects and a patient-specific method to estimate the spatial effects of stimulation. This combination creates improvement maps, i.e. 3D visualization of the intraoperative stimulation test results with therapeutic areas, adverse effect areas and anatomical structures in the stimulation test region. The 9 improvement maps generated after applying this approach to 5 ET patients who underwent DBS surgery demonstrate the potential to support and facilitate the surgical team in determining the optimal implant position of the DBS lead and to better understand the mechanism(s) of action of DBS.

## 4.1 Related work

To the best of our knowledge, commercial software solutions for DBS do not offer visualization capabilities for intraoperative stimulation tests today. Some research based software systems which are capable of visualizing DBS data have been proposed. D'Albis et al. (2015) developed PyDBS to automate tasks like image registration, image segmentation and visualization. They designed it to assist clinicians during pre-operative planning and post-operative electrode validation, but not during intraoperative electrode placement. Guo et al. (2006) used non-linear image registration to visualize digitized brain atlas, segmented deep brain nuclei and final surgical targets as well as electrophysiological information from their own database on the patient images. Although their software could be used during the surgery, it did not have provisions to visualize therapeutic or adverse effects of stimulation at a given position. The group of D'Haese (2012) developed a system consisting of a central repository (Cranial Vault), modules to interact with the repository (CRanial VAult Explorer, CRAVE) and algorithms to automate certain tasks in the DBS treatment (pre-operative, intraoperative and postoperative phases). Their system is able to visualize therapeutic and adverse effects of stimulation, which the clinical team would manually enter during the surgery. However, the use of their intraoperative module during surgeries showed that the manual task of providing information to their system was stressful for the surgical team. In addition, none of the software described above estimates the spatial effect of stimulation. Miocinovic et al. (2009) proposed a software called Cicerone which visualizes patient images with brain atlas, MER, DBS leads and the volume of tissue activated (VTA) in 3 dimensions and can be used intraoperatively. However, the estimation of VTA is not patient specific and is based only on the DBS lead. In contrast to the existing literature, the approach described in this study was specifically designed for intraoperative use. It benefits from patient-specific EF simulations to estimate the spatial effects of stimulation as well as quantitative evaluations of induced therapeutic effects by using accelerometry.

## 4.2 Improvement Map Types

In the present study, we describe a specific case of improvement maps where each voxel in the stimulation test region is assigned the maximum value of improvement as measured by the quantitative technique. In general, however, the structure of the improvement maps, i.e. the different therapeutic regions and their location, is significantly affected by the choice of the improvement value assigned to a voxel. Theoretically, this choice can be made using computationally simple functions like mean, maximum, etc. or complex functions based on fuzzy logic, weighting function based on distance from trajectory, etc. However, the practical implications of this choice have to be considered. For this study, we aimed at identifying the optimal position to implant the permanent electrode. In consequence, it is necessary to identify the highest improvement region with the least amount of current (less battery consumption), justifying our choice of assigning the maximum improvement to each voxel. In addition to the choice of improvement value assigned to a voxel, the input stimulation current amplitude used for the EF simulations also affects the improvement maps. Both these choices depend heavily on the aim set forth before the start of data analysis.

## 4.3 Improving DBS targeting

The application of the improvement map approach to five patients showed how it could assist in choosing the depth for the permanent implantation of the DBS lead (Table 2). In addition, they also show the possibility of improving DBS targeting in general. The interactions of the seven structures presented in Table 3 with the therapeutic and adverse effect regions of the improvement map concur with the findings of other published research. The highest improvement regions in the different improvement maps are either in the inferior part of the VIM or in the PSA. The VIM is the gold standard target for

treatment of ET patients and results in optimal therapy for most patients (Blomstedt et al. 2007). Stimulation in the PSA has been shown to be effective for treating proximal tremor (Kitagawa et al. 2000; Murata et al. 2003) and ET (Plaha et al. 2004; Blomstedt et al. 2010) and some researchers argue that it is a better target compared to the VIM (Sandvik et al. 2012; Hamel et al. 2007). With regards to the adverse effects, those associated with the stimulation of the pyramidal tract were observed for two implantations where the threshold outline in the improvement maps was very close to the internal capsula, supero-lateral to the thalamus. Dowsey-Limousin (2002) reported similar effects during post-operative programming of the implanted pulse generator. The dysarthria threshold outline for both implantations of patient 5 suggests that the stimulation of VCL, VCM and LaCM may be responsible for it. Similar results were observed by Reker group (2016) using post-operative stimulation tests. In contrast to the two adverse effects discussed above, paresthesia which is commonly observed in VIM DBS procedures, has been associated with different structures by different studies (Tamma et al. 2002: Subthalamic Nucleus, Krack et al. 2002; Murata et al. 2003; Keane et al. 2012: Medial lemniscus, Fytagoridis et al. 2013: Posterior sub-thalamic area, Dembek et al. 2017: Zona Incerta). As described above (Figure 5) and previously (Shah et al. 2018), the adverse effect outline can be often found in the PSA region suggesting that stimulation there might cause paresthesia, even if they do not indicate which anatomical structure or fibre tract may be responsible for them. When looking at table 3, VCL, VCM and LaCM could be candidates as well. Although VO and PLR are also listed in Table 3 for paresthesia as well as dysarthria effects, they are probably not responsible for these effects as in other implantations they are completely covered by the therapeutic regions without any adverse effect appearance. The similarities discussed here suggest that with a significantly large data set, the improvement maps could be used to improve DBS targeting and possibly support in studying the mechanisms of actions of DBS.

#### **4.4 Transferability**

In its current form described in this study, the procedure of creating the improvement maps is very specific to the type of data available from the University Hospital in Clermont-Ferrand. In general, however, the technique is very adaptable to the type of data available. In absence of pre-operative anatomical outline, the patient images can be co-registered to digitized atlases using open-source software like 3D Slicer (Fedorov et al. 2012) and segmented to outline the relevant anatomical structures. Regarding the spatial estimation of stimulation, the EF simulation procedure can be adapted to the type of MR data acquired and the type of exploration electrode used in a given surgical center. Concerning the use of accelerometers to evaluate tremor, our previous study has shown its advantages over the existing visual method and the relative ease with which it can be added to the surgical procedure without major alterations or loss of patient comfort. For DBS procedures of non-tremulous patients, e.g. Parkinson's disease patients with rigidity, some quantitative tools to evaluate rigidity exist, including ours (Shah et al. 2016a). These methods, however are in experimental stage. These situations were considered during the design phase of the improvement map method. Therefore, for making the improvement maps, the improvement in symptoms estimated using routine clinical scales and subjective methods can also be used. To do so, the surgical team has to predetermine the levels of improvement they want to visualize and to note the stimulation parameters that result in these improvements.

#### **4.5 Limitations**

Closer examination of the improvement maps reveal that the anatomical structures appear to have sharp edges and corners. Such edges and corners are not found in the original outline in the planning software, but are a resultant of the procedure used to export and reconstruct them. One possible workaround for this limitation would be to export the anatomical structures in a 3D file format, but our version of the planning software did not have any such provision. In addition, the reconstruction of this outline of anatomical structures is also limited by the voxel dimension, which can only be improved by using

imaging systems with better resolution. Apart from this, any caveats associated with the quantitative tremor evaluation and EF simulation techniques also affect the improvement maps. Our previous research has shown that the quantitative tremor evaluation depends on proper acquisition of baseline data before every stimulation test (Shah et al. 2016b). In absence of sufficient baseline recording, the baseline data of a previous stimulation test position can be used. With regards to the EF simulations, to be able to use the images with the highest resolution, image fusion was used in a manner that limited the errors associated with transformation and fusion (Zrinzo 2012). Further, we do not consider the effects of brain shift on the position of the electrode based on the observation that the largest shift occurs when the exploration electrode is replaced by the chronic DBS lead. For exhaustive description of the limitations of each method, the readers are advised to refer to the respective literature of each method (Hemm et al. 2016; Lemaire et al. 2010; Shah et al. 2016b).

#### **4.6 Future Work**

The improvement maps presented here were generated and analyzed post-operatively. Steps to generate the improvement maps in real-time have been identified. The time between pre-surgical tasks (image acquisition and surgical planning) and the actual surgery needs to be utilized for all preparatory steps (extract outline of anatomy, generate the patient-specific brain model, etc.) Additional provisions have to be made to establish communication between the accelerometer recording software and the simulation software to simulate EF in real-time. The algorithms that generates the improvement maps from the EF simulation files take a maximum of 5 minutes and can be executed once stimulation tests are completed during the surgery. Once these steps are realized, a larger clinical study will be conducted to confirm the advantages of improvement maps highlighted in the current paper and to make them available during surgical decision making after the intraoperative stimulation tests.

A likely long-term application of improvement maps would be to facilitate the use of directional DBS leads to steer the effects of stimulation in a certain direction. Schüpbach et al. (2017) recently studied the challenges that directional stimulation would bring to DBS and indicated that patient-specific visualization techniques (like improvement maps) will be required to limit alterations to targeting and intraoperative standards. Besides the intraoperative application, improvement maps provide another tool to better the understanding of the mechanisms of action of DBS. By applying this technique to a large patient cohort, an "improvement atlas" can be built to study the areas responsible for high improvement as well as adverse effects. By comparing such information to known anatomy and physiology of the disease, we can learn more about the mechanisms by which DBS alleviates symptoms.

## **5 Conclusion**

This paper describes a new technique called improvement maps to summarize and visually analyze data from intraoperative stimulation tests for deep brain stimulation surgery. Data collected from 9 implantations were analyzed with the aim to identify the optimal site to implant the chronic DBS lead. Clinicians found the visualizations intuitive and easy to interpret and to identify the region resulting in highest improvement in tremor. For 7 of the 9 improvement maps, the highest improvement region was found to be inferior and posterior to the VIM in the posterior sub-thalamic area in agreement with the scientific consensus. This method has the potential to simplify the surgical team's task in identifying the ideal implant location of the chronic DBS lead and to facilitate and expedite the use of directional leads in DBS.

## 6 References

- Abosch, A., Timmermann, L., Bartley, S., Rietkerk, H. G., Whiting, D., Connolly, P. J., et al. (2013). An international survey of deep brain stimulation procedural steps. *Stereotactic and functional neurosurgery*, *91*, 1–11 (2013). doi:10.1159/000343207
- Aström, M., Johansson, J. D., Hariz, M. I., Eriksson, O., & Wårdell, K. (2006). The effect of cystic cavities on deep brain stimulation in the basal ganglia: A simulation-based study. *Journal of Neural Engineering*, *3*, 132–138 (2006). doi:10.1088/1741-2560/3/2/007
- Aström, M., Zrinzo, L. U., Tisch, S., Tripoliti, E., Hariz, M. I., & Wårdell, K. (2009). Method for patient-specific finite element modeling and simulation of deep brain stimulation. *Medical & biological engineering & computing*, *47*, 21–28 (2009). doi:10.1007/s11517-008-0411-2
- Aström, M., Tripoliti, E., Hariz, M. I., Zrinzo, L. U., Martinez-Torres, I., Limousin, P., et al. (2010). Patient-specific model-based investigation of speech intelligibility and movement during deep brain stimulation. *Stereotactic and functional neurosurgery*, *88*, 224–233 (2010). doi:10.1159/000314357
- Blomstedt, P., Hariz, G.-M., Hariz, M. I., & Koskinen, L.-O. D. (2007). Thalamic deep brain stimulation in the treatment of essential tremor: A long-term follow-up. *British journal of neurosurgery*, *21*, 504–509 (2007). doi:10.1080/02688690701552278
- Blomstedt, P., Sandvik, U., & Tisch, S. (2010). Deep brain stimulation in the posterior subthalamic area in the treatment of essential tremor. *Movement disorders : official journal of the Movement Disorder Society*, *25*, 1350–1356 (2010). doi:10.1002/mds.22758
- Boris Delaunay. (1934). Sur la sphère vide: A la mémoire de Georges Voronoï. *Bulletin de l'Académie des Sciences de l'URSS, Classe des sciences mathématiques et naturelles.*, *6*, 793–800.
- Chaturvedi, A., Butson, C. R., Lempka, S. F., Cooper, S. E., & McIntyre, C. C. (2010). Patient-specific models of deep brain stimulation: Influence of field model complexity on neural activation predictions. *Brain stimulation*, *3*, 65–67 (2010). doi:10.1016/j.brs.2010.01.003
- Coste, J., Ouchchane, L., Sarry, L., Derost, P., Durif, F., Gabrillargues, J., et al. (2009). New electrophysiological mapping combined with MRI in parkinsonian's subthalamic region. *The European journal of neuroscience*, *29*, 1627–1633 (2009). doi:10.1111/j.1460-9568.2009.06698.x
- D'Albis, T., Haegelen, C., Essert, C., Fernandez-Vidal, S., Lalys, F., & Jannin, P. (2015). PyDBS: an automated image processing workflow for deep brain stimulation surgery. *International journal of computer assisted radiology and surgery*, *10*, 117–128 (2015). doi:10.1007/s11548-014-1007-y
- Dembek, T. A., Barbe, M. T., Astrom, M., Hoevels, M., Visser-Vandewalle, V., Fink, G. R., et al. (2017). Probabilistic mapping of deep brain stimulation effects in essential tremor. *NeuroImage. Clinical*, *13*, 164–173 (2017). doi:10.1016/j.nicl.2016.11.019
- D'Haese, P.-F., Pallavaram, S., Li, R., Remple, M. S., Kao, C., Neimat, J. S., et al. (2012). CranialVault and its CRAVE tools: a clinical computer assistance system for deep brain stimulation (DBS) therapy. *Medical image analysis*, *16*, 744–753 (2012). doi:10.1016/j.media.2010.07.009
- Dowsey-Limousin, P. (2002). Postoperative management of Vim DBS for tremor. *Movement disorders : official journal of the Movement Disorder Society*, *17 Suppl 3*, S208-11 (2002). doi:10.1002/mds.10165
- Fedorov, A., Beichel, R., Kalpathy-Cramer, J., Finet, J., Fillion-Robin, J.-C., Pujol, S., et al. (2012). 3D Slicer as an image computing platform for the Quantitative Imaging Network. *Magnetic resonance imaging*, *30*, 1323–1341 (2012). doi:10.1016/j.mri.2012.05.001
- Fytagoridis, A., Astrom, M., Wardell, K., & Blomstedt, P. (2013). Stimulation-induced side effects in the posterior subthalamic area: distribution, characteristics and visualization. *Clinical neurology and neurosurgery*, *115*, 65–71 (2013). doi:10.1016/j.clineuro.2012.04.015
- Gabriel, C., Gabriel, S., & Corthout, E. (1996). The dielectric properties of biological tissues: I. Literature survey. *Physics in Medicine and Biology*, *41*, 2231–2249 (1996). doi:10.1088/0031-9155/41/11/001
- Griffiths, R. I., Kotschet, K., Arfon, S., Xu, Z. M., Johnson, W., Drago, J., et al. (2012). Automated assessment of bradykinesia and dyskinesia in Parkinson's disease. *Journal of Parkinson's disease*, *2*, 47–55 (2012). doi:10.3233/JPD-2012-11071
- Guo, T., Finnis, K. W., Parrent, A. G., & Peters, T. M. (2006). Visualization and navigation system development and application for stereotactic deep-brain neurosurgeries. *Computer aided surgery : official journal of the International Society for Computer Aided Surgery*, *11*, 231–239 (2006). doi:10.3109/10929080600997232
- Hamel, W., Herzog, J., Kopper, F., Pinsker, M., Weinert, D., Müller, D., et al. (2007). Deep brain stimulation in the subthalamic area is more effective than nucleus ventralis intermedius stimulation for bilateral intention tremor. *Acta neurochirurgica*, *149*, 749–758 (2007). doi:10.1007/s00701-007-1230-1

- Hemm, S., & Wårdell, K. (2010). Stereotactic implantation of deep brain stimulation electrodes: a review of technical systems, methods and emerging tools. *Medical & Biological Engineering & Computing*, *48*, 611–624 (2010). doi:10.1007/s11517-010-0633-y
- Hemm, S., Mennessier, G., Vayssiere, N., Cif, L., El Fertit, H., & Coubes, P. (2005). Deep brain stimulation in movement disorders: Stereotactic coregistration of two-dimensional electrical field modeling and magnetic resonance imaging. *Journal of neurosurgery*, *103*, 949–955 (2005). doi:10.3171/jns.2005.103.6.0949
- Hemm, S., Pison, D., Alonso, F., Shah, A., Coste, J., Lemaire, J.-J., et al. (2016). Patient-Specific Electric Field Simulations and Acceleration Measurements for Objective Analysis of Intraoperative Stimulation Tests in the Thalamus. *Frontiers in Human Neuroscience*, *10*, 577(1-14) (2016). doi:10.3389/fnhum.2016.00577
- Herrington, T. M., Cheng, J. J., & Eskandar, E. N. (2016). Mechanisms of deep brain stimulation. *Journal of neurophysiology*, *115*, 19–38 (2016). doi:10.1152/jn.00281.2015
- Keane, M., Deyo, S., Abosch, A., Bajwa, J. A., & Johnson, M. D. (2012). Improved spatial targeting with directionally segmented deep brain stimulation leads for treating essential tremor. *Journal of neural engineering*, *9*, 46005 (2012). doi:10.1088/1741-2560/9/4/046005
- Kitagawa, M., Murata, J., Kikuchi, S., Sawamura, Y., Saito, H., Sasaki, H., et al. (2000). Deep brain stimulation of subthalamic area for severe proximal tremor. *Neurology*, *55*(1), 114–116.
- Krack, P., Fraix, V., Mendes, A., Benabid, A.-L., & Pollak, P. (2002). Postoperative management of subthalamic nucleus stimulation for Parkinson's disease. *Movement disorders : official journal of the Movement Disorder Society*, *17 Suppl 3*, S188-97.
- Lemaire, J.-J., Sakka, L., Ouchchane, L., Caire, F., Gabrillargues, J., & Bonny, J.-M. (2010). Anatomy of the human thalamus based on spontaneous contrast and microscopic voxels in high-field magnetic resonance imaging. *Neurosurgery*, *66*, 161–172 (2010). doi:10.1227/01.NEU.0000365617.41061.A3
- McIntyre, C. C., Grill, W. M., Sherman, D. L., & Thakor, N. V. (2004). Cellular effects of deep brain stimulation: Model-based analysis of activation and inhibition. *Journal of neurophysiology*, *91*, 1457–1469 (2004). doi:10.1152/jn.00989.2003
- Miocinovic, S., Lempka, S. F., Russo, G. S., Maks, C. B., Butson, C. R., Sakaie, K. E., et al. (2009). Experimental and theoretical characterization of the voltage distribution generated by deep brain stimulation. *Experimental Neurology*, *216*, 166–176 (2009). doi:10.1016/j.expneurol.2008.11.024
- Murata, J.-i., Kitagawa, M., Uesugi, H., Saito, H., Iwasaki, Y., Kikuchi, S., et al. (2003). Electrical stimulation of the posterior subthalamic area for the treatment of intractable proximal tremor. *Journal of neurosurgery*, *99*, 708–715 (2003). doi:10.3171/jns.2003.99.4.0708
- Palmer, J. L., Coats, M. A., Roe, C. M., Hanks, S. M., Xiong, C., & Morris, J. C. (2010). Unified Parkinson's Disease Rating Scale-Motor Exam: inter-rater reliability of advanced practice nurse and neurologist assessments. *Journal of advanced nursing*, *66*, 1382–1387 (2010). doi:10.1111/j.1365-2648.2010.05313.x
- Plaha, P., Patel, N. K., & Gill, S. S. (2004). Stimulation of the subthalamic region for essential tremor. *Journal of neurosurgery*, *101*, 48–54 (2004). doi:10.3171/jns.2004.101.1.0048
- Post, B., Merkus, M. P., de Bie, R. M.A., de Haan, R. J., & Speelman, J. D. (2005). Unified Parkinson's disease rating scale motor examination: are ratings of nurses, residents in neurology, and movement disorders specialists interchangeable? *Movement disorders : official journal of the Movement Disorder Society*, *20*, 1577–1584 (2005). doi:10.1002/mds.20640
- Reker, P., Dembek, T. A., Becker, J., Visser-Vandewalle, V., & Timmermann, L. (2016). Directional deep brain stimulation: A case of avoiding dysarthria with bipolar directional current steering. *Parkinsonism & Related Disorders*, *31*, 156–158 (2016). doi:10.1016/j.parkreldis.2016.08.007
- Sandvik, U., Koskinen, L.-O., Lundquist, A., & Blomstedt, P. (2012). Thalamic and subthalamic deep brain stimulation for essential tremor: where is the optimal target? *Neurosurgery*, *70*, 840 (2012). doi:10.1227/NEU.0b013e318236a809
- Schüpbach, W. M. M., Chabardes, S., Matthies, C., Pollo, C., Steigerwald, F., Timmermann, L., et al. (2017). Directional leads for deep brain stimulation: Opportunities and challenges. *Movement Disorders*. doi:10.1002/mds.27096
- Shah, A., Coste, J., Lemaire, J. J., Schkommodau, E., & Hemm-Ode, S. (2015). Use of quantitative tremor evaluation to enhance target selection during deep brain stimulation surgery for essential tremor. *Current Directions in Biomedical Engineering*, *1*, 488–492 (2015). doi:10.1515/cdbme-2015-0117
- Shah, A., Coste, J., Lemaire, J.-J., Schkommodau, E., Taub, E., Guzman, R., et al. (2016a). A novel assistive method for rigidity evaluation during deep brain stimulation surgery using acceleration sensors. *Journal of Neurosurgery*, *1–11* (2016). doi:10.3171/2016.8.JNS152770

- Shah, A., Coste, J., Lemaire, J.-J., Taub, E., Schüpbach, W. M. M., Pollo, C., et al. (2016b). Intraoperative acceleration measurements to quantify improvement in tremor during deep brain stimulation surgery. *Medical & Biological Engineering & Computing*. doi:10.1007/s11517-016-1559-9
- Shah, A., Alonso, F., Vogel, D., Wardell, K., Coste, J., Lemaire, J.-J., et al. (2018). Analysis of adverse effects of stimulation during deep brain stimulation surgery by patient-specific FEM simulations. *IEEE Engineering in Medicine and Biology Magazine, 40<sup>th</sup> Annual Int. Conference, Honolulu, HI, USA, July 17-21 (Accepted)*.
- Tamma, F., Caputo, E., Chiesa, V., Egidi, M., Locatelli, M., Rampini, P., et al. (2002). Anatomico-clinical correlation of intraoperative stimulation-induced side-effects during HF-DBS of the subthalamic nucleus. *Neurological sciences : official journal of the Italian Neurological Society and of the Italian Society of Clinical Neurophysiology, 23 Suppl 2*, S109-10 (2002). doi:10.1007/s100720200093
- Vassal, F., Coste, J., Derost, P., Mendes, V., Gabrillargues, J., Nuti, C., et al. (2012). Direct stereotactic targeting of the ventrointermediate nucleus of the thalamus based on anatomic 1.5-T MRI mapping with a white matter attenuated inversion recovery (WAIR) sequence. *Brain stimulation, 5*, 625–633 (2012). doi:10.1016/j.brs.2011.10.007
- Wårdell, K., Kefalopoulou, Z., Diczfalusy, E., Andersson, M., Åström, M., Limousin, P., et al. (2015). Deep brain stimulation of the pallidum internum for Gilles de la Tourette syndrome: a patient-specific model-based simulation study of the electric field. *Neuromodulation : journal of the International Neuromodulation Society, 18*, 90–96 (2015). doi:10.1111/ner.12248
- Zrinzo, L. (2012). Pitfalls in precision stereotactic surgery. *Surgical neurology international, 3*, 61 (2012). doi:10.4103/2152-7806.91612

### **Improvement maps for eight implantations described in the manuscript.**

This document contains the figures showing the 9 improvement maps generated by applying the technique described in the manuscript to 5 ET patients who underwent DBS surgery. Each figure is divided in to multiple parts: a) the first three parts (A to C) show an overview of the stimulation test region in axial, coronal and sagittal sections at the target position; b) the next three parts (D to F) show a close up of parts A to C at the target and c) the remaining parts starting from D are axial slices at the different depths along the planned trajectory at which stimulation tests were conducted. The improvement in tremor is represented by a color scale from white (least improvement) to dark green (highest improvement). The planned trajectory is represented as a gray cylinder. The anatomical structures outlined during the planning are represented with black outline for the overview and are labelled for the other close-up images. If adverse effects were observed during the stimulation tests, the first amplitude inducing these adverse effects were simulated and are indicated as red outline. The scale of the figure is indicated on the top right corner for the parts A to F and, for the axial figures, in the top right of part G. The projections of the AC and PC points on the respective planes are shown as blue circles.

Patient 1 Right:

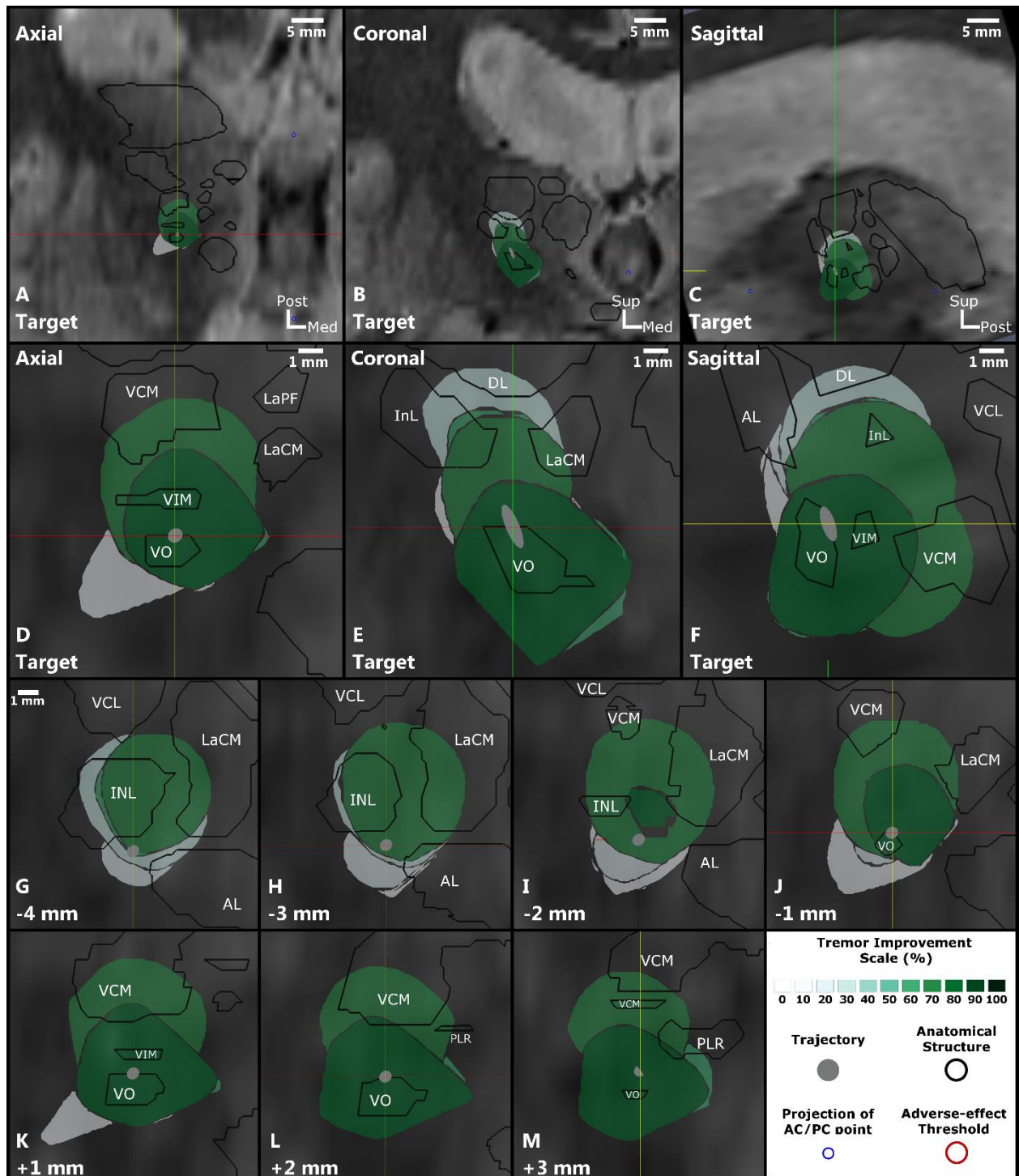


Figure S1: The target for this patient was chosen between the VO and the VIM as seen on the axial (D) and sagittal (F) slices. The deepest stimulation test position was 3 mm further along the trajectory (M). The highest improvement region for this patient encompasses the VO and the VIM and extends further to the inferior and anterior direction as seen on coronal (E) and sagittal (F) slices as well as axial slices from -2 mm to +3 mm (I to M). Adverse effects were not observed.

Patient 2 Left:

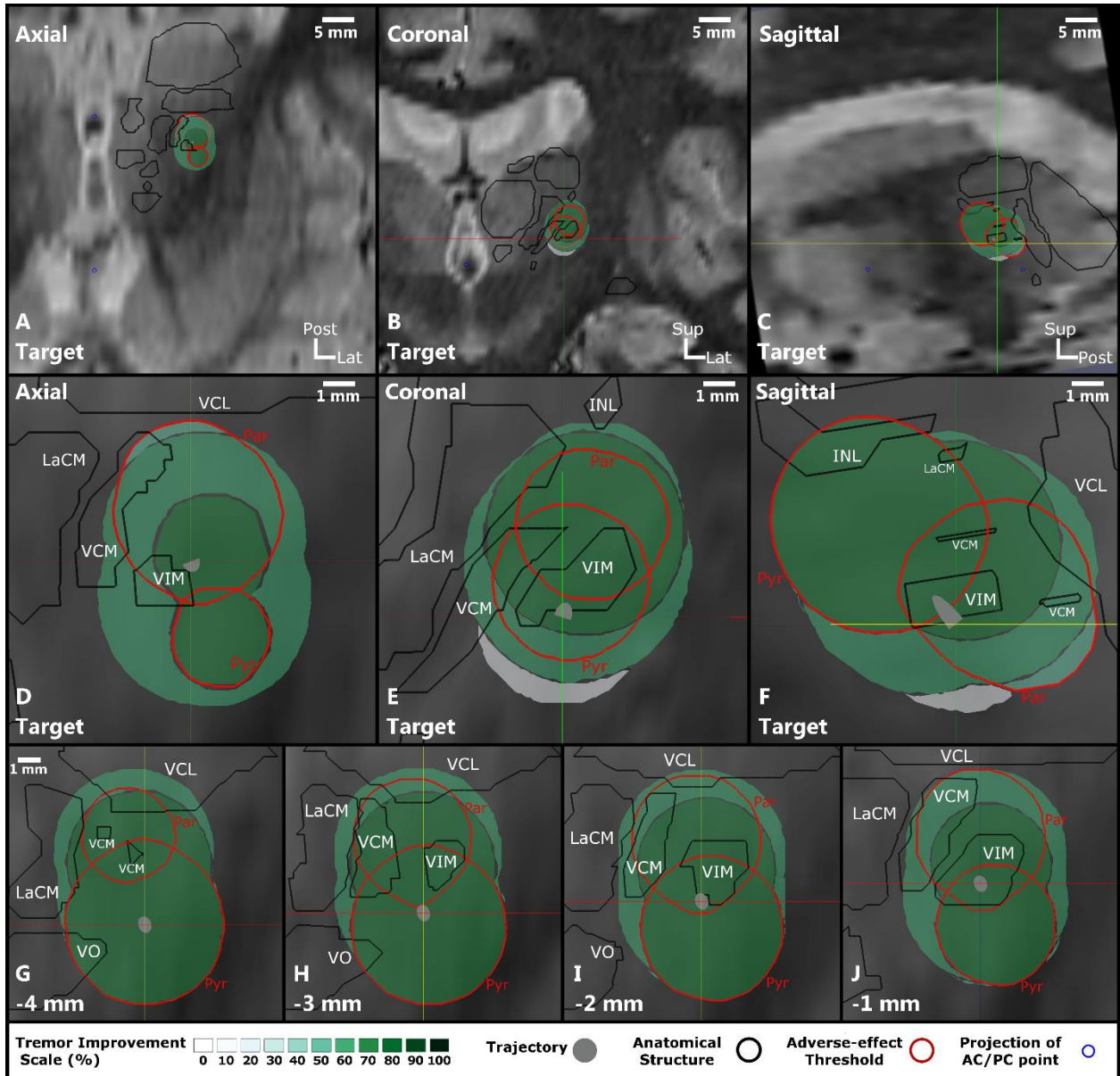


Figure S2: The planned target for the trajectories was in the middle of the VIM at the inferior border (E and F) and it was the deepest stimulation test position. The highest improvement region spans from the INL (F) to the VIM. Paresthesia and pyramidal side effects were observed at different stimulation test positions. The outline for pyramidal effects, labeled with Pyr in red, is at the supero-lateral edge of stimulation test region suggesting stimulation of the internal capsule. The outline for the paresthesia, labeled with Par in red, is posterior to the VIM in the VCL and VCM nuclei suggesting stimulation of the medial lemniscal fibres.

Patient 2 Right:

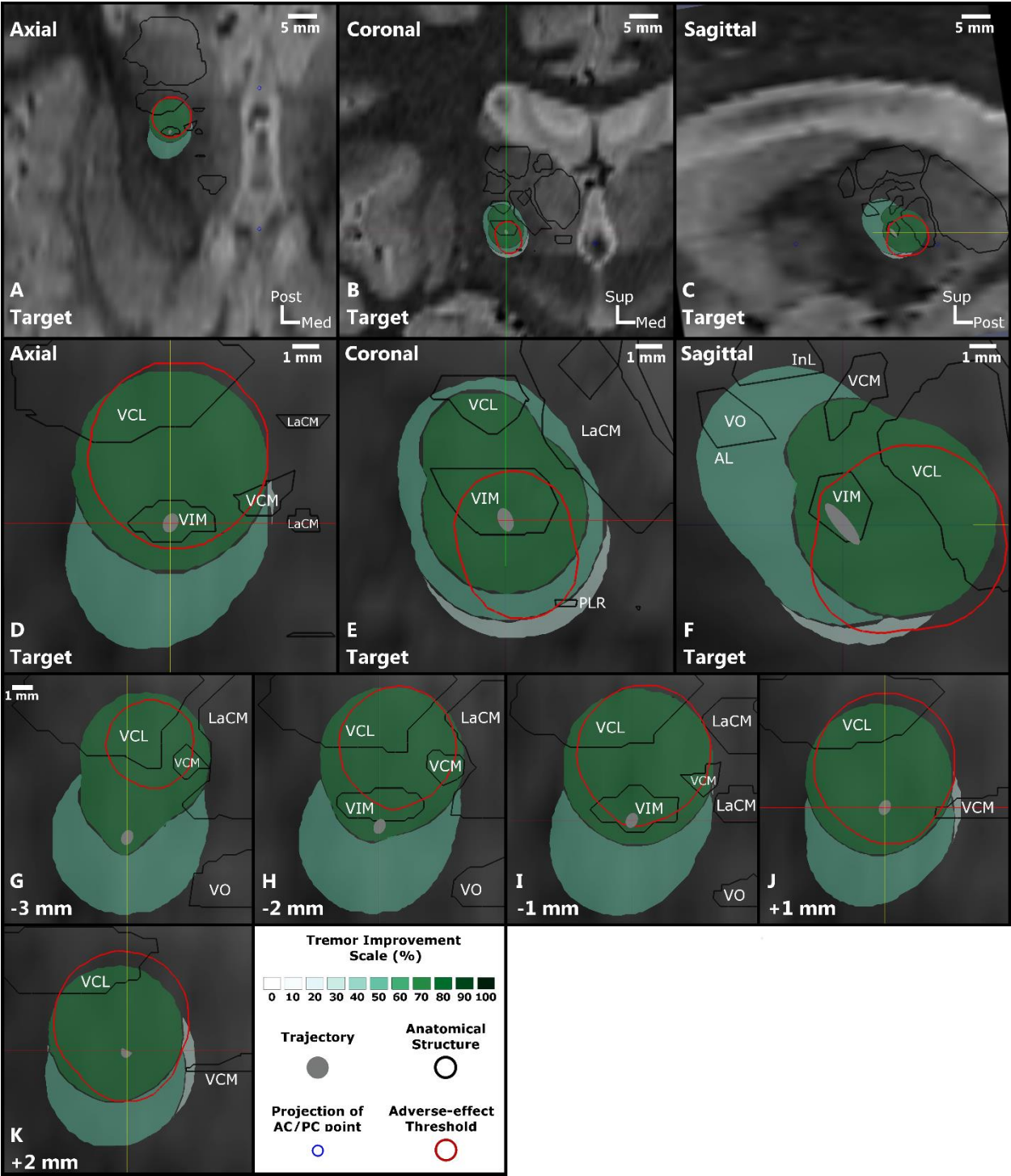


Figure S3: The VIM was the target for this patient (D to F) and the stimulation tests were performed up to 2 mm (K) further along the trajectory. The highest improvement region is found encompassing the VIM and extending posterior to it in the ventro-caudal (VCL) nuclei as visible on all slices. Paresthesia was observed during stimulation on central and posterior trajectories and the adverse effect outline extends in posterior to the VIM in the VCL and VCM nuclei.

Patient 3 Left:

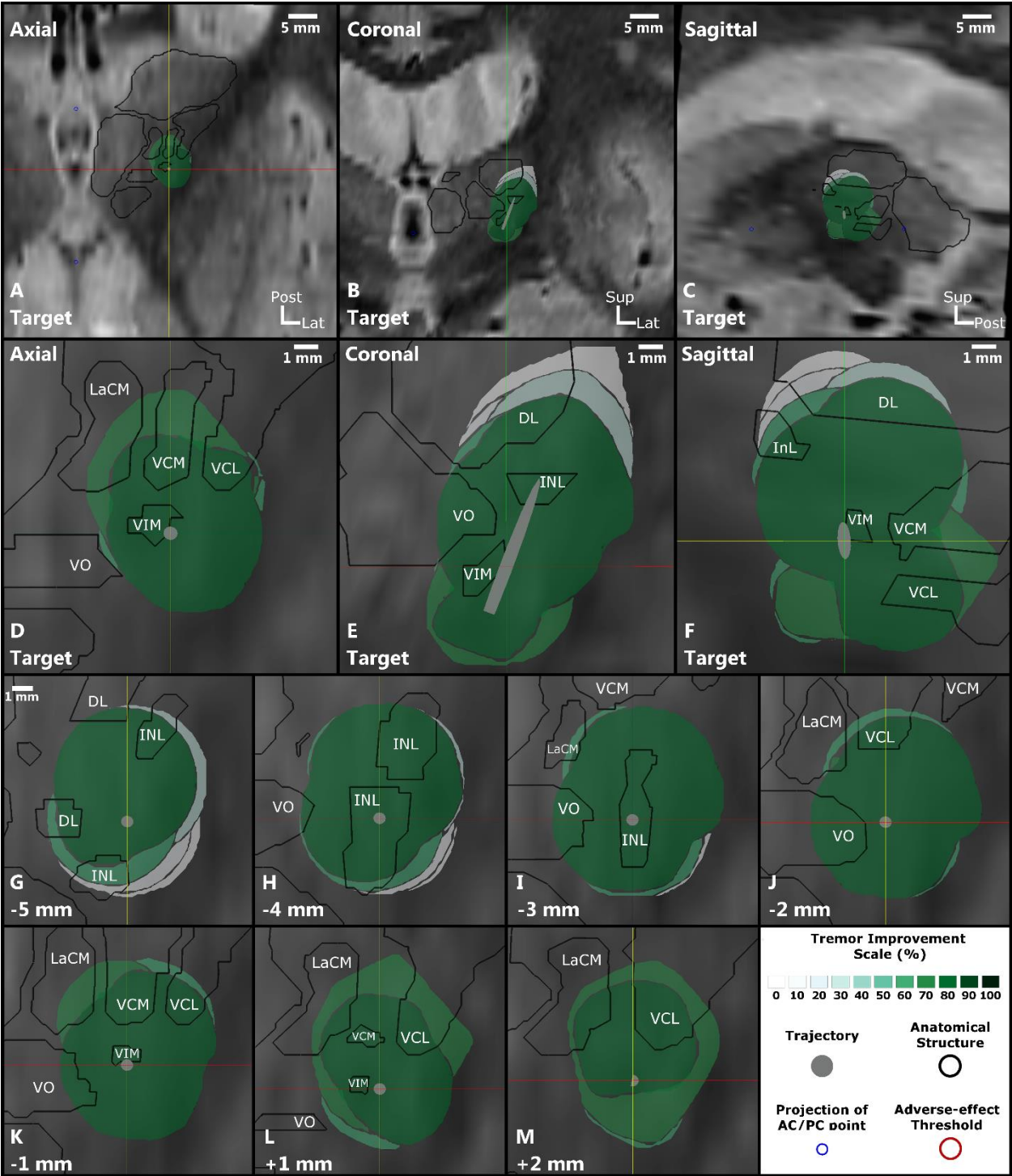


Figure S4: The antero-inferior border of the VIM was defined as the target for this patient (E, F) while stimulation tests were performed up to a depth of 2mm further on the trajectory (M). : The highest improvement region is large for this patient as visible on the coronal (B) and sagittal (C) slices. It encompasses the VIM and penetrates the InL, VCM, VCL, and the VO. The region extends further inferior to the VIM. Adverse effects were not observed during the stimulation tests.

Patient 3 Right:

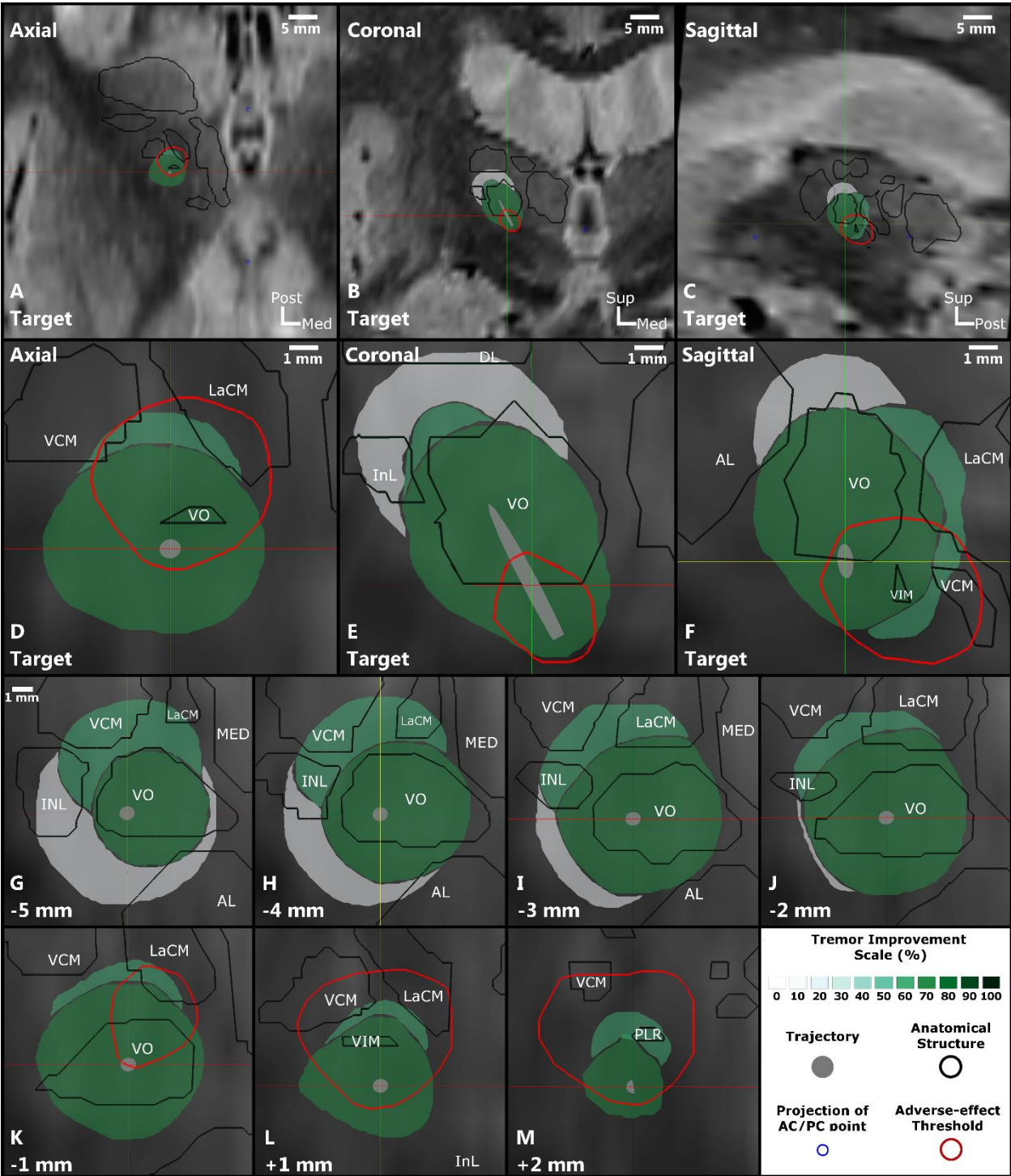


Figure S5: The planned target was at the inferior border of the VO for this patient (E and F) with stimulation tests performed until 2mm further along the trajectory (M). The highest improvement region encompasses the complete VO and the VIM and extends further in the inferior and posterior direction. Paresthesia side effects were observed on the posterior trajectory at the most inferior stimulation test positions. The adverse effect outline penetrates the VCM and LaCM nuclei posterior to the VIM.

Patient 4 Left:

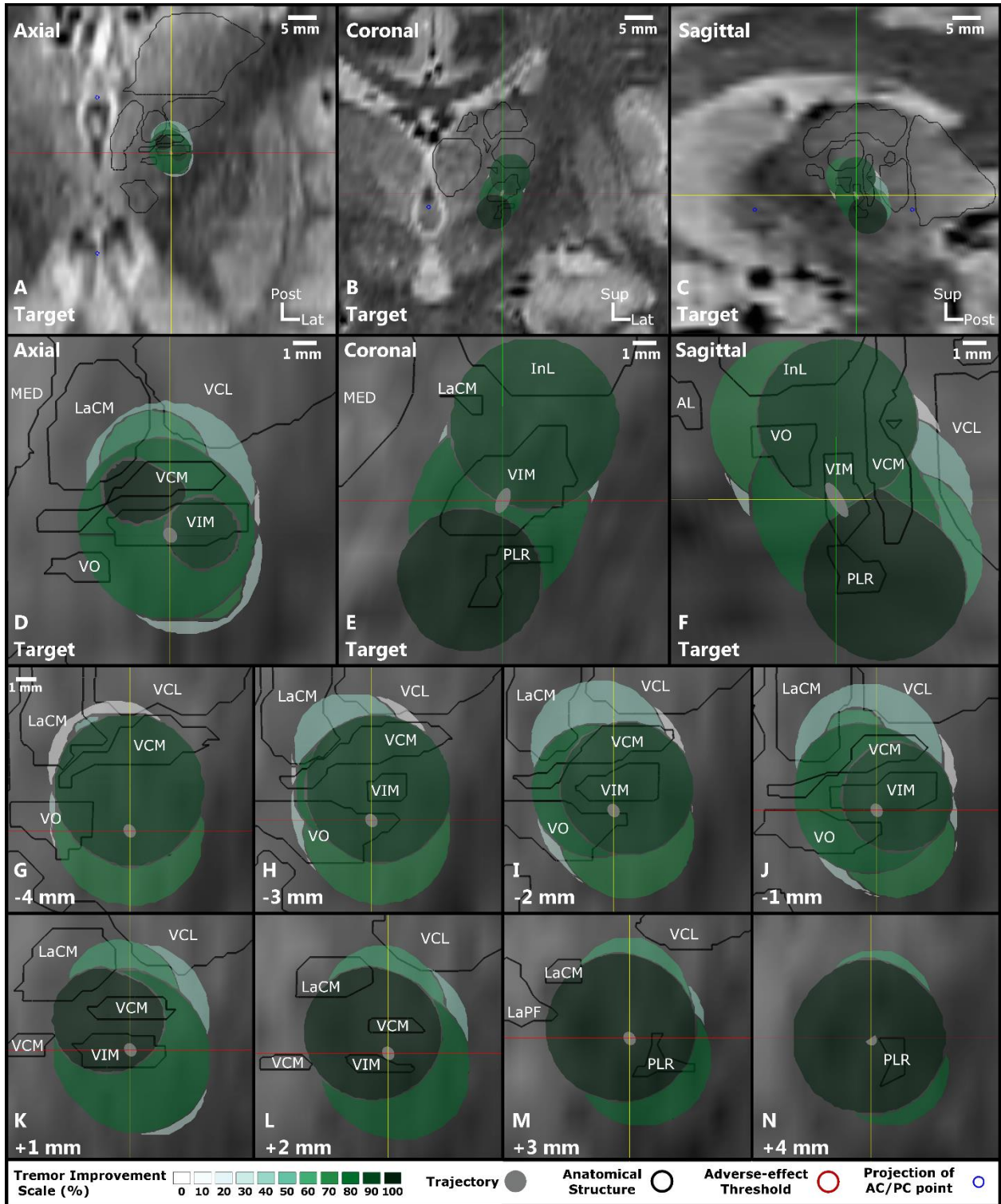


Figure S6: The planned target was located in the middle of the VIM (D, E and F) and stimulation tests were performed up to a depth of 4mm further on the trajectory (N). The highest improvement region is found to be most inferior in the stimulation test region, inferior and posterior to the VIM. It encompasses the PLR (M, N). Adverse effects were not observed during stimulation tests.

Patient 4 Right:

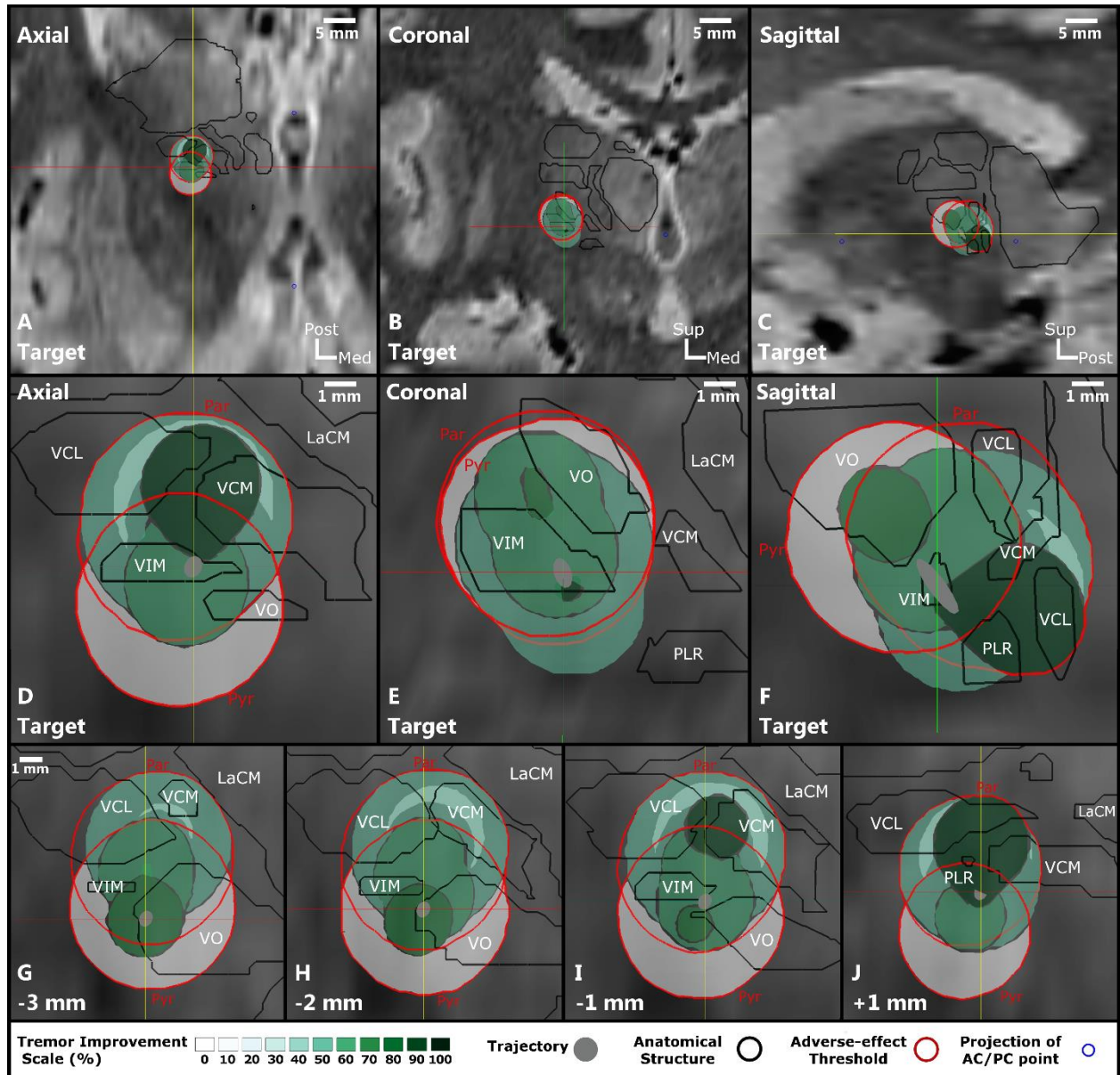


Figure S7: The medio-inferior part of the VIM was targeted (D to F) and stimulation tests were performed for 1 mm further than the target (J). The highest improvement region is inferior and posterior to the VIM penetrating the PLR, VCL and VCM (D, F, I, J). Pyramidal and paresthesia side effects were observed during stimulation on both the trajectories. The outline for pyramidal effect, labeled as Pyr in red, edges the improvement regions at the antero-superior border of the VO (E and F) indicating stimulation of the internal capsule. The paresthesia outline, labeled as Par in red, is at the posterior edge of the stimulation test region penetrating the VCL and VCM nuclei (D and F to J).

Patient 5 Left:

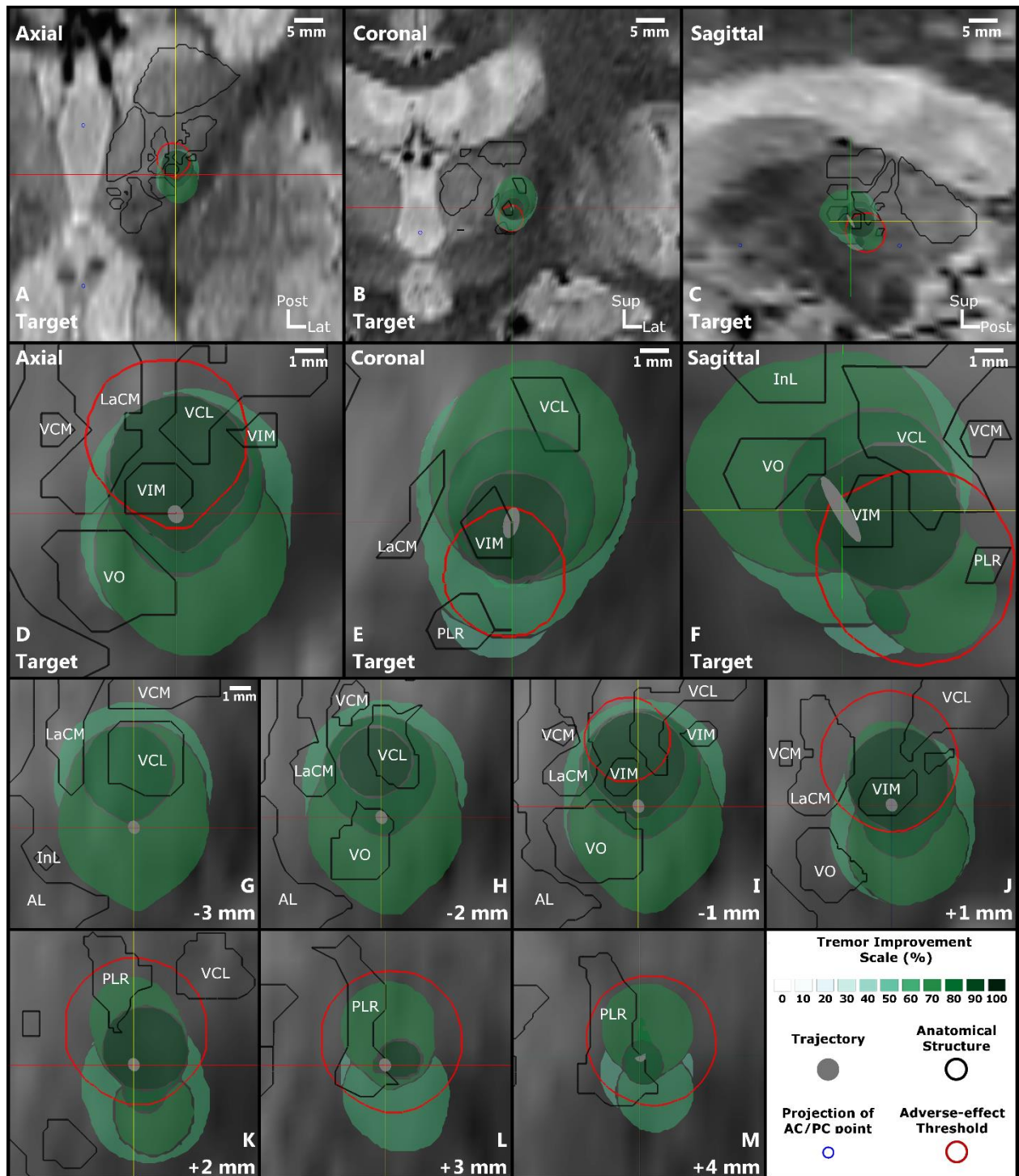


Figure S8: The antero-lateral part of VIM was planned as the target (D to F) with stimulation tests performed upto 4 mm further on the trajectory (M). The highest improvement region encompasses the VIM and extends posterior and inferior to it (D to F and I to L). Dysarthria side effects were observed during stimulation on the lowest position on the posterior trajectory. The adverse-effect outline extends into the posterior sub-thalamic area (D to F and I to M).

## Chapter 9

# Synthesis, Discussion and Perspective

This thesis describes the efforts undertaken to introduce new techniques to the traditional surgical procedure of implanting DBS leads in patient's brains for chronic stimulation to treat movement disorders. The following sections review the main results in relation to the goals that were set for this work followed by discussion of these results in context of the existing literature. The intended follow-up tasks are also described.

### 9.1 Summary of Key Findings

The results described in the seven publications in Chapters 4 to 8 relate to one or more aims out of the four that were set for this doctoral work. The first goal was **to improve the intraoperative symptom evaluation method through quantitative tools**. The publication describing the case study of using accelerometer based tremor evaluation (Section 4.1) shows the method's feasibility and its ability to identify the effective (tremor suppressing) as well as ineffective (insignificant change in tremor) stimulation current amplitudes. The larger clinical study described in Section 4.2 shows that the method can be applied to multiple clinical centers. The outcome measures extracted from raw acceleration data correlate with changes in tremor and are sensitive to minor changes in tremor. The use of accelerometer based rigidity evaluation method in Section 5.1 in 9 surgeries showed that changes in rigidity can be assessed through the variations in speed of passive movements. Outcome measures derived from acceleration data correlate with changes in rigidity and can be used to identify the stimulation current amplitude that result in suppression of rigidity. In combination, the above results clearly indicate that efforts made to reach this first goal of the study, have been successful.

The second goal of this doctoral work was to **identify the optimal target structure for implanting the DBS leads**. The first results that support this goal were obtained by comparing the efficiency of STN, FF and ZI in suppressing rigidity using the acceleration data of passive movements. Data shows that stimulation in the STN has higher chances of inducing adverse effects and the optimal target may be between STN, FF and ZI. Concerning tremor, for ET patients, the comparison of structures surrounding the VIM using accelerometer based tremor evaluation in section 6.1 similarly showed that the stimulation in the VIM may not be ideal due to adverse effect occurrence. A deeper analysis of the VIM region by estimating the spatial effects of stimulation as described in section 7.1 indeed supports the finding and also suggests that the PSA may be a better target of DBS for ET patients.

An important result of the clinical study involving evaluation of tremor using accelerometry is that, out of 26 implantations, the choice of placing the lead after intraoperative tests would have been different for 15 implantation if the accelerometry results could be considered. Furthermore, this difference in lead placement is even larger for rigidity evaluation where 12 out of 14 choices of lead placement would be altered. These results show the potential that quantitative symptom evaluation techniques have in altering the choice of lead placement after intraoperative stimulation tests. Apart from these, the improvement maps techniques proposed in section 8.2 simplifies the task of comparing the outcome of different stimulation tests in relation to patient's anatomy and through better management and visualization of intraoperatively collected data as well as estimating the spatial effects of stimulation. These results demonstrate that the efforts made to **identify the optimal position for lead placement** were successful.

The complexity associated with the study of mechanisms of actions of DBS is evident from the description in section 2.4.3. It is therefore not surprising that comprehensive knowledge about it remains elusive. In this doctoral work, the results of the anatomical analysis in sections 5.1, 6.1 and 7.1 show that the region between the thalamus and the STN seems to be the ideal target for DBS to treat ET and PD patients. Anatomically, this region is densely packed with fibre tracts. This information can be used to improve the **understanding of the mechanisms of action of DBS** by analysing it in the context of previously proposed hypotheses.

## 9.2 General Discussion

### 9.2.1 Symptom Evaluation during DBS Surgery

Various benefits of using the accelerometer based method to evaluate tremor and rigidity were identified during their use in DBS surgeries. The statistical features correlated with and can reliably estimate the changes in symptoms.

The relative evaluation with respect to baseline recorded immediately before suppresses the influence of variations in symptoms due to factors other than electrical stimulation. The results of the clinical study show that quantitative symptom evaluation is more sensitive than the subjective clinical methods. Higher sensitivity over conventional method enables the clinicians to better detect changes when baseline severity is very low. Additionally, the effective stimulation amplitudes identified through quantitative methods are lower compared to conventional methods, resulting in enlarged therapeutic windows and influencing lead placement. More importantly, these benefits are achieved without elongating the surgical procedure, without hindering the routine clinical evaluation and without any discomfort to the patient.

There are certain requirements to the proper function of the proposed methods. Acceleration sensors are influenced by gravity and all axes will contain some component of this influence based on the orientation of the sensor.<sup>267</sup> This influence can be suppressed by calculating the magnitude of the acceleration and filter this constant value in data using a high-pass filter.<sup>84</sup> Another important aspect to consider is the duration of baseline data: a minimum of 5 seconds is necessary for the method to function properly. In absence of sufficient baseline data, the baseline recorded before the previous stimulation test can be used. One significant difference between tremor evaluation method and rigidity evaluation method is that quantitative tremor evaluation can completely replace the routine visual evaluation during the surgery but the rigidity evaluation cannot. The rigidity evaluation method by design relies on the evaluator to perform the passive movements and calculates changes in rigidity indirectly. In this regard, the method is proposed as an assistive tool, which does not lessen its utility in any way as indicated by the results of the clinical study.

### 9.2.2 Anatomical Targets for DBS Lead Implantation

The incomplete understanding of the pathophysiology of PD and ET as well as that of the mechanisms of action of DBS causes the need to compare efficiency of different target structures in reducing the symptoms to identify the best one. Research studies comparing STN-DBS with GPi-DBS for PD patients<sup>7, 99, 195, 234, 240, 244, 248, 250, 252, 296, 298, 307, 341, 359, 362, 378</sup> and VIM DBS, STN DBS or PSA DBS for ET patients<sup>17, 31–33, 133, 146, 214, 242, 270, 271</sup> are plentiful, most of which compare the effects of chronic stimulation in one target structure with another. Studies have shown that some therapeutic effect of DBS may be due to neuro-plasticity i.e. adaptations in the brain's structure and function due to the introduction of DBS leads. As these effects cannot be estimated, they restrict the results of studies comparing chronic stimulation effects for identifying the ideal target structure. A possible solution to overcome this limitation is to use the intraoperative stimulation tests' data for comparison as done in the current work. An additional benefit in using our data is the use of

quantitative symptom evaluation data during intraoperative tests.

The results of the anatomical analysis of rigidity patients (Section 5.1) show that the sensorimotor part of the STN (dorso-lateral or anterior-superior-lateral<sup>53</sup>) may not be the ideal target for such patients. In terms of stimulation current amplitude, STN requires the least amount of current compared to ZI and FF. But in 30 (46.875%) out of 64 stimulation test positions in the STN, adverse effects were induced. Other studies have had similar results in chronic stimulation through DBS leads implanted inside the STN.<sup>13,20</sup> In comparison, stimulation in the ZI and FF had significantly lower occurrence of adverse effects (around 20%) with only a small increase in the stimulation current amplitude to reduce rigidity by the same amount. Various other studies have also suggested the role of ZI and FF in the therapeutic effect of STN-DBS.<sup>112,132,302,380</sup> These results collectively suggest to target the superior and lateral border of the anterior STN near ZI and FF for optimal outcome of DBS.

In a similar way, the VIM may not be the ideal target based on the results of data analysis for the ET patients who underwent VIM DBS (Section 6.1). Of the 6 anatomical structures which were compared in this study, stimulation in the VIM needed the most current amplitudes on average for 75% reduction in tremor and had the second highest chances of adverse effect occurrences. In comparison, the superiorly located VO and InL had lower occurrences of adverse effects while the PLR needed only half as much stimulation current amplitude for same reduction in tremor. Apart from these results based on the location of the stimulating contact only, in the study presenting the method of simulating electric field distribution to estimate the spatial effects of stimulation (Section 7.1), the data generated was also analysed to study the therapeutic effect of VIM and the surrounding structures. The results concurred with those of the first study indicating that the VIM may not be the only structure responsible for the therapeutic effects. Other published works also echo our results. Many papers indicate that stimulation in the PSA<sup>305</sup> that includes the ZI,<sup>63,103,133</sup> the PLR<sup>331,352</sup> and FF is either as good as or even better than VIM in suppressing tremor. Reports indicating role of VO<sup>48,352</sup> and the DRTT<sup>124</sup> in suppressing tremor have also been published.

### 9.2.3 Data Visualization for DBS Lead Placement

The success of DBS as a therapy depends heavily on the position of the lead with respect to the target structure. The percentage of patients having suboptimal outcome because of malpositioned lead and undergoing corrective surgery is reported between 1% and 8% at the same centre.<sup>92,94</sup> In a report<sup>253</sup> of unsatisfied patients who consulted a different center than the one they were operated in, 46% of them had malpositioned leads. To study the effect of using quantitative tremor evaluation and assistive rigidity evaluation on the choice of lead placement, the results of the data analysis were provided to the surgical team,

only post-operatively however and not at the time of choosing the position for lead placement as the clinical studies were approved for observational purposes only.

Out of the 26 lead placements in the tremor study (Section 4.2), the surgical team would have chosen differently for 15 of the implantations if the accelerometry results could have been considered. In the case of rigidity evaluation study (Section 5.1), the choice would have been different for 12 out of the 14 cases. To the best of my knowledge, no other published literature in the field of DBS has reported such comparison. The only studies that have some relevance to these results, in my opinion, are those that used quantitative methods to evaluate symptoms during post-operative programming of the IPG, the results of which also support the use of sensor based method over current clinical practices.<sup>140, 233, 280</sup>

An important note for the choice of lead placement for the tremor study is the stark difference in this choice between the two centers (CHU, Clermont-Ferrand: 15 of 18, Inselspital Bern: 0 of 8). These differences can be attributed to the difference in the surgical procedure and the criteria for choosing the final implant position. The team at CHU, Clermont-Ferrand tests 5 to 10 positions per trajectory and chooses the position within a group of positions with large therapeutic windows. On the other hand, the team at Inselspital tests 2 to 5 positions per trajectory and implants the lowest contact of the DBS lead at the deepest position with a large therapeutic window. Nevertheless, these differences emphasize the need to test any intraoperative system in multicentre study to understand the influence of variations in the surgical procedure. They do not in any way suggest that one procedure is better than the other.

The results of the improvement map study demonstrates that visual analysis of intraoperative stimulation test results can also potentially alter the lead placement choice. Certainly, as the improvement maps used quantitative tremor evaluation data, the influence on the final implant position is due to both techniques. It is not possible to confidently determine which of the 3 choices (based on clinical evaluation, based on accelerometer data or based on improvement maps) is better for such limited sample data. One possible way to judge it would be by comparing it to the position of the chronically stimulated DBS lead contact. But such a comparison presents its own challenge in terms of unknown changes due to neuro-plasticity, brain-shift, worsening disease, etc. In order to investigate this further, a clinical study with a large cohort is necessary.

One limitation of the improvement map method in its current state is that it can only be applied post-operatively. Nevertheless, a few modifications can enable it to be used intraoperatively. The brain model that is required to simulate the EF distribution can be generated right after the acquisition of the necessary MR images, which, in the case of CHU Clermont-Ferrand, is a day before the surgery. On completion of the planning, the trajectory and stimulation test positions

can be identified in the brain model. During the surgery, effective stimulation current amplitudes can be identified using the accelerometer method and used to simulate the EF. At the end of stimulation tests, the improvement maps can be calculated from the consolidated EFs fairly quickly (maximum 5 minutes) and visualized to identify the best position for the lead placement. The practical requirements and the feasibility of implementing the improvement maps in this way are being discussed with the research partners involved.

An important discussion concerning the visualization is about spatial accuracy. Since the visualization involves multiple datasets, their individual inaccuracies have a cumulative effect on the final visualization. As most of the information for the improvement maps is sourced from the patient images, their spatial dimensions and accuracy play a major role. MRI acquisition can cause image distortion due to magnetic field inhomogeneities,<sup>339</sup> e.g. in frame identification, but can be corrected using software. Image registration of MR with CT has been suggested to reduce distortion errors,<sup>376</sup> but studies have found that registration errors are higher than distortion errors.<sup>251</sup> High resolution stereotactic MRI acquisitions can eliminate registration errors while limiting distortion errors.<sup>383</sup> The surgical planning data also has uncertainties. The trajectory for example, can be affected by brain-shift<sup>168,235</sup> i.e. displacement and/or deformation of the brain during intracerebral procedures.<sup>326</sup> Additionally, the planning software interpolates the outline of the anatomical structures, but these outlines can only be exported after being assigned to the dimensions of an image dataset.

The FEM simulations of EF distribution to estimate the spatial effect of stimulation also have their limitations. Variations in the tissue conductivity values, voltage drop at the electrode-tissue interface and the lack of experimental validation of the models are some of them. Exhaustive discussion of all the limitations associated with the simulations can be found elsewhere.<sup>11</sup> Certainly, the quality of the image data significantly affects the outcome of simulations as the patient-specific nature relies on the image data used for creating the conductivity matrix for the brain model. Overall, it is clear that the resolution of the patient images play a large role in defining the quality of the visualization. In their current form, the datasets are based on the pre-operative CT (0.59 mm × 0.59 mm × 1.25 mm) as it has the highest resolution among the images acquired. In comparison to the diameter of the exploration electrode (0.55 mm) and the DBS lead (1.27 mm), from a purely engineering point of view, this image resolution can be used to create visualization with limited spatial accuracy. However, considering the positive results of the adverse effect maps and the simplicity offered by the improvement maps, the clinical utility of the tool has more significance than the strict engineering perspective, especially in absence of alternatives. Nevertheless, the spatial accuracy can certainly be improved by acquiring higher resolution images, which was not possible for the current retrospective application.

### 9.2.4 Mechanisms of Action of DBS

The successful results of DBS as a treatment for movement disorders were not replicated when it was applied to other neurological diseases. One of the various reasons for this lack of success is the partial understanding of the mechanisms by which DBS produces the therapeutic effects. Since the first successful DBS surgery, a significant amount of research has been undertaken to understand its mechanisms of action. Experiments have been performed to know if stimulation inhibits or excites neurons, affects the neuronal soma (cell body) or projections (axons and dendrites) or both, and influences one structure only or the whole basal-ganglia-thalamic circuit. Through the results of these experiments, researchers have collected information to better understand the mechanisms of action of DBS.

It is evident from the published literature reviewed in Section 2.4.3 that a complete understanding of mechanisms of actions of DBS is elusive and will require extensive research in numerous areas. The anatomical analysis of the data collected in this doctoral work and the visualization in the form of improvement maps can be related to the known hypothesis of mechanisms of action. The results of the analysis indicate that the region between the ventral thalamus and the subthalamic nucleus i.e. PSA containing the PLR, ZI and FF is the most effective for tremor and rigidity suppression. Detailed tractography analysis of the PSA<sup>105</sup> has shown that fibres connecting primary motor cortex, supplementary motor cortex, pallidum, ventro-lateral thalamus, brainstem and others condense together and pass through this region. Connections to the VO and the VIM are also reported. In this context, effective stimulation in the PSA could be attributed to the stimulation of these fiber tracts and consequently stimulating the neurons in the terminating structure. In terms of questions related to the mechanisms of action, these results suggest that DBS activates fiber tracts which alter the firing pattern of the functional circuit towards a healthier state. Nevertheless, these implications have low statistical confidence as they are based on data collected from few patients.

## 9.3 Perspective

The efforts made in the current doctoral work have introduced new technologies to the intraoperative stimulation tests for DBS. In addition, there are a few tasks that can further enhance the DBS therapy through technology. One such opportunity is to use the accelerometer based quantitative evaluation methods during pre-operative examination of patients. This could simplify the task of neurologists to judge if a patient's needs to and is able to undergo the surgery to fully benefit from the therapy. The use of quantitative symptom evaluation can also be extended intraoperatively during MER. This resultant data would allow correlation between neuronal firing and/or LFP with symptom changes to

better study the pathophysiology of the underlying disease. Furthermore, the use of quantitative symptom evaluation during post-operative IPG programming to identify best stimulation parameters as well as during short- and long-term follow-up examination would also benefit the neurologist and the patients. It has been shown that sensor-based algorithmic programming of IPG was successful in identifying therapeutic stimulation parameters.<sup>140</sup> To further automate the task of IPG programming, techniques to evaluate other symptoms like bradykinesia, gait disturbances, etc. as well as adverse effects of stimulation will have to be developed and tested. Further research is necessary to bring these solutions from the lab to routine clinical practice.

Apart from researching new techniques, one important task to realize the full benefits of the quantitative tremor evaluation and the assistive rigidity evaluation methods is to conduct a clinical study with the ability to use the results for lead placement and then compare the choices to a control group. Results in this thesis have shown that therapeutically effective simulation amplitudes identified through quantitative methods are lower. Certainly such a study needs to be spread across multiple clinical centers and include a large number of patients to be able to draw statistically confident conclusions. Such a large study also provides an opportunity to use the improvement maps during the surgery for choosing the lead placement. In addition, the data collected can be analyzed with respect to anatomy, not only based on the location of the electrode, but also using the patient-specific EF simulations. The results can be used to identify the best target structure for different pathologies and learn more about the mechanisms of actions of DBS.

Future research endeavours should also consider the current trends in clinical environment. One such aspect is the rise in number of DBS surgeries performed using general anaesthesia. As new lead designs allow more flexibility, experienced DBS neurosurgeons exhibit the intention to place them with fully anaesthetised patients to simplify the surgery for the patients. New techniques have to be designed and tested which can optimize lead placement under general anaesthesia to assist the neurosurgeons in improving the surgical outcome.

## Chapter 10

# Conclusion

This doctoral work successfully demonstrates that the DBS surgical procedure can be improved by using new techniques. The accelerometer based methods to evaluate changes in tremor and rigidity have been shown to overcome the subjectivity of currently used symptom evaluation methods and are more sensitive to small changes in the symptoms. The new methods also allow quantitative comparison of the role of different anatomical structures in the therapeutic effect of stimulation. The results show that stimulation in the posterior subthalamic area containing the fields of Forel, the Zona Incerta and the Prelemniscal Radiations results in significant suppression of tremor and rigidity at low amplitudes without inducing severe adverse effects. Furthermore, for ET patients, the combination of quantitative tremor evaluation with estimation of spatial effects of stimulation through electric field simulations showed that other thalamic nuclei as well as fibre tracts surrounding the ventro-intermediate nucleus may also be the responsible for therapeutic effects. Apart from this, the improvement maps method has shown that the use of patient data during the surgery can be improved. The summarized visualization of intraoperative stimulation tests can significantly simplify the task of lead placement. As a consequence of the optimization of DBS surgery through these methods, significant benefits for patients can be anticipated. The reduction in the therapeutically effective stimulation current amplitude achieved by application of these methods can reduce stimulation induced adverse effects and potentially lengthen the battery life of the IPG. These methods can also benefit the DBS therapy in general as they can be used to enhance the understanding of mechanisms of actions. The enhanced knowledge can be used to develop better hardware as well as to treat other neurological diseases using DBS.

## References

- [1] A. ABOSCH, L. TIMMERMANN, S. BARTLEY, H. G. RIETKERK, D. WHITING, P. J. CONNOLLY, D. LANCTIN, AND M. I. HARIZ, *An international survey of deep brain stimulation procedural steps*, *Stereotactic and functional neurosurgery*, 91 (2013), pp. 1–11.
- [2] F. AGNESI, A. T. CONNOLLY, K. B. BAKER, J. L. VITEK, AND M. D. JOHNSON, *Deep brain stimulation imposes complex informational lesions*, *PLoS ONE*, 8 (2013), p. e74462.
- [3] R. L. ALBIN, A. B. YOUNG, AND J. B. PENNEY, *The functional anatomy of basal ganglia disorders*, *Trends in neurosciences*, 12 (1989), pp. 366–375.
- [4] G. E. ALEXANDER, M. D. CRUTCHER, AND M. R. DELONG, *Basal ganglia-thalamocortical circuits: Parallel substrates for motor, oculomotor, prefrontal and limbic functions*, *Progress in brain research*, 85 (1990), pp. 119–146.
- [5] J. E. ALTY AND P. A. KEMPSTER, *A practical guide to the differential diagnosis of tremor*, *Postgraduate medical journal*, 87 (2011), pp. 623–629.
- [6] L. ALVAREZ, R. MACIAS, G. LOPEZ, E. ALVAREZ, N. PAVON, M. C. RODRIGUEZ-OROZ, J. L. JUNCOS, C. MARAGOTO, J. GURIDI, I. LITVAN, E. S. TOLOSA, W. KOLLER, J. VITEK, M. R. DELONG, AND J. A. OBESO, *Bilateral subthalamotomy in parkinson's disease: Initial and long-term response*, *Brain : a journal of neurology*, 128 (2005), pp. 570–583.
- [7] V. C. ANDERSON, K. J. BURCHIEL, P. HOGARTH, J. FAVRE, AND J. P. HAMMERSTAD, *Pallidal vs subthalamic nucleus deep brain stimulation in parkinson disease*, *Archives of neurology*, 62 (2005), pp. 554–560.
- [8] P. ARIDON, P. RAGONESE, M. DE FUSCO, G. SALEMI, G. CASARI, AND G. SAVETTIERI, *Further evidence of genetic heterogeneity in fa-*

- milial essential tremor*, *Parkinsonism & Related Disorders*, 14 (2008), pp. 15–18.
- [9] A. ASCHERIO AND M. A. SCHWARZSCHILD, *The epidemiology of parkinson's disease: Risk factors and prevention*, *The Lancet Neurology*, 15 (2016), pp. 1257–1272.
- [10] S. ASKARI, M. ZHANG, AND D. S. WON, *An emg-based system for continuous monitoring of clinical efficacy of parkinson's disease treatments*, *Conference proceedings : ... Annual International Conference of the IEEE Engineering in Medicine and Biology Society. IEEE Engineering in Medicine and Biology Society. Conference*, 2010 (2010), pp. 98–101.
- [11] M. ÅSTRÖM, *Modelling, simulation, and visualization of deep brain stimulation*, vol. 1384 of *Linköping studies in science and technology. Dissertations*, Department of Biomedical Engineering, Linköping University, Linköping, 2011.
- [12] M. ASTROM, E. DICZFALUSY, H. MARTENS, AND K. WARDELL, *Relationship between neural activation and electric field distribution during deep brain stimulation*, *IEEE transactions on bio-medical engineering*, 62 (2015), pp. 664–672.
- [13] M. ASTRÖM, E. TRIPOLITI, M. I. HARIZ, L. U. ZRINZO, I. MARTINEZ-TORRES, P. LIMOUSIN, AND K. WÅRDELL, *Patient-specific model-based investigation of speech intelligibility and movement during deep brain stimulation*, *Stereotactic and functional neurosurgery*, 88 (2010), pp. 224–233.
- [14] M. ASTRÖM, L. U. ZRINZO, S. TISCH, E. TRIPOLITI, M. I. HARIZ, AND K. WÅRDELL, *Method for patient-specific finite element modeling and simulation of deep brain stimulation*, *Medical & biological engineering & computing*, 47 (2009), pp. 21–28.
- [15] T. Z. AZIZ, D. PEGGS, M. A. SAMBROOK, AND A. R. CROSSMAN, *Lesion of the subthalamic nucleus for the alleviation of 1-methyl-4-phenyl-1,2,3,6-tetrahydropyridine (mptp)-induced parkinsonism in the primate*, *Movement disorders : official journal of the Movement Disorder Society*, 6 (1991), pp. 288–292.
- [16] M. G. BAKER AND L. GRAHAM, *The journey: Parkinson's disease*, *BMJ (Clinical research ed.)*, 329 (2004), pp. 611–614.
- [17] M. T. BARBE, L. LIEBHART, M. RUNGE, J. DEYNG, E. FLORIN, L. WOJTECKI, A. SCHNITZLER, N. ALLERT, V. STURM, G. R. FINK, M. MAAROUF, AND L. TIMMERMANN, *Deep brain stimulation of the ventral intermediate nucleus in patients with essential tremor: Stimula-*

*tion below intercommissural line is more efficient but equally effective as stimulation above*, *Experimental Neurology*, 230 (2011), pp. 131–137.

- [18] M. S. BARON, J. L. VITEK, R. A. BAKAY, J. GREEN, Y. KANEOKA, T. HASHIMOTO, R. S. TURNER, J. L. WOODARD, S. A. COLE, W. M. McDONALD, AND M. R. DELONG, *Treatment of advanced parkinson's disease by posterior gpi pallidotomy: 1-year results of a pilot study*, *Annals of Neurology*, 40 (1996), pp. 355–366.
- [19] A. L. BARTELS AND K. L. LEENDERS, *Parkinson's disease: The syndrome, the pathogenesis and pathophysiology*, *Cortex*, 45 (2009), pp. 915–921.
- [20] C. BAUMGARTEN, Y. ZHAO, P. SAULEAU, C. MALRAIN, P. JANIN, AND C. HAEGELEN, *Improvement of pyramidal tract side effect prediction using a data-driven method in subthalamic stimulation*, *IEEE transactions on bio-medical engineering*, 64 (2017), pp. 2134–2141.
- [21] A. L. BENABID, J. MITROFANIS, S. CHABARDES, E. SEIGNEURET, N. TORRES, B. PIALLAT, A. BENAZZOUZ, V. FRAIX, P. KRACK, P. POLLAK, S. GRAND, AND J. F. LEBAS, *Subthalamic nucleus stimulation for parkinson's disease*, in *Textbook of stereotactic and functional neurosurgery*, A. M. Lozano, P. L. Gildenberg, and R. R. Tasker, eds., Springer, Berlin, 2009, pp. 1603–1630.
- [22] A. L. BENABID, P. POLLAK, D. HOFFMANN, C. GERVASON, M. HOMMEL, J. E. PERRET, J. DE ROUGEMONT, AND D. M. GAO, *Long-term suppression of tremor by chronic stimulation of the ventral intermediate thalamic nucleus*, *The Lancet*, 337 (1991), pp. 403–406.
- [23] J. BENITO-LEÓN AND E. D. LOUIS, *Essential tremor: Emerging views of a common disorder*, *Nature clinical practice. Neurology*, 2 (2006), pp. 666–78; quiz 2p following 691.
- [24] H. BERGMAN, T. WICHMANN, AND M. R. DELONG, *Reversal of experimental parkinsonism by lesions of the subthalamic nucleus*, *Science (New York, N.Y.)*, 249 (1990), pp. 1436–1438.
- [25] H. BERGMAN, T. WICHMANN, B. KARMON, AND M. R. DELONG, *The primate subthalamic nucleus. ii. neuronal activity in the mptp model of parkinsonism*, *Journal of neurophysiology*, 72 (1994), pp. 507–520.
- [26] A. BERNEY, F. VINGERHOETS, A. PERRIN, P. GUEX, J.-G. VILLEMURE, P. R. BURKHARD, C. BENKELFAT, AND J. GHIKA, *Effect on mood of subthalamic dbs for parkinson's disease: A consecutive series of 24 patients*, *Neurology*, 59 (2002), pp. 1427–1429.
- [27] E. H. BETZ, *Centralblatt für die medicinischen Wissenschaften*, A. Hirschwald, Berlin, 1874.

- [28] R. BHATIA, A. DALTON, M. RICHARDS, C. HOPKINS, T. AZIZ, AND D. NANDI, *The incidence of deep brain stimulator hardware infection: The effect of change in antibiotic prophylaxis regimen and review of the literature*, *British journal of neurosurgery*, 25 (2011), pp. 625–631.
- [29] S. BHATIA, K. ZHANG, M. OH, C. ANGLE, AND D. WHITING, *Infections and hardware salvage after deep brain stimulation surgery: A single-center study and review of the literature*, *Stereotactic and functional neurosurgery*, 88 (2010), pp. 147–155.
- [30] M. J. BIRDNO, A. M. KUNCCEL, A. D. DORVAL, D. A. TURNER, AND W. M. GRILL, *Tremor varies as a function of the temporal regularity of deep brain stimulation*, *NeuroReport*, 19 (2008), pp. 599–602.
- [31] P. BLOMSTEDT, P. LINDVALL, J. LINDER, M. OLIVECRONA, L. FORSGREN, AND M. I. HARIZ, *Reoperation after failed deep brain stimulation for essential tremor*, *World Neurosurgery*, 78 (2012), pp. 554.e1–554.e5.
- [32] P. BLOMSTEDT, U. SANDVIK, M. I. HARIZ, A. FYTAGORIDIS, L. FORSGREN, G.-M. HARIZ, AND L.-O. D. KOSKINEN, *Influence of age, gender and severity of tremor on outcome after thalamic and subthalamic dbs for essential tremor*, *Parkinsonism & related disorders*, 17 (2011), pp. 617–620.
- [33] P. BLOMSTEDT, U. SANDVIK, J. LINDER, A. FREDRICKS, L. FORSGREN, AND M. I. HARIZ, *Deep brain stimulation of the subthalamic nucleus versus the zona incerta in the treatment of essential tremor*, *Acta neurochirurgica*, 153 (2011), pp. 2329–2335.
- [34] C. BOSCH-BOUJU, B. I. HYLAND, AND L. C. PARR-BROWNLIE, *Motor thalamus integration of cortical, cerebellar and basal ganglia information: Implications for normal and parkinsonian conditions*, *Frontiers in computational neuroscience*, 7 (2013), p. 163.
- [35] H. BRAAK, K. DEL TREDICI, U. RUB, R. A. I. DE VOS, E. N. H. JANSEN STEUR, AND E. BRAAK, *Staging of brain pathology related to sporadic parkinson's disease*, *Neurobiology of aging*, 24 (2003), pp. 197–211.
- [36] S. BREIT, R. BOUALI-BENAZZOUZ, R. C. POPA, T. GASSER, A. L. BENABID, AND A. BENAZZOUZ, *Effects of 6-hydroxydopamine-induced severe or partial lesion of the nigrostriatal pathway on the neuronal activity of pallido-subthalamic network in the rat*, *Experimental Neurology*, 205 (2007), pp. 36–47.
- [37] A. R. BROWN, M. C. ANTLE, B. HU, AND G. C. TESKEY, *High frequency stimulation of the subthalamic nucleus acutely rescues*

- motor deficits and neocortical movement representations following 6-hydroxydopamine administration in rats*, *Experimental Neurology*, 231 (2011), pp. 82–90.
- [38] P. BROWN, *Oscillatory nature of human basal ganglia activity: Relationship to the pathophysiology of parkinson's disease*, *Movement disorders : official journal of the Movement Disorder Society*, 18 (2003), pp. 357–363.
- [39] P. BROWN AND C. D. MARSDEN, *What do the basal ganglia do?*, *Lancet* (London, England), 351 (1998), pp. 1801–1804.
- [40] P. BROWN, A. OLIVIERO, P. MAZZONE, A. INSOLA, P. TONALI, AND V. DI LAZZARO, *Dopamine dependency of oscillations between subthalamic nucleus and pallidum in parkinson's disease*, *The Journal of neuroscience : the official journal of the Society for Neuroscience*, 21 (2001), pp. 1033–1038.
- [41] S. F. BUCHER, K. C. SEELOS, R. C. DODEL, M. REISER, AND W. H. OERTEL, *Activation mapping in essential tremor with functional magnetic resonance imaging*, *Annals of Neurology*, 41 (1997), pp. 32–40.
- [42] P. R. BURKHARD, F. J. G. VINGERHOETS, A. BERNEY, J. BOGOU-SLAVSKY, J.-G. VILLEMURE, AND J. GHKA, *Suicide after successful deep brain stimulation for movement disorders*, *Neurology*, 63 (2004), pp. 2170–2172.
- [43] J. A. BURNE, M. W. HAYES, V. S. C. FUNG, C. YIANNIKAS, AND D. BOLJEVAC, *The contribution of tremor studies to diagnosis of parkinsonian and essential tremor: A statistical evaluation*, *Journal of clinical neuroscience : official journal of the Neurosurgical Society of Australasia*, 9 (2002), pp. 237–242.
- [44] P. BURRESI, *Sopra un caso di tremore essenziale. memore originali. conferenza raccolta dallo studente alfredo rubini (22 febbraio, 1874, siena)*, *Lo Sperimentale*, 33 (1874), pp. 475–481.
- [45] C. R. BUTSON, S. E. COOPER, J. M. HENDERSON, AND C. C. MCINTYRE, *Patient-specific analysis of the volume of tissue activated during deep brain stimulation*, *NeuroImage*, 34 (2007), pp. 661–670.
- [46] C. R. BUTSON, A. M. NOECKER, C. B. MAKS, AND C. C. MCINTYRE, *Stimexplorer: deep brain stimulation parameter selection software system*, *Acta neurochirurgica. Supplement*, 97 (2007), pp. 569–574.
- [47] F. CAIRE, D. RANOUX, D. GUEHL, P. BURBAUD, AND E. CUNY, *A systematic review of studies on anatomical position of electrode contacts used for chronic subthalamic stimulation in parkinson's disease*, *Acta neurochirurgica*, 155 (2013), pp. 1647–54; discussion 1654.

- [48] D. CAPARROS-LEFEBVRE, S. BLOND, M.-P. FELTIN, P. POLLAK, AND A. L. BENABID, *Improvement of levodopa induced dyskinesias by thalamic deep brain stimulation is related to slight variation in electrode placement: Possible involvement of the centre median and parafascicularis complex*, *Journal of neurology, neurosurgery, and psychiatry*, 67 (1999), pp. 308–314.
- [49] V. CHANDRAN, P. K. PAL, J. Y. C. REDDY, K. THENNARASU, R. YADAV, AND N. SHIVASHANKAR, *Non-motor features in essential tremor*, *Acta neurologica Scandinavica*, 125 (2012), pp. 332–337.
- [50] C. C. CHEN, V. LITVAK, T. GILBERTSON, A. KÜHN, C. S. LU, S. T. LEE, C. H. TSAI, S. TISCH, P. LIMOUSIN, M. HARIZ, AND P. BROWN, *Excessive synchronization of basal ganglia neurons at 20 hz slows movement in parkinson's disease*, *Experimental Neurology*, 205 (2007), pp. 214–221.
- [51] S. CHIKEN AND A. NAMBU, *High-frequency pallidal stimulation disrupts information flow through the pallidum by gabaergic inhibition*, *The Journal of neuroscience : the official journal of the Society for Neuroscience*, 33 (2013), pp. 2268–2280.
- [52] L. N. CLARK, N. PARK, S. KISSELEV, E. RIOS, J. H. LEE, AND E. D. LOUIS, *Replication of the lingo1 gene association with essential tremor in a north american population*, *European journal of human genetics : EJHG*, 18 (2010), pp. 838–843.
- [53] V. A. COENEN, A. PRESCHER, T. SCHMIDT, P. PICOZZI, AND F. L. H. GIELEN, *What is dorso-lateral in the subthalamic nucleus (stn)?—a topographic and anatomical consideration on the ambiguous description of today's primary target for deep brain stimulation (dbs) surgery*, *Acta neurochirurgica*, 150 (2008), pp. 1163–5; discussion 1165.
- [54] V. A. COENEN, T. E. SCHLAEPFER, N. ALLERT, AND B. MÄDLER, *Diffusion tensor imaging and neuromodulation: Dti as key technology for deep brain stimulation*, *International review of neurobiology*, 107 (2012), pp. 207–234.
- [55] G. C. COTZIAS, P. S. PAPAVALIOU, AND R. GELLENE, *Modification of parkinsonism—chronic treatment with l-dopa*, *The New England journal of medicine*, 280 (1969), pp. 337–345.
- [56] P. COUBES, N. VAYSSIERE, H. EL FERTIT, S. HEMM, L. CIF, J. KIENLEN, A. BONAFE, AND P. FREREBEAU, *Deep brain stimulation for dystonia. surgical technique*, *Stereotactic and functional neurosurgery*, 78 (2002), pp. 183–191.

- [57] T. D'ALBIS, C. HAEGELEN, C. ESSERT, S. FERNANDEZ-VIDAL, F. LALYS, AND P. JANNIN, *Pydbs: an automated image processing workflow for deep brain stimulation surgery*, International journal of computer assisted radiology and surgery, 10 (2015), pp. 117–128.
- [58] A. DANIELE, A. ALBANESE, M. F. CONTARINO, P. ZINZI, A. BARBIER, F. GASPARINI, L. M. A. ROMITO, A. R. BENTIVOGLIO, AND M. SCERRATI, *Cognitive and behavioural effects of chronic stimulation of the subthalamic nucleus in patients with parkinson's disease*, Journal of neurology, neurosurgery, and psychiatry, 74 (2003), pp. 175–182.
- [59] C. DE HEMPTINNE, N. C. SWANN, J. L. OSTREM, E. S. RYAPOLOVA-WEBB, M. SAN LUCIANO, N. B. GALIFIANAKIS, AND P. A. STARR, *Therapeutic deep brain stimulation reduces cortical phase-amplitude coupling in parkinson's disease*, Nature neuroscience, 18 (2015), pp. 779–786.
- [60] E. DELLA FLORA, C. L. PERERA, A. L. CAMERON, AND G. J. MADDERN, *Deep brain stimulation for essential tremor: A systematic review*, Movement Disorders, 25 (2010), pp. 1550–1559.
- [61] M. R. DELONG, *Possible involvement of central pacemakers in clinical disorders of movement*, Federation proceedings, 37 (1978), pp. 2171–2175.
- [62] M. R. DELONG, *Primate models of movement disorders of basal ganglia origin*, Trends in neurosciences, 13 (1990), pp. 281–285.
- [63] T. A. DEMBEK, M. T. BARBE, M. ASTROM, M. HOEVELS, V. VISSER-VANDEWALLE, G. R. FINK, AND L. TIMMERMANN, *Probabilistic mapping of deep brain stimulation effects in essential tremor*, Neurolmage. Clinical, 13 (2017), pp. 164–173.
- [64] H. DENG, S. GU, AND J. JANKOVIC, *Lingo1 variants in essential tremor and parkinson's disease*, Acta neurologica Scandinavica, 125 (2012), pp. 1–7.
- [65] H. DENG, W. LE, AND J. JANKOVIC, *Genetics of essential tremor*, Brain : a journal of neurology, 130 (2007), pp. 1456–1464.
- [66] P.-P. DEROST, L. OUCHCHANE, D. MORAND, M. ULLA, P.-M. LLORCA, M. BARGET, B. DEBILLY, J.-J. LEMAIRE, AND F. DURIF, *Is dbs-stn appropriate to treat severe parkinson disease in an elderly population?*, Neurology, 68 (2007), pp. 1345–1355.
- [67] G. DEUSCHL, P. BAIN, AND M. BRIN, *Consensus statement of the movement disorder society on tremor. ad hoc scientific committee*, Movement disorders : official journal of the Movement Disorder Society, 13 Suppl 3 (1998), pp. 2–23.

- [68] G. DEUSCHL, J. RAETHJEN, M. LINDEMANN, AND P. KRACK, *The pathophysiology of tremor*, *Muscle & nerve*, 24 (2001), pp. 716–735.
- [69] A. DEVOR, *The great gate: Control of sensory information flow to the cerebellum*, *Cerebellum* (London, England), 1 (2002), pp. 27–34.
- [70] P.-F. D’HAESE, S. PALLAVARAM, R. LI, M. S. REMPLE, C. KAO, J. S. NEIMAT, P. E. KONRAD, AND B. M. DAWANT, *Cranialvault and its crave tools: a clinical computer assistance system for deep brain stimulation (dbs) therapy*, *Medical image analysis*, 16 (2012), pp. 744–753.
- [71] O. DOGU, E. D. LOUIS, S. SEVIM, H. KALEAGASI, AND M. ARAL, *Clinical characteristics of essential tremor in mersin, turkey—a population-based door-to-door study*, *Journal of neurology*, 252 (2005), pp. 570–574.
- [72] O. DOGU, E. D. LOUIS, L. TAMER, O. UNAL, A. YILMAZ, AND H. KALEAGASI, *Elevated blood lead concentrations in essential tremor: A case-control study in mersin, turkey*, *Environmental health perspectives*, 115 (2007), pp. 1564–1568.
- [73] O. DOGU, S. SEVIM, H. CAMDEVIREN, T. SASMAZ, R. BUGDAYCI, M. ARAL, H. KALEAGASI, S. UN, AND E. D. LOUIS, *Prevalence of essential tremor: Door-to-door neurologic exams in mersin province, turkey*, *Neurology*, 61 (2003), pp. 1804–1806.
- [74] A. D. DORVAL AND W. M. GRILL, *Deep brain stimulation of the subthalamic nucleus reestablishes neuronal information transmission in the 6-ohda rat model of parkinsonism*, *Journal of neurophysiology*, 111 (2014), pp. 1949–1959.
- [75] P. K. DOSHI, *Expanding indications for deep brain stimulation*, *Neurology India*, 66 (2018), pp. S102–S112.
- [76] J. O. DOSTROVSKY, R. LEVY, J. P. WU, W. D. HUTCHISON, R. R. TASKER, AND A. M. LOZANO, *Microstimulation-induced inhibition of neuronal firing in human globus pallidus*, *Journal of neurophysiology*, 84 (2000), pp. 570–574.
- [77] L. M. F. DOYLE, A. A. KÜHN, M. HARIZ, A. KUPSCH, G.-H. SCHNEIDER, AND P. BROWN, *Levodopa-induced modulation of subthalamic beta oscillations during self-paced movements in patients with parkinson’s disease*, *The European journal of neuroscience*, 21 (2005), pp. 1403–1412.
- [78] J. DOYON, *Motor sequence learning and movement disorders*, *Current opinion in neurology*, 21 (2008), pp. 478–483.

- [79] M. J. DUPUIS, P. J. DELWAIDE, D. BOUCQUEY, AND R. E. GONSETTE, *Homolateral disappearance of essential tremor after cerebellar stroke*, *Movement disorders : official journal of the Movement Disorder Society*, 4 (1989), pp. 183–187.
- [80] R. ELBLE, C. COMELLA, S. FAHN, M. HALLETT, J. JANKOVIC, J. L. JUNCOS, P. LEWITT, K. LYONS, W. ONDO, R. PAHWA, K. SETHI, N. STOVER, D. TARSY, C. TESTA, R. TINTNER, R. WATTS, AND T. ZESIEWICZ, *Reliability of a new scale for essential tremor*, *Movement Disorders*, 27 (2012), pp. 1567–1569.
- [81] R. J. ELBLE, *Diagnostic criteria for essential tremor and differential diagnosis*, *Neurology*, 54 (2000), pp. S2–6.
- [82] R. J. ELBLE, *Essential tremor is a monosymptomatic disorder*, *Movement disorders : official journal of the Movement Disorder Society*, 17 (2002), pp. 633–637.
- [83] R. J. ELBLE, *Gravitational artifact in accelerometric measurements of tremor*, *Clinical neurophysiology : official journal of the International Federation of Clinical Neurophysiology*, 116 (2005), pp. 1638–1643.
- [84] R. J. ELBLE AND J. MCNAMES, *Using portable transducers to measure tremor severity*, *Tremor and other hyperkinetic movements* (New York, N.Y.), 6 (2016), p. 375.
- [85] R. J. ELBLE, S. L. PULLMAN, J. Y. MATSUMOTO, J. RAETHJEN, G. DEUSCHL, AND R. TINTNER, *Tremor amplitude is logarithmically related to 4- and 5-point tremor rating scales*, *Brain : a journal of neurology*, 129 (2006), pp. 2660–2666.
- [86] T. ENDO, R. OKUNO, M. YOKOE, K. AKAZAWA, AND S. SAKODA, *A novel method for systematic analysis of rigidity in parkinson's disease*, *Movement disorders : official journal of the Movement Disorder Society*, 24 (2009), pp. 2218–2224.
- [87] EUROPEAN MEDICINES AGENCY, *Guideline on clinical investigation of medicinal products in the guideline on clinical investigation of medicinal products in the treatment of parkinson's disease. [document reference: Ema/chmp/330418/2012 rev. 2;online]*, 2012.
- [88] S. FAHN, *The medical treatment of parkinson disease from james parkinson to george cotzias*, *Movement Disorders*, 30 (2015), pp. 4–18.
- [89] S. FAHN, C. D. MARSDEN, M. GOLDSTEIN, AND D. B. CALNE, eds., *Recent developments in Parkinson's disease*, Macmillan Healthcare Information, Florham Park, 1987.

- [90] S. FAHN, E. TOLOSA, AND C. MARÍN, *Clinical rating scale for tremor*, Parkinson's disease and movement disorders. Baltimore: Williams and Wilkins, (1993), pp. 271–280.
- [91] D. FARINA, C. CESCONE, AND R. MERLETTI, *Influence of anatomical, physical, and detection-system parameters on surface emg*, Biological cybernetics, 86 (2002), pp. 445–456.
- [92] S. FARRIS AND M. GIROUX, *Retrospective review of factors leading to dissatisfaction with subthalamic nucleus deep brain stimulation during long-term management*, Surgical neurology international, 4 (2013), p. 69.
- [93] A. FASANO, J. HERZOG, J. RAETHJEN, F. E. M. ROSE, M. MUTHURAMAN, J. VOLKMANN, D. FALK, R. ELBLE, AND G. DEUSCHL, *Gait ataxia in essential tremor is differentially modulated by thalamic stimulation*, Brain : a journal of neurology, 133 (2010), pp. 3635–3648.
- [94] A. J. FENOY AND R. K. SIMPSON, *Risks of common complications in deep brain stimulation surgery: management and avoidance*, Journal of neurosurgery, 120 (2014), pp. 132–139.
- [95] F. S. FERNÁNDEZ, M. A. ALVAREZ VEGA, A. ANTUÑA RAMOS, F. FERNÁNDEZ GONZÁLEZ, AND B. LOZANO ARAGONESES, *Lead fractures in deep brain stimulation during long-term follow-up*, Parkinson's disease, 2010 (2010), p. 409356.
- [96] M. M. FILIPPI, M. OLIVERI, P. PASQUALETTI, P. CICINELLI, R. TRAVERSA, F. VERNIERI, M. G. PALMIERI, AND P. M. ROSSINI, *Effects of motor imagery on motor cortical output topography in parkinson's disease*, Neurology, 57 (2001), pp. 55–61.
- [97] L. J. FINDLEY, *The economic impact of parkinson's disease*, Parkinsonism & Related Disorders, 13 Suppl (2007), pp. S8–S12.
- [98] A. FLÖEL, C. BREITENSTEIN, F. HUMMEL, P. CELNIK, C. GINGERT, L. SAWAKI, S. KNECHT, AND L. G. COHEN, *Dopaminergic influences on formation of a motor memory*, Annals of Neurology, 58 (2005), pp. 121–130.
- [99] K. A. FOLLETT, F. M. WEAVER, M. STERN, K. HUR, C. L. HARRIS, P. LUO, W. J. MARKS, J. ROTHLIND, O. SAGHER, C. MOY, R. PAHWA, K. BURCHIEL, P. HOGARTH, E. C. LAI, J. E. DUDA, K. HOLLOWAY, A. SAMII, S. HORN, J. M. BRONSTEIN, G. STONER, P. A. STARR, R. SIMPSON, G. BALTUCH, A. DE SALLES, G. D. HUANG, AND D. J. REDA, *Pallidal versus subthalamic deep-brain stimulation for parkinson's disease*, The New England journal of medicine, 362 (2010), pp. 2077–2091.

- [100] J. FROMENT AND H. GARDÈRE, *Parkinsonisme fruste et perte des mouvements automatiques associés, sans rigidité apparente. De la rigidité latente et des moyens de la rendre évidente, par MM. J. Froment et H. Gardère (de Lyon)*, Société française d'imprimerie, 1926.
- [101] V. S. FUNG, J. A. BURNE, AND J. G. MORRIS, *Objective quantification of resting and activated parkinsonian rigidity: a comparison of angular impulse and work scores*, *Movement disorders : official journal of the Movement Disorder Society*, 15 (2000), pp. 48–55.
- [102] A. FYTAGORIDIS, M. ASTROM, K. WARDELL, AND P. BLOMSTEDT, *Stimulation-induced side effects in the posterior subthalamic area: distribution, characteristics and visualization*, *Clinical neurology and neurosurgery*, 115 (2013), pp. 65–71.
- [103] A. FYTAGORIDIS, U. SANDVIK, M. ASTROM, T. BERGENHEIM, AND P. BLOMSTEDT, *Long term follow-up of deep brain stimulation of the caudal zona incerta for essential tremor*, *Journal of neurology, neurosurgery, and psychiatry*, 83 (2012), pp. 258–262.
- [104] C. GANTERT, J. HONERKAMP, AND J. TIMMER, *Analyzing the dynamics of hand tremor time series*, *Biological cybernetics*, 66 (1992), pp. 479–484.
- [105] M. G. GARCÍA-GOMAR, J. SOTO-ABRAHAM, F. VELASCO-CAMPOS, AND L. CONCHA, *Anatomic characterization of prelemniscal radiations by probabilistic tractography: implications in parkinson's disease*, *Brain Structure and Function*, (2016), pp. 1–11.
- [106] I. M. GARONZIK, S. E. HUA, S. OHARA, AND F. A. LENZ, *Intra-operative microelectrode and semi-microelectrode recording during the physiological localization of the thalamic nucleus ventral intermediate*, *Movement disorders : official journal of the Movement Disorder Society*, 17 Suppl 3 (2002), pp. S135–44.
- [107] P. GATEV, O. DARBIN, AND T. WICHMANN, *Oscillations in the basal ganglia under normal conditions and in movement disorders*, *Movement disorders : official journal of the Movement Disorder Society*, 21 (2006), pp. 1566–1577.
- [108] M. S. GAZZANIGA, R. B. IVRY, AND G. R. MANGUN, *Cognitive neuroscience: The biology of the mind*, W. W. Norton & Company Inc, New York N.Y., fourth edition ed., 2013.
- [109] C. R. GERFEN, T. M. ENGBER, L. C. MAHAN, Z. SUSEL, T. N. CHASE, F. J. MONSMA, AND D. R. SIBLEY, *D1 and d2 dopamine receptor-regulated gene expression of striatonigral and striatopallidal neurons*, *Science (New York, N.Y.)*, 250 (1990), pp. 1429–1432.

- [110] C. GHEZ, CLAUDE P. J., AND S. FAHN, *The cerebellum*, in Principles of neural science, E. R. Kandel, J. H. Schwartz, and T. M. Jessell, eds., Elsevier, 1991, pp. 502–522.
- [111] A. GIRONELL, J. KULISEVSKY, L. RAMI, N. FORTUNY, C. GARCÍA-SÁNCHEZ, AND B. PASCUAL-SEDANO, *Effects of pallidotomy and bilateral subthalamic stimulation on cognitive function in parkinson disease. a controlled comparative study*, Journal of neurology, 250 (2003), pp. 917–923.
- [112] F. GODINHO, S. THOBOIS, M. MAGNIN, M. GUENOT, G. POLO, I. BENATRU, J. XIE, A. SALVETTI, L. GARCIA-LARREA, E. BROUS-SOLLE, AND P. MERTENS, *Subthalamic nucleus stimulation in parkinson's disease: Anatomical and electrophysiological localization of active contacts*, Journal of neurology, 253 (2006), pp. 1347–1355.
- [113] C. G. GOETZ, Y. LIU, G. T. STEBBINS, L. WANG, B. C. TILLEY, J. A. TERESI, D. MERKITCH, AND S. LUO, *Gender-, age-, and race/ethnicity-based differential item functioning analysis of the movement disorder society-sponsored revision of the unified parkinson's disease rating scale*, Movement Disorders, 31 (2016), pp. 1865–1873.
- [114] C. G. GOETZ, W. POEWE, O. RASCOL, C. SAMPAIO, G. T. STEBBINS, C. COUNSELL, N. GILADI, R. G. HOLLOWAY, C. G. MOORE, G. K. WENNING, M. D. YAHR, AND L. SEIDL, *Movement disorder society task force report on the hoehn and yahr staging scale: status and recommendations*, Movement disorders : official journal of the Movement Disorder Society, 19 (2004), pp. 1020–1028.
- [115] C. G. GOETZ, W. POEWE, O. RASCOL, C. SAMPAIO, G. T. STEBBINS, S. FAHN, A. E. LANG, P. MARTINEZ-MARTIN, B. TILLEY, B. VAN HILTEN, C. KLECZKA, AND L. SEIDL, *The unified parkinson's disease rating scale (updrs): status and recommendations*, Movement disorders : official journal of the Movement Disorder Society, 18 (2003), pp. 738–750.
- [116] C. G. GOETZ, G. T. STEBBINS, T. A. CHMURA, S. FAHN, H. L. KLAWANS, AND C. D. MARSDEN, *Teaching tape for the motor section of the unified parkinson's disease rating scale*, Movement disorders : official journal of the Movement Disorder Society, 10 (1995), pp. 263–266.
- [117] C. G. GOETZ, B. C. TILLEY, S. R. SHAFTMAN, G. T. STEBBINS, S. FAHN, P. MARTINEZ-MARTIN, W. POEWE, C. SAMPAIO, M. B. STERN, R. DODEL, B. DUBOIS, R. HOLLOWAY, J. JANKOVIC, J. KULISEVSKY, A. E. LANG, A. LEES, S. LEURGANS, P. A. LEWITT, D. NYENHUIS, C. W. OLANOW, O. RASCOL, A. SCHRAG, J. A. TERESI, VAN HILTEN, JACOBUS J, AND N. LAPELLE, *Move-*

- ment disorder society-sponsored revision of the unified parkinson's disease rating scale (mds-updrs): scale presentation and clinimetric testing results*, *Movement disorders : official journal of the Movement Disorder Society*, 23 (2008), pp. 2129–2170.
- [118] J. A. GOLDBERG, T. BORAUD, S. MARATON, S. N. HABER, E. VAADIA, AND H. BERGMAN, *Enhanced synchrony among primary motor cortex neurons in the 1-methyl-4-phenyl-1,2,3,6-tetrahydropyridine primate model of parkinson's disease*, *The Journal of neuroscience : the official journal of the Society for Neuroscience*, 22 (2002), pp. 4639–4653.
- [119] V. GRADINARU, M. MOGRI, K. R. THOMPSON, J. M. HENDERSON, AND K. DEISSEROTH, *Optical deconstruction of parkinsonian neural circuitry*, *Science (New York, N.Y.)*, 324 (2009), pp. 354–359.
- [120] A. M. GRAYBIEL, J. J. CANALES, AND C. CAPPER-LOUP, *Levodopa-induced dyskinesias and dopamine-dependent stereotypies: A new hypothesis*, *Trends in neurosciences*, 23 (2000), pp. S71–7.
- [121] R. I. GRIFFITHS, K. KOTSCHET, S. ARFON, Z. M. XU, W. JOHNSON, J. DRAGO, A. EVANS, P. KEMPSTER, S. RAGHAV, AND M. K. HORNE, *Automated assessment of bradykinesia and dyskinesia in parkinson's disease*, *Journal of Parkinson's disease*, 2 (2012), pp. 47–55.
- [122] W. M. GRILL, A. N. SNYDER, AND S. MIOCINOVIC, *Deep brain stimulation creates an informational lesion of the stimulated nucleus*, *NeuroReport*, 15 (2004), pp. 1137–1140.
- [123] G. GRIMALDI AND M. MANTO, *Neurological tremor: Sensors, signal processing and emerging applications*, *Sensors (Basel, Switzerland)*, 10 (2010), pp. 1399–1422.
- [124] S. GROPPA, J. HERZOG, D. FALK, C. RIEDEL, G. DEUSCHL, AND J. VOLKMANN, *Physiological and anatomical decomposition of subthalamic neurostimulation effects in essential tremor*, *Brain : a journal of neurology*, 137 (2014), pp. 109–121.
- [125] C. GROSS, A. ROUGIER, D. GUEHL, T. BORAUD, J. JULIEN, AND B. BIOULAC, *High-frequency stimulation of the globus pallidus internalis in parkinson's disease: A study of seven cases*, *Journal of neurosurgery*, 87 (1997), pp. 491–498.
- [126] D. GUEHL, M. PESSIGLIONE, C. FRANÇOIS, J. YELNIK, E. C. HIRSCH, J. FÉGER, AND L. TREMBLAY, *Tremor-related activity of neurons in the 'motor' thalamus: Changes in firing rate and pattern in the mptp vervet model of parkinsonism*, *The European journal of neuroscience*, 17 (2003), pp. 2388–2400.

- [127] J. R. GULCHER, P. JÓNSSON, A. KONG, K. KRISTJÁNSSON, M. L. FRIGGE, A. KÁRASON, I. E. EINARSDÓTTIR, H. STEFÁNSSON, A. S. EINARSDÓTTIR, S. SIGURTHOARDÓTTIR, S. BALDURSSON, S. BJÖRNSDÓTTIR, S. M. HRAFNKELSDÓTTIR, F. JAKOBSSON, J. BENEDICKZ, AND K. STEFÁNSSON, *Mapping of a familial essential tremor gene, fet1, to chromosome 3q13*, *Nature genetics*, 17 (1997), pp. 84–87.
- [128] T. GUO, K. W. FINNIS, A. G. PARRENT, AND T. M. PETERS, *Visualization and navigation system development and application for stereotactic deep-brain neurosurgeries*, *Computer aided surgery : official journal of the International Society for Computer Aided Surgery*, 11 (2006), pp. 231–239.
- [129] J. GURIDI, M. T. HERRERO, R. LUQUIN, J. GUILLEN, AND J. A. OBESO, *Subthalamotomy improves mptp-induced parkinsonism in monkeys*, *Stereotactic and functional neurosurgery*, 62 (1994), pp. 98–102.
- [130] G. HALLIDAY, A. LEES, AND M. STERN, *Milestones in parkinson's disease—clinical and pathologic features*, *Movement disorders : official journal of the Movement Disorder Society*, 26 (2011), pp. 1015–1021.
- [131] C. HAMANI, J. A. SAINT-CYR, J. FRASER, M. KAPLITT, AND A. M. LOZANO, *The subthalamic nucleus in the context of movement disorders*, *Brain : a journal of neurology*, 127 (2004), pp. 4–20.
- [132] W. HAMEL, U. FIETZEK, A. MORSNOWSKI, B. SCHRADER, J. HERZOG, D. WEINERT, G. PFISTER, D. MÜLLER, J. VOLKMAN, G. DEUSCHL, AND H. M. MEHDORN, *Deep brain stimulation of the subthalamic nucleus in parkinson's disease: evaluation of active electrode contacts*, *Journal of neurology, neurosurgery, and psychiatry*, 74 (2003), pp. 1036–1046.
- [133] W. HAMEL, J. HERZOG, F. KOPPER, M. PINSKER, D. WEINERT, D. MÜLLER, P. KRACK, G. DEUSCHL, AND H. M. MEHDORN, *Deep brain stimulation in the subthalamic area is more effective than nucleus ventralis intermedius stimulation for bilateral intention tremor*, *Acta neurochirurgica*, 149 (2007), pp. 749–758.
- [134] C. HAMMOND, H. BERGMAN, AND P. BROWN, *Pathological synchronization in parkinson's disease: networks, models and treatments*, *Trends in Neurosciences*, 30 (2007), pp. 357–364.
- [135] M. I. HARIZ, *From functional neurosurgery to "interventional" neurology: Survey of publications on thalamotomy, pallidotomy, and deep brain stimulation for parkinson's disease from 1966 to 2001*, *Movement disorders : official journal of the Movement Disorder Society*, 18 (2003), pp. 845–853.

- [136] M. I. HARIZ, P. KRACK, R. MELVILL, J. V. JORGENSEN, W. HAMEL, H. HIRABAYASHI, M. LENDERS, N. WESSLEN, M. TENGVAR, AND T. A. YOUSRY, *A quick and universal method for stereotactic visualization of the subthalamic nucleus before and after implantation of deep brain stimulation electrodes*, *Stereotactic and functional neurosurgery*, 80 (2003), pp. 96–101.
- [137] T. HASHIMOTO, C. M. ELDER, M. S. OKUN, S. K. PATRICK, AND J. L. VITEK, *Stimulation of the subthalamic nucleus changes the firing pattern of pallidal neurons*, *The Journal of neuroscience : the official journal of the Society for Neuroscience*, 23 (2003), pp. 1916–1923.
- [138] B. HASLINGER, P. ERHARD, N. KÄMPFE, H. BOECKER, E. RUMMENY, M. SCHWAIGER, B. CONRAD, AND A. O. CEBALLOS-BAUMANN, *Event-related functional magnetic resonance imaging in parkinson's disease before and after levodopa*, *Brain : a journal of neurology*, 124 (2001), pp. 558–570.
- [139] D. HAUBENBERGER, G. ABBRUZZESE, P. G. BAIN, N. BAJAJ, J. BENITO-LEÓN, K. P. BHATIA, G. DEUSCHL, M. J. FORJAZ, M. HALLETT, E. D. LOUIS, K. E. LYONS, T. A. MESTRE, J. RAETHJEN, M. STAMELOU, E.-K. TAN, C. M. TESTA, AND R. J. ELBLE, *Transducer-based evaluation of tremor*, *Movement Disorders*, 31 (2016), pp. 1327–1336.
- [140] D. A. HELDMAN, C. L. PULLIAM, E. URREA MENDOZA, M. GARTNER, J. P. GIUFFRIDA, E. B. MONTGOMERY, JR, A. J. ESPAY, AND F. J. REVILLA, *Computer-guided deep brain stimulation programming for parkinson's disease*, *Neuromodulation : journal of the International Neuromodulation Society*, 19 (2016), pp. 127–132.
- [141] C. HELMCHEN, A. HAGENOW, J. MIESNER, A. SPRENGER, H. RAMBOLD, R. WENZELBURGER, W. HEIDE, AND G. DEUSCHL, *Eye movement abnormalities in essential tremor may indicate cerebellar dysfunction*, *Brain : a journal of neurology*, 126 (2003), pp. 1319–1332.
- [142] R. C. HELMICH, M. HALLETT, G. DEUSCHL, I. TONI, AND B. R. BLOEM, *Cerebral causes and consequences of parkinsonian resting tremor: a tale of two circuits?*, *Brain : a journal of neurology*, (2012).
- [143] S. HEMM, G. MENNESSIER, N. VAYSSIERE, L. CIF, H. EL FERITIT, AND P. COUBES, *Deep brain stimulation in movement disorders: Stereotactic coregistration of two-dimensional electrical field modeling and magnetic resonance imaging*, *Journal of neurosurgery*, 103 (2005), pp. 949–955.
- [144] S. HEMM AND K. WÄRDELL, *Stereotactic implantation of deep brain stimulation electrodes: a review of technical systems, methods and emerg-*

- ing tools*, Medical & Biological Engineering & Computing, 48 (2010), pp. 611–624.
- [145] S. HERCULANO-HOUZEL, *Coordinated scaling of cortical and cerebellar numbers of neurons*, Frontiers in neuroanatomy, 4 (2010), p. 12.
- [146] J. HERZOG, W. HAMEL, R. WENZELBURGER, M. PÖTTER, M. O. PINSKER, J. BARTUSSEK, A. MORSNOWSKI, F. STEIGERWALD, G. DEUSCHL, AND J. VOLKMANN, *Kinematic analysis of thalamic versus subthalamic neurostimulation in postural and intention tremor*, Brain : a journal of neurology, 130 (2007), pp. 1608–1625.
- [147] J. J. HIGGINS, L. T. PHO, AND L. E. NEE, *A gene (etm) for essential tremor maps to chromosome 2p22-p25*, Movement disorders : official journal of the Movement Disorder Society, 12 (1997), pp. 859–864.
- [148] O. HIKOSAKA, K. NAKAMURA, K. SAKAI, AND H. NAKAHARA, *Central mechanisms of motor skill learning*, Current opinion in neurobiology, 12 (2002), pp. 217–222.
- [149] A. HINTZEN, E. A. PELZER, AND M. TITTEMEYER, *Thalamic interactions of cerebellum and basal ganglia*, Brain Structure and Function, (2017).
- [150] T. HIRAI AND E. G. JONES, *A new parcellation of the human thalamus on the basis of histochemical staining*, Brain Research Reviews, 14 (1989), pp. 1–34.
- [151] E. C. HIRSCH, P. JENNER, AND S. PRZEDBORSKI, *Pathogenesis of parkinson's disease*, Movement disorders : official journal of the Movement Disorder Society, 28 (2013), pp. 24–30.
- [152] M. M. HOEHN AND M. D. YAHR, *Parkinsonism: onset, progression and mortality*, Neurology, 17 (1967), pp. 427–442.
- [153] A. HOSSEN, M. MUTHURAMAN, J. RAETHJEN, G. DEUSCHL, AND U. HEUTE, *Discrimination of parkinsonian tremor from essential tremor by implementation of a wavelet-based soft-decision technique on emg and accelerometer signals*, Biomedical Signal Processing and Control, 5 (2010), pp. 181–188.
- [154] A. HRISTOVA, K. LYONS, A. I. TRÖSTER, R. PAHWA, S. B. WILKINSON, AND W. C. KOLLER, *Effect and time course of deep brain stimulation of the globus pallidus and subthalamus on motor features of parkinson's disease*, Clinical neuropharmacology, 23 (2000), pp. 208–211.
- [155] J. P. HUBBLE, K. L. BUSENBARK, R. PAHWA, K. LYONS, AND W. C. KOLLER, *Clinical expression of essential tremor: Effects of gender*

- and age*, *Movement disorders : official journal of the Movement Disorder Society*, 12 (1997), pp. 969–972.
- [156] A. J. HUGHES, S. E. DANIEL, L. KILFORD, AND A. J. LEES, *Accuracy of clinical diagnosis of idiopathic parkinson's disease: A clinico-pathological study of 100 cases*, *Journal of neurology, neurosurgery, and psychiatry*, 55 (1992), pp. 181–184.
- [157] S. JAIN, S. E. LO, AND E. D. LOUIS, *Common misdiagnosis of a common neurological disorder: How are we misdiagnosing essential tremor?*, *Archives of neurology*, 63 (2006), pp. 1100–1104.
- [158] S. C. JANICKI, S. COSENTINO, AND E. D. LOUIS, *The cognitive side of essential tremor: What are the therapeutic implications?*, *Therapeutic advances in neurological disorders*, 6 (2013), pp. 353–368.
- [159] J. JANKOVIC, *Parkinson's disease: clinical features and diagnosis*, *Journal of neurology, neurosurgery, and psychiatry*, 79 (2008), pp. 368–376.
- [160] J. JANKOVIC AND J. D. FROST, *Quantitative assessment of parkinsonian and essential tremor: Clinical application of triaxial accelerometry*, *Neurology*, 31 (1981), p. 1235.
- [161] J. JANKOVIC, M. MCDERMOTT, J. CARTER, S. GAUTHIER, C. GOETZ, L. GOLBE, S. HUBER, W. KOLLER, C. OLANOW, AND I. SHOULSON, *Variable expression of parkinson's disease: A base-line analysis of the datatop cohort. the parkinson study group*, *Neurology*, 40 (1990), pp. 1529–1534.
- [162] J. JANKOVIC AND E. TOLOSA, eds., *Parkinson's disease & movement disorders*, Lippincott Williams & Wilkins, Philadelphia, PA, USA, 6th edition ed., 2015.
- [163] K. A. JELLINGER, *Formation and development of lewy pathology: A critical update*, *Journal of neurology*, 256 Suppl 3 (2009), pp. 270–279.
- [164] M. D. JOHNSON, S. MIOCINOVIC, C. C. MCINTYRE, AND J. L. VITEK, *Mechanisms and targets of deep brain stimulation in movement disorders*, *Neurotherapeutics*, 5 (2008), pp. 294–308.
- [165] W. H. JOST, *Autonomic dysfunctions in idiopathic parkinson's disease*, *Journal of neurology*, 250 Suppl 1 (2003), pp. 128–30.
- [166] H. L. JOURNEE, A. A. POSTMA, AND M. J. STAAL, *Intraoperative neurophysiological assessment of disabling symptoms in dbs surgery*, *Neurophysiologie clinique = Clinical neurophysiology*, 37 (2007), pp. 467–475.
- [167] H. L. JOURNÉE, A. A. POSTMA, M. SUN, AND M. J. STAAL, *Detection of tremor bursts by a running second order moment function and*

- analysis using interburst histograms*, Medical engineering & physics, 30 (2008), pp. 75–83.
- [168] M. F. KHAN, K. MEWES, R. E. GROSS, AND O. SKRINJAR, *Assessment of brain shift related to deep brain stimulation surgery*, Stereotactic and functional neurosurgery, 86 (2008), pp. 44–53.
- [169] S. KLEBE, H. STOLZE, K. GRENSING, J. VOLKMANN, R. WENZELBURGER, AND G. DEUSCHL, *Influence of alcohol on gait in patients with essential tremor*, Neurology, 65 (2005), pp. 96–101.
- [170] J. C. KLEIN, B. LORENZ, J.-S. KANG, S. BAUDREXEL, C. SEIFRIED, S. VAN DE LOO, H. STEINMETZ, R. DEICHMANN, AND R. HILKER, *Diffusion tensor imaging of white matter involvement in essential tremor*, Human brain mapping, 32 (2011), pp. 896–904.
- [171] J. H. KO, C. C. TANG, AND D. EIDELBERG, *Brain stimulation and functional imaging with fmri and pet*, Handbook of clinical neurology, 116 (2013), pp. 77–95.
- [172] J. KOERTS, K. L. LEENDERS, M. KONING, A. T. PORTMAN, AND M. VAN BEILEN, *Striatal dopaminergic activity (fdopa-pet) associated with cognitive items of a depression scale (madr) in parkinson's disease*, The European journal of neuroscience, 25 (2007), pp. 3132–3136.
- [173] J. KOJIMA, Y. YAMAJI, M. MATSUMURA, A. NAMBU, M. INASE, H. TOKUNO, M. TAKADA, AND H. IMAI, *Excitotoxic lesions of the pedunculopontine tegmental nucleus produce contralateral hemiparkinsonism in the monkey*, Neuroscience letters, 226 (1997), pp. 111–114.
- [174] M. J. KOVACH, J. RUIZ, K. KIMONIS, S. MUEED, S. SINHA, C. HIGGINS, S. ELBLE, R. ELBLE, AND V. E. KIMONIS, *Genetic heterogeneity in autosomal dominant essential tremor*, Genetics in medicine : official journal of the American College of Medical Genetics, 3 (2001), pp. 197–199.
- [175] S. L. KOWAL, T. M. DALL, R. CHAKRABARTI, M. V. STORM, AND A. JAIN, *The current and projected economic burden of parkinson's disease in the united states*, Movement disorders : official journal of the Movement Disorder Society, 28 (2013), pp. 311–318.
- [176] S. E. KRAHL, F. C. MARTIN, AND A. HANDFORTH, *Vagus nerve stimulation inhibits harmaline-induced tremor*, Brain research, 1011 (2004), pp. 135–138.
- [177] Y. KWON, S. H. PARK, J. W. KIM, Y. HO, H. M. JEON, M. J. BANG, S. B. KOH, J. H. KIM, AND G. M. EOM, *Quantitative evaluation of parkinsonian rigidity during intra-operative deep brain stimulation*, Bio-medical materials and engineering, 24 (2014), pp. 2273–2281.

- [178] L. V. LAITINEN, *Pallidotomy for parkinson's disease*, *Neurosurgery clinics of North America*, 6 (1995), pp. 105–112.
- [179] F. LALYS, C. HAEGELEN, M. MEHRI, S. DRAPIER, M. VÉRIN, AND P. JANNIN, *Anatomo-clinical atlases correlate clinical data and electrode contact coordinates: Application to subthalamic deep brain stimulation*, *Journal of Neuroscience Methods*, 212 (2013), pp. 297–307.
- [180] J. LANGSTON, P. BALLARD, J. TETRUD, AND I. IRWIN, *Chronic parkinsonism in humans due to a product of meperidine-analog synthesis*, *Science (New York, N.Y.)*, 219 (1983), pp. 979–980.
- [181] M. LAUK, J. TIMMER, B. GUSCHLBAUER, B. HELLWIG, AND C. H. LÜCKING, *Variability of frequency and phase between antagonistic muscle pairs in pathological human tremors*, *Muscle & nerve*, 24 (2001), pp. 1365–1370.
- [182] A. LEE AND R. M. GILBERT, *Epidemiology of parkinson disease*, *Neurologic Clinics*, 34 (2016), pp. 955–965.
- [183] S.-M. LEE, M. KIM, H. M. LEE, K.-Y. KWON, AND S.-B. KOH, *Nonmotor symptoms in essential tremor: Comparison with parkinson's disease and normal control*, *Journal of the Neurological Sciences*, 349 (2015), pp. 168–173.
- [184] A. J. LEES, *Unresolved issues relating to the shaking palsy on the celebration of james parkinson's 250th birthday*, *Movement disorders : official journal of the Movement Disorder Society*, 22 Suppl 17 (2007), pp. S327–34.
- [185] G. LEISMAN, R. MELILLO, AND F. R., *Clinical motor and cognitive neurobehavioral relationships in the basal ganglia*, in *Basal Ganglia - An Integrative View*, F. A. Barrios, ed., InTech, 2013.
- [186] J. J. LEMAIRE, F. CAIRE, J. M. BONY, J. L. KEMENY, VILLEGER A, AND J. CHAZAL, *Contribution of 4.7 tesla mri in the analysis of the mri anatomy of the human subthalamic area*, *Acta neurochirurgica*, 146 (2004), pp. 906–907.
- [187] J.-J. LEMAIRE, L. SAKKA, L. OUCHCHANE, F. CAIRE, J. GABRIL-LARGUES, AND J.-M. BONNY, *Anatomy of the human thalamus based on spontaneous contrast and microscopic voxels in high-field magnetic resonance imaging*, *Neurosurgery*, 66 (2010), pp. 161–172.
- [188] F. A. LENZ, J. O. DOSTROVSKY, R. R. TASKER, K. YAMASHIRO, H. C. KWAN, AND J. T. MURPHY, *Single-unit analysis of the human ventral thalamic nuclear group: Somatosensory responses*, *Journal of neurophysiology*, 59 (1988), pp. 299–316.

- [189] F. A. LENZ, R. R. TASKER, H. C. KWAN, S. SCHNIDER, R. KWONG, Y. MURAYAMA, J. O. DOSTROVSKY, AND J. T. MURPHY, *Single unit analysis of the human ventral thalamic nuclear group: Correlation of thalamic "tremor cells" with the 3-6 hz component of parkinsonian tremor*, *Journal of Neuroscience*, 8 (1988), pp. 754–764.
- [190] S. LESAGE AND A. BRICE, *Parkinson's disease: From monogenic forms to genetic susceptibility factors*, *Human molecular genetics*, 18 (2009), pp. R48–59.
- [191] J. LEVIN, S. KRAFCZYK, P. VALKOVIC, T. EGGERT, J. CLAASSEN, AND K. BÖTZEL, *Objective measurement of muscle rigidity in parkinsonian patients treated with subthalamic stimulation*, *Movement disorders : official journal of the Movement Disorder Society*, 24 (2009), pp. 57–63.
- [192] R. LEVY, W. D. HUTCHISON, A. M. LOZANO, AND J. O. DOSTROVSKY, *Synchronized neuronal discharge in the basal ganglia of parkinsonian patients is limited to oscillatory activity*, *The Journal of neuroscience : the official journal of the Society for Neuroscience*, 22 (2002), pp. 2855–2861.
- [193] D. LINDENBACH AND C. BISHOP, *Critical involvement of the motor cortex in the pathophysiology and treatment of parkinson's disease*, *Neuroscience and biobehavioral reviews*, 37 (2013), pp. 2737–2750.
- [194] S. LITTLE, A. POGOSYAN, A. A. KUHN, AND P. BROWN,  *$\beta$  band stability over time correlates with parkinsonian rigidity and bradykinesia*, *Experimental Neurology*, 236 (2012), pp. 383–388.
- [195] M. C. LOCKE, S. S. WU, K. D. FOOTE, M. SASSI, C. E. JACOBSON, R. L. RODRIGUEZ, H. H. FERNANDEZ, AND M. S. OKUN, *Weight changes in subthalamic nucleus vs globus pallidus internus deep brain stimulation: Results from the compare parkinson disease deep brain stimulation cohort*, *Neurosurgery*, 68 (2011), pp. 1233–7; discussion 1237–8.
- [196] D. LORENZ AND G. DEUSCHL, *Update on pathogenesis and treatment of essential tremor*, *Current opinion in neurology*, 20 (2007), pp. 447–452.
- [197] D. LORENZ, H. FREDERIKSEN, H. MOISES, F. KOPPER, G. DEUSCHL, AND K. CHRISTENSEN, *High concordance for essential tremor in monozygotic twins of old age*, *Neurology*, 62 (2004), pp. 208–211.
- [198] E. D. LOUIS, *Environmental epidemiology of essential tremor*, *Neuroepidemiology*, 31 (2008), pp. 139–149.
- [199] E. D. LOUIS, *Essential tremors: A family of neurodegenerative disorders?*, *Archives of neurology*, 66 (2009), pp. 1202–1208.

- [200] E. D. LOUIS, *Essential tremor: Evolving clinicopathological concepts in an era of intensive post-mortem enquiry*, *The Lancet. Neurology*, 9 (2010), pp. 613–622.
- [201] E. D. LOUIS, *Essential tremor and other forms of kinetic tremor*, in *Mechanisms and emerging therapies in tremor disorders*, G. Grimaldi and M.-U. Manto, eds., *Contemporary Clinical Neuroscience*, Springer, New York, NY, 2013, pp. 167–201.
- [202] E. D. LOUIS, *Diagnosis and management of tremor*, *Continuum (Minneapolis, Minn.)*, 22 (2016), pp. 1143–1158.
- [203] E. D. LOUIS, *Essential tremor then and now: How views of the most common tremor diathesis have changed over time*, *Parkinsonism & Related Disorders*, 46 Suppl 1 (2018), pp. S70–S74.
- [204] E. D. LOUIS, L. F. BARNES, B. FORD, S. L. PULLMAN, AND Q. YU, *Ethnic differences in essential tremor*, *Archives of neurology*, 57 (2000), pp. 723–727.
- [205] E. D. LOUIS, E. BROUSSOLLE, C. G. GOETZ, P. KRACK, P. KAUFMANN, AND P. MAZZONI, *Historical underpinnings of the term essential tremor in the late 19th century*, *Neurology*, 71 (2008), pp. 856–859.
- [206] E. D. LOUIS AND O. DOGU, *Does age of onset in essential tremor have a bimodal distribution? data from a tertiary referral setting and a population-based study*, *Neuroepidemiology*, 29 (2007), pp. 208–212.
- [207] E. D. LOUIS AND J. J. FERREIRA, *How common is the most common adult movement disorder? update on the worldwide prevalence of essential tremor*, *Movement Disorders*, 25 (2010), pp. 534–541.
- [208] E. D. LOUIS, L. S. HONIG, J. P. G. VONSATTEL, D. M. MARAGANORE, S. BORDEN, AND C. B. MOSKOWITZ, *Essential tremor associated with focal nonnigral lewy bodies: A clinicopathologic study*, *Archives of neurology*, 62 (2005), pp. 1004–1007.
- [209] E. D. LOUIS AND R. OTTMAN, *How familial is familial tremor? the genetic epidemiology of essential tremor*, *Neurology*, 46 (1996), pp. 1200–1205.
- [210] E. D. LOUIS AND R. OTTMAN, *Is there a one-way street from essential tremor to parkinson's disease? possible biological ramifications*, *European journal of neurology*, 20 (2013), pp. 1440–1444.
- [211] E. D. LOUIS, R. OTTMAN, B. FORD, S. PULLMAN, M. MARTINEZ, S. FAHN, AND W. A. HAUSER, *The washington heights-inwood genetic study of essential tremor: Methodologic issues in essential-tremor research*, *Neuroepidemiology*, 16 (1997), pp. 124–133.

- [212] E. D. LOUIS, S. P. THAWANI, AND H. F. ANDREWS, *Prevalence of essential tremor in a multiethnic, community-based study in northern manhattan, new york, n.y.*, *Neuroepidemiology*, 32 (2009), pp. 208–214.
- [213] E. D. LOUIS AND J. P. G. VONSATTEL, *The emerging neuropathology of essential tremor*, *Movement Disorders*, 23 (2008), pp. 174–182.
- [214] A. M. LOZANO AND R. LEVY, *Reoperation of deep brain stimulation in patients with essential tremor*, *World neurosurgery*, 78 (2012), pp. 442–444.
- [215] C. LOZZA, J.-C. BARON, D. EIDELBERG, M. J. MENTIS, M. CARBON, AND R.-M. MARIÉ, *Executive processes in parkinson's disease: Fdg-pet and network analysis*, *Human brain mapping*, 22 (2004), pp. 236–245.
- [216] S. MA, T. L. DAVIS, M. A. BLAIR, J. Y. FANG, Y. BRADFORD, J. L. HAINES, AND P. HEDERA, *Familial essential tremor with apparent autosomal dominant inheritance: Should we also consider other inheritance modes?*, *Movement disorders : official journal of the Movement Disorder Society*, 21 (2006), pp. 1368–1374.
- [217] A. MAERCKER, A. PERKONIGG, M. PREISIG, K. SCHALLER, AND M. WELLER, *The costs of disorders of the brain in switzerland: An update from the european brain council study for 2010*, *Swiss medical weekly*, 143 (2013), p. w13751.
- [218] C. MAGARIÑOS-ASCONE, J. PAZO, O. MACADAR, AND W. BUÑO, *High-frequency stimulation of the subthalamic nucleus silences subthalamic neurons: A possible cellular mechanism in parkinson's disease*, *Neuroscience*, 115 (2002), pp. 1109–1117.
- [219] L. MALLET, M. POLOSAN, N. JAAFARI, N. BAUP, M.-L. WELTER, D. FONTAINE, S. T. DU MONTCEL, J. YELNIK, I. CHÉREAU, C. ARBUS, S. RAOUL, B. AOUIZERATE, P. DAMIER, S. CHABARDÈS, V. CZERNECKI, C. ARDOUIN, M.-O. KREBS, E. BARDINET, P. CHAYNES, P. BURBAUD, P. CORNU, P. DEROST, T. BOUGEROL, B. BATAILLE, V. MATTEI, D. DORMONT, B. DEVAUX, M. VÉRIN, J.-L. HOUETO, P. POLLAK, A.-L. BENABID, Y. AGID, P. KRACK, B. MILLET, AND A. PELISSOLO, *Subthalamic nucleus stimulation in severe obsessive-compulsive disorder*, *The New England journal of medicine*, 359 (2008), pp. 2121–2134.
- [220] MARTENS, H C F, E. TOADER, DECRÉ, M M J, D. J. ANDERSON, R. VETTER, D. R. KIPKE, K. B. BAKER, M. D. JOHNSON, AND J. L. VITEK, *Spatial steering of deep brain stimulation volumes using a novel lead design*, *Clinical neurophysiology : official journal of the International Federation of Clinical Neurophysiology*, 122 (2011), pp. 558–566.

- [221] F. C. MARTIN AND A. HANDFORTH, *Carbenoxolone and mefloquine suppress tremor in the harmaline mouse model of essential tremor*, *Movement disorders : official journal of the Movement Disorder Society*, 21 (2006), pp. 1641–1649.
- [222] R. C. R. MARTINEZ, C. HAMANI, M. C. DE CARVALHO, A. R. DE OLIVEIRA, E. ALHO, J. NAVARRO, M. G. DOS SANTOS GHI-LARDI, E. BOR-SENG-SHU, H. HEINSEN, J. P. OTOCH, M. L. BRANDÃO, E. R. BARBOSA, M. J. TEIXEIRA, AND E. T. FONOFF, *Intraoperative dopamine release during globus pallidus internus stimulation in parkinson's disease*, *Movement Disorders*, 28 (2013), pp. 2027–2032.
- [223] P. MARTÍNEZ-MARTÍN, A. GIL-NAGEL, L. M. GRACIA, J. B. GÓMEZ, J. MARTÍNEZ-SARRIÉS, AND F. BERMEJO, *Unified parkinson's disease rating scale characteristics and structure. the cooperative multicentric group*, *Movement disorders : official journal of the Movement Disorder Society*, 9 (1994), pp. 76–83.
- [224] A. MATHAI AND Y. SMITH, *The corticostriatal and corticosubthalamic pathways: Two entries, one target. so what?*, *Frontiers in Systems Neuroscience*, 5 (2011), p. 64.
- [225] A. R. D. MATHY, *Structure and Function in the Inferior Olivary Nucleus*, doctoral thesis, University College London, London, 2012.
- [226] C. C. MCINTYRE, W. M. GRILL, D. L. SHERMAN, AND N. V. THAKOR, *Cellular effects of deep brain stimulation: Model-based analysis of activation and inhibition*, *Journal of neurophysiology*, 91 (2004), pp. 1457–1469.
- [227] C. C. MCINTYRE, M. SAVASTA, L. KERKERIAN-LE GOFF, AND J. L. VITEK, *Uncovering the mechanism(s) of action of deep brain stimulation: activation, inhibition, or both*, *Clinical Neurophysiology*, 115 (2004), pp. 1239–1248.
- [228] R. J. MEARA AND F. W. CODY, *Stretch reflexes of individual parkinsonian patients studied during changes in clinical rigidity following medication*, *Electroencephalography and clinical neurophysiology*, 89 (1993), pp. 261–268.
- [229] S. H. MEHTA, J. C. MORGAN, AND K. D. SETHI, *Sleep disorders associated with parkinson's disease: Role of dopamine, epidemiology, and clinical scales of assessment*, *CNS spectrums*, 13 (2008), pp. 6–11.
- [230] A. Y. MEIGAL, S. M. RISSANEN, M. P. TARVAINEN, O. AIRAKSINEN, M. KANKAANPÄÄ, AND P. A. KARJALAINEN, *Non-linear emg*

- parameters for differential and early diagnostics of parkinson's disease*, *Frontiers in neurology*, 4 (2013), p. 135.
- [231] A. Y. MEIGAL, S. M. RISSANEN, M. P. TARVAINEN, S. D. GEORGIADIS, P. A. KARJALAINEN, O. AIRAKSINEN, AND M. KANKAANPAA, *Linear and nonlinear tremor acceleration characteristics in patients with parkinson's disease*, *Physiological measurement*, 33 (2012), pp. 395–412.
- [232] S. J. MELDRUM AND B. W. WATSON, *Tremor recording in parkinson's disease*, *Physics in Medicine and Biology*, 15 (1970), pp. 249–254.
- [233] T. MERA, J. L. VITEK, J. L. ALBERTS, AND J. P. GIUFFRIDA, *Kinematic optimization of deep brain stimulation across multiple motor symptoms in parkinson's disease*, *Journal of Neuroscience Methods*, 198 (2011), pp. 280–286.
- [234] A. MINGUEZ-CASTELLANOS, F. ESCAMILLA-SEVILLA, M. J. KATATI, J. M. MARTIN-LINARES, M. MEERSMANS, A. ORTEGA-MORENO, AND V. ARJONA, *Different patterns of medication change after subthalamic or pallidal stimulation for parkinson's disease: Target related effect or selection bias?*, *Journal of Neurology, Neurosurgery & Psychiatry*, 76 (2005), pp. 34–39.
- [235] Y. MIYAGI, F. SHIMA, AND T. SASAKI, *Brain shift: An error factor during implantation of deep brain stimulation electrodes*, *Journal of neurosurgery*, 107 (2007), pp. 989–997.
- [236] G. F. MOLNAR, A. PILLIAR, A. M. LOZANO, AND J. O. DOSTROVSKY, *Differences in neuronal firing rates in pallidal and cerebellar receiving areas of thalamus in patients with parkinson's disease, essential tremor, and pain*, *Journal of neurophysiology*, 93 (2005), pp. 3094–3101.
- [237] E. B. MONTGOMERY AND J. T. GALE, *Mechanisms of action of deep brain stimulation(dbs)*, *Neuroscience and biobehavioral reviews*, 32 (2008), pp. 388–407.
- [238] G. P. MOORE, L. DING, AND H. M. BRONTE-STEWART, *Concurrent parkinson tremors*, *The Journal of physiology*, 529 Pt 1 (2000), pp. 273–281.
- [239] R. MORIGAKI AND S. GOTO, *Deep brain stimulation for essential tremor*, in *Deep Brain Stimulation for Neurological Disorders*, T. Itakura, ed., Springer International Publishing and Imprint: Springer, Cham, 2015, pp. 135–155.
- [240] E. MORO, A. M. LOZANO, P. POLLAK, Y. AGID, S. REHNCRONA, J. VOLKMANN, J. KULISEVSKY, J. A. OBESO, A. ALBANESE, M. I. HARIZ, N. P. QUINN, J. D. SPEELMAN, A. L. BENABID, V. FRAIX,

- A. MENDES, M.-L. WELTER, J.-L. HOUETO, P. CORNU, D. DORMONT, A. L. TORNQVIST, R. EKBERG, A. SCHNITZLER, L. TIMMERMANN, L. WOJTECKI, A. GIRONELL, M. C. RODRIGUEZ-OROZ, J. GURIDI, A. R. BENTIVOGLIO, M. F. CONTARINO, L. ROMITO, M. SCERRATI, M. JANSSENS, AND A. E. LANG, *Long-term results of a multicenter study on subthalamic and pallidal stimulation in parkinson's disease*, *Movement Disorders*, 25 (2010), pp. 578–586.
- [241] F. MUNDINGER, *Stereotaxic interventions on the zona incerta area for treatment of extrapyramidal motor disturbances and their results*, *Confinia neurologica*, 26 (1965), pp. 222–230.
- [242] J.-I. MURATA, M. KITAGAWA, H. UESUGI, H. SAITO, Y. IWASAKI, S. KIKUCHI, K. TASHIRO, AND Y. SAWAMURA, *Electrical stimulation of the posterior subthalamic area for the treatment of intractable proximal tremor*, *Journal of neurosurgery*, 99 (2003), pp. 708–715.
- [243] M. MYSLOBODSKY, F. M. LALONDE, AND L. HICKS, *Are patients with parkinson's disease suicidal?*, *Journal of geriatric psychiatry and neurology*, 14 (2001), pp. 120–124.
- [244] K. NAKAMURA, C. W. CHRISTINE, P. A. STARR, AND W. J. MARKS, *Effects of unilateral subthalamic and pallidal deep brain stimulation on fine motor functions in parkinson's disease*, *Movement Disorders*, 22 (2007), pp. 619–626.
- [245] A. NAMBU, H. TOKUNO, AND M. TAKADA, *Functional significance of the cortico-subthalamo-pallidal 'hyperdirect' pathway*, *Neuroscience research*, 43 (2002), pp. 111–117.
- [246] D. NANDI, T. Z. AZIZ, N. GILADI, J. WINTER, AND J. F. STEIN, *Reversal of akinesia in experimental parkinsonism by gaba antagonist microinjections in the pedunculopontine nucleus*, *Brain : a journal of neurology*, 125 (2002), pp. 2418–2430.
- [247] A. NOWACKI, I. DEBOVE, M. FIECHTER, F. ROSSI, M. F. OERTEL, R. WIEST, M. SCHÜPBACH, AND C. POLLO, *Targeting accuracy of the subthalamic nucleus in deep brain stimulation surgery: Comparison between 3 t t2-weighted magnetic resonance imaging and microelectrode recording results*, *Operative neurosurgery (Hagerstown, Md.)*, (2017).
- [248] J. A. OBESO, C. W. OLANOW, M. C. RODRIGUEZ-OROZ, P. KRACK, R. KUMAR, AND A. E. LANG, *Deep-brain stimulation of the subthalamic nucleus or the pars interna of the globus pallidus in parkinson's disease*, *The New England journal of medicine*, 345 (2001), pp. 956–963.

- [249] J. A. OBESO, M. C. RODRÍGUEZ-OROZ, B. BENITEZ-TEMINO, F. J. BLESÁ, J. GURIDI, C. MARIN, AND M. RODRIGUEZ, *Functional organization of the basal ganglia: Therapeutic implications for parkinson's disease*, *Movement disorders : official journal of the Movement Disorder Society*, 23 (2008), pp. S548–S559.
- [250] V. J. J. ODEKERKEN, T. VAN LAAR, M. J. STAAL, A. MOSCH, C. F. E. HOFFMANN, P. C. G. NIJSSEN, G. N. BEUTE, J. P. P. VAN VUGT, M. W. P. M. LENDERS, M. F. CONTARINO, M. S. J. MINK, J. LO BOUR, P. VAN DEN MUNCKHOF, B. A. SCHMAND, R. J. DE HAAN, P. R. SCHUURMAN, AND R. M. A. DE BIE, *Subthalamic nucleus versus globus pallidus bilateral deep brain stimulation for advanced parkinson's disease (nsteps study): A randomised controlled trial*, *The Lancet. Neurology*, 12 (2013), pp. 37–44.
- [251] R. L. O'GORMAN, J. M. JAROSZ, M. SAMUEL, C. CLOUGH, R. P. SELWAY, AND K. ASHKAN, *Ct/mr image fusion in the postoperative assessment of electrodes implanted for deep brain stimulation*, *Stereotactic and functional neurosurgery*, 87 (2009), pp. 205–210.
- [252] M. S. OKUN, H. H. FERNANDEZ, S. S. WU, L. KIRSCH-DARROW, D. BOWERS, F. BOVA, M. SUELTER, C. E. JACOBSON, X. WANG, C. W. GORDON, P. ZEILMAN, J. ROMRELL, P. MARTIN, H. WARD, R. L. RODRIGUEZ, AND K. D. FOOTE, *Cognition and mood in parkinson's disease in subthalamic nucleus versus globus pallidus interna deep brain stimulation: The compare trial*, *Annals of Neurology*, 65 (2009), pp. 586–595.
- [253] M. S. OKUN, M. TAGLIATI, M. POURFAR, H. H. FERNANDEZ, R. L. RODRIGUEZ, R. L. ALTERMAN, AND K. D. FOOTE, *Management of referred deep brain stimulation failures: A retrospective analysis from 2 movement disorders centers*, *Archives of neurology*, 62 (2005), pp. 1250–1255.
- [254] D. A. OLSZEWSKA, S. FAHN, R. A. WALSH, AND T. LYNCH, *Parkinson's disease*, in *Neurodegenerative disorders*, O. Hardiman and C. P. Doherty, eds., Springer, Cham, 2016, pp. 85–115.
- [255] J. L. OSTREM, C. A. RACINE, G. A. GLASS, J. K. GRACE, M. M. VOLZ, S. L. HEATH, AND P. A. STARR, *Subthalamic nucleus deep brain stimulation in primary cervical dystonia*, *Neurology*, 76 (2011), pp. 870–878.
- [256] P. E. O'SUILLEABHAIN AND J. Y. MATSUMOTO, *Time-frequency analysis of tremors*, *Brain : a journal of neurology*, 121 ( Pt 11) (1998), pp. 2127–2134.

- [257] A. OSWAL, V. LITVAK, P. SAULEAU, AND P. BROWN, *Beta reactivity, prospective facilitation of executive processing, and its dependence on dopaminergic therapy in parkinson's disease*, *The Journal of neuroscience : the official journal of the Society for Neuroscience*, 32 (2012), pp. 9909–9916.
- [258] P. A. PAHAPILL, *The pedunculopontine nucleus and parkinson's disease*, *Brain : a journal of neurology*, 123 (2000), pp. 1767–1783.
- [259] R. PAHWA, S. A. FACTOR, K. E. LYONS, W. G. ONDO, G. GRONSETH, H. BRONTE-STEWART, M. HALLETT, J. MIYASAKI, J. STEVENS, AND W. J. WEINER, *Practice parameter: Treatment of parkinson disease with motor fluctuations and dyskinesia (an evidence-based review): report of the quality standards subcommittee of the american academy of neurology*, *Neurology*, 66 (2006), pp. 983–995.
- [260] J. L. PALMER, M. A. COATS, C. M. ROE, S. M. HANKO, C. XIONG, AND J. C. MORRIS, *Unified parkinson's disease rating scale-motor exam: inter-rater reliability of advanced practice nurse and neurologist assessments*, *Journal of advanced nursing*, 66 (2010), pp. 1382–1387.
- [261] S. PAPAPETROPOULOS, J. R. JAGID, C. SENGUN, C. SINGER, AND B. V. GALLO, *Objective monitoring of tremor and bradykinesia during dbs surgery for parkinson disease*, *Neurology*, 70 (2008), pp. 1244–1249.
- [262] S. PAPAPETROPOULOS, H. L. KATZEN, B. K. SCANLON, A. GUEVARA, C. SINGER, AND B. E. LEVIN, *Objective quantification of neuromotor symptoms in parkinson's disease: implementation of a portable, computerized measurement tool*, *Parkinson's disease*, 2010 (2010), p. 760196.
- [263] S. L. PARISI, M. E. HÉROUX, E. G. CULHAM, AND K. E. NORMAN, *Functional mobility and postural control in essential tremor*, *Archives of physical medicine and rehabilitation*, 87 (2006), pp. 1357–1364.
- [264] B. K. PARK, Y. KWON, J. W. KIM, J. H. LEE, G. M. EOM, S. B. KOH, J. H. JUN, AND J. HONG, *Analysis of viscoelastic properties of wrist joint for quantification of parkinsonian rigidity*, *IEEE transactions on neural systems and rehabilitation engineering : a publication of the IEEE Engineering in Medicine and Biology Society*, 19 (2011), pp. 167–176.
- [265] J. PARKINSON, *An essay on the shaking palsy*, Whittingham and Rowland (London), 1817.
- [266] S. PATEL, K. LORINCZ, R. HUGHES, N. HUGGINS, J. GROWDON, D. STANDAERT, M. AKAY, J. DY, M. WELSH, AND P. BONATO, *Monitoring motor fluctuations in patients with parkinson's disease using wearable sensors*, *IEEE transactions on information technology in*

- biomedicine : a publication of the IEEE Engineering in Medicine and Biology Society, 13 (2009), pp. 864–873.
- [267] T. PERERA, S. A. C. YOHANANDAN, AND H. J. MCDERMOTT, *A simple and inexpensive test-rig for evaluating the performance of motion sensors used in movement disorders research*, Medical & biological engineering & computing, 54 (2015), pp. 333–339.
- [268] M. PESSIGLIONE, D. GUEHL, A.-S. ROLLAND, C. FRANÇOIS, E. C. HIRSCH, J. FÉGER, AND L. TREMBLAY, *Thalamic neuronal activity in dopamine-depleted primates: Evidence for a loss of functional segregation within basal ganglia circuits*, The Journal of neuroscience : the official journal of the Society for Neuroscience, 25 (2005), pp. 1523–1531.
- [269] P. PIBOOLNURAK, A. E. LANG, A. M. LOZANO, J. M. MIYASAKI, J. A. SAINT-CYR, Y.-Y. W. POON, W. D. HUTCHISON, J. O. DOSTROVSKY, AND E. MORO, *Levodopa response in long-term bilateral subthalamic stimulation for parkinson's disease*, Movement disorders : official journal of the Movement Disorder Society, 22 (2007), pp. 990–997.
- [270] P. PLAHA, Y. BEN-SHLOMO, N. K. PATEL, AND S. S. GILL, *Stimulation of the caudal zona incerta is superior to stimulation of the subthalamic nucleus in improving contralateral parkinsonism*, Brain : a journal of neurology, 129 (2006), pp. 1732–1747.
- [271] P. PLAHA, N. K. PATEL, AND S. S. GILL, *Stimulation of the subthalamic region for essential tremor*, Journal of neurosurgery, 101 (2004), pp. 48–54.
- [272] E. D. PLAYFORD, I. H. JENKINS, R. E. PASSINGHAM, J. NUTT, R. S. FRACKOWIAK, AND D. J. BROOKS, *Impaired mesial frontal and putamen activation in parkinson's disease: A positron emission tomography study*, Annals of Neurology, 32 (1992), pp. 151–161.
- [273] O. POGARELL, T. GASSER, J. J. VAN HILTEN, S. SPIEKER, S. POLLENTIER, D. MEIER, AND W. H. OERTEL, *Pramipexole in patients with parkinson's disease and marked drug resistant tremor: A randomised, double blind, placebo controlled multicentre study*, Journal of neurology, neurosurgery, and psychiatry, 72 (2002), pp. 713–720.
- [274] M. H. POLYMEROPOULOS, C. LAVEDAN, E. LEROY, S. E. IDE, A. DEHEJIA, A. DUTRA, B. PIKE, H. ROOT, J. RUBENSTEIN, R. BOYER, E. S. STENROOS, S. CHANDRASEKHARAPPA, A. ATHANASSIADOU, T. PAPAPETROPOULOS, W. G. JOHNSON, A. M. LAZZARINI, R. C. DUVOISIN, G. DI IORIO, L. I. GOLBE, AND R. L. NUSSBAUM, *Mutation in the alpha-synuclein gene identi-*

- fied in families with parkinson's disease*, *Science* (New York, N.Y.), 276 (1997), pp. 2045–2047.
- [275] B. POST, M. P. MERKUS, R. M. DE BIE, R. J. DE HAAN, AND J. D. SPEELMAN, *Unified parkinson's disease rating scale motor examination: are ratings of nurses, residents in neurology, and movement disorders specialists interchangeable?*, *Movement disorders : official journal of the Movement Disorder Society*, 20 (2005), pp. 1577–1584.
- [276] K. L. POSTON AND D. EIDELBERG, *Functional brain networks and abnormal connectivity in the movement disorders*, *NeuroImage*, 62 (2012), pp. 2261–2270.
- [277] R. B. POSTUMA, D. BERG, M. STERN, W. POEWE, C. W. OLANOW, W. OERTEL, J. OBESO, K. MAREK, I. LITVAN, A. E. LANG, G. HALLIDAY, C. G. GOETZ, T. GASSER, B. DUBOIS, P. CHAN, B. R. BLOEM, C. H. ADLER, AND G. DEUSCHL, *Mds clinical diagnostic criteria for parkinson's disease*, *Movement disorders : official journal of the Movement Disorder Society*, 30 (2015), pp. 1591–1601.
- [278] A. PROCHAZKA, D. J. BENNETT, M. J. STEPHENS, S. K. PATRICK, R. SEARS-DURU, T. ROBERTS, AND J. H. JHAMANDAS, *Measurement of rigidity in parkinson's disease*, *Movement disorders : official journal of the Movement Disorder Society*, 12 (1997), pp. 24–32.
- [279] S. PRZEDBORSKI, *Neuroinflammation and parkinson's disease*, *Handbook of clinical neurology*, 83 (2007), pp. 535–551.
- [280] C. L. PULLIAM, D. A. HELDMAN, T. H. ORCUTT, T. O. MERA, J. P. GIUFFRIDA, AND J. L. VITEK, *Motion sensor strategies for automated optimization of deep brain stimulation in parkinson's disease*, *Parkinsonism & Related Disorders*, 21 (2015), pp. 378–382.
- [281] J. RAETHJEN, M. LINDEMANN, H. SCHMALJOHANN, R. WENZELBURGER, G. PFISTER, AND G. DEUSCHL, *Multiple oscillators are causing parkinsonian and essential tremor*, *Movement disorders : official journal of the Movement Disorder Society*, 15 (2000), pp. 84–94.
- [282] S. RAEVA, *Localization in human thalamus of units triggered during 'verbal commands,' voluntary movements and tremor*, *Electroencephalography and clinical neurophysiology*, 63 (1986), pp. 160–173.
- [283] A. RAJPUT, C. A. ROBINSON, AND A. H. RAJPUT, *Essential tremor course and disability: A clinicopathologic study of 20 cases*, *Neurology*, 62 (2004), pp. 932–936.

- [284] A. H. RAJPUT, K. MAXOOD, AND A. RAJPUT, *Classic essential tremor changes following cerebellar hemorrhage*, *Neurology*, 71 (2008), pp. 1739–1740.
- [285] A. H. RAJPUT, C. A. ROBINSON, M. L. RAJPUT, AND A. RAJPUT, *Cerebellar purkinje cell loss is not pathognomonic of essential tremor*, *Parkinsonism & Related Disorders*, 17 (2011), pp. 16–21.
- [286] A. K. RAO, A. GILLMAN, AND E. D. LOUIS, *Quantitative gait analysis in essential tremor reveals impairments that are maintained into advanced age*, *Gait & posture*, 34 (2011), pp. 65–70.
- [287] M. RAPOPORT, R. VAN REEKUM, AND H. MAYBERG, *The role of the cerebellum in cognition and behavior: A selective review*, *Journal of Neuropsychiatry*, 12 (2000), pp. 193–198.
- [288] I. RAUTAKORPI, J. TAKALA, R. J. MARTTILA, K. SIEVERS, AND U. K. RINNE, *Essential tremor in a finnish population*, *Acta Neurologica Scandinavica*, 66 (1982), pp. 58–67.
- [289] M. RICHARDS, K. MARDER, L. COTE, AND R. MAYEUX, *Interrater reliability of the unified parkinson's disease rating scale motor examination*, *Movement disorders : official journal of the Movement Disorder Society*, 9 (1994), pp. 89–91.
- [290] S. M. RISSANEN, M. KANKAANPÄÄ, A. MEIGAL, M. P. TARVAINEN, J. NUUTINEN, I. M. TARKKA, O. AIRAKSINEN, AND P. A. KARJALAINEN, *Surface emg and acceleration signals in parkinson's disease: feature extraction and cluster analysis*, *Medical & biological engineering & computing*, 46 (2008), pp. 849–858.
- [291] S. M. RISSANEN, M. KANKAANPÄÄ, M. P. TARVAINEN, V. NOVAK, P. NOVAK, KUN HU, B. MANOR, O. AIRAKSINEN, AND P. A. KARJALAINEN, *Analysis of emg and acceleration signals for quantifying the effects of deep brain stimulation in parkinson's disease*, *IEEE Transactions on Biomedical Engineering*, 58 (2011), pp. 2545–2553.
- [292] C. N. RIVIERE, S. G. REICH, AND N. V. THAKOR, *Adaptive fourier modeling for quantification of tremor*, *Journal of Neuroscience Methods*, 74 (1997), pp. 77–87.
- [293] M. RIVLIN-ETZION, O. MARMOR, G. HEIMER, A. RAZ, A. NINI, AND H. BERGMAN, *Basal ganglia oscillations and pathophysiology of movement disorders*, *Current opinion in neurobiology*, 16 (2006), pp. 629–637.
- [294] E. ROCON, J. L. PONS, A. O. ANDRADE, AND S. J. NASUTO, *Application of emd as a novel technique for the study of tremor time series*, *Conference proceedings : ... Annual International Conference of*

- the IEEE Engineering in Medicine and Biology Society. IEEE Engineering in Medicine and Biology Society. Annual Conference, Suppl (2006), pp. 6533–6536.
- [295] C. RODRIGUEZ-BLAZQUEZ, M. J. FORJAZ, L. LIZAN, S. PAZ, AND P. MARTINEZ-MARTIN, *Estimating the direct and indirect costs associated with parkinson's disease*, Expert review of pharmacoeconomics & outcomes research, 15 (2015), pp. 889–911.
- [296] M. C. RODRIGUEZ-OROZ, J. A. OBESO, A. E. LANG, J.-L. HOUE TO, P. POLLAK, S. REHNCRONA, J. KULISEVSKY, A. ALBANESE, J. VOLKMANN, M. I. HARIZ, N. P. QUINN, J. D. SPEELMAN, J. GURIDI, I. ZAMARBIDE, A. GIRONELL, J. MOLET, B. PASCUAL-SEDANO, B. PIDOUX, A. M. BONNET, Y. AGID, J. XIE, A.-L. BENABID, A. M. LOZANO, J. SAINT-CYR, L. ROMITO, M. F. CONTARINO, M. SCERRATI, V. FRAIX, AND N. VAN BLERCOM, *Bilateral deep brain stimulation in parkinson's disease: A multicentre study with 4 years follow-up*, Brain : a journal of neurology, 128 (2005), pp. 2240–2249.
- [297] P. J. ROSSI, A. GUNDUZ, J. JUDY, L. WILSON, A. MACHADO, J. J. GIORDANO, W. J. ELIAS, M. A. ROSSI, C. L. BUTSON, M. D. FOX, C. C. MCINTYRE, N. POURATIAN, N. C. SWANN, C. DE HEMPTINNE, R. E. GROSS, H. J. CHIZECK, M. TAGLIATI, A. M. LOZANO, W. GOODMAN, J.-P. LANGEVIN, R. L. ALTERMAN, U. AKBAR, G. A. GERHARDT, W. M. GRILL, M. HALLETT, T. HERRINGTON, J. HERRON, C. VAN HORNE, B. H. KOPELL, A. E. LANG, C. LUNGU, D. MARTINEZ-RAMIREZ, A. Y. MOGILNER, R. MOLINA, E. OPRI, K. J. OTTO, K. G. OWEISS, Y. PATHAK, A. SHUKLA, J. SHUTE, S. A. SHETH, L. C. SHIH, G. K. STEINKE, A. I. TRÖSTER, N. VANEGAS, K. A. ZAGHLOUL, L. CENDEJAS-ZARAGOZA, L. VERHAGEN, K. D. FOOTE, AND M. S. OKUN, *Proceedings of the third annual deep brain stimulation think tank: A review of emerging issues and technologies*, Frontiers in neuroscience, 10 (2016), p. 119.
- [298] T. ROUAUD, T. DONDAINE, S. DRAPIER, C. HAEGELEN, F. LALLEMENT, J. PÉRON, S. RAOUL, P. SAULEAU, AND M. VÉRIN, *Pallidal stimulation in advanced parkinson's patients with contraindications for subthalamic stimulation*, Movement Disorders, 25 (2010), pp. 1839–1846.
- [299] U. SABATINI, K. BOULANOUAR, N. FABRE, F. MARTIN, C. CAREL, C. COLONNESE, L. BOZZAO, I. BERRY, J. L. MONTASTRUC, F. CHOLLET, AND O. RASCOL, *Cortical motor reorganization in akinetic patients with parkinson's disease*, Brain : a journal of neurology, 123 (2000), pp. 394–403.

- [300] P. S. SACHDEV, A. MOHAN, E. CANNON, J. D. CRAWFORD, P. SILBERSTEIN, R. COOK, T. COYNE, AND P. A. SILBURN, *Deep brain stimulation of the antero-medial globus pallidus interna for tourette syndrome*, PLoS ONE, 9 (2014), p. e104926.
- [301] V. M. SAENGER, J. KAHAN, T. FOLTYNIE, K. FRISTON, T. Z. AZIZ, A. L. GREEN, T. J. VAN HARTEVELT, J. CABRAL, A. B. A. STEVNER, H. M. FERNANDES, L. MANCINI, J. THORNTON, T. YOUSRY, P. LIMOUSIN, L. ZRINZO, M. HARIZ, P. MARQUES, N. SOUSA, M. L. KRINGELBACH, AND G. DECO, *Uncovering the underlying mechanisms and whole-brain dynamics of deep brain stimulation for parkinson's disease*, Scientific reports, 7 (2017), p. 9882.
- [302] J. A. SAINT-CYR, T. HOQUE, L. C. M. PEREIRA, J. O. DOSTROVSKY, W. D. HUTCHISON, D. J. MIKULIS, A. ABOSCH, E. SIME, A. E. LANG, AND A. M. LOZANO, *Localization of clinically effective stimulating electrodes in the human subthalamic nucleus on magnetic resonance imaging*, Journal of neurosurgery, 97 (2002), pp. 1152–1166.
- [303] G. SALEMI, P. ARIDON, G. CALAGNA, M. MONTE, AND G. SAVETTIERI, *Population-based case-control study of essential tremor*, Italian journal of neurological sciences, 19 (1998), pp. 301–305.
- [304] A. SAMII, J. G. NUTT, AND B. R. RANSOM, *Parkinson's disease*, Lancet (London, England), 363 (2004), pp. 1783–1793.
- [305] U. SANDVIK, L.-O. KOSKINEN, A. LUNDQUIST, AND P. BLOMSTEDT, *Thalamic and subthalamic deep brain stimulation for essential tremor: where is the optimal target?*, Neurosurgery, 70 (2012), pp. 840–5; discussion 845–6.
- [306] J. SARNTHEIN, D. PÉUS, H. BAUMANN-VOGEL, C. R. BAUMANN, AND O. SÜRÜCÜ, *Stimulation sites in the subthalamic nucleus projected onto a mean 3-d atlas of the thalamus and basal ganglia*, Acta neurochirurgica, 155 (2013), pp. 1655–1660.
- [307] P. SAULEAU, E. LERAY, T. ROUAUD, S. DRAPIER, D. DRAPIER, S. BLANCHARD, G. DRILLET, J. PÉRON, AND M. VÉRIN, *Comparison of weight gain and energy intake after subthalamic versus pallidal stimulation in parkinson's disease*, Movement Disorders, 24 (2009), pp. 2149–2155.
- [308] C. SCHMIDT, P. GRANT, M. LOWERY, AND U. VAN RIENEN, *Influence of uncertainties in the material properties of brain tissue on the probabilistic volume of tissue activated*, IEEE transactions on bio-medical engineering, 60 (2013), pp. 1378–1387.

- [309] E. A. SCHON AND S. PRZEDBORSKI, *Mitochondria: The next (neurode)generation*, *Neuron*, 70 (2011), pp. 1033–1053.
- [310] A. SCHRAG, L. HORSFALL, K. WALTERS, A. NOYCE, AND I. PETERSEN, *Prediagnostic presentations of parkinson's disease in primary care: A case-control study*, *The Lancet. Neurology*, 14 (2015), pp. 57–64.
- [311] A. SCHRAG, A. MUENCHAU, K. P. BHATIA, N. P. QUINN, AND C. D. MARSDEN, *Overdiagnosis of essential tremor*, *Lancet (London, England)*, 353 (1999), pp. 1498–1499.
- [312] A. SCHRAG, A. MÜNCHAU, K. P. BHATIA, N. P. QUINN, AND C. D. MARSDEN, *Essential tremor: An overdiagnosed condition?*, *Journal of neurology*, 247 (2000), pp. 955–959.
- [313] N. SCHWEIGHOFER, E. J. LANG, AND M. KAWATO, *Role of the olivocerebellar complex in motor learning and control*, *Frontiers in neural circuits*, 7 (2013), p. 94.
- [314] C. A. SEGER, *The basal ganglia in human learning*, *The Neuroscientist : a review journal bringing neurobiology, neurology and psychiatry*, 12 (2006), pp. 285–290.
- [315] C. A. SEGER AND B. J. SPIERING, *A critical review of habit learning and the basal ganglia*, *Frontiers in Systems Neuroscience*, 5 (2011), p. 66.
- [316] S. SENOVA, D. QUERLIOZ, C. THIRIEZ, P. JEDYNAK, B. JARRAYA, AND S. PALFI, *Using the accelerometers integrated in smartphones to evaluate essential tremor*, *Stereotactic and functional neurosurgery*, 93 (2015), pp. 94–101.
- [317] B. SEPEHRI, A. ESTEKI, E. EBRAHIMI-TAKAMJANI, G. A. SHAHIDI, F. KHAMSEH, AND M. MOINODIN, *Quantification of rigidity in parkinson's disease*, *Annals of biomedical engineering*, 35 (2007), pp. 2196–2203.
- [318] D. SERVELLO, M. PORTA, M. SASSI, A. BRAMBILLA, AND M. M. ROBERTSON, *Deep brain stimulation in 18 patients with severe gilles de la tourette syndrome refractory to treatment: The surgery and stimulation*, *Journal of neurology, neurosurgery, and psychiatry*, 79 (2008), pp. 136–142.
- [319] R. R. SHAMIR, R. EITAN, S. SHEFFER, O. MARMOR-LEVIN, D. VALSKY, S. MOSHEL, A. ZAIDEL, H. BERGMAN, AND Z. ISRAEL, *Intra-operative identification of the subthalamic nucleus motor zone using goniometers*, in *Information Processing in Computer-Assisted Interventions*, D. Hutchison, T. Kanade, J. Kittler, J. M. Kleinberg, F. Mattern, J. C. Mitchell, M. Naor, O. Nierstrasz, C. Pandu Rangan, B. Steffen,

- M. Sudan, D. Terzopoulos, D. Tygar, M. Y. Vardi, G. Weikum, D. Barratt, S. Cotin, G. Fichtinger, P. Jannin, and N. Navab, eds., vol. 7915 of *Lecture Notes in Computer Science*, Springer Berlin Heidelberg, Berlin, Heidelberg, 2013, pp. 21–29.
- [320] R. R. SHAMIR, A. NOECKER, AND C. C. MCINTYRE, *Deep brain stimulation*, *Frontiers for Young Minds*, 2 (2014), p. 2096.
- [321] M. B. SHAPIRO, D. E. VAILLANCOURT, M. M. STURMAN, L. V. METMAN, R. A. E. BAKAY, AND D. M. CORCOS, *Effects of stn dbs on rigidity in parkinson's disease*, *IEEE transactions on neural systems and rehabilitation engineering : a publication of the IEEE Engineering in Medicine and Biology Society*, 15 (2007), pp. 173–181.
- [322] A. SHATUNOV, N. SAMBUUGHIN, J. JANKOVIC, R. ELBLE, H. S. LEE, A. B. SINGLETON, A. DAGVADORJ, J. JI, Y. ZHANG, V. E. KIMONIS, J. HARDY, M. HALLETT, AND L. G. GOLDFARB, *Genomewide scans in north american families reveal genetic linkage of essential tremor to a region on chromosome 6p23*, *Brain : a journal of neurology*, 129 (2006), pp. 2318–2331.
- [323] H. A. SHILL, C. H. ADLER, AND T. G. BEACH, *Pathology in essential tremor*, *Parkinsonism & Related Disorders*, 18 (2012), pp. S135–S137.
- [324] J. L. SHILS, M. TAGLIATI, AND R. L. ALTERMAN, *Neurophysiological monitoring during neurosurgery for movement disorders*, in *Neurophysiology in Neurosurgery*, Elsevier, 2002, pp. 405–IX.
- [325] P. SILBERSTEIN, A. POGOSYAN, A. A. KÜHN, G. HOTTON, S. TISCH, A. KUPSCH, P. DOWSEY-LIMOUSIN, M. I. HARIZ, AND P. BROWN, *Cortico-cortical coupling in parkinson's disease and its modulation by therapy*, *Brain : a journal of neurology*, 128 (2005), pp. 1277–1291.
- [326] K. A. SILLAY, L. M. KUMBIER, C. ROSS, M. BRADY, A. ALEXANDER, A. GUPTA, N. ADLURU, G. S. MIRANPURI, AND J. C. WILLIAMS, *Perioperative brain shift and deep brain stimulating electrode deformation analysis: Implications for rigid and non-rigid devices*, *Annals of biomedical engineering*, 41 (2013), pp. 293–304.
- [327] A. B. SINGLETON, M. J. FARRER, AND V. BONIFATI, *The genetics of parkinson's disease: progress and therapeutic implications*, *Movement disorders : official journal of the Movement Disorder Society*, 28 (2013), pp. 14–23.
- [328] H. M. M. SMEDING, J. D. SPEELMAN, M. KONING-HAANSTRA, P. R. SCHURMAN, P. NIJSSEN, T. VAN LAAR, AND B. SCHMAND,

- Neuropsychological effects of bilateral stn stimulation in parkinson disease: A controlled study*, *Neurology*, 66 (2006), pp. 1830–1836.
- [329] L. SMELTERE, V. KUZNECOVS, AND R. ERTS, *Depression and social phobia in essential tremor and parkinson's disease*, *Brain and behavior*, 7 (2017), p. e00781.
- [330] P. F. SOWMAN AND K. S. TÜRKER, *Methods of time and frequency domain examination of physiological tremor in the human jaw*, *Human movement science*, 24 (2005), pp. 657–666.
- [331] R. SPIEGELMANN, O. NISSIM, D. DANIELS, A. OCHERASHVILLI, AND Y. MARDOR, *Stereotactic targeting of the ventrointermediate nucleus of the thalamus by direct visualization with high-field mri*, *Stereotactic and functional neurosurgery*, 84 (2006), pp. 19–23.
- [332] M. STACY, *Medical treatment of parkinson disease*, *Neurologic Clinics*, 27 (2009), pp. 605–631.
- [333] P. A. STARR, *Placement of deep brain stimulators into the subthalamic nucleus or globus pallidus internus: Technical approach*, *Stereotactic and functional neurosurgery*, 79 (2002), pp. 118–145.
- [334] H. STEFANSSON, S. STEINBERG, H. PETURSSON, O. GUSTAFSSON, I. H. GUDJONSDOTTIR, G. A. JONSDOTTIR, S. T. PALSSON, T. JONSSON, J. SAEMUNSDOTTIR, G. BJORNSDOTTIR, Y. BÖTTCHER, T. THORLACIUS, D. HAUBENBERGER, A. ZIMPRICH, E. AUFF, C. HOTZY, C. M. TESTA, L. A. MIYATAKE, A. R. ROSEN, K. KRISTLEIFSSON, D. RYE, F. ASMUS, L. SCHÖLS, M. DICHGANS, F. JAKOBSSON, J. BENEDIKZ, U. THORSTEINSDOTTIR, J. GULCHER, A. KONG, AND K. STEFANSSON, *Variant in the sequence of the lingo1 gene confers risk of essential tremor*, *Nature genetics*, 41 (2009), pp. 277–279.
- [335] E. STEIN, *Olgierd c. zienkiewicz, a pioneer in the development of the finite element method in engineering science*, *Steel Construction*, 2 (2009), pp. 264–272.
- [336] H. STOLZE, G. PETERSEN, J. RAETHJEN, R. WENZELBURGER, AND G. DEUSCHL, *The gait disorder of advanced essential tremor*, *Brain : a journal of neurology*, 124 (2001), pp. 2278–2286.
- [337] M. M. STURMAN, D. E. VAILLANCOURT, L. V. METMAN, BAKAY, ROY A E, AND D. M. CORCOS, *Effects of subthalamic nucleus stimulation and medication on resting and postural tremor in parkinson's disease*, *Brain : a journal of neurology*, 127 (2004), pp. 2131–2143.

- [338] K. SUGIYAMA, *Complications of deep brain stimulation*, in *Deep Brain Stimulation for Neurological Disorders*, T. Itakura, ed., Springer International Publishing and Imprint: Springer, Cham, 2015, pp. 195–206.
- [339] T. S. SUMANAWEEERA, J. R. ADLER, S. NAPEL, AND G. H. GLOVER, *Characterization of spatial distortion in magnetic resonance imaging and its implications for stereotactic surgery*, *Neurosurgery*, 35 (1994), pp. 696–703; discussion 703–4.
- [340] S. SVEINBJORNSDOTTIR, *The clinical symptoms of parkinson's disease*, *Journal of neurochemistry*, 139 Suppl 1 (2016), pp. 318–324.
- [341] H. A. TABA, S. S. WU, K. D. FOOTE, C. J. HASS, H. H. FERNANDEZ, I. A. MALATY, R. L. RODRIGUEZ, Y. DAI, P. R. ZEILMAN, C. E. JACOBSON, AND M. S. OKUN, *A closer look at unilateral versus bilateral deep brain stimulation: Results of the national institutes of health compare cohort*, *Journal of neurosurgery*, 113 (2010), pp. 1224–1229.
- [342] T. TAIRA, *Deep brain stimulation for dystonia*, in *Deep Brain Stimulation for Neurological Disorders*, T. Itakura, ed., Springer International Publishing and Imprint: Springer, Cham, 2015, pp. 121–134.
- [343] S. TAKESHITA, K. KURISU, L. TROP, K. ARITA, T. AKIMITSU, AND N. P. L. G. VERHOEFF, *Effect of subthalamic stimulation on mood state in parkinson's disease: Evaluation of previous facts and problems*, *Neurosurgical review*, 28 (2005), pp. 179–86; discussion 187.
- [344] F. TAMMA, E. CAPUTO, V. CHIESA, M. EGIDI, M. LOCATELLI, P. RAMPINI, C. CINNANTE, A. PESENTI, AND A. PRIORI, *Anatomo-clinical correlation of intraoperative stimulation-induced side-effects during hf-dbs of the subthalamic nucleus*, *Neurological sciences : official journal of the Italian Neurological Society and of the Italian Society of Clinical Neurophysiology*, 23 Suppl 2 (2002), pp. S109–10.
- [345] C. M. TANNER, S. M. GOLDMAN, K. E. LYONS, D. A. ASTON, J. W. TETRUD, M. D. WELSH, J. W. LANGSTON, AND W. C. KOLLER, *Essential tremor in twins: An assessment of genetic vs environmental determinants of etiology*, *Neurology*, 57 (2001), pp. 1389–1391.
- [346] THE FEDERAL COUNCIL OF SWITZERLAND, *Medical devices ordinance: Meddo 812.213 art 8 para. 1*, 2002.
- [347] THE FEDERAL COUNCIL OF SWITZERLAND, *Ordinance on human research with the exception of clinical trials: Hro 810.301 art 7*, 2014.
- [348] O.-B. TYSNES AND A. STORSTEIN, *Epidemiology of parkinson's disease*, *Journal of neural transmission (Vienna, Austria : 1996)*, 124 (2017), pp. 901–905.

- [349] K. UDUPA AND R. CHEN, *The mechanisms of action of deep brain stimulation and ideas for the future development*, Progress in Neurobiology, 133 (2015), pp. 27–49.
- [350] U. UNGERSTEDT, *Postsynaptic supersensitivity after 6-hydroxydopamine induced degeneration of the nigro-striatal dopamine system*, Acta physiologica Scandinavica. Supplementum, 367 (1971), pp. 69–93.
- [351] X. VASQUES, L. CIF, O. HESS, S. GAVARINI, G. MENNESSIER, AND P. COUBES, *Stereotactic model of the electrical distribution within the internal globus pallidus during deep brain stimulation*, Journal of computational neuroscience, 26 (2009), pp. 109–118.
- [352] F. VASSAL, J. COSTE, P. DEROST, V. MENDES, J. GABRILLARGUES, C. NUTI, F. DURIF, AND J. J. LEMAIRE, *Direct stereotactic targeting of the ventrointermediate nucleus of the thalamus based on anatomic 1.5-t mri mapping with a white matter attenuated inversion recovery (wair) sequence*, Brain stimulation, 5 (2012), pp. 625–633.
- [353] N. VAYSSIERE, N. VAN DER GAAG, L. CIF, S. HEMM, R. VERDIER, P. FREREBEAU, AND P. COUBES, *Deep brain stimulation for dystonia confirming a somatotopic organization in the globus pallidus internus*, Journal of neurosurgery, 101 (2004), pp. 181–188.
- [354] R. VIARO, M. MORARI, AND G. FRANCHI, *Progressive motor cortex functional reorganization following 6-hydroxydopamine lesioning in rats*, The Journal of neuroscience : the official journal of the Society for Neuroscience, 31 (2011), pp. 4544–4554.
- [355] F. S. C. VICTOR AND P. D. THOMPSON, *Rigidity and spasticity*, in Parkinson's disease & movement disorders, J. Jankovic and E. Tolosa, eds., Lippincott Williams & Wilkins, Philadelphia, PA, USA, 2015.
- [356] C. VILARIÑO-GÜELL, C. WIDER, O. A. ROSS, B. JASINSKA-MYGA, J. KACHERGUS, S. A. COBB, A. I. SOTO-ORTOLAZA, B. BEHROUZ, M. G. HECKMAN, N. N. DIEHL, C. M. TESTA, Z. K. WSZOLEK, R. J. UITTI, J. JANKOVIC, E. D. LOUIS, L. N. CLARK, A. RAJPUT, AND M. J. FARRER, *Lingo1 and lingo2 variants are associated with essential tremor and parkinson disease*, Neurogenetics, 11 (2010), pp. 401–408.
- [357] J. L. VITEK, *Mechanisms of deep brain stimulation: Excitation or inhibition*, Movement disorders : official journal of the Movement Disorder Society, 17 Suppl 3 (2002), pp. S69–72.
- [358] J. L. VITEK, R. A. E. BAKAY, A. FREEMAN, M. EVATT, J. GREEN, W. McDONALD, M. HABER, H. BARNHART, N. WAHLAY, S. TRICHE, K. MEWES, V. CHOCKKAN, J.-Y. ZHANG, AND M. R.

- DELONG, *Randomized trial of pallidotomy versus medical therapy for parkinson's disease*, *Annals of Neurology*, 53 (2003), pp. 558–569.
- [359] J. VOLKMANN, A. ALBANESE, J. KULISEVSKY, A.-L. TORNQVIST, J.-L. HOUETO, B. PIDOUX, A.-M. BONNET, A. MENDES, A.-L. BENABID, V. FRAIX, N. VAN BLERCOM, J. XIE, J. OBESO, M. C. RODRIGUEZ-OROZ, J. GURIDI, A. SCHNITZLER, L. TIMMERMANN, A. A. GIRONELL, J. MOLET, B. PASCUAL-SEDANO, S. REHNCRONA, E. MORO, A. C. LANG, A. M. LOZANO, A. R. BENTIVOGLIO, M. SCERRATI, M. F. CONTARINO, L. ROMITO, M. JANSSENS, AND Y. AGID, *Long-term effects of pallidal or subthalamic deep brain stimulation on quality of life in parkinson's disease*, *Movement Disorders*, 24 (2009), pp. 1154–1161.
- [360] V. VOON, P. KRACK, A. E. LANG, A. M. LOZANO, K. DUJARDIN, M. SCHÜPBACH, J. D'AMBROSIA, S. THOBOIS, F. TAMMA, J. HERZOG, J. D. SPEELMAN, J. SAMANTA, C. KUBU, H. ROSSIGNOL, Y.-Y. POON, J. A. SAINT-CYR, C. ARDOUIN, AND E. MORO, *A multicentre study on suicide outcomes following subthalamic stimulation for parkinson's disease*, *Brain : a journal of neurology*, 131 (2008), pp. 2720–2728.
- [361] R. L. WATTS AND A. S. MANDIR, *The role of motor cortex in the pathophysiology of voluntary movement deficits associated with parkinsonism*, *Neurologic Clinics*, 10 (1992), pp. 451–469.
- [362] F. WEAVER, K. FOLLETT, K. HUR, D. IPPOLITO, AND M. STERN, *Deep brain stimulation in parkinson disease: A metaanalysis of patient outcomes*, *Journal of neurosurgery*, 103 (2005), pp. 956–967.
- [363] F. M. WEAVER, K. FOLLETT, M. STERN, K. HUR, C. HARRIS, W. J. MARKS, J. ROTHLIND, O. SAGHER, D. REDA, C. S. MOY, R. PAHWA, K. BURCHIEL, P. HOGARTH, E. C. LAI, J. E. DUDA, K. HOLLOWAY, A. SAMII, S. HORN, J. BRONSTEIN, G. STONER, J. HEEMSKERK, AND G. D. HUANG, *Bilateral deep brain stimulation vs best medical therapy for patients with advanced parkinson disease: A randomized controlled trial*, *JAMA*, 301 (2009), pp. 63–73.
- [364] F. M. WEAVER, K. A. FOLLETT, M. STERN, P. LUO, C. L. HARRIS, K. HUR, W. J. MARKS, J. ROTHLIND, O. SAGHER, C. MOY, R. PAHWA, K. BURCHIEL, P. HOGARTH, E. C. LAI, J. E. DUDA, K. HOLLOWAY, A. SAMII, S. HORN, J. M. BRONSTEIN, G. STONER, P. A. STARR, R. SIMPSON, G. BALTUCH, A. DE SALLES, G. D. HUANG, AND D. J. REDA, *Randomized trial of deep brain stimulation for parkinson disease: Thirty-six-month outcomes*, *Neurology*, 79 (2012), pp. 55–65.

- [365] D. D. WEBSTER, *Dynamic measurement of rigidity, strength, and tremor in parkinson patients before and after destruction of mesial globus pallidus*, *Neurology*, 10 (1960), pp. 157–163.
- [366] L. M. WEISE, C. SEIFRIED, S. EIBACH, T. GASSER, J. ROEPER, V. SEIFERT, AND R. HILKER, *Correlation of active contact positions with the electrophysiological and anatomical subdivisions of the subthalamic nucleus in deep brain stimulation*, *Stereotactic and functional neurosurgery*, 91 (2013), pp. 298–305.
- [367] M.-L. WELTER, J.-L. HOUETO, A.-M. BONNET, P.-B. BEJANI, V. MESNAGE, D. DORMONT, S. NAVARRO, P. CORNU, Y. AGID, AND B. PIDOUX, *Effects of high-frequency stimulation on subthalamic neuronal activity in parkinsonian patients*, *Archives of neurology*, 61 (2004), pp. 89–96.
- [368] T. WICHMANN AND J. SOARES, *Neuronal firing before and after burst discharges in the monkey basal ganglia is predictably patterned in the normal state and altered in parkinsonism*, *Journal of neurophysiology*, 95 (2006), pp. 2120–2133.
- [369] WIKIMEDIA COMMONS: MALYSZKZ, *Sir william richard gowers parkinson disease sketch*, 1886.
- [370] A. J. WILLS, I. H. JENKINS, P. D. THOMPSON, L. J. FINDLEY, AND D. J. BROOKS, *Red nuclear and cerebellar but no olivary activation associated with essential tremor: A positron emission tomographic study*, *Annals of Neurology*, 36 (1994), pp. 636–642.
- [371] K. WITT, C. DANIELS, J. REIFF, P. KRACK, J. VOLKMANN, M. O. PINSKER, M. KRAUSE, V. TRONNIER, M. KLOSS, A. SCHNITZLER, L. WOJTECKI, K. BÖTZEL, A. DANEK, R. HILKER, V. STURM, A. KUPSCH, E. KARNER, AND G. DEUSCHL, *Neuropsychological and psychiatric changes after deep brain stimulation for parkinson's disease: A randomised, multicentre study*, *The Lancet Neurology*, 7 (2008), pp. 605–614.
- [372] K. WITT, O. GRANERT, C. DANIELS, J. VOLKMANN, D. FALK, T. VAN EIMEREN, AND G. DEUSCHL, *Relation of lead trajectory and electrode position to neuropsychological outcomes of subthalamic neurostimulation in parkinson's disease: Results from a randomized trial*, *Brain : a journal of neurology*, 136 (2013), pp. 2109–2119.
- [373] D. WRIGHT, K. NAKAMURA, T. MAEDA, K. KUTSUZAWA, K. MIYAWAKI, AND K. NAGATA, *Research and development of a portable device to quantify muscle tone in patients with parkinsons disease*, *Conference proceedings : ... Annual International Conference of the*

- IEEE Engineering in Medicine and Biology Society. IEEE Engineering in Medicine and Biology Society. Conference, 2008 (2008), pp. 2825–2827.
- [374] H. H. YIN AND B. J. KNOWLTON, *The role of the basal ganglia in habit formation*, *Nature reviews. Neuroscience*, 7 (2006), pp. 464–476.
- [375] W. YIN, W. LIN, W. LI, S. QIAN, AND X. MOU, *Resting state fmri demonstrates a disturbance of the cerebello-cortical circuit in essential tremor*, *Brain topography*, 29 (2016), pp. 412–418.
- [376] C. YU, M. L. APUZZO, C. S. ZEE, AND Z. PETROVICH, *A phantom study of the geometric accuracy of computed tomographic and magnetic resonance imaging stereotactic localization with the leksell stereotactic system*, *Neurosurgery*, 48 (2001), pp. 1092–8; discussion 1098–9.
- [377] H. YU, D. STERNAD, D. M. CORCOS, AND D. E. VAILLANCOURT, *Role of hyperactive cerebellum and motor cortex in parkinson's disease*, *NeuroImage*, 35 (2007), pp. 222–233.
- [378] L. B. ZAHODNE, M. S. OKUN, K. D. FOOTE, H. H. FERNANDEZ, R. L. RODRIGUEZ, S. S. WU, L. KIRSCH-DARROW, C. E. JACOBSON, C. ROSADO, AND D. BOWERS, *Greater improvement in quality of life following unilateral deep brain stimulation surgery in the globus pallidus as compared to the subthalamic nucleus*, *Journal of neurology*, 256 (2009), pp. 1321–1329.
- [379] A. ZERROUG, J. GABRILLARGUES, G. COLL, F. VASSAL, B. JEAN, E. CHABERT, B. CLAISE, T. KHALIL, L. SAKKA, F. FESCHET, F. DURIF, L. BOYER, J. COSTE, AND J.-J. LEMAIRE, *Personalized mapping of the deep brain with a white matter attenuated inversion recovery (wair) sequence at 1.5-tesla: Experience based on a series of 156 patients*, *Neurochirurgie*, 5014 (2016), pp. 183–231.
- [380] Z. ZHENG, Y. Q. ZHANG, J. Y. LI, X. H. ZHANG, P. ZHUANG, AND Y. J. LI, *Subthalamic deep brain stimulation for parkinson's disease: correlation of active contacts and electrophysiologically mapped subthalamic nucleus*, *Chin Med J (Engl) (Chinese medical journal)*, 122 (2009), pp. 2419–2422.
- [381] A. ZIMPRICH, S. BISKUP, P. LEITNER, P. LICHTNER, M. FARRER, S. LINCOLN, J. KACHERGUS, M. HULIHAN, R. J. UITTI, D. B. CALNE, A. J. STOESSL, R. F. PFEIFFER, N. PATENGE, I. C. CARBAJAL, P. VIEREGGE, F. ASMUS, B. MÜLLER-MYHSOK, D. W. DICKSON, T. MEITINGER, T. M. STROM, Z. K. WSZOLEK, AND T. GASSER, *Mutations in *Irrk2* cause autosomal-dominant parkinsonism with pleomorphic pathology*, *Neuron*, 44 (2004), pp. 601–607.

- [382] M. ZONENSHAYN, D. STERIO, P. J. KELLY, A. R. REZAI, AND A. BERIC, *Location of the active contact within the subthalamic nucleus (stn) in the treatment of idiopathic parkinson's disease*, *Surgical neurology*, 62 (2004), pp. 216–25; discussion 225–6.
- [383] L. ZRINZO, *Pitfalls in precision stereotactic surgery*, *Surgical neurology international*, 3 (2012), pp. S53–61.
- [384] P. ZSIGMOND, N. DERNROTH, A. KULLMAN, L.-E. AUGUSTINSSON, AND N. DIZDAR, *Stereotactic microdialysis of the basal ganglia in parkinson's disease*, *Journal of Neuroscience Methods*, 207 (2012), pp. 17–22.

## **Schriftliche Erklärung**

Ich erkläre, dass ich die Dissertation

“Investigation of intraoperative accelerometer data recording for safer and improved target selection for deep brain stimulation”

nur mit der darin angegebenen Hilfe verfasst und bei keiner anderen Universität und keiner anderen Fakultät der Universität Basel eingereicht habe.

Ich bin mir bewusst, dass eine unwahre Erklärung rechtliche Folgen haben kann.

Basel, 13.08.2018

---

(Ort, Datum)



---

Ashesh Shah (Unterschrift)